Sodium Circulation in *Vibrio cholerae*

by

Judith L. Winogrodzki

A Thesis
Submitted to the Faculty of Graduate Studies in Partial Fulfillment
of the Requirement for the Degree of

DOCTOR OF PHILOSOPHY

Department of Microbiology
University of Manitoba
Winnipeg, Manitoba
CANADA

July, 2006

THE UNIVERSITY OF MANITOBA

FACULTY OF GRADUATE STUDIES

*****

COPYRIGHT PERMISSION

Sodium Circulation in *Vibrio cholerae*

BY

Judith L. Winogrodzki

A Thesis/Practicum submitted to the Faculty of Graduate Studies of The University of Manitoba in partial fulfillment of the requirement of the degree

OF

DOCTOR OF PHILOSOPHY

ABSTRACT

The present research is focused on the physiology and biochemistry of Na^+ circulation in the important human pathogen *Vibrio cholerae*. In the course of this work, Vc-NhaD, representing a new family of Na^+/H^+ antiporters, was cloned from the *V. cholerae* genome, functionally expressed in *Escherichia coli* and characterized in inside-out sub-bacterial vesicles. Extensive site-directed mutagenesis of the *nhaD* gene identified a number of functionally important amino acid residues presumably involved in cation transfer and pH regulation of the antiporter. The intramolecular distribution of these residues revealed an unexpected similarity of molecular organization of Vc-NhaD and the phylogenetically unrelated bacterial Na^+/H^+ antiporter, NhaA, indicating an exciting possibility of common mechanism of transmembrane ion transfer shared by these antiporters, namely, alternating-access mechanism. However, the experiments employing the *V. cholerae* chromosomal *nhaD*$^-$ mutant constructed in this work, demonstrated that the physiological role of Vc-NhaD differs significantly from that of NhaA. In contrast to NhaA, a major Na^+-extruding mechanism in many bacterial species, Vc-NhaD *in vivo* operates to import Na^+ ions in exchange for cytoplasmic protons. This is what makes Vc-NhaD unique, because previously described bacterial Na^+/H^+ antiporters export rather than import alkali cations under physiological conditions. The unusual physiology of Vc-NhaD suggests its important role in completing the Na^+ cycle and regulating intracellular pH. The growth properties of the *nhaD*$^-$ mutant indicate that through its role in ion homeostasis, Vc-NhaD apparently influences such physiological traits in *V. cholerae* as phosphate uptake, arsenate sensitivity and survival at elevated temperatures.

At the beginning of this project, there were no experimental data concerning the energy requirements of the central bioenergetic process, oxidative phosphorylation, in *V.*

cholerae. Using an *atpE*⁻ mutant and sub-bacterial vesicles derived from wild type and mutant cells, it has been found that, despite the presence in the membrane of two primary Na^+ pumps, the respiratory Na^+-translocating ubiquinone oxidoreductase (NQR) and the Na^+-translocating oxaloacetate decarboxylase, oxidative phosphorylation in this bacterium is mediated by a proton-motive F_1F_0-ATPase. The significance of this finding is three-fold: (i) it provides, for the first time, experimental data on the energization of oxidative phosphorylation in *V. cholerae*; (ii) it is a direct experimental confirmation of earlier bioinformatics assignments based on the Na^+-binding model; and (iii) it shows how Na^+ and H^+ circulation are integrated in the overall energization of the membrane of marine vibrios, such as *V. cholerae* and another NQR-possessing marine vibrio, *V. alginolyticus*, where the F_1F_0-ATPase is H^+-specific, as well.

In a related study, the possible role of the primary Na^+ pump, NQR, as a specific target for micromolar Ag^+ in *V. cholerae* was investigated. Although the therapeutic antimicrobial effects of Ag^+ have been known for a long time, the molecular mechanism of the bactericidal action of low concentrations of Ag^+ has not been elucidated. On the other hand, it has been previously shown that preparations of isolated NQR are highly sensitive to low concentrations of Ag^+. However, data presented in this study showed that NQR is not a determinant of the high sensitivity of *V. cholerae* to Ag^+ ions. Both growth experiments and analysis of sub-bacterial vesicles isolated from wild type and the ΔNQR mutant of *V. cholerae* revealed that micromolar concentrations of Ag^+ induce a massive H^+ leakage through the *V. cholerae* membrane irrespectively of the presence of NQR, causing complete deenergization and cell death.

ACKNOWLEDGEMENTS

I would like to thank my supervisor, Dr. Pavel Dibrov, for his guidance, giving me the courage to succeed and mostly for believing in me. I would also like to thank others who significantly helped in this process including:

Dr. Rahim Habibian who constructed and characterized a number of mutant forms of Vc-NhaD discussed in this thesis.

Dr. Elena Ostroumov who also constructed and characterized a couple of Vc-NhaD mutants discussed in this thesis.

Dr. Jeannine Barrett for her attempts at over-expressing and purifying Vc-NhaD.

Dr. Arthur Winogrodzki who cloned Vc-NhaA and Vc-NhaD. He was also involved in the preliminary characterization of both antiporters.

A number of summer/project students especially Leon Espira for his attempts at over-expressing Vc-NhaD, Katarzyna Godlewski who helped me significantly with a number of growth experiments and Olga Winogrodzki for helping me characterize a couple of mutant forms of Vc-NhaD.

Our collaborator, Dr. Claudia Häse, for generating and donating various knock-out strains of *V. cholerae* and who is involved in a number of projects conducted in the laboratory.

Dr. Peter Loewen for generating an assortment of computer models of Vc-NhaD.

Dr. Elizabeth Worobec and Dr. Harry Duckworth for sitting on my committee and for thier care, as well as my external examiner Dr. Oleg Dmitriev for his advice.

I would also like to thank NSERC, MHRC, the Winnipeg Foundation, the Canadian Foundation of Innovation and the University of Manitoba for funding.

Thank you to all of my friends and family for supporting me throughout this whole time.

Saving the best for last, I would like to thank my husband, Arthur, for absolutely everything! Mojemu najbardziej ukochanemu przyjacielowi i mezowi. Dziekuje za wiare we mnie, i za podpore w ciezkim czasie.

TABLE OF CONTENTS

LIST OF PUBLICATIONS

Habibian, R., **Dzioba, J.**, Barrett, J., Galperin, M. Y., Loewen, P. C. and Dibrov, P. (2005) Functional analysis of conserved polar residues in Vc-NhaD, Na^+/H^+ antiporter of *Vibrio cholerae*. *J. Biol. Chem.* **280**, 39637-39643.

Dibrov, P., Rimon, A., **Dzioba, J.**, Winogrodzki, A., Shalitin, Y. and Padan, E. (2005) 2-Aminoperimidine, a specific inhibitor of bacterial NhaA Na^+/H^+ antiporters. *FEBS Lett.* **579**, 373-378.

Dzioba, J., Häse, C. C., Gosink, K., Galperin, M. Y. and Dibrov, P. (2003) Experimental verification of a sequence-based prediction: F_1F_0-type ATPase of *Vibrio cholerae* transports protons, no Na^+ ions. *J. Bacteriol.* **185**, 674-678.

Dibrov, P., **Dzioba, J.**, Gosink, K. K. and Häse, C. C. (2002) Chemiosmotic mechanism of the antimicrobial activity of Ag^+ in *Vibrio cholerae*. *Antimicrob. Agents Chemother.* **46**, 2668-2670.

Ostroumov, E., **Dzioba, J.**, Loewen, P. C. and Dibrov, P. (2002) Asp(344) and Thr(345) are critical for cation exchange mediated by NhaD, Na^+/H^+ antiporter of *Vibrio cholerae*. *Biochim. Biophys. Acta.* **1564**, 99-106.

Dzioba, J., Ostroumov, E., Winogrodzki, A. and Dibrov, P. (2002) Cloning, functional expression in *Escherichia coli* and primary characterization of a new Na^+/H^+ antiporter, NhaD, of *Vibrio cholerae*. *Mol. Cell. Biochem.* **1-2**, 119-124.

Manuscripts in Progress

Dzioba-Winogrodzki, J., Loewen, P. C. and Dibrov, P. (2006) Mutation of a single residue, R305, affects coupling of $Na^+(Li^+)$ and H^+ fluxes as well as pH response in Vc-NhaD, Na^+/H^+ antiporter of *Vibrio cholerae*. *Manuscript in progress.*

Dzioba-Winogrodzki, J., Godlewski, K., Habibian, R., Barrett, J., Loewen, P. C., Padan, E. and Dibrov, P. (2006) Specific Na^+/H^+ antiporter, Vc-NhaD, modulates the arsenate resistance and net inorganic phosphate transport in *Vibrio cholerae*. *Manuscript in progress.*

Dzioba-Winogrodzki, J., Godlewski, K., Häse, C. C., Galperin, M. Y. and Dibrov. P. (2006) The role of the Na^+ cycle in the survival of the mesophilic bacterium, *Vibrio cholerae*, at elevated temperatures. *Manuscript in progress.*

Dzioba-Winogrodzki, J., Winogrodzki, O., Häse, C. C., Krulwich, T. A. and Dibrov, P. (2006) Characterization of the *Vibrio cholerae* multifunctional *mrp*-encoded cation/proton antiporter affecting intestinal colonization and conferring resistance to bile salts in heterologous host. *Manuscript in progress.*

LIST OF FIGURES **Page**

LIST OF TABLES **Page**

LIST OF ABBREVIATIONS

ABC	ATP-binding cassette
ADP	adenine diphosphate
AP	2-aminoperimidine
ATP	adenine triphosphate
ATPase	adenine triphosphate synthase
ATR	acid tolerance response
cAMP	cyclic AMP
C_i	inorganic carbon
COG	cluster of orthologous groups of proteins
DCCD	N,N'-dicyclohexylcarbodiimide
Ec	*E. coli*
g	gram
G3P	glycerol-3-phosphate
HA	high affinity
HAP	hemagglutin protease
H-NS	histone-like nucleoid structuring protein
HQNO	2-heptyl-4-hydroxyquinoline-N-oxide
IC_{50}	inhibitory concentration 50%
IT	ion transporter
kDa	kilodalton
kV	kilovolt
L	litre
LA	low affinity
LPS	lipopolysaccharide
M	molar
MATE	multidrug and toxic compound extrusion
MFS	major facilitator superfamily
mg	milligram
MIC	minimum inhibitory concentration
ml	millillitre
mM	millmolar
NADH	nicotinamide adenine dinucleotide hydroxide
ng	nanogram
NQR	Na^+-translocating NADH:ubiquinone oxidoreductase
OAD	oxaloacetate decarboxylase
ORF	open reading frame
PAGE	polyacrylamide gel electrophoresis
PCR	polymerase chain reaction
Pho-box	phosphate box
P_i	inorganic phosphate
pmf	proton-motive force
PMSF	phenylmethylsulfonyl flouride
RND	resistance nodulation cell division
rpm	rotations per minute

SDS	sodium dodecyl sulphate
smf	sodium-motive force
SMR	small multidrug resistance
TCP	toxin co-regulated pilus
TMS	transmembrane segment
V	volt
Vc	*Vibrio cholerae*
Vp	*Vibrio parahaemolyticus*
VPI	*Vibrio* pathogenicity island
μg	microgram
μl	microlitre
μM	micromolar

1. LITERATURE REVIEW

1. LITERATURE REVIEW

1.1. *Vibrio cholerae*: An Overview

V. cholerae, the causative agent of the often-fatal diarrheal disease cholera, is a highly motile, Gram negative bacterium that belongs to the γ-subdivision of the family *Proteobacteriaceae*. The *V. cholerae* genome consist of two mega-replicons, 2,961,146 and 1,072,314 base pairs respectively, comprising 3885 predicted ORFs. Chromosome 1 (large one) contains most of the genes for cellular function where as chromosome 2 (small one) contains a larger fraction of hypothetical genes. Of the many serogroups, O1 and O139 are associated with major epidemics of the disease and, the non-O1 and non-O139 serogroups are associated with moderate to severe gastroenteritis [Faruque, et al., 2004]. There are two phenotypes of pathogenic *V. cholerae*, El Tor and classical. The El Tor type is different from the classical one in that it produces hemolysins. Moreover, it remains inside the host for a longer period of time and is capable of surviving in the environment for a greater duration, thereby making this strain more virulent than the classical. The different serogroups of *V. cholerae* have distinct cell surface lipopolysaccharide (LPS) antigens and the epidemiology and virulence of *V. cholerae* relies on its antigenic variation. Until the emergence of the Bengal strain, which is a new O139 type, all strains of *V. cholerae* responsible for epidemic disease were classified into the O1 serogroup. There are three O1 biotypes and these are Ogawa, Inaba and Hikojima [Torodor, 2005].

The disease cholera is a very old one and today, still affects millions of people in developing countries such as Asia, Africa and Latin America. Since the first pandemic in 1817, six more have been reported [Faruque, et. al., 2004].

The most important advances into the understanding of *V. cholerae* include the characterization of the major virulence determinants, cholera toxin (CT) and toxin co-regulated pilus (TCP). However, despite these progresses, there are many aspects of *V. cholerae* that still remain under-investigated (see Faruque, et. al., 2004 and references therein).

1.2. The Life Cycle of *V. cholerae*

Through its life cycle, *V. cholerae* must endure an immense range of physiological conditions. It must overcome the host's immunological defense mechanisms, as well as survive in an environment outside the host between infections [Colwell & Huq, 1994; Reidl & Klose, 2002]. Some of the changes *V. cholerae* encounters when it invades the human intestine include abrupt variations in temperature, nutrients, salinity, pH, oxygen concentration, inorganic phosphate (P_i) and others [Colwell & Huq, 1994; Reidl & Klose, 2002; Peterson, 2002].

Because of these variations, the life cycle of *V. cholerae* is considered to consist of two phases, the Environmental Phase and the Host Phase (Fig. 1.1).

1.2.1. The Environmental Phase

V. cholerae is an autochthonous species in estuarine and brackish waters, a type of environment ideally suited for its proliferation and persistence [Singleton, et al., 1982; Huq et al., 1984; Colwell, 1996; Häse & Barquera, 2001; Peterson, 2002]. It has been isolated from areas with salt concentrations ranging from 0.2-2.0%. The optimum pH for growth seems to be slightly alkaline, ranging from 8.0 to 9.0 according to different sources [Miller et al., 1984; Tamplin et al, 1990; Colwell & Huq, 1994; Häse & Barquera,

2001]. In vitro, *V. cholerae* can be cultured in as high as 3.0% sodium, but the ideal concentration is considered to be 2.0% [Miller et al., 1984; Tamplin et al., 1990].

Aquatic organisms are continuously subjected to alternations in temporal and spacial gradients of nutrients. Under adverse living conditions, such as decreased temperature, reduced organic content, lowered salinity or differences in osmotic pressure, pH and many other factors, *V. cholerae* will enter a dormant/spore-like state, though it can still remain infectious [Bennish, 1994]. Such cells maintain viability and will resume a vegetative form once favourable living conditions prevail [Colwell & Huq, 1994; Bennish, 1994].

In its environment, *V. cholerae* exists as a free-living organism [Miller et al., 1984], but can be found associated with marine plants, phytoplankton, cyanobacteria, algae and zooplankton such as copepods [Tokuda & Kogure, 1989; Colwell, 1996; Peterson, 2002]. It can likewise survive on molluscs, crustaceans, fish and shellfish [Huq et. al., 1986; Colwell, 1996; Peterson, 2002]. It has been suggested the ability of *V. cholerae* to generate biofilms may enhance its survivability and lend an adaptive benefit in an aquatic environment [Watnick & Kolter, 1999]. For instance, *V. cholerae* can metabolize chitin, so attachment to various chitinaceous surfaces may provide nutrition directly to the bacterium [Fletcher, 1996; Watnick & Kolter, 1999].

1.2.2. The Host Phase

On the basis of human volunteer studies, an infectious dose of *V. cholerae* is estimated to be 10^8-10^9 cells, though certain strains are reported as being more virulent [Bennish, 1994; Colwell, 1996]. The severity of the disease appears to be dependent

Fig. 1.1. Natural history and life cycle of *V. cholerae* (after, Raskin et al., 2004). Infection begins when contaminated food or water is ingested. *V. cholerae* that survive passage through the stomach, go on to colonize the epithelium of the small intestine where it secretes a toxin that causes the intestinal mucosal cells to secrete copious amounts of solutes into the lumen. *V. cholerae* proliferates rapidly, with densities reaching as high as 1,000,000 bacteria/ml of intestinal fluid. The voluminous diarrhea associated with cholera infection promotes the spread of *V. cholerae* back in to the environment to begin its life cycle once again [Reidl & Klose, 2002; Peterson, 2002; Colwell, 1996; Finkelstein, 1996; Bennish, 1994].

Fig. 1.1

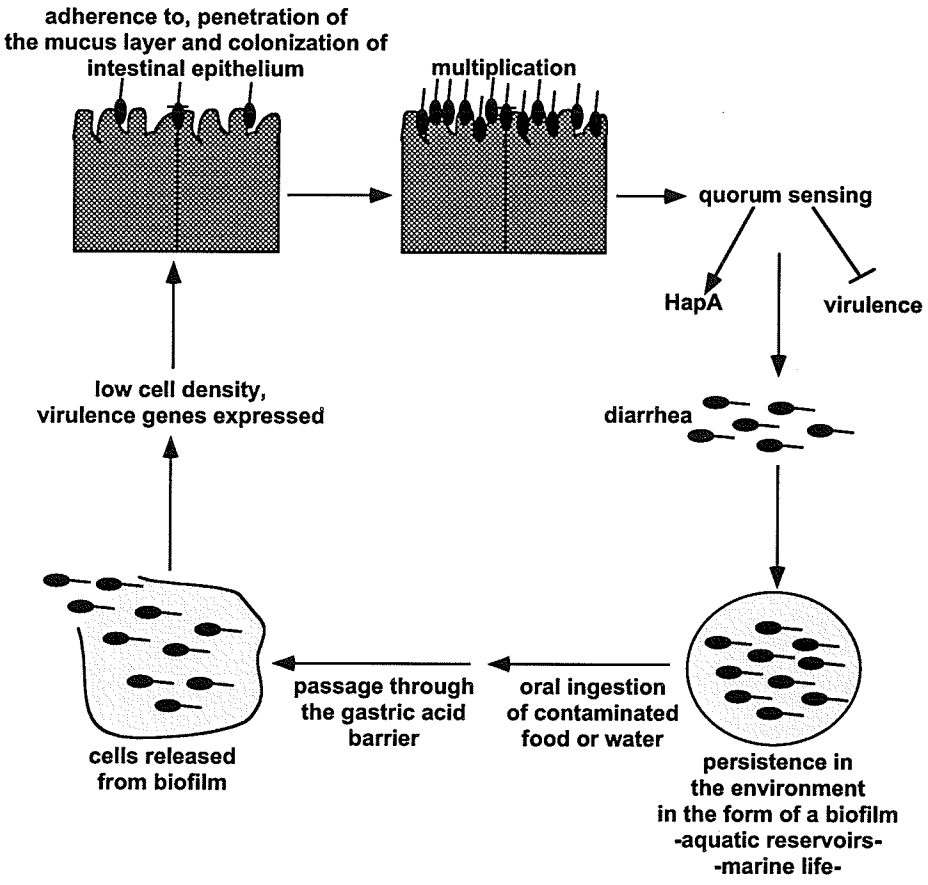
adherence to, penetration of
the mucus layer and colonization of
intestinal epithelium
multiplication
quorum sensing
HapA
virulence
diarrhea
persistence in
the environment
in the form of a biofilm
-aquatic reservoirs-
-marine life-
oral ingestion
of contaminated
food or water
passage through
the gastric acid
barrier
cells released
from biofilm
low cell density,
virulence genes expressed

upon the dosage size and health status of the individual [Bennish, 1994]. Previous attempts to infect healthy volunteers with *V. cholerae*, revealed that an inoculum-size of up to approximately 1000 cells caused little to no disease and in fact, these organisms could not be retrieved from the stools of these individuals. However, when bicarbonate was simultaneously administered to neutralize the gastric acidity, cholera ensued in most volunteers when given a much lower dose of 100 cells [Finkelstein, 1996]. Therefore, stomach acidity is a very effective natural resistance mechanism and explains the requirement for the large initial dose to effectively cause disease [Finkelstein, 1996; Ding & Waldor, 2003].

Once inside the host, *V. cholerae* must evade the innate immunological defense mechanisms (gastric acid barrier, mucoid secretion and peristalsis), permeate the mucus layer protecting the intestinal villi, adhere to and colonize the epithelium of the small intestine, change to a nonmotile form, replicate and cause disease by secreting the potent enterotoxin, CT at the site of infection [Peterson, 2002].

Upon entering the acidic environment of the stomach, *V. cholerae* is able to mount an acid tolerance response (ATR) to acid challenge, by inducing the *cadCBA* operon. Acid tolerance in *V. cholerae* is dependent upon lysine decarboxylation, but not ornithine decarboxylation [Merrell & Camilli, 1999; and Merrell & Camilli, 2000]. The second gene in the operon, *cadA*, encodes an inducible lysine decarboxylase, upstream to this, the gene *cadB* encodes a lysine/cadaverine antiporter and *cadB* is preceded by *cadC*, an acid responsive positive transcriptional regulator of the operon [Merrell & Camilli, 2000]. Interestingly, acid-exposed *V. cholerae* has a competitive advantage in colonization over cells that were not pre-exposed [Merrell & Camilli, 1999]. *V. cholerae* cells that survive

the acid environment of the stomach, use motility and chemotaxis to ultimately colonize the intestinal epithelium [Merrell & Camilli, 1999; Faruque et al., 2004].

1.2.2.1. Virulence Factors in *V. cholerae*

V. cholerae pathogenicity is reliant upon a number of virulence genes forming the ToxR regulon, which is the subject of complex regulation aimed to prevent expression of virulence factors outside the host, but ensure high expression levels in the host intestine (Fig. 1.2).

The two most important virulence factors are cholera toxin (CT) and the colonization factor, TCP (toxin-coregulated pilus). CT is an A-B type ADP-ribosylating toxin that, being exported into intestinal lumen, causes severe diarrhea in cholera patients [Gill, 1976; Mekalanos et al., 1983]. TCP is a type IV bundle-forming pilus [Taylor et al., 1987; Herrington et al., 1988]. It also serves as the receptor for the CTXϕ bacteriophage whose genome contains the *ctxAB* operon encoding CT [Waldor & Mekalanos, 1996]. TCP biogenesis is governed by the *tcpA-F* operon, whose first gene encodes TcpA, the major pilin subunit of TCP that is required for its proper assembly and function [Manning, 1997; Chiang et al., 1995]. Together with the upstream *tcpPH* operon (encoding membrane-bound regulatory proteins TcpP and TcpH) and downstream genes *toxT* (encoding a master transcriptional regulator of CT production, ToxT) and *acf* (encoding an accessory colonization factor), *tcpA-F* constitutes the so-called TCP pathogenicity island or *Vibrio* pathogenicity island (VPI) [Kovach, 1996; Faruque et al, 2004].

When production of CT and TCP is not desirable, their expression is down-regulated by at least two distinct mechanisms (see Fig. 1.2). First, an abundant histone-like, nucleoid structuring protein, H-NS, directly silences the expression from *tcpA-F*,

toxT and *ctxAB* genes by binding to their AT-rich promoters [Nye, et al., 2000; Yu & DiRita, 2002]. Deletion of the *hns* gene which encodes H-NS results in high constitutive expression of CT, TCP and ToxT [Nye, et al., 2000]. The H-NS-based mechanism ensures the efficient repression of the virulence determinant expression in the absence of inducing stimuli. The second mechanism includes quorum-sensing regulators LuxO and HapR [Zhu, 2002; Kovacikova & Skorupski, 2002]. At low cell density, LuxO is active and represses the expression of HapR, which is a negative regulator of *aphA* transcription. Therefore, under these conditions the TcpP signaling protein, which should be activated by AphA/B, is produced and can (in concert with TcpH and the ToxR/S pair) activate the expression of CT and TCP. However, at high cell density, quorum sensing signals (i.e., accumulation of autoinducer) inactivates LuxO. As a result, accumulating HapR represses *tcpP* transcription, which eventually switches off production of virulence factors. The *luxO* mutant showed both overall repression of the ToxT regulon in gene array essays and a severe defect in colonization in an infant mouse model of infection [Zhu et al., 2002]. Thus, in contrast to the H-NS-dependent repression, the quorum-sensing mediated control mechanism stops the on-going expression of virulence factors. HapR also activates the expression of hemagglutinin protease (HAP), a major extracellular protease serving as a "detachase" during colonization [Finkelstein et al., 1992]. It has been suggested that at advanced stages of infection, when critical cell density is reached, HapR acts to promote detachment of *V. cholerae* cells (through the simultaneous expression of HAP and repression of TCP, which is involved in bacterial-bacterial and bacterial-epithelial adhesion) in order to establish new loci of infection elsewhere in the gut or to allow the organism to leave the host altogether [Zhu et al., 2002].

Fig. 1.2. The key elements of the ToxR regulon in *V. cholerae*. CT, cholera toxin; TCP, toxin co-regulated pilus; VPI, *Vibrio* pathogenicity island. Arrows and T bars denote positive and negative effects, respectively. H-NS prevents expression of virulence factors in the absence of external stimuli. The quorum sensing-based branch can switch off the on-going expression of CT and TCP. ToxT acts as a ToxR-dependent master transcriptional activator in the cascade. In the presence of bile, ToxR can directly bind to the *ctxA* promoter, activating synthesis of CT in a ToxT-independent manner. The exact nature of external signals is still unknown. See the text for further details.

Fig. 1.2

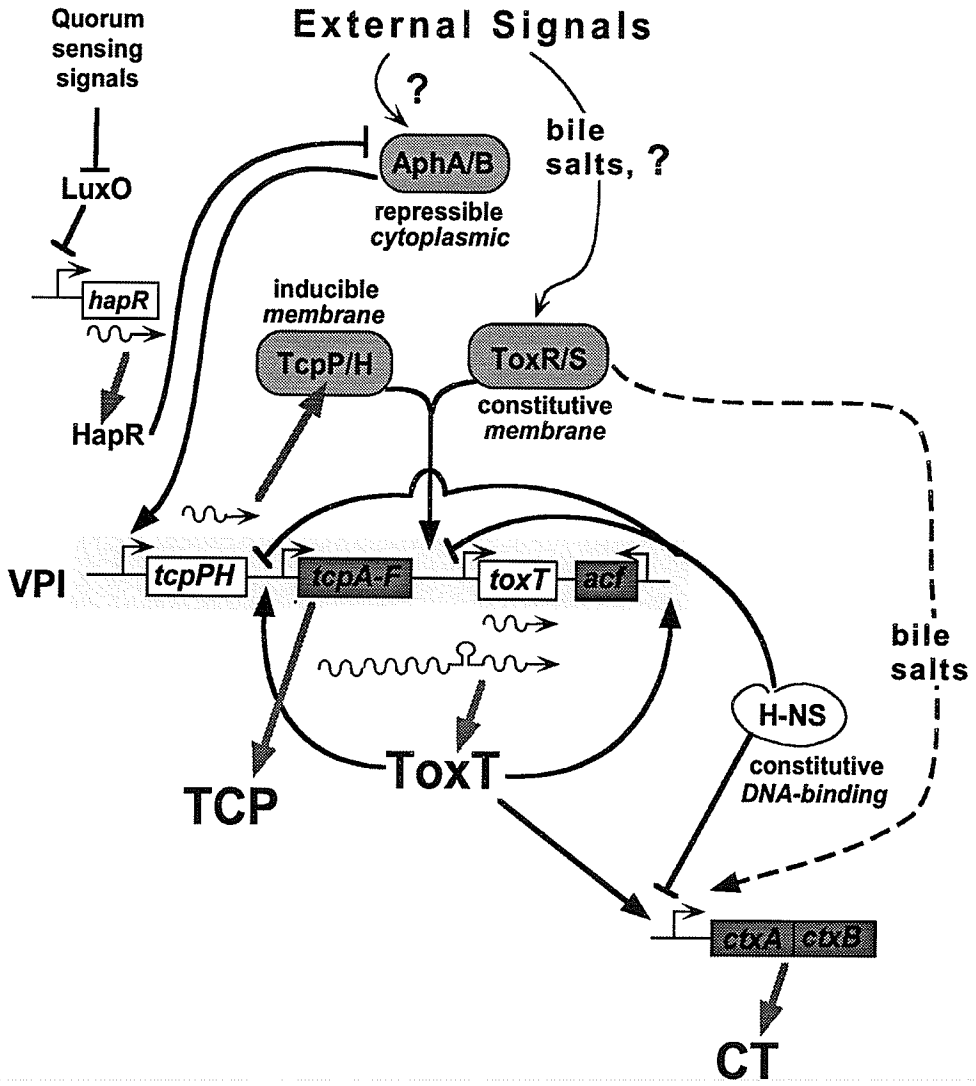
Quorum sensing signals
External Signals
?
bile salts, ?
AphA/B
repressible cytoplasmic
LuxO
hapR
HapR
inducible membrane
TcpP/H
ToxR/S
constitutive membrane
VPI
tcpPH
tcpA-F
toxT
acf
bile salts
H-NS
constitutive DNA-binding
TCP
ToxT
ctxA
ctxB
CT

Once *V. cholerae* successfully enters the intestine, external signals (of which the true nature remains unknown) activate a complex positive regulatory cascade leading to CT and TCP expression. From *in vitro* induction studies, it is believed that the first event is the transcription of *tcpPH*, which is activated by cytoplasmic regulators AphA/B [DiRita et al., 1991; Skorupski & Taylor, 1999; Kovacikova & Skorupski, 2001]. The TcpP/H complex then reaches the cytoplasmic membrane and interacts with constitutive membrane-bound ToxR/S complexes, activating them [Häse & Mekalanos, 1998]. Activated ToxR is able to bind to the *toxT* promoter, apparently displacing H-NS "silencers" and activating transcription of *toxT* [Miller et al., 1987]. ToxT serves as a master transcriptional activator of the whole ToxR regulon (Fig. 1.2). It binds to the AT-rich promoters of *ctxAB*, *acf* and *tcpA*, displaces H-NS and activates transcription. As a result, not only CT, TCP and other virulence determinants are produced, but more ToxT is synthesized from the read-through transcript due to the activation of the *tcpA* promoter (see Fig. 1.2). This autoregulatory loop of positive feedback maintains a high level of expression of virulence factors under inducing conditions [Yu & DiRita, 1999]. Interestingly, in the presence of bile salts ToxR/S can bind to the *ctxA* promoter directly, activating it [Hung & Mekalanos, 2005].

In *V. cholerae*, expression of the virulence factors TCP and CT *in vitro* is known to depend on temperature. Paradoxically, maximal induction of virulence gene expression is seen at 30°C, whereas repression is observed at 37°C [Parsot & Mekalanos, 1990]. Interestingly, immediately upstream of the *toxR* gene and transcribed in the opposite direction, is the gene encoding the heat shock protein, *htpG*. In fact, these genes are in such close proximity, that it has been hypothesized that only one RNA polymerase is capable of binding to the upstream region of *toxR* at any given time. It has been proposed

that at decreased temperature, the σ^{70} RNA polymerase binds to the *toxR* promoter and at increased temperatures, the σ^{32} RNA polymerase binds to the promoter of *htpG*, thereby repressing the expression of *toxR* [Parsot & Mekalanos, 1990]. Why virulence factors are adequately expressed *in vivo* in the intestine still remains to be explained. Perhaps, it is due to the presence of a signal found *in vivo*, but lacking *in vitro* [Parsot & Mekalanos, 1990].

1.2.2.2. Cholera Toxin and the Disease

Once secreted, CT acts as an A-B type toxin, causing ADP-ribosylation of a small G-protein in host cells and activating adenylate cyclase, resulting in an abnormally high production of cyclic AMP (cAMP). The subsequent cAMP-mediated flow of reactions is not well characterized, but eventually there is an over-stimulation of the mucosal cells to continuously pump out large amounts of chloride and bicarbonate into the intestinal lumen from the blood and tissues. This is followed by the loss of water, sodium and other electrolytes resulting in the characteristic sudden onset of massive diarrhea [Finkelstein, 1996]. The cholera stool contains shedded mucus and intestinal epithelial cells ("rice-water" stool) along with an enormous number of *V. cholerae* cells [Bennish, 1994; Finkelstein, 1996].

In hospitalized patients, the loss of fluid from diarrhea can be as high as 20 litres or more per day, ultimately leading to dehydration, anuria, acidosis and shock. The loss of potassium ions may result in cardiac complications and circulatory failure. If left untreated, cholera frequently results in death, with the mortality rate reaching sometimes 60% [Finkelstein, 1996].

The acute diarrhea associated with cholera leads to the dissipation of *V. cholerae* cells back into the environment and thus a return to the Environmental Phase of the life cycle (for review, see Reidl & Klose, 2002; Peterson, 2002) (Fig. 1.1).

1.3. Na^+ and H^+ Cycles in Bacteria

Generally, bacteria use pmf generated by primary H^+ pumps as the ultimate source of energy for osmotic, chemical and mechanical work (for review see [Harold & Maloney, 1996, Maloney & Wilson, 1996]). However, analysis of bacterial genomes shows that many species, including a number of human and animal pathogens encode primary Na^+-motive pumps, such as Na^+-transporting dicarboxylate decarboxylases and/or Na^+-translocating NADH:ubiquinone oxidoreductase (NQR), as well as a variety of Na^+-dependent permeases [Häse et al., 2001]. These bacteria can utilize Na^+ as a coupling ion instead of, or (typically) in addition to the H^+ ion. The list of microorganisms that have the capacity to utilize the chemiosmotic Na^+ cycle includes diverse bacterial pathogens, such as *C. trachomatis, C. pneumoniae, Treponema palladium, Haemophilus influenzae, V. cholerae, Pseudomonas aeruginosa, Salmonella enterica, Klebsiella pneumonia* and *Yersinia pestis,* as well as many archaeal species [Häse et al., 2001]. Some of these microorganisms also have Na^+-specific membrane ATPases (F_1F_0-type or A_1A_0-type ATP synthases), suggesting that they rely on smf, rather than on pmf for such an important function as oxidative phosphorylation (see [Häse et al., 2001]).

1.3.1. Primary Na^+ Pumping at Lowered Proton-Motive Force: Alkalophiles and Thermophiles

Obvious adaptive advantages should be provided to bacteria, including pathogens, that possess primary Na^+ pumps and accompanying smf consumers (discussed in [Häse et al., 2001]), and have a free-living phase in their life cycle. In these cases, energetics employing Na^+ rather than H^+ as a primary coupling ion (Na^+-cycle) would enhance their survival under conditions where the pmf is dangerously low.

In particular, in alkaline environments, the total level of pmf on the bacterial membrane becomes significantly lowered due to the opposite direction of its electric ($\Delta\psi$) and osmotic (ΔpH) components. The ability to switch from a H^+ to Na^+ cycle under these circumstances could be crucial for survival of the bacterium [Skulachev, 1989; Skulachev, 1991].

Growth of bacteria and archaea at high temperatures is also limited in particular because of increased permeability of the membrane for ions (leakiness), resulting in lowered levels of pmf on the membrane [van de Vossenberg et. al., 1995]. Importantly, it turns out that Na^+ ions are far less permeable compared to H^+ at any temperature [van de Vossenberg et. al., 1995].

Different microorganisms apparently use three distinct major strategies to cope with the arising proton leakage (see [van de Vossenberg et. al., 1998, Albers et. al., 2001] and references therein): (i) psychrophilic and mesophilic bacteria, as well as archaea, are able to adjust the lipid composition of their membranes in order to limit the H^+ permeability at higher temperatures (the so-called "homeo-proton permeability adaptation"); (ii) some thermophiles respond to elevated temperatures by a sharp increase in the H^+-extruding respiration [De Vrij et. al., 1988]; and, (iii) anaerobic thermophiles use the Na^+ cycle

instead of the H^+ cycle. The use of a less permeable coupling cation in the latter case allows avoidance of the futile transmembrane circulation of H^+, thus enhancing the overall efficiency of energy transduction. For instance, the thermophile *Caloramator fervidus* (previously *Clostridium fervidus*) relies solely on the energy derived from the Na^+ gradient generated by the Na^+ pumping V-type ATPase. The smf can then be used for the uptake of various amino acids [Speelmans et al., 1993].

Since some mesophilic bacteria, including a number of important pathogens, possess both primary Na^+ pumps and various smf consumers (see [Häse et. al, 2001]), the question arises whether the Na^+ cycle may contribute to the survival of these organisms at elevated temperature. We attempted to investigate this possibility in the case of *V. cholerae* (Section 4.7).

1.3.2. Secondary Na^+/H^+ Exchange: Removal of Toxic Alkali Cations and Regulation of Internal pH

Na^+/H^+ antiporters are universal components of a functional bacterial membrane (reviewed in Padan & Schuldiner, 1996; Padan & Krulwich, 2000; Padan et al., 2001).

They create a secondary smf at the expense of the pre-established pmf generated by primary proton pumps, or vice versa, thereby linking H^+ and Na^+ circulation across the membrane [Padan & Schuldiner, 1994; Padan & Schuldiner, 1996; Padan & Krulwich, 2000; Padan et al., 2001]. Coupling Na^+ and H^+ transmembrane fluxes, Na^+/H^+ antiporters are essential for maintaining cytoplasmic pH homeostasis during growth in an alkaline environment [Padan et al., 1981], removing toxic Na^+ and Li^+ ions from the cytoplasm, and controlling cell volume [Padan & Schuldiner, 1996; Padan & Krulwich, 2000]. The significance of these membrane proteins is highlighted by the fact that

bacteria often possess more than one type of Na^+/H^+ antiporter. For instance, *B. subtilis* possesses at least five Na^+/H^+ antiporters, TetA(L) [Cheng et al., 1996; Krulwich et al., 2001], MleN (previously YqkI) [Wei et al., 2000], NhaC [Pragai et al., 2001], NhaK [Fujisawa et al., 2005] and Mrp [Ito et al., 1999]. Aside from NhaA and NhaB, two antiporters common in enterobacteria, *E. coli* has two others, ChaA and MdfA.

1.3.3. Possible Linkage of Na^+/H^+ Antiport to Individual Physiological Traits

The multiplicity of bacterial Na^+/H^+ antiporters mentioned above might be due to the fact that they are not only key elements in maintaining intracellular ion balance and osmoregulation, but as it has been uncovered during the past few years, are related to specific physiological functions in bacteria (for review see Krulwich et al., 2005).

For instance, Tet(K) and Tet(L) proteins from gram-positive organisms can exchange external H^+ not only for Na^+, but also for tetracycline-divalent-metal complex [Krulwich et al., 2001]. Another Na^+/H^+ antiporter, NhaC of *B. subtilis*, influences the expression of alkaline phosphatases through the modulation of transcription of the Pho operon [Pragai et al., 2001]. In the same microorganism, the MrpA (also named ShaA) Na^+/H^+ antiporter (product of *mrpA* belonging to the *mrp* operon, see below) is required for the initiation of sporulation [De la Horra et al., 2000] and MleN (previously YqkI) is unique in that it mediates simultaneous Na^+/H^+ and malate/lactate antiport [Wei et al., 2000]. An endospore germination factor, GerN of *Bacillus cereus* was recently identified as a Na^+/H^+-K^+ antiporter [Southworth, et al., 2001]. The NhaP Na^+/H^+ antiporter isolated from *Pseudomonas aeruginosa* has been reported to carry out Na^+/H^+ exchange, but Li^+ is a very poor substrate [Utsugi et al., 1998]. Other NhaP homologues have been identified as being capable of carrying out Ca^{2+}/H^+ antiport as well [Waditee et al., 2001].

The multidrug resistance transporter MdfA of *E. coli* has been recently shown to confer extreme alkaline tolerance, which is dependent on the presence of Na^+ or K^+. In addition to exporting multiple drugs, MdfA also catalyses $Na^+(K^+)/H^+$ antiport [Lewinson et al., 2004]. ChaA of *E. coli* is a Ca^{2+}/H^+ antiporter [Ivey et al., 1993] that functions to remove Na^+ ions at alkaline pH [Ohyama et al., 1994]. Expression of *chaA* appears to be regulated by osmolarity and pH [Shijuku et al., 2002].

Another interesting class of cation/H^+ antiporters includes the Mrp, multisubunit antiport system (reviewed in [Swartz et al., 2005]). These cation/H^+ antiporters are thought to function as hetero-oligimers. They have been shown to be important in overall pH homeostasis and Na^+ resistance in *Bacillus* species at alkaline pH [Ito et al., 1999; Kitada et al., 2000; Krulwich et al., 2001]. They also play an important role in the physiology of the nitrogen-fixing organism *Sinorhizobium meliloti* [Putnoky et al., 1998] and in cyanobacterium *Anabaena* [Blanco-Rivero et al., 2005], as well as in the pathogens *Staphylococcus aureus* [Tsuchiya et al., 1998] and *P. aeruginosa* [Kosono et al., 2005].

Thus, different Na^+/H^+ antiporters occupying the same membrane can be associated with a diverse set of individual pathways. This then raises the question about the possible specific roles of Na^+ transporting enzymes, including Na^+/H^+ antiporters, in pathogenic bacteria. Possible involvement of sodium circulation in particular aspects of physiology of *V. cholerae* will be discussed below in Section 1.5, following the consideration of Na^+-transporting systems of this bacterium.

1.4. Transmembrane Na^+ Circulation in *Vibrio cholerae*

The physiology of *V. cholerae* relies on transmembrane circulation of both H^+ and Na^+ ions. The cellular membrane of *V. cholerae* contains two primary Na^+ pumps, the

Fig. 1.3. Hypothetical role of the sodium cycle in *V. cholerae* virulence. Intestinal environmental conditions result in lowering of membrane potential ($\Delta\psi$) and slowing down of flagellar rotation. This effects TcpP/H regulatory proteins, which activate transcription of the ToxT-dependent virulence factors. Primary Na^+ pumping via NQR represses ToxT. The influence of sodium exchange via the Na^+/H^+ antiporters on $\Delta\psi$ modulation and toxin production is still unknown [Häse & Mekalanos, 1999; Häse & Barquera, 2001].

Fig. 1.3

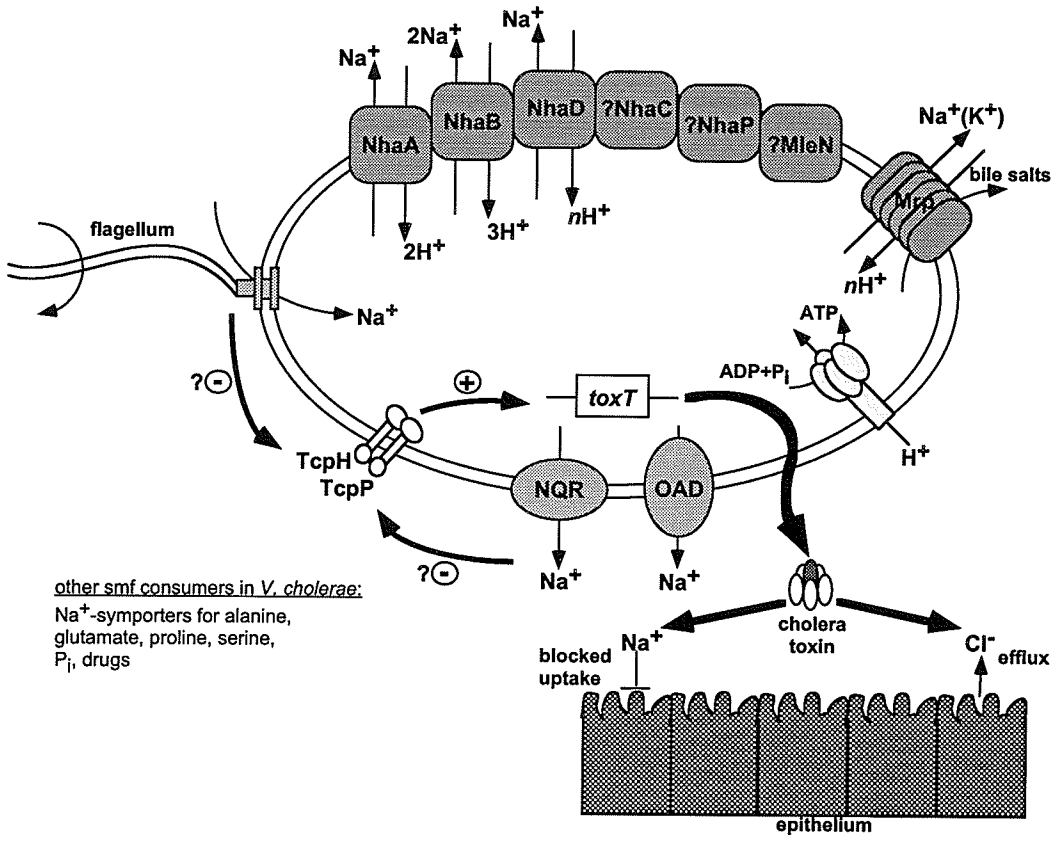
Na+
2Na+
Na+
Na+
NhaA
NhaB
NhaD
?NhaC
?NhaP
?MleN
Na+(K+)
bile salts
Mrp
2H+
3H+
nH+
nH+
flagellum
Na+
ATP
ADP+Pi
?
toxT
TcpH
TcpP
NQR
OAD
H+
?
Na+
Na+
other smf consumers in V. cholerae:
Na+-symporters for alanine,
glutamate, proline, serine,
Pi, drugs
cholera
toxin
blocked
uptake
Na+
Cl- efflux
epithelium

Na^+-translocating NADH:ubiquione oxidoreductase (NQR) [Häse & Mekalanos, 1998; Häse & Mekalanos, 1999; Barquera et al., 2002a] and the newly discovered and characterized Na^+-translocating oxaloacetate decarboxylase [Dahinden et al., 2005].

The *V. cholerae* genome also encodes at least seven putative Na^+/H^+ antiporters, namely NhaA, NhaB, NhaD, Mrp, MleN (YqkI), NhaC and NhaP [Vimont & Berche, 2000; Häse et al., 2001; Herz et al., 2003]. These *V. cholerae* antiporters and/or their characterized homologues from other bacterial species will be discussed below in more detail.

Also present is a battery of various consumers of smf, such as a Na^+-dependent flagellar motor [Häse & Mekalanos, 1999; Kojima et al., 1999; Gosink & Häse, 2000], Na^+-dependent multidrug efflux pumps [Huda et al., 2001; Huda et al., 2003], as well as putative Na^+ symporters for alanine, glutamate, proline, serine, citrate and inorganic phosphate [reviewed in Häse et al., 2001; Lebens et al., 2002] (Fig. 1.3). Furthermore, Na^+ circulation apparently influences the expression of virulence factors in *V. cholerae* [Häse & Mekalanos, 1999]. However, despite the progress made in categorization and primary characterization of the components of the Na^+ cycle in *V. cholerae*, Na^+ circulation in this bacterium remains under-investigated [Häse et al., 2001].

1.4.1. Primary Sodium Pumps in *V. cholerae*

In an alkaline environment, the employment of various pH homeostatic mechanisms keep the bacterial cytoplasm more acidic than the extracellular medium (for review, see Krulwich, 1983; Kuroda et al., 1994; Padan & Schuldiner, 1994; Nakamura et al., 1994; Padan & Schuldiner, 1996; Nozaki et al., 1996). As a consequence, the maintenance of

pmf across the membrane becomes increasingly difficult. As mentioned, certain organisms that flourish in a high Na^+ environment at moderate alkalinity are capable of using Na^+ rather than H^+ as a chemiosmotic ion. Therefore, Mitchell's model of the H^+ cycle in membrane bioenergetics [Mitchell, 1961; Mitchell, 1966] should include Na^+ as an alternative coupling ion as well [Skulachev, 1989; Skulachev, 1991]. Primary Na^+ pumps establish an electrochemical gradient of Na^+ across the membrane, minimizing the internal concentration of the toxic cation and establishing a thermodynamic force which can substitute for pmf at alkaline pH [Steuber et al., 1997; Zhou et al., 1999; Kato & Yumoto, 2000]. The resultant smf can be used as a driving force for ATP synthesis [Avetisyan et. al, 1993; Dibrov et al., 1986b; Dimroth et al., 1999], Na^+/solute symport [Sarker et al., 1996; reviewed in Jung, H., 2001] and in some cases, multidrug efflux [Huda et al., 2001; Huda et al., 2003], phosphate uptake [Lebens et al., 2002] and motility [Dibrov et al., 1986a; Kojima et al., 1999; Häse & Mekalanos, 1999; Gosink & Häse, 2000].

In *V. cholerae*, the primary generation of smf occurs by the direct pumping of Na^+ out of the cell, against its concentration gradient, via the Na^+-translocating NADH:ubiquinone oxidoreductase (NQR) [Barquera et al., 2002a] and via the newly discovered and characterized Na^+-translocating oxaloacetate decarboxylase [Dahinden et al., 2005].

1.4.1.1. Na^+-translocating Ubiquinone Oxidoreductase (NQR)

NQR is a redox-driven sodium pump and is the main entry route for electrons into the respiratory chain of many organisms. DNA sequence encoding NQR has now been identified in the genomes of a number of marine and pathogenic bacteria [Tokuda & Kogure, 1989; Steuber et al., 1997; Nakayama, Y., et al., 1998; Krebs, et al., 1999; Zhou

Fig. 1.4. Schematic of the NQR enzyme complex (after Häse & Barquera, 2001). The enzyme has been divided into two domains, a hydrophilic domain containing the NADH dehydrogenase and a hydrophobic domain containing the quinone reductase [Häse & Barquera, 2001]. NQR is a complex of six subunits, NqrA-F. It contains a 2Fe-2S centre, a noncovalently bound FAD [Pfenninger-Li, et al., 1996; Steuber et al., 1997; Nakayama et al., 1998; Zhou et al., 1999; Barquera et al., 2002a] and perhaps two covalently bound FMN cofactors [Nakayama et al., 1998; Zhou et al., 1999; Barquera et al., 2002a]. Riboflavin is also a cofactor of NQR in *V. cholerae* [Barquera et al., 2002b]. The FAD and 2Fe-2S are believed to be associated with NqrF [Steuber et al., 1997; Nakayama et al., 1998; Zhou et al., 1999; Häse & Barquera, 2000; reviewed in Hayashi et al., 2001]. The two FMNs may be bound to NqrB and NqrC [Nakayama et al., 1998; Zhou et al., 1999; Barquera et al., 2002a] through a threonine attachment site [Barquera et al., 2001; Hayashi et al., 2001]. Very little is known about the other subunits NqrA, D and E [Häse & Barquera, 2001]. Electrons from NADH are donated to FAD in the NqrF subunit. The electrons are then transferred from the 2Fe-2S centre to the tightly bound quinone (QA) [Pfenninger-Li et al., 1996; Häse & Barquera, 2001]. The resulting intermediate is the ubisemiquinone radical. This negatively charged quinone species then forms a complex with Na^+ ion taken from the cytoplasm. Once the second electron is received by the neutral Na^+-quinone complex, Na^+ ion is pumped out of enzyme at the opposite side of the membrane [Pfenninger-Li et al., 1996]. The semiquinone is then re-oxidized back to QA. [Pfenninger-Li et al., 1996]. See the text for details.

Fig. 1.4

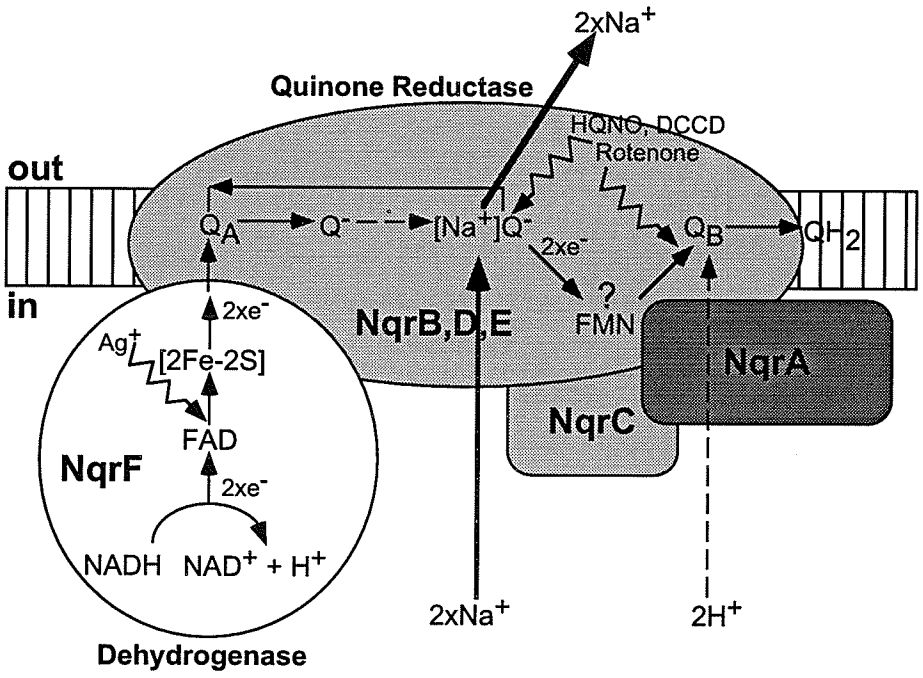
2xNa+
Quinone Reductase
HQNO, DCCD
Rotenone
out
QA
Q·-
[Na+]Q-
2xe-
QB
QH2
in
2xe-
Ag+
[2Fe-2S]
NqrB,D,E
FMN
?
NqrA
NqrC
FAD
NqrF
2xe-
NADH
NAD+ + H+
2xNa+
2H+
Dehydrogenase

et al., 1999; Kato & Yumoto, 2000; reviewed in Unemoto & Hayashi, 1993], in addition to *V. cholerae* [Barquera et al., 2002a]. NQR catalyzes the oxidation of NADH and the reduction of ubiquinone, coupling the energy derived from this redox reaction solely to the pumping of sodium ions across the membrane, resulting in the formation of smf [Steuber, 2001; Steuber et al., 1997; Dibrov, 1986a, Dibrov, 1986b]. The enzyme has now been isolated from three *Vibrio* species, *V. alginolyticus* [Nakayama et. al., 1998], *V. harveyi* [Zhou et al., 1999] and *V. cholerae* [Barquera et al., 2002a].

In *Vibrios*, NQR is a complex of six subunits, NqrA-F (Fig. 1.4), five containing transmembrane helices. The genes for all six subunits are organized in a single operon. The subunits share no significant homology with the subunits of the H^+-translocating NADH:quinone oxidoreductase (Complex I) [Steuber et al., 1997; Zhou et al., 1999; Barquera et al., 2002a]. Therefore, NQR represents a unique family of sodium-motive NADH:quinone oxidoreductases [Barquera et al., 2002a]. NQR contains a 2Fe-2S centre, a noncovalently bound FAD [Pfenninger-Li, et al., 1996; Steuber et al., 1997; Nakayama et al., 1998; Zhou et al., 1999; Barquera et al., 2002a] and perhaps two covalently bound FMN cofactors [Nakayama et al., 1998; Zhou et al., 1999; Barquera et al., 2002a] (Fig. 1.4.). Riboflavin itself has also been determined to be a cofactor of NQR in *V. cholerae* [Barquera et al., 2002b]. The FAD and 2Fe-2S are thought to be associated with NqrF, which represents the dehydrogenase segment of the enzyme (Fig. 1.4) [Steuber et al., 1997; Nakayama et al., 1998; Zhou et al., 1999; Häse & Barquera, 2000; reviewed in Hayashi et al., 2001]. This subunit also contains a sequence most probably associated with NADH binding (G^{279}GGAGMAP and Y^{375}MCGPPMM in the *V. alginolyticus* enzyme), suggesting that electrons are donated here [Rich et al., 1995]. The two FMNs may be bound to NqrB and NqrC [Nakayama et al., 1998; Zhou et al., 1999; Barquera et

al., 2002a] through a threonine attachment site [Barquera et al., 2001; Hayashi et al., 2001] (Fig. 1.4). Very little is known about the other subunits NqrA, D and E [Häse & Barquera, 2001].

Electrons from NADH are donated to FAD in the NqrF subunit. The electrons are then transferred from the 2Fe-2S centre to the tightly bound quinone (QA), completing the NADH dehydrogenase segment of the reaction [Pfenninger-Li et al., 1996; Häse & Barquera, 2001]. The resulting intermediate is the ubisemiquinone radical. According to the model suggested initially by P. Dimroth, this negatively charged quinone species, located in a hydrophobic environment, forms a complex with Na^+ ion taken from the cytoplasm; receiving of the second electron by the now neutral Na^+-quinone complex pushes this Na^+ ion towards exit from the enzyme at the opposite side of the membrane [Pfenninger-Li et al., 1996]. This is how primary Na^+ pumping is believed to occur in NQR. The semiquinone can again be re-oxidized back to QA, thereby producing a redox cycle [Pfenninger-Li et al., 1996]. As one can see, the suggested mechanism is a variation of a "built-in" Mitchellian Q-cycle resulting in translocation of Na^+ instead of H^+ (Fig. 1.4).

Electrons are then donated to the second quinone, QB, which becomes further reduced to ubiquinol, taking up protons from the cytoplasm [Pfenninger-Li et al., 1996]. At least one of the FMN cofactors may participate in this electron transfer [Häse & Barquera, 2001]. QB is not as tightly bound to the enzyme as QA; it could be exchanged with quinones of the membrane pool [Pfenninger-Li et al., 1996]. This constitutes the quinone reductase portion of the reaction, which is dependent upon the presence of sodium ion [Pfenninger-Li, et al., 1996; Nakayama et al., 1999; Zhou et al., 1999; Bogachev, et al., 2001; Steuber et al., 2001; Barquera et. al., 2002a] (Fig. 1.4).

The NADH dehydrogenase activity is not sensitive to the Na^+ pump inhibitor, 2-heptyl-4-hydroxyquinoline-N-oxide (HQNO) [Pfenniger-Li et al., 1996; Nakayama et al., 1999; Zhou et al., 1999; Barquera et al., 2002a], but it is inhibited by sub-micromolar concentrations of Ag^+ [Pfenninger-Li et al., 1996; Steuber et al., 1997; Nakayama et al., 1999]. The quinone reductase activity is inhibited by HQNO [Pfenninger-Li, et al., 1996; Nakayama et al., 1999; Zhou et al., 1999; Barquera et. al., 2002a], the electron transport (Complex I) inhibitor rotenone and the cross-linking reagent N,N'-dicyclohexylcarbodiimide (DCCD) [Pfenninger-Li et al., 1996]. It is also inhibited by the antibiotic korormicin [Nakayama et al., 1999] in a similar mechanism to HQNO. As mentioned, the dehydrogenase activity, catalysed by NqrF is strongly inhibited by Ag^+ [Pfenninger-Li et al., 1996; Steuber et al., 1997; Nakayama et al., 1999]. As it was once believed, Ag^+ does not cause a direct uncoupling of FAD from NqrF, [Steuber et al., 1997], but rather it causes partial denaturation of the enzyme resulting in slow release of FAD from the subunit F [Nakayama et al., 1999].

The operon encoding all six subunits of NQR was cloned and successfully over-expressed in *V. cholerae* [Barquera et al., 2002a]. For this purpose, a *V. cholerae* strain with a chromosomal deletion of the entire operon was constructed [Barquera et al., 2002a]. A six-histidine tag placed at the C-terminus of subunit F (last subunit in the operon) allowed purification of significant quantities of a highly active enzyme [Barquera et al., 2002a].

The recombinant *V. cholerae* enzyme could oxidize NADH specifically in the presence of Na^+, but not K^+ or Li^+ [Barquera et al., 2002a]. As in other NQRs, the quinone reductase activity was markedly sensitive to the addition of HQNO [Barquera et al., 2002a]. When purified protein was incorporated into proteoliposomes, NADH:Q1

oxidoreduction in sodium-containing medium dramatically affected the absorbance of the $\Delta\psi$-sensitive dye Oxonol VI, indicating the formation of an electric potential (positive interior). This data strongly indicated that NQR functioned as an electrogenic Na^+ pump [Barquera et al., 2002a]. In contrast to more complex H^+-motive NADH:quinone oxidoreductases, purified Na^+-motive NQR retained its Na^+-pumping ability when incorporated into proteoliposomes [Pfenninger-Li et al., 1996].

1.4.1.2. Na^+-Translocating Oxaloacetate Decarboxylase

Another, somewhat unusual, class of primary Na^+ pumps is exemplified by the Na^+-translocating dicarboxylate decarboxylases, which couple anaerobic fermentation to the generation of smf. Na^+-translocating dicarboxylate decarboxylases have been found in a number of bacteria that are capable of growing anaerobically on dicarboxylic acids [Häse et al., 2001].

This pump itself was first discovered in the anaerobe *Propionigenium modestum* when it was established that Na^+-dependent decarboxylation of oxaloacetate was coupled to the export of Na^+ into the external medium [Dimroth, 1980]. In this way, part of the free energy released during the reaction could be conserved in the form of a transmembrane Na^+ gradient [Dimroth, 1980]. Oxaloacetate decarboxylases contain three subunits, alpha, beta and gamma (Fig. 1.5), encoded in an *oadGAB* operon [Dimroth, 1980; Laussermai, 1989].

The enzyme functions to convert oxaloacetate to pyruvate and CO_2 in the presence of Na^+ ion, coupling this reaction to the export of Na^+ against its electrochemical gradient from the cytoplasm to the external medium [reviewed in Dimroth, 1987; Dimroth & Thomer, 1993]. It is localized to the cytoplasmic membrane [reviewed in Dimroth, 1987]

Fig. 1.5. Schematic of the OAD enzyme complex (after Schmid et al., 2002). The OAD enzyme complex consists of a hydrophilic α subunit that is divided into two domains and which binds biotin at the C-terminal domain [Schwarz et al., 1988]. It also contains a very hydrophobic β subunit and a small γ subunit [Schmid et al., 2002]. See the text for details.

Fig. 1.5

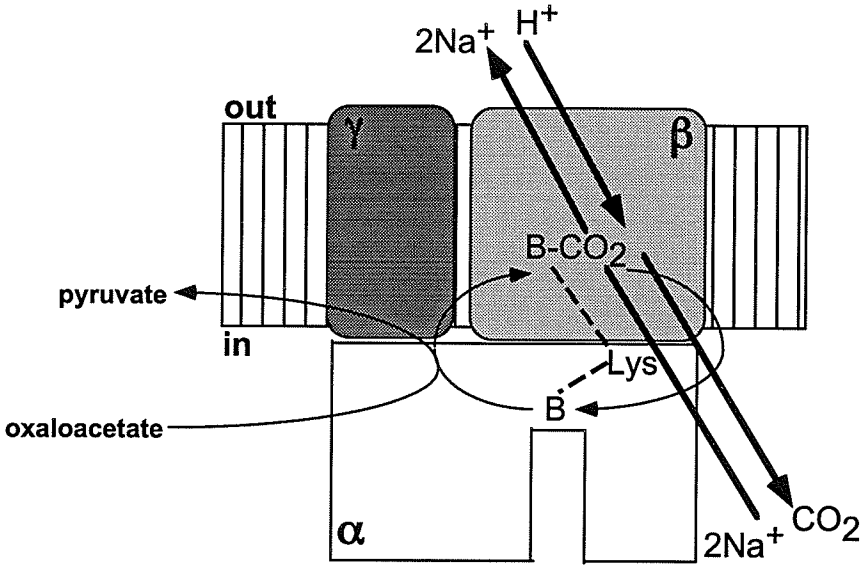

and contains biotin [Schwarz et al., 1988] (see Fig. 1.5). It carries out the following overall reaction.

$$\textbf{Oxaloacetate} + 2\ \textbf{Na}^{+}_{\textbf{in}} + \textbf{H}^{+} \rightarrow \textbf{Pyruvate} + 2\ \textbf{Na}^{+}_{\textbf{out}} + \textbf{CO}_2$$

The α subunit is hydrophilic and consists of two domains. A lysine residue responsible for biotin-binding, is located in the smaller C-terminal domain, just 35 residues from the terminus; cryoelectron microscopy has revealed the presence of a deep cleft, which divides the α subunit into these two domains [Schwartz et al., 1988] (Fig. 1.5).The β subunit is very hydrophobic and was thought to contain 11 transmembrane segments according to hydropathy analysis, but *phoA* and *lacZ* fusion studies showed that this subunit is made up of threeN-terminal and six C-terminal membrane spanning alpha-helices, connected by a hydrophobic segment (Fig. 1.5) [Jockel et al., 1999].

The smallest γ subunit (Fig. 1.5) contains a series of histidine residues near the C-terminus. This motif provides a binding-site for Zn^{2+}, which is firmly bound to the enzyme [Schmid et al., 2002].

The catalytic cycle is initiated by the transfer of the carboxyl group from oxaloacetate to the prosthetic biotin group, producing a carboxybiotin intermediate. Then this intermediate is transferred to the decarboxylase site in the β subunit and decarboxylation of the carboxybiotin with H^+ is coupled to Na^+ translocation across the membrane:

$$\textbf{E-biotin-COO}^{-} + \textbf{nNa}^{+}_{\textbf{in}} + \textbf{H}^{+}_{\textbf{out}} \leftrightarrow \textbf{E-biotin} + \textbf{CO}_2 + \textbf{nNa}^{+}_{\textbf{out}}$$

Note that H^+ consumed from the external medium in the course of the reaction, crosses the membrane to bind to biotin instead of released CO_2. Eventually, biotin transfers this H^+ to pyruvate, so that H^+ does not accumulate within the cytoplasm.

Therefore, the only bioenenergetic effect of this reaction is the transfer of Na^+ ions across the membrane. The generated CO_2 leaves the cell through passive diffusion [reviewed in Dimroth, et al., 2001].

The above reaction is reversible, as was demonstrated in proteoliposomes containing purified decarboxylase [Dimroth & Thomer, 1993]. When they were loaded with high concentrations of NaCl and rapidly diluted in buffer containing a low concentration of $^{22}NaCl$, some uptake of $^{22}Na^+$ ions against the concentration gradient occurred. The process required the presence of dissolved CO_2 (bicarbonate) and could be completely inhibited by the biotin-binding inhibitor avidin. Therefore, $^{22}Na^+$ uptake involved the exchange of internal and external sodium in accordance with the above reaction. Hence, the outwardly directed efflux of non-radiactive Na^+ down its concentration gradient could drive carboxylation of biotin and the resulting carboxybiotin, upon its decarboxylation, could power the uptake of $^{22}Na^+$ against its concentration gradient [Dimroth & Thomer, 1993].

The reversible reaction also affects the overall stoichiometry of Na^+ transfer. At low smf, two Na^+ ions are pumped for each decarboxylation event, producing a progressively larger smf on the membrane. Once a high smf is obtained, the enzyme still exports two Na^+ per decarboxylated oxaloacetate, but this is compensated by the import of Na^+ that drives the coupled reaction of biotin carboxylation. Since the enzyme at equilibrium catalyses two opposing Na^+ fluxes, the net Na^+ transported per single decarboxylation is much lower than two. In proteoliposomes, even at steady state when there was no net Na^+ flux, decarboxylation still occurred suggesting a balance between Na^+ pumping on both sides of the membrane [Dimroth & Thomer, 1993].

Fig. 1.6. Coupling of decarboxylation to Na^+ transfer (after Di Berardino & Dimroth, 1996). A model describing the mechanism of coupling decarboxylation to Na^+ as suggested by P. Dimroth [Di Berardino & Dimroth, 1996]. In the first step of the cycle (E→A), when the biotin group gets carboxylated by the carboxyl transfer from oxaloacetate, the negatively charged carboxybiotin moves into the binding pocket in the β-subunit, where it becomes a part of the HA Na^+ binding site. Na^+ then binds. In the second step (A→B), after Na^+ has bound to the HA site, the protein assumes a closed conformation, where the Na^+ ion can be delivered to D203. In the third step (B→C), the enzyme again assumes an open conformation, the carboxybiotin gets released from its binding pocket and Na^+ in the LA binding site is exchanged with H^+. The second Na^+ ion then binds to the HA site. In the fourth step (C→D), the protein resumes a closed conformation and the H^+ in the LA binding site is exchanged with the second Na^+ ion bound to the HA site. In the fifth step (D→E), the H^+, which is now near the carboxybiotin, substitutes CO_2, which then is released. The decarboxylated, protonated biotin then moves out its binding pocket, the protein resumes an open conformation and the whole cycle can be repeated [Di Berardino & Dimroth, 1996]. See the text for details.

Fig. 1.6

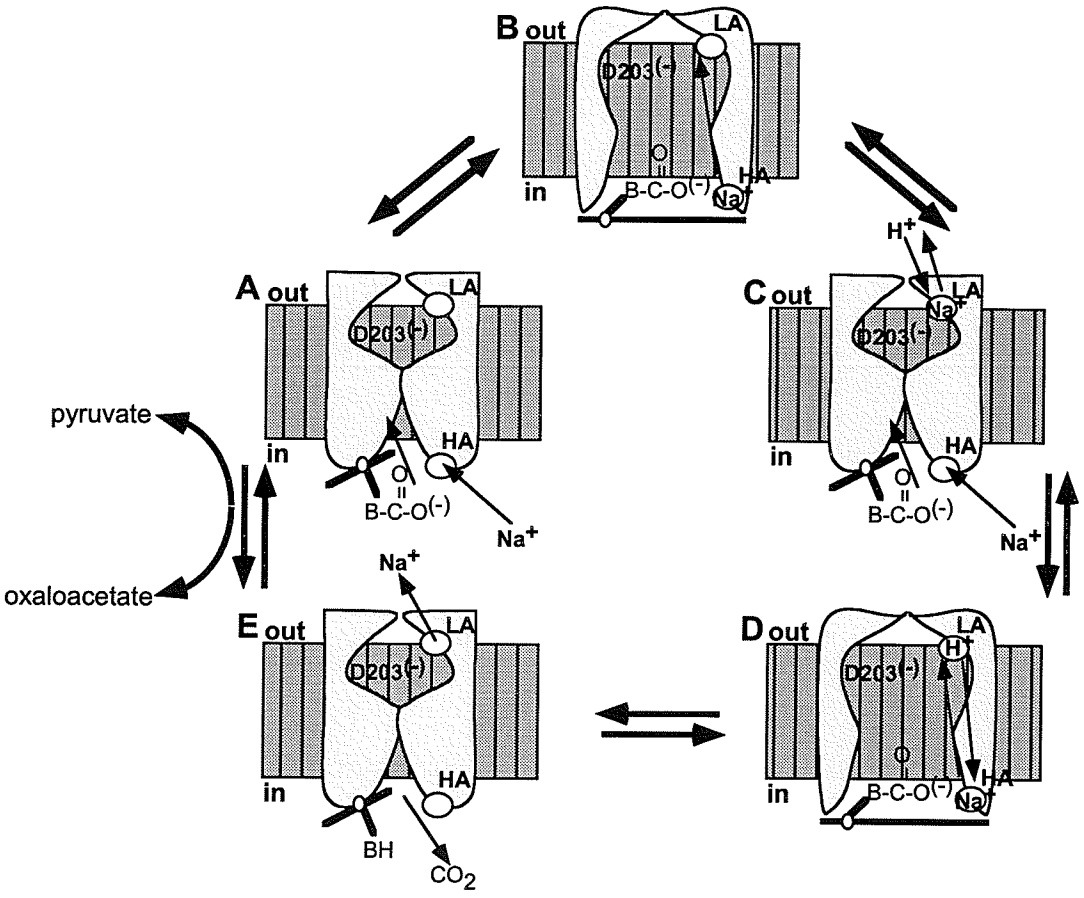
B out
LA
D203(-)
O
B-C-O(-)
HA
Na+
in
A out
LA
D203(-)
HA
O
B-C-O(-)
Na+
in
pyruvate
oxaloacetate
C out
H+
LA
Na+
D203(-)
HA
O
B-C-O(-)
Na+
in
E out
Na+
LA
D203(-)
HA
BH
CO2
in
D out
LA
H+
D203(-)
O
B-C-O(-)
HA
Na+
in

Fig. 1.7. Na^+-dependent citrate fermentation pathway (after Häse, 2001). Citrate is pumped into the cell in symport with Na^+ via CitS. This is further broken down into acetate and oxaloacetate via citrate lyase (CitDEF). The oxaloacetate is then decarboxylated into pyruvate by oxaloacetate decarboxylase (OadGAB), which also transports Na^+, restoring the Na^+ gradient. Pyruvate is then broken down to formate and acetyl-CoA, which is converted into acetylphosphate by phosphotransacetylase (Pta). Acetylphosphate is then dephosphorylated by acetate kinase (AckA) yielding ATP, resulting in the conservation of energy. The fermentation end-products are outlined [Bott, 1997].

Fig. 1.7

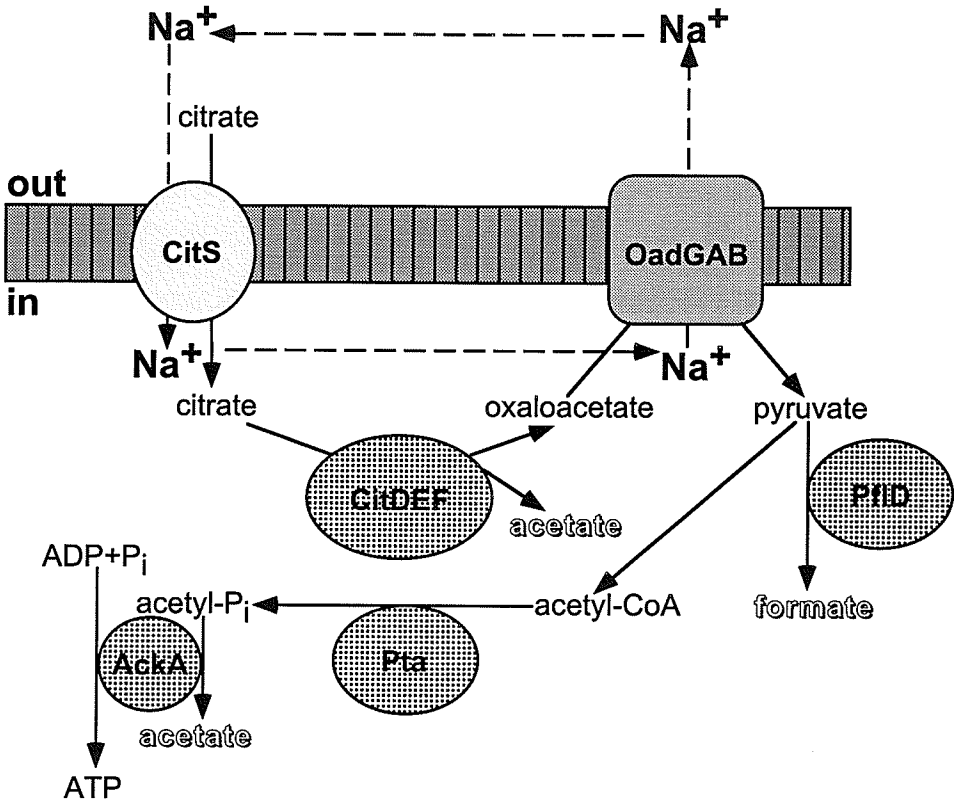
Na+
Na+
citrate
out
CitS
OadGAB
in
Na+
Na+
citrate
oxaloacetate
pyruvate
CitDEF
acetate
PflD
ADP+Pi
acetyl-Pi
acetyl-CoA
formate
AckA
Pta
acetate
ATP

A model describing the mechanism of coupling decarboxylation to Na^+ transfer has been suggested by P. Dimroth [Di Berardino & Dimroth, 1996]. It is based on experiments performed on various mutant forms of the enzyme in proteoliposomes. According to the model, there are two different binding sites for Na^+. The first binding site has a high affinity for Na^+ (HA in Fig. 1.6) and is located near the carboxybiotin residue bound to the β subunit in the second step of the catalytic cycle. The second binding site has a low affinity for Na^+ (LA in Fig. 1.6) and is located near the conserved aspartate residue (D203) that is a part of the LA site. The HA site is accessible from the cytoplasm and must be occupied with Na^+ if decarboxylation is to occur. The LA site at D203 is accessible from the periplasm and may be occupied with Na^+, H^+ or could remain empty. It is assumed that only one of the two Na^+ binding sites can be occupied by Na^+ at any time. Fig. 1.6 shows the major steps of the proposed process of coupled ion transfer based on P. Dimroth's model [Di Berardino & Dimroth, 1996].

Genomic sequence comparison reveals that Na^+-translocating decarboxylases are restricted to mostly anaerobic bacteria [Dimroth & Schink, 1998; Häse et al., 2001]. However, in *V. cholerae* there exist two gene clusters representing oxaloacetate decarboxylases, called *oad-1* and *oad-2* [Dahinden et al., 2005]. In constrast to the *oad-2* gene cluster, which forms a part of a citrate fermentation operon that includes a citrate transporter, citrate lyase and a two-component regulatory system, the *oad-1* cluster is not flanked by genes involved in any fermentative pathway and is therefore predicted not to be involved in metabolic catalysis [Dahinden, 2005]. In the citrate fermentative pathway, which has been studied extensively in *Klebsiella pneumoniae* (reviewed in [Dimroth, 1994]), citrate is first transported into the cell at the expense of the pre-established smf and split to form acetate and oxaloacetate by citrate lyase. Then, decarboxylation of

oxaloacetate by the Na^+-translocating decarboxylase restores the Na^+ gradient and yields pyruvate, which is further metabolized to form formate, acetyl-CoA and acetyl phosphate intermediates. Finally, energy is regained by the ATP-generating conversion of acetyl phosphate to acetate catalyzed by acetate kinase [Bott, 1997] (Fig. 1.7).

When *V. cholerae* was cultivated anaerobically on citrate and the oxaloacetate decarboxylase was purified, N-terminal sequencing of the α subunit and analysis of protein bands isolated from SDS-PAGE revealed that expression occurred solely from the *oad-2* set of genes. Purification of the *oad-2* product yielded a highly active and stable enzyme. The enzyme was inactive in the absence of Na^+ and its activity rose with increasing Na^+ concentrations. It was also shown that two Na^+ ions bound concurrently suggesting that two Na^+ are transported in every decarboxylation event by the *V. cholerae* enzyme. The enzyme was also inhibited by oxalate as well as oxomalonate [Dahinden, Reconstitution of the *oad-2* gene product into proteoliposomes revealed it to function as a Na^+ pump [Dahinden, 2005].

1.4.1.3. F_1F_0-ATPase: Na^+ or H^+ Translocating?

Given the fact that *V. cholerae* has smf generating enzymes present in the cytoplasmic membrane, one might expect that oxidative phosphorylation in this organism would be energized by smf rather than pmf. Indeed, in organisms such as *Propionigenum modestum* [Laubinger & Dimroth, 1987] and *Acetobacterium woodii* [Heise et al., 1992], F_1F_0-type ATPases transport Na^+ ions. Furthermore, Na^+-coupled ATP synthesis driven by respiration or an artificial sodium ion gradient has been reported in pathogenic *Vibrio parahaemolyticus*, an organism that is similar to *V. cholerae* [Sakai et al., 1989; Sakai-Tomita et al., 1991]. However, this activity was evident only in a mutant devoid of H^+-translocating ATPase [Sakai-Tomita et al., 1991]. It has also been suggested that the

free-living marine bacterium *V. alginolyticus* is able to use smf to energize ATP synthesis [Dibrov et al., 1986b; Dibrov et al., 1988]. Yet, following studies exploiting the reconstituted *V. alginolyticus* F_1F_0 enzyme, have demonstrated that it translocates H^+ ions rather than Na^+ [Dmitriev et al., 1991].

The *V. cholerae* genome contains the *atp* operon encoding the F_1F_0-ATPase very similar to the enzyme from *V. alginolyticus.* This indicated that both ATPases are most probably H^+-motive. However, at the moment there were no experimental data on *V. cholerae* F_1F_0 ATPase to support or disprove this conjecture. Also, keeping in mind the situation with *V. parahaemolyticus*, one could argue for the existence of an alternative Na^+-motive ATPase, perhaps of different architecture, whose activity could be masked by the presence of active F_1F_0-type enzyme.

Indeed, there are at least three classes of ATP-dependent primary Na^+ pumps that generate sodium gradients at the expense of ATP hydrolysis, namely the ATP-binding cassette (ABC)-type transporters, Na^+-transporting F_1F_0-ATPases and archaeal/vacuolar (A/V-type) ATP synthases operating in the opposite direction. Recently, a P-type Na^+-transporting ATPase has been isolated from the facultative alkalophilic anaerobe, *Exioguobacterium aurantiacum* [Ueno et al., 2000].

In addition to the *atp* operon encoding the F_1F_0-ATPase (analysed in detail in Section 4.5), examination of the *V. cholerae* genome reveals three open reading frames (VC1033, VC1437, and VC2215), which encode P-type cation transport ATPases (E1-E2 ATPases [Silver, 1996; Rensing et al., 1999]). However, since the sequence of VC1033 is similar to the *E. coli* Zn^{2+} transporter ZntA [Rensing et al., 1997], and VC1437 and VC2215 to the *E. coli* Cu^+ transporter CopA [Rensing et al., 2000; Fan & Rosen, 2002], it

Fig. 1.8. The role of Na^+/H^+ antiporters in bacterial bioenenergetics. In *Vibrio* species, the circulation of Na^+ and H^+ ions is maintained across the cytoplasmic membrane. Na^+/H^+ antiporters couple these ion circulations, playing a central role in H^+ and Na^+ homeostasis [Padan & Schuldiner, 1994; Padan & Schuldiner, 1996; Padan & Krulwich, 2000; Padan et al., 2001]. There may be as many as seven Na^+/H^+ antiporters in *V. cholerae* [Häse, 2001]. Na^+ porters and H^+ porters consume smf and pmf to perform useful work. See the text for details.

Fig. 1.8

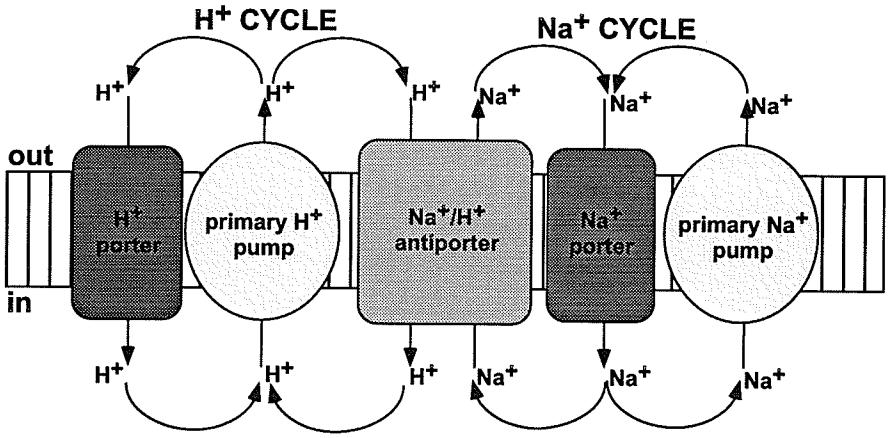
H+ CYCLE
Na+ CYCLE
H+
H+
H+
Na+
Na+
Na+
out
in
H+ porter
primary H+ pump
Na+/H+ antiporter
Na+ porter
primary Na+ pump
H+
H+
H+
Na+
Na+
Na+

is probable that *in vivo* they use the energy of ATP hydrolysis to transport divalent cations.

An inducible, two-gene ABC-type system extruding Na^+ ions, NatAB, has been reported in *Bacillus subtilis* [Cheng et al., 1997]. This transport system is proposed to expel toxic Na^+ from the cytoplasm when the barrier function of the cytoplasmic membrane is affected by uncouplers or alcohols [Cheng et al., 1997]. Multiple genes encoding putative ABC-type transporters could be found in the *V. cholerae* genome (for example, ORF VC1486), but neither of them are similar to the bacillar *natAB* genes [Häse et al, 2001]. These putative traffic ATPases of *V. cholerae* still require characterization.

1.4.2. Secondary Sodium Pumps in *V. cholerae*

In addition to a sodium cycle, a proton cycle is operative in the same membrane of *V. cholerae*, the major constituents of which are the pmf respiratory pumps [Häse et al., 2001; Häse & Barquera, 2001] and the H^+-F_1F_0 ATPase, (see Section 4.5). The chemiosmotic linkage between the two ion cycles is mediated by Na^+/H^+ antiporters (Fig. 1.8).

1.4.2.1. NhaA and NhaB Na^+/H^+ Antiporters

Two specific $Na^+(Li^+)/H^+$ antiporters, NhaA (for reviews see Padan & Schuldiner, 1994; Padan et. al., 2001; Padan et al., 2004; Padan et al., 2005 and references therein) and NhaB [Pinner et al., 1992; Pinner et al., 1994; Schuldiner & Padan, 1994; Pinner et al., 1995], are regarded as "standard" ones for enterobacteria. They were extensively studied in *E. coli* (see [Padan & Krulwich, 2000; Padan et al., 2001] for a comprehensive review). This antiporter pair has been documented also in *V. cholerae* (see below).

The most characterized bacterial Na^+/H^+ antiporter to date is NhaA from *E. coli*. Deletion of the *nhaA* gene in this organism impairs cell growth at alkaline pH in the presence of NaCl or LiCl [Padan et al., 1989]. In contrast, the Δ*nhaB* strain is able to grow in the presence of Na^+ or Li^+ ions at elevated pH [Pinner et al., 1992; Pinner et al., 1994; Pinner et al., 1995] suggesting that Ec-NhaA alone is vital for coping with high salt and pH stress [Padan et al., 1989]. The double mutant, Δ*nhaA*Δ*nhaB* grows extremely poorly in Na^+-containing medium [Schuldiner & Padan, 1994]. Still, Ec-NhaB confers limited Na^+ resistance in the cell and becomes important when Ec-NhaA is not expressed [Pinner et al., 1993]. Both antiporters are electrogenic, the stoichiometry of exchange for Ec-NhaA being two H^+ per each Na^+ [Taglicht et al., 1993] and Ec-NhaB exchanging three H^+ per two Na^+ [Pinner et al., 1994]. The activity of Ec-NhaB, but not Ec-NhaA is inhibited by amiloride derivatives [Pinner et al., 1995].

When Ec-NhaA was analysed in inside-out membrane vesicles isolated from the Δ*nhaA*Δ*nhaB* strain of *E. coli* EP432, it revealed a pH-dependent profile of activity as opposed to the pH-independent Ec-NhaB [Pinner et al., 1992]. The V_{max} increased more than 10^3-fold over the pH range 7.0 to 8.0, above which it plateaued [Gerchman, et al., 1993; Rimon et al., 1995; Olami et al., 1997]. The apparent K_m for Na^+ was affected by the external pH, being 3.0 mM at pH 7.5 versus 0.6 mM at pH 8.5 [Gerchman, et al., 1993].

A series of studies in E. Padan's laboratory revealed, the important role of H225 in the pH control of Ec-NhaA. Substitutions H225S and H225C did not affect the pH profile of activity, whereas H225R shifted it toward acidic pH and H225D toward alkaline pH. The authors concluded that the capacity of a residue in position 225 to form

hydrogen bonds might be important for pH regulation of the antiporter [Gerchman, et al., 1993; Rimon et al., 1995]. Of note, the motif containing H225 is conserved among different NhaA antiporters from different *Vibrio* species. Most interestingly, a similar sequence is also present in NhaD-type antiporters from *V. parahaemolyticus*, *V. vulnificus* and *V. cholerae* [Nozaki et al., 1998; Dzioba et al., 2002]. From the similarities of their pH profiles of activity, it has been hypothesized that H249 of Vp-NhaD is a functional analog of H225 of Ec-NhaA [Nozaki et al., 1998]. In an another study, the point mutation G338S in Ec-NhaA, resulted in an antiporter that was active throughout the pH range [Rimon et al., 1998].

It is known that *E. coli* NhaA has a dual mode of regulation of transcription, involving two separate promoters [Dover & Padan, 2001]. During exponential growth, *nhaA* expression is positively regulated by NhaR (a regulator belonging to the LysR family) [Rahav-Manor et al., 1992], is induced by Na^+ and is transcribed by σ^{70} via the specific Na^+-induced promoter, P_1 [Dover & Padan, 2001]. In stationary phase, σ^s transcribes *nhaA* through the P_2 promoter in a manner independent of NhaR and the presence of Na^+ [Dover & Padan, 2001].

Homologues of Ec-NhaA and Ec-NhaB exist in other bacteria. For instance, Hp-NhaA, from *Helicobacteri pylori*, shows significant homology to Ec-NhaA, aside from the presence of an intergenic sequence of approximately 40 amino acids. Interestingly, the pH profile of activity is markedly different in Hp-NhaA compared to Ec-NhaA, showing maximal activity throughout the pH range 6.5 to 8.5 [Inoue et al., 1999]. Another Ec-NhaA homologue from *Vibrio parahaemolyticus*, showing 59% identity and 87% similarity, demonstrates the same pH-dependent pattern of activity of NhaA from *E*

coli, displaying increased activity from pH 7.0 to 8.5 [Kuroda, et al., 1994]. However, in constrast to Ec-NhaA, Vp-NhaA is inhibited by amiloride [Kuroda et al., 1997]. A homologue, showing 58% identity to Ec-NhaA, has also been isolated from *Vibrio alginolyticus* [Nakamura et al., 1994]. It confers NaCl resistance up to 500 mM in an antiporterless strain of *E. coli* and it functions as an electrogenic antiporter. Moreover, three conserved aspartate residues in membrane-spanning segments in the same antiporter play a role in the transport activity of the antiporter [Nakamura et al., 1995].

A gene showing 72% identity to Ec-NhaB has been isolated from *V. parahaemolyticus*. It confers Na^+ resistance up to 200 mM and LiCl resistance up to 10 mM in an antiporterless strain of *E. coli*. Moreover, $Na^+(Li^+)/H^+$ antiport activity was detected in inside-out membrane vesicles isolated from the same transformants [Nozaki et al., 1996]. An NhaB homologue from *P. aeruginosa*, showing 60% identity and 90% similarity to NhaB from *E. coli* and *V. parahaemolyticus* has been isolated. In contrast to Ec-NhaB, this antiporter shows pH-dependent activity with a broad optimum range between pH 7.5 and 8.5 [Kuroda et al., 2004]. Like Ec-NhaB, this antiporter was inhibited by amiloride. In *V. alginolyticus* an Ec-NhaB homologue showing 58% identity has also been cloned [Nakamura et al., 1996]. It confers resistance up to 200 mM NaCl in an antiporterless strain of *E. coli*. It also shows a pH-dependence of activity, being active at pH 7.5 to 8.5 but not at pH 6.5 [Nakamura et al., 2001], in contrast to Ec-NhaB, which shows activity at pH 6.5 [Padan & Schuldiner, 1996].

Simultaneous to us in an independent study, *nhaA* and *nhaB* were cloned out and functional NhaA and NhaB homologues were documented in *V. cholerae* [Vimont & Berche, 2000; Herz et al., 2003] as well. In addition, a homolog of the *E. coli* NhaR has

previously been described [Williams et al., 1998], indicating similar regulation of NhaA activity in both *E. coli* and *V. cholerae*.

Vc-NhaA and Vc-NhaB conferred salt resistance in the Δ*nhaA*Δ*nhaB* strain of *E. coli* EP432 and the activity of Vc-NhaA in inside-out sub-bacterial vesicles isolated from the same transformants was similar to that of Ec-NhaA. However, in the same study, the authors failed to demonstrate the activity of Vc-NhaB in vesicles. Reasons for that failure are not clear at the moment, but Vc-NhaB was clearly physiologically active in intact cells of EP432 [Herz et al., 2003].

To ascertain the physiological significance of these antiporters in *V. cholerae*, a series of mutants inactivated by insertion was generated. Inactivation of these genes had almost no effect on the growth of *V. cholerae* in high Na^+ [Herz et al., 2003]. In the presence of LiCl, however, the growth of mutants lacking *nhaA* was inhibited [Herz et al., 2003]. As discussed, NQR functions to specifically export Na^+, but not Li^+ ions [Steuber et al, 1997; Zhou et al, 1999; Barquera et al., 2002a] from the cytoplasm. Therefore in a Na^+/H^+ antiporter mutant background, this pump could compensate for the loss of Na^+/H^+ antiport activity but not Li^+/H^+ antiport activity, resulting in a Na^+-insensitive, but Li^+-sensitive phenotype. Indeed, upon the addition of HQNO, a specific inhibitor of NQR, a functional NhaA antiporter became paramount for the survival of *V. cholerae* in high salt at alkaline pH [Herz et al., 2003]. Therefore, Na^+ resistance in *V. cholerae* appears to rely upon NQR as well as Na^+/H^+ antiport activity. It is also apparent that NhaA is important in maintaining Na^+ and H^+ homeostasis at alkaline pH [Vimont & Berche, 2000], and this is more prevalent in the absence of NQR activity [Herz et al., 2003].

A series of NhaA and NhaB inactivation mutants in *V. parahaemolyticus* has also been generated. In that study it was found that Δ*nhaA* and Δ*nhaA*Δ*nhaB* strains were both sensitive to growth in LiCl compared to the wild-type [Kuroda et al., 2005]. As in *V. cholerae*, the results obtained in that study established the role of Na^+/H^+ antiporters, in particular NhaA, in LiCl resistance and resistance to high concentrations of NaCl. Based on activity in inside-out sub-bacterial membrane vesicles, it was surmised that the expression of *nhaA* and *nhaB* was somehow controlled by external pH. For instance, vesicles isolated from cells grown at pH 7.0, exhibited lower NhaA activity and increased NhaB activity. However, when vesicles were isolated from cells cultured at pH 8.5, NhaA activity was increased two-fold. Basing on their results, the authors concluded that Na^+/H^+ antiporters contribute to ion homeostasis in this organism [Kuroda et al., 2005].

Summing up, Vc-NhaA and its physiological role in *V. cholerae* appear to be very similar to what is documented in other organisms, whereas the situation with NhaB still remains somewhat unclear. However, it most probably functions similarly to that characterized in other bacteria.

Very recently, the 3-D crystal structure of Ec-NhaA has been obtained [Hunte et al., 2005], but this will be discussed in detail below in connection to our structural studies of Vc-NhaD (see Section 4.2).

1.4.2.2. NhaD Na^+/H^+ Antiporter

Another Na^+/H^+ antiporter in *V. cholerae* is NhaD [Ostroumov et al., 2002] (see Section 4.1). Interestingly, this type of antiporter is present only in the pathogenic vibrios including *V. parahaemolyticus* [Nozaki et al., 1998] and *V. vulnificus*, but not in nonpathogenic, free-living *V. alginolyticus*. NhaD homologues are also found in the genomes of the obligate intracellular parasites *C. trachomatis* and *C. pneumoniae* as their

sole Na^+/H^+ antiporter [Dibrov et al., 2005]. Such distribution indicates that NhaD-type antiporters might be associated with the pathogenicity of these organisms. However, NhaD homologues are also found in the genomes of nitrogen-fixing symbionts, magnetotactic cocci, photosynthetic bacteria, as well as in higher plants. Analysis of the genome sequences of the thermophilic bacterium *Rhodothermus marinus*, reveals the occurrence of NhaD homologues in operons encoding NADH:menaquinone oxidoreductases (Nqo), an enzyme present in the respiratory chain of this organism [Melo et al., 2005]. Genomic analysis also shows the presence of NhaD homologues in operons that also contain genes encoding sulfate permeases of the SulP family in different species [Felce & Saier, 2004]. Functionally characterized carriers of SulP group include anion/H^+ symporters and anion/anion antiporters [Felce & Saier, 2004].

To date, four NhaD-type Na^+/H^+ antiporters have been cloned, functionally expressed and at least partially characterized, namely NhaD from *V. cholerae* (see Sections 4.1 and 4.2), NhaD from *V. parahaemolyticus* [Nozaki et al., 1998], NhaD from the soda lake haloalkaliphile *Alkalimonas amylolytica* [Liu et al., 2005], as well as an NhaD homologue from the higher plant *Populus euphratica* [Ottow et al., 2005].

All four antiporters complemented an antiporterless strain of *E. coli* [Nozaki et al., 1998; Ottow et al., 2005; Liu et al., 2005] (see Section 4.1). Vc-NhaD restored the ability of the Δ*nhaA*Δ*nhaB* strain of *E. coli* EP432 to grow in the presence of 0.1 M LiCl or 0.3 M NaCl up to pH 7.6 (see Section 4.1, Fig. 4.2) whereas NhaD from *P. euphratica* complemented only up to pH 5.5 [Ottow et al., 2005]. The activity of Vc-NhaD in inside-out sub-bacterial membrane vesicles appeared to be pH-dependent with a sharp optimum at pH ~7.75. No activity was registered at pH 6.75 or pH 8.75 (see Section 4.1, Fig. 4.4). NhaD from *V. parahaemolyticus* enabled an antiporterless strain of *E. coli* to grow in 10

mM LiCl or 0.2 M NaCl under conditions normally lethal. The activity of this antiporter was also pH-dependent, showing maximal activity at pH 8.5 to 9.0 and no activity at pH 7.5 and below [Nozaki et al., 2005]. In *A. amylolytica*, NhaD activity could not be observed at pH below 8.5, having an optimum at pH 9.5 [Lui et al., 2005].

In *V. cholerae* and *V. parahaemolyticus*, NhaD inactivation mutants have been generated [Herz et al., 2003; Kuroda et al., 2005]. It was noted that NhaD in *V. cholerae* did not contribute much to the overall Na^+ and Li^+ resistance under the conditions tested (high sodium load, alkaline pH). In fact in the same study, the Δ*nhaD* strain after 12 hours of overnight growth lysed for unknown reasons, whereas the wild-type nor any other inactivation mutant did not [Herz et al., 2003]. However, in *V. parahaemolyticus*, NhaD became important at neutral pH in the presence of high LiCl concentrations, when the activity of NhaA and NhaB was absent [Kuroda et al., 2005].

The physiological role of NhaD in *V. cholerae* is still being investigated in our laboratory and will be discussed in more detail below (see Results & Discussion).

1.4.2.3. Mrp Na^+/H^+ Antiporter

Mrp Na^+/H^+ antiporters are encoded in operons consisting typically of six to seven subunits and form apart of the cation:proton antiporter-3 (CPA-3) family [http://www.tcdb.org/tcdb/family2.php?tc=2.A.63/]. The Mrp antiporter was first discovered in *Bacillus halodurans* C-125 [Hamamoto et al., 1994] and homologues have now been characterized in *B. subtilis* and *Bacillus pseudofirmus* OF4 [Ito et al., 1999; Kitada et al., 2000; Krulwich et al., 2001]. In these studies, it was noted that this antiporter contributed to the overall pH homeostasis and alkali resistance in *Bacillus* species [Kitada et al., 2000; Krulwich et al., 2001]. Homologues have also been

Fig. 1.9. Gene arrangement of *mrp* operons (after Swartz et al., 2005). Group 1 operons consist of a cluster of seven genes, *mrpA-G*. *mrpA* contains two *mrpB* domains. Group 2 operons consist of a cluster of six genes, *mrpA'C-G*. *mrpA'* has two *mrpB* domains. A representative member of each group is noted above each gene cluster (Swartz et al., 2005)

Fig. 1.9

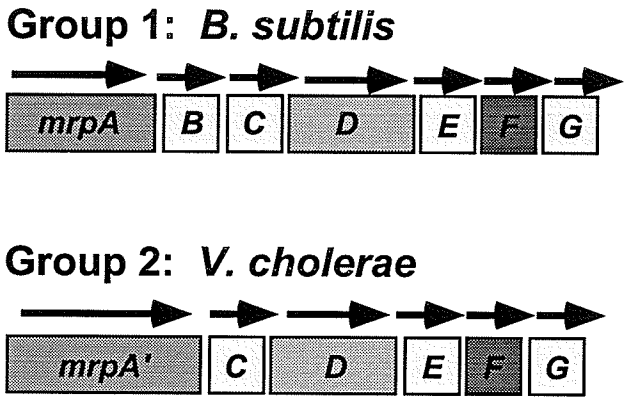

characterized in *S. meliloti* [Putnoky et al., 1998], *S. aureus* [Tsuchiya et al., 1998], *P. aeruginosa* [Kosono et al., 2005] and cyanobacterium *Anabaena* [Blanco-Rivero et al., 2005].

Apart from their role in Na^+-dependent pH homeostasis, Mrp antiporters seem to be involved in several different tasks. For instance, the *S. meliloti* enzyme appears to function as a K^+/H^+ antiporter and is important in symbiotic nitrogen fixation [Putnoky et al, 1998]. In *B. halodurans* C-125 and *B. pseudofirmus* OF-4 it functions as a Na^+/H^+ antiporter whereas in *B. subtilis*, it acts as a $Na^+(K^+)/H^+$ antiporter as well as exports cholate [Ito et al., 1999; Ito et al., 2000]. Moreover, in the same organism, a mutation in MrpA (or ShaA) renders it incapable of sporulation [Kosono et al., 2000]. Deletion of MrpA in cyanobacterium *Anabaena* results in severe sensitivity to Na^+ and alkaline pH. Based on *in vivo* expression assays, induction of *mrpA* in this organism occurs in the presence of high concentrations of Na^+ and at alkaline pH, as well as when the inorganic carbon (C_i) supply becomes limited [Blanco-Rivera et al., 2005]. In *P. aeruginosa*, deletion of MrpA (also called ShaA) results in Na^+ sensitivity and decreased Na^+ efflux. This mutant also exhibits attenuated virulence in mice with respect to systemic, pulmonary and urinary tract infections and in general, shows diminished colonization in infected organs [Kosono et al., 2005]. In *S. aureus*, Mrp functions as a Na^+/H^+ antiporter [Hiramatsu et al., 1998].

The two most common arrangements of genes within the *mrp* operon are depicted in Fig. 1.9. Note that these arrangements can vary amongst different organisms. Group 1 and Group 2 *mrp* operons differ with respect to their *mrpA* and *mrpB* genes. In Group 1, *mrpA* and *mrpB* are encoded by separate ORFs. *mrpA* also contains a *mrpB* domain (Fig. 1.9). Group 2 on the other hand, contains no *mrpB* subunits, but instead *mrpA* contains

two *mrpB* domains (Fig. 1.9). In other words, *mrpA* and *mrpB* are encoded by one ORF as opposed to two [Swartz et al., 2005].

Interestingly, Mrp subunits A, C and D show sequence similarity to NADH:quinone oxidoreductase ion-translocating complexes. For instance, MrpA of *B. halodurans* C-125 shows similarities to NuoL of *E. coli* Complex I [Swartz et al., 2005]. Also, the MrpF subunit of *B. subtilis*, which is responsible for cholate efflux [Ito et al., 1999; Ito et al., 2000], shows sequence similarity to eukaryotic Na^+-coupled bile acid transporters [Ito et al., 1999]. Analysis of the sequence of MrpG reveals that it contains motifs found in Na^+/solute symporters [Swartz et al., 2005].

According to studies carried out in *B. subtilis*, all Mrp subunits are required for Na^+/H^+ antiport, but subunit A appears to be a most important one because a single mutation in it prevents antiport [Ito et al., 2000].

The genome of *V. cholerae* contains a typical Group 2 *mrp* operon (VCA0152, VCA0153, VCA0154, VCA0155, VCA0156, VCA0157) on its small chromosome. It has recently been cloned and is being characterized in our laboratory in a collaborative project with Dr. Claudia Häse. Preliminary results show that this antiporter is functional when expressed in the Δ*nhaA*Δ*nhaB* strain of *E. coli* EP432 allowing growth of this Na^+-sensitive strain in media containing up to 400 mM NaCl (Winogrodzki, O. and Winogrodzki, J., unpublished results). Like the Mrp protein in *B. subtilis* [Ito et al., 1999; Ito et al., 2000], this antiporter also contributes to cholate resistance in *E. coli*. Recently a Δ*mrp* strain of *V. cholerae* has been produced and studies are currently underway in our laboratory to ascertain the physiological role Mrp has in this bacterium.

1.4.2.4. NhaC, NhaP and MleN Na^+/H^+ Antiporters

In addition to chemiosmotically active NhaA, NhaB and NhaD [Vimont & Berche, 2000; Herz et al., 2003; also see Sections 4.1 and 4.2], as well as the multisubunit antiporter Mrp, the genome of *V. cholerae* contains three other distinct open reading frames annotated as putative structural genes for Na^+/H^+ antiporters [Häse et al., 2001]. These are VC2037, VCA0193 and VC0389 [Häse et al., 2001]. VC2037 and VCA0193 encode proteins similar to the MleN (previously YqkI) [Wei et al., 2000] and NhaC [Pragai et al., 2001] antiporters of *B. subtilus*. As mentioned above, the latter protein is known to be involved in regulating alkaline phosphatase production [Pragai et al., 2001] and the other functions as a simultaneous Na^+/H^+ and malate/lactate antiporter [Wei et al., 2000]. Also, two other NhaC paralogues VCA0213 and VC1131 are present in the *V. cholerae* genome. Finally, putative protein VC0389 shows significant identity/similarity to the Na^+/H^+ antiporter-encoding gene, *nhaP* of the pathogen *P. aeruginosa* [Utsugi et al., 1998]. Two more paralogues of NhaP, VC0689 and VC2703, also exist in the genome of *V. cholerae*. Not much is known about NhaP-type antiporters apart from their role in Na^+ extrusion (Li^+ is a poor substrate) in *P. aeruginosa* [Utsugi et al., 1998; Kuroda et al., 2004], in transporting Ca^{2+} in cyanobacterium *Synechocystis* sp. PCC 6803 [Waditee et al., 2001] and in functioning as a $Na^+(Li^+)/H^+$ antiporter in *Methanococcus jannaschii* [Hellmer et al., 2002]. Molecular biology and biochemistry of NhaC, NhaP and MleN antiporters in *V. cholerae* remain to be investigated.

As the above discussion shows, the Na^+/H^+ antiport machinery of *V. cholerae* is complex. Elucidation of the precise biochemical/physiological roles of individual antiporters as well as their effect on overall physiology is therefore important. From this viewpoint, *V. cholerae*, with as many as seven Na^+/H^+ antiporters belonging to different

families, provides a rare opportunity to study different routes of Na^+/H^+ exchange, their interplay and their impact on metabolism in one single organism. Some of the *V. cholerae* Na^+/H^+ antiporters may regulate other pathogenicity-related aspects of cellular metabolism, for instance, phosphate metabolism [von Krüger et al., 1999] similarly to NhaC from *B. subtilis* [Pragai et al., 2001]. To sum up, studying Na^+/H^+ exchange in *V. cholerae* may help to reveal the molecular mechanism linking Na^+ homeostasis and virulence.

1.4.3 Sodium-Motive Force Consumers in *V. cholerae*

As discussed previously, once chemiosmotic energy in the form of an electrochemical Na^+ gradient is produced, it can be used to carry out various cellular functions such as energization of motility, drug efflux and solute accumulation. [Dibrov et al., 1986a; Dibrov et al., 1986b; Avetisyan et al., 1993; Dimroth et al., 1999; Kojima et al., 1999; Häse & Mekalanos, 1999; Gosink & Häse, 2000; Huda et al., 2001; Huda et al., 2003; Lebens et al., 2002]. Moreover, Na^+ influx is essential for providing substrate for Na^+/H^+ antiporters, so that pH homeostasis can be maintained and for keeping the Na^+ concentration above the K_m for other Na^+ pumps, for example NQR. Various Na^+ re-entry routes in *V. cholerae* are discussed below.

1.4.3.1. Na^+/Solute Symporters

There is not much experimental data concerning Na^+/solute symporters in *V. cholerae*. Applying the methodology derived from the Classification of Transporters (TC) [Saier, 2000; Häse et al., 2001] to the *V. cholerae* Genome Database, one can identify open reading frames encoding putative Na^+-dependent uptake systems for the

amino acids alanine, glutamate, proline and serine [Häse & Barquera, 2001; Häse et al., 2001].

Also, analysis of the genome sequence reveals that *V. cholerae* encodes a homologue to the Na^+/citrate symporter CitS [Häse, et al., 2001; Dahinden et al., 2005]. This protein, studied extensively in *Klebsiella pneumoniae* [van der Rest et al., 1992a; van der Rest et al., 1992b; van Geest & Lolkema, 1996], is the first enzyme involved in the Na^+-dependent anaerobic fermentation of citrate (Fig.1.7). The true substrate for CitS appears to be the divalent (singly protonated) form of citrate, transported in symport with two Na^+ ions. Therefore, it is actually a $H^+/2Na^+$/citrate symporter [van der Rest, et al., 1992b]. As discussed above, *V. cholerae* also contains a functional oxaloacetate decarboxylase and is able to grow anaerobically on citrate [Dahinden et al., 2005]. Therefore, citrate catabolic pathway does function in *V. cholerae*. Moreover, these genes appear to be situated in a single operon similar to that seen in *K. pneumoniae* and *Salmonella enterica* serovar Typhimurium [Wifling & Dimroth, 1989; Bott et al., 1995; Dahinden et al., 2005].

A gene (*nptA*) encoding a *V. cholerae* homologue to the type II eukaryotic Na^+/phosphate symporters, was cloned and sequenced [Lebens et al., 2003]. Although analogous systems have been described in eukaryotes, including vertebrates (for review, see [Takeda et al., 1996; Biber et al., 1996; Werner & Kinne, 2001]), this is the first to be characterized in prokaryotes [Lebens et al., 2003].

In the absence of Na^+, *V. cholerae* can import ^{32}P-labelled phosphate. This is more prevalent when the cells are starved for phosphate, suggesting the presence of an inducible, Na^+-independent uptake system. However, addition of Na^+ does result in a

further influx of phosphate, indicating the presence of an inducible Na^+-dependent system as well [Lebens et al., 2003].

When the *nptA* gene was cloned into an expression vector and placed under the control of an inducible promoter, analysis in *E. coli* showed that Vc-NptA catalysed phosphate uptake, but only in the presence of Na^+. Moreover, the addition of monensin, an ionophore that dissipates ΔpNa on the membrane, inhibited the Na^+-dependent phosphate uptake as well. Taken together, the results showed that NptA was a Na^+/P_i symporter. The K_m values for phosphate and Na^+ were estimated to be 300 μM and 75 mM respectively; the V_{max} for phosphate was approximately 8.85 pmol min^{-1} mg^{-1} of protein [Lebens et al., 2003]. As was observed in eukaryotic systems [de la Horra, et al., 2000], the activity of NptA was affected by pH, showing decreased function by about one-half at pH 6.5 compared to that at pH 9.0 [Lebens et al., 2003].

In the light of the presence in *V. cholerae* of the "standard" bacterial phosphate-uptake systems Pst and Pit (for a review on phosphate transport in prokaryotes, see van Veen, 1997, and references therein), the role of NptA in *V. cholerae* and why there is the need for an additional P_i-symporter still remains unclear and requires further clarification.

1.4.3.2. Na^+-Dependent Motility

V. cholerae is a highly motile organism by means of rotation of a single polar flagellum [Kojima et al., 1999, Gosink & Häse, 2000]. Bacterial flagella are driven by a membrane-embedded reversible rotatory motor, which can be powered by either smf [Kojima et al., 1999; Kosono et al., 2000; Gosink & Häse, 2000; Yorimutsu, 2001] or pmf (for review, see references [Blair, 1995; Macnab, 1996; DeRosier, 1998]). The proton-driven motors of *E. coli* and *S. enterica* serovar Typhimurium have been

Fig. 1.10. Na^+-driven flagellar motor (after Okabe et al., 2002). An electrochemical gradient of Na^+ ions provides the energy required for flagellar rotation. MotX and MotY co-localize to the outer membrane and they may participate in the transfer of Na^+ to PomA/PomB (Okabe et al., 2002).

Fig. 1.10

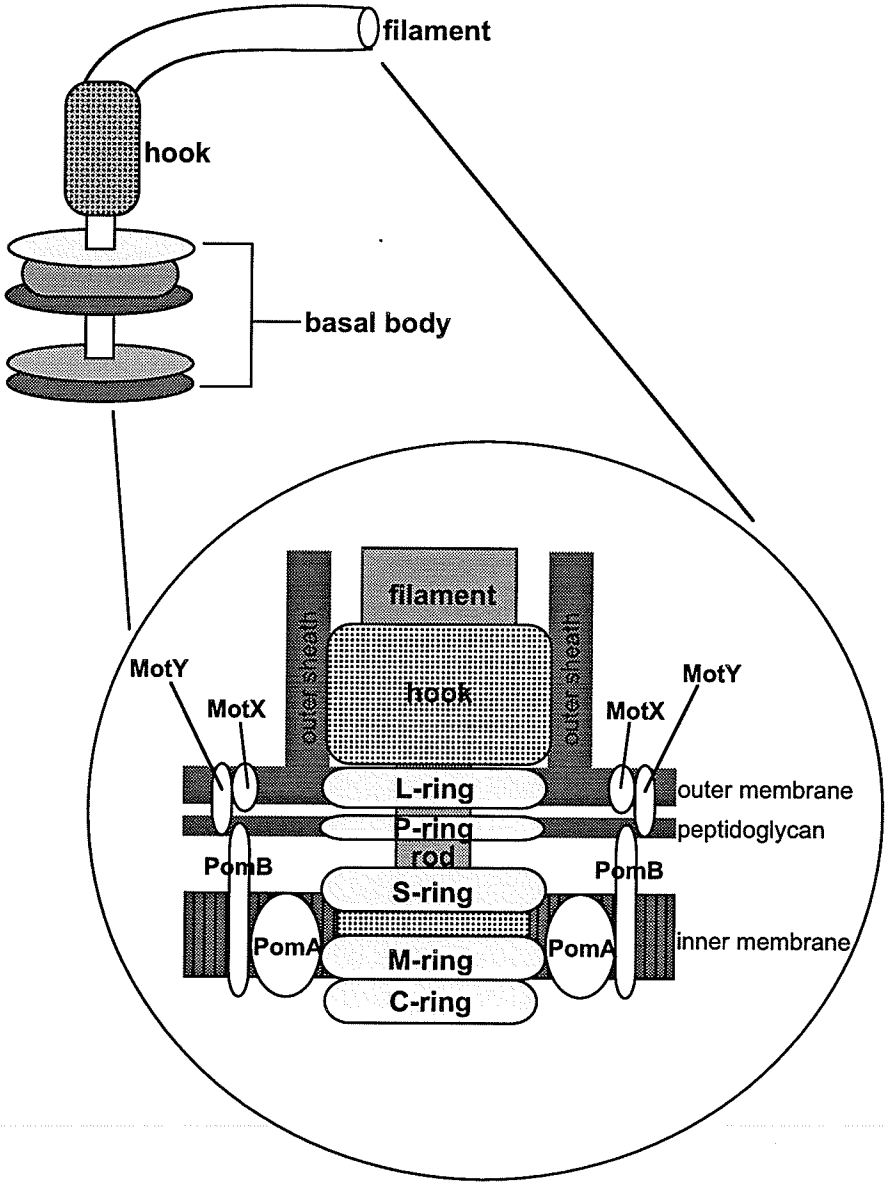
filament
hook
basal body
filament
outer sheath
outer sheath
MotY
MotX
hook
MotX
MotY
L-ring
outer membrane
P-ring
peptidoglycan
rod
PomB
PomB
S-ring
PomA
PomA
inner membrane
M-ring
C-ring

extensively studied [Blair, 1995; Macnab, 1996; DeRosier, 1998; reviewed in Blair, 2003], while the sodium-motive one is still being actively investigated at the molecular level [Kojima et al., 1999; Gosink & Häse, 2000; reviewed in Yorimitsu & Homma, 2001; recent developments are discussed in Okabe et al., 2002; Yakushi et al., 2004; Fukuoka et al., 2005; Okabe et al., 2005]. Nevertheless, experimental data from different laboratories clearly show that in marine *Vibrios* such as *V. alginolyticus* and *V. parahaemolyticus*, the polar flagella use smf rather than pmf (for review, see references [Kosono et al., 2000; Yorimitsu & Homma, 2001]). *V. cholerae* also shows Na^+-dependent motility [Kojima et al., 1999]. The swimming speed of *V. cholerae* cells is clearly limited upon the addition of the Na^+-motor inhibitor phenamil, which provides further indication that smf powers the flagellar motor in this organism [Kojima et al., 1999]. On the assumption that the structure/function of the Na^+-motive flagellum is similar amongst different vibrios, the *V. cholerae* flagellum and/or the characterized flagellar components of other *Vibrio* species are discussed below in more detail.

The bacterial flagellum consists of a long, hollow flagellar filament composed of globules of proteins called flagellin. This filament is joined to the basal body by means of a flexible hook. The structure of the basal body consists of set of rings threaded on a common rod. In Gram-negative bacteria, these rings correspond to different layers in the cell envelope (L – **l**ipopolysaccaride; P – **p**eptidoglycan; S – **s**upramembrane; M – **m**embrane). On the cytoplasmic side of the M ring, is the C-ring (C – **c**ytoplasm) or switch complex (Ueno et al., 1992; Francis et al., 1994; reviewed in Blair, 2003) (Fig. 1.10).

Fig. 1.11. Membrane location of the components of the Na^+ driven motor (after Yorimitsu & Homma, 2001). The predicted location and membrane topology of the four gene products of the Na^+-driven flagellar motor are shown [Yorimitsu & Homma, 2001; Okabe et al., 2002; Okabe et al., 2005].

Fig. 1.11

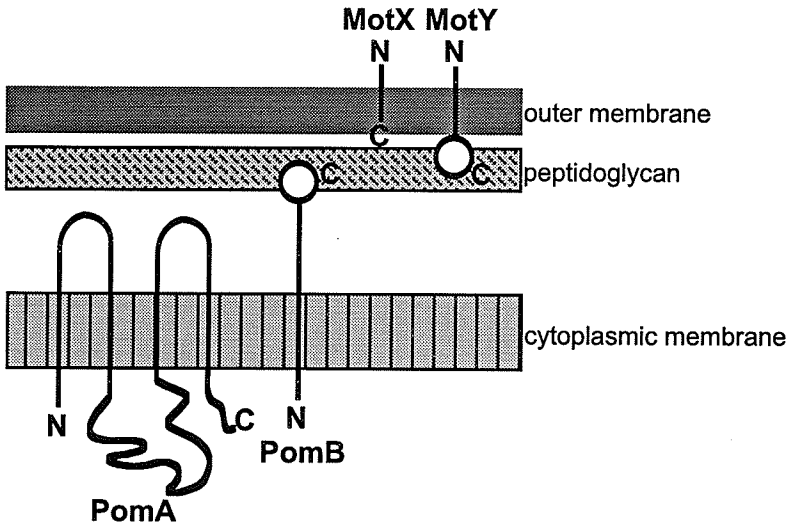
MotX MotY
N N
C
C C
outer membrane
peptidoglycan
cytoplasmic membrane
N
C N
PomB
PomA

In *E. coli* and *S. enterica* serovar Typhimurium, extensive research has shown that the proteins MotA, MotB, FliG, FliM and FliN are involved in motor rotation [Tang et al., 1996]. The FliG, FliM and FliN complex of proteins make up the rotor part of the flagellar motor [Tang et al., 1996]. This complex is essential for switching from clockwise to counterclockwise rotation as well as for flagellar assembly [Yamaguchi et al., 1986]; FliG is responsible for the generation of torque [Lloyd et al., 1996]. The stator is comprised of two integral membrane proteins, MotA (four TMS) and MotB (one TMS) [Dean et al., 1984; Stader et al., 1986; Tang et al., 1996], which form a proton-conducting channel through interaction of their transmembrane regions [Blair & Berg, 1990; Stolz & Berg, 1991]. An aspartate residue at position 32 in MotB is essential for H^+ transport; its side chain carboxyl acts as the proton binding site [Zhou et al., 1998]. The MotA/MotB complex is critical for coupling ion translocation to force generation in the motor possibly by communicating with the C-terminal domain of the FliG protein (see [Häse & Gosink, 2000; Yorimitsu & Homma, 2001], and references therein). Null mutants in *motA* and *motB* result in flagella are unable to rotate [Muramoto & Macnab, 1998].

In *V. alginolyticus* and *V. parahaemolyticus*, four rather than two integral membrane proteins, PomA, PomB, MotX and MotY, are essential for generating force in the Na^+-driven flagellar motor (Fig. 1.11). PomA (four TMS) and PomB (one TMS) show sequence similarities to MotA and MotB; they also form a membrane complex through interaction of their transmembrane segments (PomA TMSIII and PomB TMS) [Asai et al., 1997; Yakushi et al., 2004]. Like MotB, PomB is responsible for Na^+ translocation and an aspartate residue at position 24 is required for this function [Yakushi et al., 2004]. The next pair of proteins, MotX and MotY, shares no sequence homology

to MotA and MotB [McCarter, 1994a; McCarter, 1994b], however the C-terminus of MotY shows similarity to members of the OmpA family [McCarter, 1994a] (overall 34.2% identity and 55.6% similarity to Vc-OmpA according to TIGR). It is also annotated as a paralog of PomB [www.tigr.org/tdb]. MotX interacts with MotY in the outer membrane; moreover, MotX and MotY are mutually required for efficient targeting to the outer membrane [Okabe et al., 2002]. MotX also appears to interact with the PomA/PomB complex through PomB. [Okabe et al., 2002; Okabe et al., 2005] (Fig. 1.10). MotX is thought to form a part of the Na^+ channel since over-expression in *E. coli* is lethal in the presence of sodium and this can be prevented by the addition of amiloride, which blocks transmembrane Na^+ flux [McCarter, 1994b]. The other proteins, FliG, FliM and FliN in *V. parahaemolyticus* are important for assembly of the flagellum [Kosono et al, 2000]. The cytoplasmic region between TMSII and TMSIII of PomA interacts with FliG, resulting in the generation of torque [Yakushi et al., 2004].

Genes homologous to *pomA*, *pomB*, *motX*, *motY* and *fliG* are present in the *V. cholerae* genome as well [Häse & Gosink, 2000]. To clarify the involvement of the PomA, PomB, MotX, MotY and FliG proteins in *V. cholerae* flagellar activity and assembly, a series of different mutants was constructed [Häse & Gosink, 2000]. These strains either carried a single chromosomal deletion of each gene, or had a deletion of the four stator components (*pomA*, *pomB*, *motX*, *motY*), or were lacking all genes. All mutations resulted in a nonmotile phenotype. However, electron microscopy confirmed that the Δ*pomA,pomB,motX,motY* derivative had a normal-looking flagellum (lack of motility could not be ascribed to its absence), while the Δ*fliG* strain was aflagellate [Häse

& Gosink, 2000]. Therefore, PomA/B and MotX/Y appeared to make up the Na^+ conducting part of the flagellar motor.

It has been suggested that Na^+ influx through the flagellar motor is active enough that no other system needs to be implemented to bring Na^+ back into the cell [Sugiyama, 1994]. The rotation rates of H^+-motors in *Streptococcus sp.*, *E. coli*, *S. typhimurium* are approximately 6,000 r.p.m. [Lowe et al., 1987], 16,000 r.p.m. [Lowe et al., 1987] and 10,000 r.p.m. [Kudo et al., 1990], respectively. Interestingly, for the Na^+-motor of *V. alginolyticus*, Magariyama and co-authors reported amazingly high 100,000 r.p.m. [Magariyama et al., 1994]. Perhaps, this reflects the difference in the concentration of H^+ and Na^+ in the environment. Indeed, in natural marine habitats the concentration of Na^+ ions exceeds that of H^+ by at least four orders of magnitude. If binding of ions to the motor is the limiting step in the overall ion transfer through the basal body and the motor affinities for transported ions are comparable, one would expect Na^+-motors would be considerably faster than H^+-motors.

The number of protons required to make one revolution of the H^+-motor is reported as being 1,000 in *Streptococcus sp.* [Meister et al., 1987]. In *V.alginolyticus*, if the motor actually rotates at 100,000 r.p.m. [Magariyama et al., 1994] and Na^+ influx through the motor is assumed to be equivalent to the number of H^+ transported in *Streptococcus sp.* H^+-motor [Meister et al., 1987], the Na^+ re-entry rate would be 1×10^8 $cell^{-1}$ min^{-1}. Taking into account, Avogadro's number ($N = 6 \times 10^{23}$) and assuming the protein content of a single *Vibrio* cell is 240 fg [Zubkov et al., 1999], this corresponds to approximately 0.67 μmol of Na^+ min^{-1} mg $protein^{-1}$, similar to what has been reported for Na^+ efflux mediated by the Na^+/H^+ antiport in *Bacillus alcalophilus* (0.35 to 1.0 μmol min^{-1} mg

protein^{-1}) [Garcia et al., 1983]. Therefore, Na^+ influx through the flagellar motors could be the major route for Na^+ re-entry in the cell as originally suggested by Sugiyama [Sugiyama, 1994]. However, such a re-entry route for Na^+ would apparently depend on the motility status of the cell. As mentioned above, *V. cholerae* cells lose their flagella when they reach the intestine and enter a state of colonization [Finkelstein, 1996]. Under these circumstances, what would mediate effective Na^+ uptake? Data obtained in our laboratory would suggest that, at least under some conditions, Vc-NhaD could serve this purpose (discussed in "Results & Discussion").

1.4.3.2. Na^+-Dependent Drug Efflux

Several clinical isolates of *V. cholerae* have been reported to be highly resistant to the antibiotics ampicillin, penicillin, streptomycin, nitrofurantoin and erythromycin as well as the toxic metals, Pb^{2+} and Zn^{2+} [Huda et al., 2001; Huda et al., 2003; Begum et al., 2005].

Based on the discovery of a Na^+-dependent drug efflux pump, NorM in *V. parahaemolyticus* [Morita et al., 1998; Morita et al., 2000], it was hypothesized that similar systems could be operative in the *V. cholerae* membrane as well. Indeed, homologues of NorM are present in the genome sequences of many other bacteria, but it is not known whether these are Na^+-dependent or H^+-dependent [Nishino & Yamaguchi, 2001]. Nevertheless, it is likely that smf can serve as an energy source for drug efflux systems in a number of pathogens.

Multidrug efflux pumps are structurally diverse and are members of one of five super-families (for review, see reference [Brown et al., 1999]): i) ATP-binding cassette (ABC) family, ii) major facilitator superfamily (MFS) family, iii) small multidrug resistance (SMR) family, iv) resistance nodulation cell division (RND) family, and v) the

multidrug and toxic compound extrusion (MATE) family [Bolhius et al., 1997]. Proteins belonging to the ABC family require ATP as an energy source whereas members from the MFS, SMR and RND families are typically secondary transporters, dependent upon protons [Brown et al., 1999]. Some members of the MATE family have been documented as requiring Na^+ as a coupling ion [Bolhius et al., 1997; Morita et al., 1999; Morita et al., 2000; Chen et al., 2002], but some use H^+ [Bolhius et al., 1997].

The *V. cholerae* genome encodes at least five putative drug efflux systems, VcmA [Huda et al., 2001], VcrM [Huda et al., 2003], VcmB, VcmD and VcmH [Begum et al., 2005], all belonging to the MATE family [Bolhius et al., 1997]. All of them reside on chromosome 1 [Begum et al., 2005].

VcmA, the first Na^+/drug antiporter to be characterized in *V. cholerae*, is a 457 amino acid polypeptide with a molecular mass of 49.438 kDa [Huda et al., 2001]. Multiple sequence alignment of deduced amino acid sequences shows that VcmA is homologous to the Na^+-dependent drug efflux pump, NorM of *V. parahaemolyticus* [Morita et al., 1998; Morita et al., 2000; Chen et al., 2000] and the putative Na^+-dependent drug efflux pumps, YdhE of *E. coli* and YdhE of *H. influenzae* [Nishino & Yamaguchi, 2001]. Alignment also reveals several conserved aspartate and glutamate residues, believed to be responsible for Na^+-binding and transport [Huda et al., 2001]. Hydropathy analysis predicts VcmA to have 12 putative TMS placing it in the MATE family of transporters [Bolhius et al., 1997; Huda et al., 2001].

VcrM is a protein consisting of 445 amino acid residues and has 12 TMS according to hydropathy profiling. Dendrogram analysis suggests that VcrM is a member of the DinF subfamily, which belongs to the MATE family of multidrug efflux pumps [Bolhius et al., 1997; Huda et al., 2003].

Based on sequence analysis, the others, VcmB, VcmD and VcmH are predicted to be putative MATE drug transporters [Begum et al., 2005].

Each gene was introduced and expressed in the drug hypersensitive host *E. coli* KAM32 [Huda et al., 2001; Huda et al., 2003; Begum et al., 2005]. An increased MIC (mean inhibitory concentration) for a number of antimicrobials was noted in cells expressing each putative pump. It was found that fluoroquinolones were substrates for all of the transporters, except VcrM. Aminoglycosides appeared to be substrates for VcmB and VcmH. Ethidium bromide and Hoescht 33342 were substrates for all the pumps [Begum et al., 2005]. Upon energization of energy-starved cells, ethidium bromide or Hoechst 33342 loaded cells showed Na^+-dependent efflux in KAM32 transformed with the above putative MATE drug pumps [Huda et al., 2001; Huda et al., 2003; Begum et al., 2005]. In fact, in VcmA [Huda et al., 2001] and VcrM [Huda et al., 2003], Na^+ efflux could be evoked upon imposition of an artificial drug gradient. Notable, no Na^+ flux has ever been detected secondary to H^+-coupled transporters, demonstrating strict cation selectivity in these two groups of drug transporters [Huda et al., 2001]. Importantly, according to RT-PCR, each pump was found to be expressible in *V. cholerae* [Begum et al., 2005].

1.5. The Na^+ Cycle in the Context of *V. cholerae* Physiology

As already mentioned, transmembrane circulation of sodium ions plays a fundamental role in the physiology of *Vibrio cholerae*. The general chemiosmotic role of Na^+ circulation in *V. cholerae* was discussed above. Now, possible links of Na^+ cycling to particular physiological mechanisms in this organism will be discussed.

1.5.1. Regulation of Expression of Virulence Factors

It has been suggested that one of the functions of CT is to generate a Na^+-rich environment to enhance the efficacy of sodium circulation in *V. cholerae* surviving in the alkaline environment of the small intestine [Bakeeva et al., 1986]. Although the connection between Na^+ circulation and virulence gene expression in *V. cholerae* is a well-documented phenomenon, the underlying mechanism still remains unclear [Häse & Mekalanos, 1999]. However, it is known that environmental stimuli [Gardel & Mekalanos, 1994; Gardel and Mekalanos, 1996; Gupta & Chowdhury, 1997; Klose, 2001; Peterson, 2002; Zhu et al., 2002; Krukonis & DiRita, 2003; Krishnan et al., 2004], including temperature, pH, cell density, growth phase, motility and a number of regulatory proteins influence the expression of the main virulence factors CT and TCP, required for colonization.

Initially, a mutant strain of *V. cholerae* with a transposon insertion in *nqr* was isolated, which produced TCP even when cells were grown under non-inducing conditions (pH 8.5, 37°C) [Häse & Mekalanos, 1998]. The observation that TCP is constitutively expressed when *toxT* is over-expressed [DiRita et al., 1991] prompted a further look into how *nqr* might affect virulence gene expression in *V. cholerae* [Häse & Mekalanos, 1999]. Through transposon mutagenesis and a *V. cholerae* strain carrying a *toxT::lacZ* reporter construct, proteins affecting *toxT* transcription were isolated [Häse & Mekalanos, 1998; Häse & Mekalanos, 1999; for review see Faruque et al., 2004].

In those studies, it was shown that dissipation of sodium-motive force by ionophores, mutations in *nqr* or NQR inhibitors such as HQNO caused an increase in the transcription of *toxT* [Häse & Mekalanos, 1999]. Also, very high or very low concentrations of Na^+ decreased the expression of *toxT*, but not in the *nqr* mutant. To

ascertain if the effect of *nqr* on *toxT* transcription was modulated by ToxR/S or TcpP/H, a *nqr::TnMar* transposon was introduced into a Δ*toxR*Δ*tcpP toxT::lacZ* strain of *V. cholerae.* Both Δ*toxR*Δ*tcpP* and Δ*toxR*Δ*tcpP nqr::TnMar* strains showed decreased *toxT* transcription. Over-expression of TcpP/H alone compensated for the *toxR* and *tcpP* mutations in activating ToxT. However, when TcpP/H was over-expressed in the *nqr* mutant background, a significant increase in *toxT* transcription was noted compared to the parental strain. The same effect could be elicited by the addition of HQNO suggesting that pumping of Na^+ via NQR has a negative effect on TcpP/H. Moreover, *toxT* expression mediated by TcpP/H was reduced in the presence of high Na^+ concentrations. In addition, ionophores such as monensin, which disturb the smf on the membrane, modulated the transcription of *toxT* [Häse & Mekalanos, 1999]. Taken together, these observations support the notion that virulence gene expression in *V. cholerae* is sensitive to (or even governed by) the changes in net Na^+ flux across the membrane [Häse & Mekalanos, 1999].

Motility in *V. cholerae* has been shown to be driven by smf [Kojima et al., 1999; Häse & Mekalanos, 1999; Gosink & Häse, 2000]. Motility is also believed to be an important virulence factor in many pathogens, for it allows penetration through different tissues and may provide assistance in attachment to the epithelial surface [Otterman & Miller, 1997]. Its relationship to the toxigenicity of *V. cholerae* is not well understood, however, although it has been established that production of CT and TCP is influenced by the motility phenotype of the bacterium [Gardel & Mekalanos, 1996; Häse & Mekalanos, 1999]]. Some studies have demonstrated that virulence gene expression and motility are reciprocally related. *toxR* mutants display a hypermotile phenotype on swarm-plate

assays, while examination of some spontaneous hyperswarmers of *V. cholerae* revealed them to have a defect in TCP and CT production even under normal induction conditions (pH 6.5, 30°C) [Gardel & Mekalanos, 1996]. All non-motile mutants of *V. cholerae* constitutively expressed TCP and CT [Gardel and Mekalanos, 1996]. Moreover, increased *toxT* expression is observed by decelerating the Na^+-driven flagellar motor by the addition of the inhibitor phenamil or by growth in viscous media, or by the introduction of a single mutation leading to the non-motile phenotype [Gardel & Mekalanos, 1996; Häse & Mekalanos, 1999].

To ascertain further the role of flagellar activity in *toxT* expression, several non-motile mutants were generated and analysed under various growth conditions as well as in the presence of different ionophores. Like the wild-type parent, the non-motile mutants showed similar levels of *toxT* transcription under the growth conditions tested indicating that the particular situation and energy status of the membrane was sensed, but this did not occur at the level of the flagellum. Therefore, the observed change in *toxT* transcription does not occur solely through modulation of flagellar activity, but may occur through an as yet uncharacterized signaling pathway [Häse, 2001]. It is clear, however, that the motility phenotype of *V. cholerae* is somehow linked to the expression of multiple ToxR-regulated and non-ToxR-regulated virulence determinants [Gardel & Mekalanos, 1996].

Fig. 1.12. Arsenate detoxification in prokaryotes (after Rosen, 1999). Arsenate gains entrance into the cytoplasm via molecular mimicry through the phosphate transport systems. Arsenate is then reduced to arsenite by ArsC and this is extruded either through the ArsA-B complex, ArsB or YqcL [Rosen, 1999].

Fig. 1.12

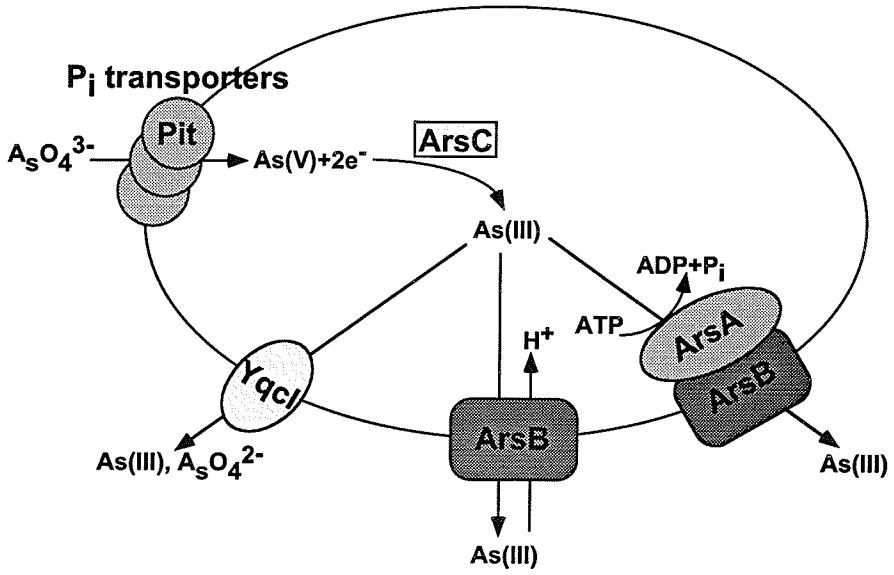
P$_i$ transporters
Pit
$A_sO_4^{3-}$
As(V)+2e$^-$
ArsC
As(III)
ADP+P$_i$
ATP
ArsA
ArsB
H$^+$
Yqcl
ArsB
As(III), $A_sO_4^{2-}$
As(III)
As(III)

1.5.2. Possible Link of Na^+/H^+ Antiport, Arsenate Detoxification and P_i Transport

Besides influence of Na^+ circulation on the expression of virulence factors in *V. cholerae* discussed above, bioinformatic analysis suggested a possible relation of Vc-NhaD antiporter to arsenate/phosphate metabolism in this organism. Therefore in the following sections, this analysis will be presented followed by a brief discussion of key aspects of arsenical detoxification and phosphate metabolism in bacteria, including *V. cholerae*.

1.5.2.1. The ArsB/NhaD Superfamily

The Membrane Transport Protein Classification database maintained by M. Saier and colleagues (http://www-biology.ucsd.edu/~msaier/transport) places Vc-NhaD into the 2.A.62 family "The NhaD Na^+:H^+ Antiporter (NhaD)," which is a part of the Ion Transporter (IT) superfamily [Prakash et al., 2003] that contains, among others, the family 2.A.45 ("The Arsenite-Antimonite (ArsB) Efflux Family"). According to the NCBI Conserved Domain Database (http://www.ncbi.nlm.nih.gov/Structure/cdd), NhaD-type antiporters form a part of the ArsB/NhaD superfamily of permeases translocating sodium, arsenate, arsenite, sulfate, and organic anions. Search of the NCBI Clusters of Orthologous Groups of proteins (http://www.ncbi.nlm.nih.gov/COG) yields a COG 1055 named "Na^+/H^+ antiporter NhaD and related arsenite permeases."

Phylogenetic association of NhaD-type proteins with ArsB/NhaD superfamily of permeases and COG 1055 indicates possible relation of Vc-NhaD to arsenite/arsenate/phosphate metabolism in V. *cholerae* (see Fig. 4.22A).

To probe possible physiological roles of Vc-NhaD, a chromosomal *nhaD* deletion mutant of *V. cholerae* was constructed as described below.

1.5.2.2. Arsenical Detoxification in Bacteria

In *E. coli*, the major arsenical detoxification system is encoded by the *ars* operon (for review see [Rosen 1999; Rosen, 2002]). The pathway includes reduction of As(V) to As(III) by arsenate reductase, ArsC, and subsequent removal of As(III) in the form of arsenite either by the ArsB carrier alone (via electrogenic antiport with H^+) or by the ArsAB complex operating as an arsenite-motive ATPase [Rosen, 1999; Rosen, 2002; Meng et al., 2004] (Fig. 1.12). In *Bacillus subtilis* and a few other bacteria, an urelated YqcL-type arsenite transporter has also been reported [Sato & Kobayashi, 1998; Rosen, 2002] (Fig. 1.12). In *E. coli*, ArsR is a *trans*-acting negative regulator [Xu et al., 1996; Wu & Rosen, 1991], controlling the basal level of expression of the operon, whereas ArsD is a *trans*-acting repressor [Wu & Rosen, 1993], controlling maximal expression (for review see [Rosen, 1999; Rosen, 2002]). ArsR and ArsD are distinct and act separately from each other (for review see [Rosen, 1999; Rosen, 2002]).

1.5.2.3. The *phoBR* Regulatory Circuit

Phosphorus is an important element in bacteria as it is necessary for energy (ATP generation) as well as for DNA, RNA and phospholipid synthesis. The preferred source of phosphorus is inorganic phosphate (P_i), but bacteria can use the degradation products of organo-phosphates as an alternative source. After being degraded, the P_i esters cross the outer membrane where they become further hydrolysed. The P_i is then transported across the cytoplasmic membrane through specific transport systems (for an excellent review on phosphate transport systems in prokaryotes, see van Veen, 1997) to be used in various cellular reactions.

Interestingly, phosphate limitation can have an effect on virulence factor expression in some pathogenic bacteria such as *P. aeruginosa*, *S. typhimurium* and entero-invasive *E. coli* [Ostroff et al., 1989; Libby et al., 1990; Sinai & Bavoil, 1993; Buckles et al., 2006]. On the other hand, mutation of the *phoBR* element in another *E. coli* strain, which is pathogenic to pigs, results in avirulence [Daigle et al., 1995].

The *phoBR* regulatory element ("phosphate box" or "Pho-box") is an 18-base consensus sequence that is a part of the promoter of genes belonging to the phosphate (Pho) regulon [Wanner & Chang, 1987]. It serves as the binding site for the transcriptional activator PhoB. In *E. coli*, the PhoB protein activates genes of the phosphate regulon, which include *phoA* and *pstS* that are induced upon phosphate deprivation. Under these circumstances, a protein called PhoR activates PhoB when phosphate is limiting and inactivates it when phosphate is in excess [Wanner & Chang, 1987]. The *V. cholerae* genome contains an operon homologous to the *E. coli* PhoBR regulatory system, which has been characterized (von Kruger et al., 1999). Because of the presence of a sequence similar to a Pho box in the promoter region of Vc-PhoB, it was suggested that expression of the putative *V. cholerae phoBR* operon could be regulated by levels of inorganic phosphate. A *V. cholerae* mutant devoid of PhoB could not grow in low phosphate media and failed to induce the synthesis of PhoA as well as the expression of the putative Pho regulon. The PhoB mutation had no effect on cholera toxin production, whether the cells were grown in high or low phosphate media, but the mutant was not able to colonize the rabbit intestine as effectively as the wild type [von Kruger et al., 1999]. Production of CT was reduced in the absence of amino acids [Sagar et al., 1981; Miller & Mekalanos, 1988]. However, in the presence of amino acids and at high

phosphate levels, cells were able to produce a much more significant amount of the toxin [Sagar et al., 1981; Miller & Mekalanos, 1988; von Kruger et al., 1999].

1.5.2.4. P_i Transport Systems in *V. cholerae*

Analysis of the genome sequence suggests that phosphate import in *Vibrio cholerae* is mediated by a variety of transport systems (for an excellent review on microbial phosphate transporters see [van Veen, 1997]).

There are two *pstSCAB*-like operons, VC0721-25 & VCA0070-73. In *E. coli*, Pst is a high affinity, low-velocity system for P_i uptake (K_m = 0.2 μM, V_{max} = 15.9 nmol P_i per minute per mg protein). It is an ABC-type transporter, induced when $[P_i]_{out}$ is less than 20 μM. It is apparently repressed when $[P_i]_{out}$ is greater than 1 mM. Pst has a 100-fold higher affinity to P_i than to arsenate [Rosenberg, et al., 1977; reviewed in van Veen, 1997].

There is also the presence of a *pit*-like transporter, VC2442. In *E. coli*, Pit is the major route for P_i uptake. It is a constitutive, pmf-driven, low-affinity, high-capacity system (K_m is approximately equal to 25-38 μM for P_i or arsenate). It co-transports neutral $MeHPO_4$ ($MeHAsO_4$) with H^+ [Willsky et al., 1973; Rosenberg et al., 1977; Rosenberg et al., 1979; van Veen et al., 1994; reviewed in van Veen, 1997].

Another putative phosphate transporter in *V. cholerae*, VCA0137, is homologous to GlpT. In *E. coli* as well as in other bacteria, this secondary transporter mediates the electroneutral antiport of phosphate with glycerol-3-phosphate (G3P) (reviewed in [van Veen, 1997]). It can also undergo electroneutral P_i/P_i and G3P/G3P antiport as well. Arsenate can freely substitute for P_i in all three exchange reactions. Its expression is

regulated by extracellular G3P and not P_i. GlpT also appears to have a much better selectively for H_2PO^{4-} over HPO_4^{2-} [van Veen, 1997].

Another entry route of P_i in *V. cholerae* is through the NptA transporter, VC0676 (discussed above), which is homologous to the animal Type II Na^+-dependent P_i cotransporters [Lebens, 2002]. Compared to other transport systems, it has a rather low affinity for P_i (300 mM) and Na^+ (75 mM). Interestingly, the activity of Vc-NptA when expressed in *E. coli* is found to be dependent upon external pH, doubling with a pH rise from 6.5 to 9.0 [Lebens, 2002]. Its contribution to the overall P_i uptake in *V. cholerae*, however, remains to be elucidated [Lebens, 2002]. One possibility is that it mediates rapid Pi uptake in preparation for growth in nutrient rich environments such as in the intestine (perhaps for establishing infection).

2. RESEARCH OBJECTIVES

2. RESEARCH OBJECTIVES

2.1. Cloning of the *nhaD* Gene from *V. cholerae* and Characterization of the Biochemical Properties of Vc-NhaD

At the beginning of this work, the complete genome of *V. cholerae* had just been sequenced revealing a number of Na^+ transporting mechanisms. Unusual for a bacterium, was the presence of as many as seven Na^+/H^+ antiporters (see Fig. 1.3) namely, NhaA and NhaB typical for enterobacteria, NhaC, NhaP and MleN named after homologues found in other bacteria, Mrp multisubunit Na^+/H^+ antiporter, which we are currently characterizing in our laboratory and is beyond the scope of this thesis and NhaD (Fig. 1.3). Interestingly, NhaD was only found in pathogenic *Vibrios*, *V. parahaemolyticus* [Nozaki et al., 1998] and *V. cholerae*, but not in the free-living, non-pathogenic similar species *V. alginolyticus.* Because of this, the main research objective of this project was to clone-out the *nhaD* gene and characterize it at the biochemical level in the antiporterless strain of *E. coli* EP432.

2.2. Elucidation of the Possible Physiological Role of NhaD in *V. cholerae*

Because NhaD could only be found in pathogenic *Vibrios* as mentioned above, we felt it important to ascertain the physiological role of this antiporter in *V. cholerae* as it seemed possible that it may be related to the pathogenicity of this organism.

2.3. Study of the Role of Vc-F_1F_0-ATPase in Oxidative Phosphorylation and Determination of the Ion Specificity of the Enzyme

The *V. cholerae* genome also appeared to contain an operon encoding a typical F_1F_0-ATPase. Given the variety of Na^+-exporting systems, it seemed important to determine whether oxidiative phosphorylation in *V. cholerae* was mediated by a proton-

motive or sodium-motive F_1F_0-ATPase. Partial sequence alignment of the *c* subunit, which determines the ionic specificity of the enzyme, and the experimental data obtained concerning the same enzyme in *V. alginolyticus* [Dmitriev et al., 1991] predicted it to most probably be protonic. However, there was no experimental data concerning the ionic specificity of this enzyme in *V. cholerae*. We therefore wanted to determine this.

2.4. Examination of the Role of Vc-NQR in the Survival and Sensitivity of *V. cholerae* to Ag^+

It had been well established that NQR functioned as a Na^+ pumping NADH ubiquinone oxidoreductase in *V. alginolyticus* (for a review see Hayashi et al., 2001) and had also been shown to be a target for low concentrations of Ag^+ [Steuber et al., 1997; Nakayama et al., 1999]. Since *V. cholerae* was very sensitive to Ag^+, we wanted to ascertain whether NQR was responsible for this. We also wanted to examine the role of NQR in the survival of *V. cholerae*.

2.5. Probing of the Role of Vc-NhaD and Vc-NQR in the Survival of *V. cholerae* at Elevated Temperature

Since Na^+ ions are much less permeable than H^+ at any given temperature [van de Vossenberg et al., 1995], some anaerobic thermophiles use the Na^+ cycle instead of the H^+ cycle [van de Vossenberg et al., 1998; Albers et al., 2001]. Using a less permeable coupling cation in this case would disallow the futile cycling of H^+, therefore enhancing the efficiency of energy transduction. Since *V. cholerae* contains both primary Na^+ pumps and smf consumers, it seemed interesting to determine whether the Na^+ cycle contributed to the survival of this mesophilic organism at elevated temperatures.

3. MATERIALS AND METHODS

3. MATERIALS AND METHODS

3.1. Bacterial Strains and Plasmids

The bacterial strains and plasmids used are listed in Tables 1 and 2 respectively. The *V. cholerae* strains used in this study were strain O395N1 (kindly provided by Dr. J. J. Mekalanos, Harvard Medical School) and its isogenic Δ*atpE*, Δ*nqrA-F*, and Δ*nhaD* derivatives, DATPE1 (this work), DNQR1 (gift from Dr. C. Häse, Oregon State University), and DD1 (this work). EP432 (kindly provided by Dr. E. Padan, Hebrew University of Jerusalem) is a Na^+/H^+ antiporter-deficient *E. coli* K-12 derivative, which is *mel*BLid, Δ*nha*A1::*kan*, Δ*nha*B::*cat*, Δ*lac*ZY, *thr*1 [Harel-Bronstein et al., 1995]. For routine cloning and plasmid construction, DH5α (U.S. Biochemical Corp.) or XL1-Blue (Stratagene) was used as a host.

3.2. Growth Media and Storage Conditions

LB Medium [Sambrook et al., 1989]

10 g	Bacto-Tryptone (DIFCO)
5 g	Yeast Extract (DIFCO)
5 g	NaCl
	per litre of distilled water

For plates, 7.5 g of Bacto-agar (DIFCO) was added, then sterilized by autoclaving for 20 minutes.
Where indicated, appropriate antibiotics were added after autoclaving and sufficient cooling.
For colour selection, 0.1 M IPTG was added at 1:1000 and 20 mg/ml X-gal at 1:500 after autoclaving.

LBK Medium [Padan et al., 1989]

10 g	Bacto-Tryptone (DIFCO)
5 g	Yeast Extract (DIFCO)
5 g	KCl
	per litre of distilled water

For plates, 7.5 g of Bacto-agar (DIFCO) was added, then sterilized by autoclaving for 20 minutes.

Table 1. **List of bacteria**
See "Materials and Methods" for further details.

Strain		Relevant Genotype or Phenotype
E. coli		
	DH5α	*supE*44 *hsdR*17 *recA*1 *endA*1 *gyrA*96 *thi*-1 *relA*1
	XL1-Blue	*supE*44 *hsdR*17 *recA*1 *endA*1 *gyrA*96 *thi*-1 *relA*1 *lac*$^-$ F' [*proAB*$^+$ *lacI*^{q} *lacZ*ΔM15 Tn*10*(Tet^R)]
	EP432[a]	*mel*BLid, Δ*nha*A1::*kan*, Δ*nha*B::*cat*, Δ*lac*ZY, *thr*1
V. cholerae		
	O395N1[b]	Δ*ctxAB* *toxT*::*lacZ*, Str^R
	DD1	O395N1 Δ*nhaD*, Str^R
	DATP1[c]	O395N1 Δ*atpE*, Str^R
	DNQR 1[c]	O395N1 Δ*nqrA-F*, Str^R

[a]kindly provided by Dr. E. Padan, Hebrew University of Jerusalem
[b]kindly provided by Dr. J. J. Mekalanos, Harvard Medical School
[c]kindly provided by Dr. C. Häse, Oregon State University

Table 2. **List of plasmids**
See "Materials and Methods" for details on construction.

Plasmid	Description
pBluescript	cloning vector, *amp*^{R}
pBLDL	pBluescript containing Vc-*nhaD* with 154 bp 5'- and 230 bp 3'-flanks
pBA[a]	pBluescript containing Vc-*nhaA* with 5'- and 3'- flanks
pBELD	pBluescript containing Vc-*nhaD* with 919 bp 5'- and 230 bp 3'-flanks
pΔSnaBL	pBELD containing in-frame Vc-*nhaD* deletion of 241 residues (S60-K301)
pMAKSACB	suicidal vector, contains *sacB* and *oriT* of replication, *cat*^{R}
pWM91	suicidal vector, contains *sacB* and R6K origin of replication, *amp*^{R}
pMADL	pMAKSACB containing Ecl136II/HincII fragment from pΔSnaBL
pH93A	pBLDL bearing H93A mutation
pH210A	pBLDL bearing H210A mutation
pH274A	pBLDL bearing H274A mutation
pH278A	pBLDL bearing H278A mutation
pH450A	pBLDL bearing H450A mutation
pH468A	pBLDL bearing H468A mutation
pR305A	pBLDL bearing R305A mutation
pR305C	pBLDL bearing R305C mutation
pR305D	pBLDL bearing R305D mutation
pR305H	pBLDL bearing R305H mutation
pR305S	pBLDL bearing R305S mutation
pR305T	pBLDL bearing R305T mutation
pK301A	pBLDL bearing K301A mutation
pT302A	pBLDL bearing T302A mutation
pS306A	pBLDL bearing S306A mutation
pC163S[b]	pBLDL bearing C163S mutation
pC181S[b]	pBLDL bearing C181S mutation
pC355S[b]	pBLDL bearing C355S mutation
pTM[b]	pBluescript containing *cys*-less Vc-*nhaD*
pS150A[b]	pBLDL bearing S150A mutation
pD154A[b]	pBLDL bearing D154A mutation
pN155A[b]	pBLDL bearing N155A mutation
pT157A[b]	pBLDL bearing T157A mutation
pN189A[b]	pBLDL bearing N189A mutation
pD199A[b]	pBLDL bearing D199A mutation
pT201A[b]	pBLDL bearing T201A mutation
pT202A[b]	pBLDL bearing T202A mutation
pD344A[c]	pBLDL bearing D344A mutation

pT345A[c]	pBLDL bearing T345A mutation
pS389A[b]	pBLDL bearing S389A mutation
pS390A[b]	pBLDL bearing S390A mutation
pN394A[b]	pBLDL bearing N394A mutation
pS425A[b]	pBLDL bearing S425A mutation
pS428A[b]	pBLDL bearing S428A mutation
pS431A[b]	pBLDL bearing S431A mutation

[a]kindly constructed by Dr. Arthur Winogrodzki, University of Manitoba
[b]kindly constructed and analysed by Dr. Rahim Habibian, University of Manitoba
[c]kindly constructed and analysed by Dr. Elena Ostroumov

Where indicated, appropriate antibiotics wer added after autoclaving and sufficient cooling.

M9 Minimal Medium [Sambrook et al., 1989]

200 ml Sterile 5X M9 Salts
800 ml Autoclaved distilled water
The appropriate carbon source was added after autoclaving.

Trace Elements

5.0 mM $MgSO_4$
0.1 µg/ml Thiamine
2 µM $FeSO_4$
0.2 mM $CaCl_2$
Trace elements were added to minimal medium after autoclaving.

5X M9 Salts

64 g Na_2HPO_4
15 g KH_2PO_4
2.5 g NaCl
5.0 g NH_4Cl
per litre of distilled water
5X M9 salts were divided into 200 ml aliquots and sterilized by autoclaving for 20 minutes.

Unless otherwise indicated, cells were grown either in LB or LBK and stock cultures were stored at –80°C in 25% glycerol.

3.3. Bacterial Growth Conditions

3.3.1. Growth of *E. coli* EP432

If not indicated otherwise, cells were grown in liquid LBK or on LBK-agar plates supplemented with 100 µg/ml ampicillin, 15 µg/ml kanamycin and 17.5 µg/ml chloramphenicol. For growth experiments with EP432 transformants, LBK medium with or without 0.1 M LiCl was used where the starting pH was adjusted from 5.6 to 8.8 by the addition of MES-Tris (pH 5.6 to 6.0) or HEPES-Tris (pH 6.4 to 8.0) to a final

concentration of 60 mM. All media were supplemented with 100 μg/ml ampicillin, 30 μg/ml kanamycin and 17.5 μg/ml chloramphenicol as indicated. Cells were inoculated at OD_{600}=0.05 and grown aerobically at 37°C for 15 hours. The resulting growth was measured as the optical density of the bacterial suspension at 600 nm.

3.3.2. Growth of *V. cholerae*

If not indicated otherwise, cells were grown in LB or on LB-agar plates supplemented with 100 μg/ml streptomycin or for transformants, 100 μg/ml streptomycin plus 300 μg/ml carbenicillin. The antibiotics did not affect the cellular growth rate.

3.3.2.1. Growth in the Presence of LiCl

For growth experiments of *V. cholerae* in the presence of LiCl, the above protocol for *E. coli* EP432 was modified as follows: LB-based medium (10 g/L Bacto-Tryptone and 5 g/L yeast extract) plus 0.180 M KCl or 0.180 M LiCl was used where the starting pH was adjusted to 6.0 by the addition of 60 mM MES-Tris or pH 8.0 by the addition of 60 mM HEPES-Tris. Single colonies from LB-agar plates containing 100 μg/ml streptomycin or 100 μg/ml streptomycin plus 300 μg/ml carbenicillin (for transformants) were inoculated into 2 ml of liquid medium containing 100 μg/ml streptomycin or 100 μg/ml streptomycin plus 300 μg/ml carbenicillin (for transformants), and grown aerobically at 37°C for 15 hours. The resulting growth was measured as the optical density of the bacterial suspension at 600 nm.

3.3.2.2. Growth in the Presence of Ag^+ Ions

In the case of growth in the presence of silver nitrate, LB medium, where NaCl was replaced by equimolar Na_2SO_4 or M9 minimal medium containing no chloride ions was

used and the concentration of added silver adjusted as indicated. The resulting growth was measured as the optical density of the bacterial suspension at 600 nm.

3.3.2.3. Growth in the Presence of Various Substrates

In the case of growth in the presence of various substrates, overnight cultures of *V. cholerae* in LB were inoculated at OD_{600}=0.05 into 20 ml of M9 minimal medium supplemented with 0.4% glucose, 25 mM succinate or 0.4% glycerol and grown aerobically in 250 ml Erlenmeyer flasks at 37°C for 18 hours, as indicated. The resulting growth was measured as the optical density of the bacterial suspension at 600 nm.

3.3.2.4. Growth with Sodium Arsenate or Sodium Arsenite.

In the case of growth in the presence of sodium arsenate, *V. cholerae* was grown in LBK plus or minus 7.5 mM sodium arsenate where 60 mM MES-Tris was used for pH below 6.5 and 60 mM HEPES-Tris was used for pH 6.5-8.2. In the case of growth in the presence of sodium arsenite, LBK medium was used where the concentration of added arsenite was adjusted as indicated. Single colonies from LB-agar plates containing 100 μg/ml streptomycin or 100 μg/ml streptomycin plus 300 μg/ml carbenicillin (for transformants) were inoculated into 2 ml of liquid medium, containing 100 μg/ml streptomycin or 100 μg/ml streptomycin plus 300 μg/ml carbenicillin (for transformants), and grown aerobically at 37°C for 15 hours. The resulting growth was measured as the optical density of the bacterial suspension at 600 nm.

3.3.2.5. Growth at Elevated Temperatures

In the case of heat-shock experiments, overnight cultures of *V. cholerae* were grown at 28°C in LB containing 100 μg/ml streptomycin or 100 μg/ml streptomycin plus 300 μg/ml carbenicillin (for transformants) for no longer than 15 hours were inoculated

into pre-warmed LB containing 100 μg/ml streptomycin or 100 μg/ml streptomycin plus 300 μg/ml carbenicillin (for transformants) at OD_{600}=0.05. The resulting growth at optical density 600 nm was monitored for at least 6 hours.

3.4. Isolation of DNA

3.4.1. Chromosomal DNA Isolation

Lysis Buffer

40 mM	Tris-Acetate (pH 7.8)
20 mM	Sodium Acetate
1 mM	EDTA
1%	SDS

The solution was sterilized by syringe filtration through a 0.4 μM filter.

TE Buffer [Sambrook et al, 1989]

10 mM	Tris-HCl (pH 8.0)
1.0 mM	EDTA (pH 8.0)

The solution was sterilized by syringe filtration through a 0.4 μM filter.

Chromosomal DNA was isolated as described in [Chen & Kuo, 1993]. Cells were grown in LB at 37°C to OD_{600}=1.0 or higher. In an Eppendorf tube, 1.0 ml of saturated culture was centrifuged for three minutes at 14,000 x g, the resulting pellet resuspended in 200 μl of Lysis Buffer and the cells lysed by vigorous pipetting. RNase was added to the suspension at a concentration of 10 μg/ml and incubated for 30 minutes at 37°C. To remove cellular debris, 66 μl of 5M NaCl was added and mixed well. The resulting viscous solution was centrifuged at 14,000 x g for 15 minutes at 4°C. The clear supernatant was transferred into a new Eppendorf tube. An equal volume of chloroform was added and the tubes gently inverted at least 50 times to get a milky solution. The solution was then spun for three minutes at 14,000 x g and the extracted supernatant

transferred into a fresh Eppendorf tube. The DNA was precipitated with 95% ethanol and washed twice with 70% ethanol. The DNA pellet was dried in a speed-vacuum or on the bench for 20 minutes and re-dissolved in 50 µl of TE buffer.

The concentration and purity of the DNA was measured as described below.

3.4.2. Plasmid DNA Isolation

Resuspension Buffer

50 mM	Glucose
10 mM	EDTA (pH 8.0)
25 mM	Tris-HCl (pH 8.0)

Lysis Buffer

0.2 M	NaOH
1%	SDS

Neutralization Buffer

3 M	Potassium Acetate
pH to 4.8 with glacial acetic acid	

Plasmid DNA was isolated as described in [Sambrook et al., 1989; Birnboim, 1983]. 3.0 ml of cells were aliquoted into Eppendorf tubes and spun-down in a microcentrifuge set at high-speed (14,000 x g) for two to three minutes. 200 µl of Resuspension Buffer was added to each pellet along with 20 µl of 10 mg/ml RNase solution and the pellet was resuspended completely. 300 µl of Lysis Buffer was then added, the tubes mixed by inverting five times and incubated at room temperature for five minutes. Then, 300 µl of Neutralization Buffer was added, the tubes mixed by inversion five times and incubated at room temperature for five minutes. The suspension was then spun at 14,000 x g in a microcentrifuge for 20 minutes. The supernatant was carefully decanted into fresh Eppendorf tubes, extracted once by adding 450 µl of chloroform and shaking vigorously for 30 seconds. The mixture was spun for three to four minutes in a

microcentrifuge set at 14,000 x g and the upper layer drawn off into new tubes. The plasmid DNA was precipitated by adding 700 µl of ice-cold 95% ethanol and spinning at 14,000 x g for 15 to 20 minutes. The ethanol was carefully suctioned off and the DNA pellets washed once by the addition of 500 µl of ice-cold 70% ethanol and spinning at 14,000 x g for three to five minutes. After careful suctioning of the ethanol, the DNA was dried on the bench for 20 to 30 minutes and resuspended in 40 to 50 µl of TE buffer (pH 8.0) or sterile double-distilled water. The concentration and purity of the DNA was measured as described below.

3.5. Purification of DNA Products

3.5.1. DNA Purification by Binding to Glass Powder

NaI Solution

90.8 g	Sodium Iodide
1.5 g	Na_2SO_3
	per 100 ml of sterile distilled water.

The solution was filtered through Whatman No.1 and then 0.5 g of Na_2SO_4 was added to the solution to keep it saturated.
It was stored foil-wrapped at 4°C.

New Wash

100 mM	NaCl
1 mM	EDTA
50%	ethanol
10 mM	Tris-HCl (pH 7.5)

The solution was stored at –20°C.

The following was based on the Gene-Clean (Bio101) procedure.

Three volumes of NaI was added to the DNA sample, then approximately 10 µl of glass milk, mixed and the solution placed on ice for 30 minutes for DNA binding to occur. The glass milk was then pelleted by centrifugation in a microcentrifuge at 14,000

x g for one minute, washed by adding 1.0 ml of New Wash, spinning for one minute at 14,000 x g and decanting the supernatent. This was then repeated twice more. On the last spin, the New Wash was aspirated off, the pellet dried at room temperature for two minutes and resuspended in 25 to 50 µl of sterile distilled water or TE buffer. The DNA was eluted off of the glass milk by incubation at 65°C for 15 minutes, after which it was spun for two minutes in a microcentrifuge at 14,000 x g and the supernatent containing the purified DNA transferred into a fresh Eppendorf tube. The concentration and purity of the DNA was measured as described below.

3.5.2. DNA Purification by Ethanol Precipitation

One volume of DNA was mixed with 0.5 volumes of sodium acetate (3 M, pH 5.0) and 3.5 volumes of 95% ethanol. The mixture was then incubated at –80°C for 30 minutes or –20°C overnight. The DNA was precipitated, by spinning at 14,000 x g in a microcentrifuge for 20 minutes at room temperature. The supernatant was removed by aspiration and 2.5 volumes of 75% ethanol added. The mixture was spun again at 14,000 x g in a microcentrifuge for five minutes at room temperature. The supernatant was removed by aspiration, the DNA allowed to dry for 30 minutes and then it was resuspended in 0.5 volumes TE buffer or sterile distilled water. The concentration and purity of the DNA was measured as described below.

3.5.3. Determination of DNA Concentration and Purity

Concentration of DNA

1 OD_{260} Unit of dsDNA = 50 µg/ml H_20

1 OD_{260} Unit of ssDNA = 33 µg/ml H_20

Purity of DNA

Pure DNA $OD_{260}/OD_{280} \geq 1.8$

The concentration of DNA was determined on a Ultrospec 3000 UV/visible spectrophotometer (Pharmacia Biotech) by reading the absorbance of the sample at 260 nm. As stated above, one absorbance unit is equal to 50 μg of DNA, but this value is based on the extinction coefficient of nucleic acids in water. Therefore, it may differ in other buffers or solutions.

The purity of the sample was then determined by measuring the ratio of OD_{260} to OD_{280}. As above, a pure sample should have a value of approximately 1.8. If this ratio is determined to be greater than 1.8, then the preparation is contaminated with proteins or aromatic substances such as phenol. If it is greater than 2.0, then the sample is contaminated with RNA.

3.6. Cloning of DNA Products

3.6.1. PCR Amplification of DNA

PCR Reaction Components

100-300 ng	Template DNA
10 μl	10X PCR Buffer
10 μl	50 mM $MgSO_4$
10 μl	10 mM dNTPs (Invitrogen)
10 μl	10 mM Forward Primer
10 μl	10 mM Reverse Primer
1 to 2 μl	DNA Polymerase

The volume was brought up to 100 μl with sterile double distilled water.

PCR Reaction Cycling Parametres

Segment 1	1X	94°C	5 minutes (Denaturation)
Segment 2	30X	94°C	30 seconds (Denaturation)
		55-60°C[a]	30 seconds (Annealing)
		68°C	1 minute per kb (Synthesis)
Segment 3	1X	68°C	7 minutes (Final Synthesis)
		4°C	∞

Table 3A. List of primers used for mutagenesis

Primer	Primer Sequence	Codon Change	Restriction Site (+) or (-)
H93A	CAGGCCTTAGAA**GC**CAATTTGCT TGA**GT**ACGCAGAGCTGCTG	CAC – GCC	+ *Rsa*I
H210A	GTGGCAGGCTGGG**GC**TGTTAGCTT CCTTGAG	CAT – GCT	+ *Nsp*I
H274A	CCATCCTCTCGGCCATCGGTTGC**GC** TGCATTTTTCCACTTCCC	CAT – GCT	+ *Nsi*I
H278A	CATGCATTTTTC**GC**CTTCCCGCC**GG** TGATCGGCATGATGATGG	CAC – GCC	+ *Bsl*I
H450A	CACGTTCTTGAGC**GC**CTTGAAATGG ACTCC	CAC – GCC	+ *HhaI*
H468A	CAGTATCGTGTTG**GC**CTTGCTGCT CAATC	CAT – GCC	+ *Hae*I
R305A	CGTAAAACGCTGGCA**GC**G**T**CATGG CTAAGAAAACGGCG	AGA – GCG	- *Dpn*I
R305C	CGTAAAACGCTGGCA**T**G**T**TCATGG CTAAGAAAACGGCG	AGA – TGT	+ *Nsp*I
R305D	CGTAAAACGCTGGCA**GA**T**T**CATGG CTAAGAAAACGGCG	AGA – GAT	+ *Tfi*I
R305H	CGTAAAACGCTGGCA**CA**C**T**CATGG CTAAGAAAACGGCG	AGA – CAC	- *Dpn*I
R305S	CGTAAAACGCTGGCAAG**C**TCATGG CTAAGAAAACGGCG	AGA – AGC	- *Dpn*I
R305T	CGTAAAACGCTGGCAAA**C**ACATGG CTAAGAAAACGGCG	AGA – ACA	- *Dpn*I
K301A	GGCTATTTCCTACGT**GC**AACGCTGGC AAGATCAC	AAA – GCA	- *SnaB*I
S306A	CGTAAAACGCTGGCAAGA**GC**CCTGG CTAAGAAAACGGCG	TCA – GCC	+ *Eco*RII
R305A,S306A	CGTAAAACGCTGGCA**GCTGC**GCTGG CTAAGAAAACGGCG	AGA – GCT (R) TCA – GCG (S)	+ *Pvu*II
T302A	CTATTCCTACGTAAA**GC**GCTGGCAAG ATCACTGGC	ACG – GCG	+ *Eco47*III
S150A	GCGTTTTTCATT**GC**G**C**CGATTGCCG ATAACC	TCC – GCG	+ *Hha*I
D154G	CCGATTGCCG**GA**AACCTCACCACG	GAT – GGA	+ *Hpa*II
N155A	CCGATTGCCGAT**GC**G**C**TCACCACG GCG	AAC – GCG	+ *Hha*I
T157A	CCGATAACCTC**GC**GACGGCGTTATTG	ACC – GCG	+ *Bsp68*I
N189A	GTGATTGCTGCC**GC**CGCGGGAGGA GCC	AAC – GCC	+ *Sac*II

D199A	CAGTCCCTTTGGCG**C**TATCACCACTC	GAT – GCT	- *EcoR*V
T201A	CTTTGGCGATATC**GC**G**A**CTCTTATG GTG	ACC – GCG	+ *Bsp68*I
T202A	GCGATATCACC**GC**G**C**TTATGGTGT GG	ACT – GCG	+ *Hha*I
S389A	GTTGGGCTGCTT**GC**G**T**CGGTGGTC GATAAC	TCT – GCG	+*Hga*I
S390A	GTTGGGCTGCTTTCT**G**C**A**GTGGTC GATAAC	TCG – GCA	+*Pst*I
N394A	CGGTGGTCGAT**GGA**ATTCCTGTCAT GTTTGC	AAC – GGA	+ *EcoR*I
S425A	GGAGTCGGCGGC**GC**C**C**TTGCTATCG ATTGG	AGT – GCC	+ *Ehe*I
S428A	GCAGTTTGCTA**G**CGATTGGCTCTGC	TCG – GCG	+ *Taq*I
S431A	CTATCGATTGGC**GC**A**G**CAGCAGGTG TGG	TCT – GCG	- *Pst*I

Table 3B. List of primers used for construction of plasmids

Primer	Primer Sequence	Construct
ECF	TAGCATGAATTCTAAAAAATGATG AATAAACAACCATTTCTAAGC	pBLDL (forward primer)
BM	CATTACGGATCCAGATCCGTAATAACTCC	pBLDL (reverse primer)
NHAAF	AAGCCGGAATGGGCCCTCAGCCTTTTCGG ATGTGG	pBA (foward primer)
NHAAR	TTTGGATGGTCGACCAGAGTCGAGTTGTG CTTTCAGTGC	pBA (reverse primer)
PMADLF	CATCGACATCCATGCATCAATCAACACCGC	pMADLS (forward primer)
PRIMER 1	GGACTAGTCTCCGGCTCGAATAATAA	pΔ*atp*E (downstream region)
PRIMER 2	GGAATTCCACTTTAGGGGGTAG	pΔ*atp*E (downstream region)
PRIMER 3	GGAATTCTCCAAAGATTCAATGGGTATTA	pΔ*atp*E (upstream region)
PRIMER 4	AATGGTCGACATCTCGTTTAT	pΔ*atp*E (upstream region)
FORWARD	GCCGGCCTGCGTCCTGTCGCTCGT	pNQR (forward primer)
REVERSE	GGAACACCATCACGGTTCAGT	pNQR (reverse primer)

[a]This is the step at which primers anneal, therefore the temperature was adjusted accordingly (typically approximately 5°C below the T_m of the primer). The T_m of the primer, however, should be about 60°C.

PCR primers used in this study are listed in Table 3A and 3B. A typical PCR reaction for cloning was performed as above in a 0.5 ml Eppendorf tube, in a total volume of 100 µl using High Fidelity Taq (Invitrogen), Pfx (Invitrogen) or Pfu (Fermentas or Stratagene) DNA polymerase. Amplification was then carried out in a Techne PCR machine using the program settings as described.

3.6.2. Restriction Endonuclease Digestion of DNA Products

Restriction endonucleases were purchased from Invitrogen, Fermentas or New England Biolabs. Restriction digest of DNA was typically carried out in a volume of 20 µl using 1 to 10 units of enzyme per reaction as well as the recommended buffer. If a double digestion (using two enzymes) was performed, a buffer that gave 100% activity for both enzymes was used. All digestions were incubated for two hours at the recommended temperature.

3.6.3. Agarose Gel Electrophoresis of DNA Products

3.6.3.1. Preparation of the Agarose Gel

5X TAE Buffer

48.4 g	Tris Base
11.42 ml	Glacial Acetic Acid
20 ml	0.5 M EDTA (pH 8.0)

6X Loading Buffer (Fermantas)

0.09%	Bromophenol Blue

0.09%	Xylene Cyanol FF
60%	Glycerol
60 mM	EDTA

0.7 to 1.5% agarose gels were prepared by adding the appropriate amount of agarose (Gibco-BRL Ultra-Pure) to 30 ml of 1X TAE buffer in a 125 ml Erlenmeyer flask. The solution was heated to boiling, cooled slightly and 4 µl of 10 mg/ml ethidium bromide added. The agarose solution was then poured into a gel mold, the well-divider submerged and allowed to polymerize. Once the agarose was solidified, the well-divider was removed and the mold placed into a DNA electrophoresis chamber (Tyler Research Instruments) containing 1X TAE. 6X DNA loading buffer was added to all DNA samples to a concentration of approximately 1:5, prior to loading into each well. Electrophoresis took place at approximately 60 to 80 Volts for one to two hours.

3.6.3.2. Visualization of Agarose Gels

The agarose gel was visualized either using the FluorChem 8600 Version 3.2.3 program (Alphainnotech Corporation) on an ultraviolet transilluminator set at 302 nm, outfitted with a camera or by using the GelDoc1000 system (BioRad), on a transilluminator, equipped with a camera utilizing the Quantity One Version 4.5.0. program (BioRad). The final photograph was printed on standard white paper using a HPLaserJet1300 printer in the aforementioned case or a Mitsubishi Video Copy Processor in the latter case. The sizes of the DNA fragments were compared to known DNA markers, namely the 1 Kb^+ DNA ladder (Invitrogen).

3.6.4. Isolation of DNA from Agarose Gels

The DNA band selected for purification was excised from the agarose gel under low ultraviolet light and the slice placed in an Eppendorf tube. It was then weighed, three

volumes of NaI added and the tube incubated at 55°C to 60°C to solubilize the agarose (about 15 minutes). After that, the Geneclean protocol described above was followed.

3.6.5. Ligation of DNA Products

Ligation reactions were typically carried out in a volume of 20 µl, using T4 DNA Ligase purchased from Invitrogen. After running 3 to 5 µl samples of both vector and insert on an agarose gel, an overnight reaction at room temperature was set-up that contained a 3:1 insert to vector ratio, ligation buffer at a final concentration of 1X and 2 units of T4 DNA ligase. In a parallel control, water replaced the insert.

3.6.6. Transformation of DNA

3.6.6.1. Preparaton of Chemically Component *E. coli* Cells

Transformation Storage Buffer

85%	LB (pH 6.5)
10%	PEG (molecular weight 8,000)
5%	DMSO
50 mM	$MgSO_4$

Sterilize by syringe filtration using a 0.4 µM filter.
Store at 4°C for no longer than four weeks.

Transformation of *E. coli* was performed as per (Transformer Site-Directed Mutagenesis Kit Manual, Catolog No. K1600-1; Protocol No. PT1130-1; Version No., PR13832; Chung, 1989). Typically, 10 ml of cells were grown in LB or LBK until OD_{600}=0.4 to 0.5, pelleted at 17,400 x g in 50 ml centrifuge bottles in a JA-20 Beckman Rotor and then resuspended in Transformation Storage Buffer at $1/20^{th}$ the original culture volume (500 µl).

3.6.6.2. Chemical Transformation of *E. coli*

5 to 20 µl of DNA (depending on the concentration) was mixed with 100 µl of chemically competent cells, placed on ice for 30 minutes, incubated at 42°C for 90 seconds and then placed on ice again for five minutes. 1.0 ml of LB or LBK was then added to the Eppendorf tube, the tubes placed in a beaker and recuperated in a 37°C shaker (250 rpm) for one hour. The cells were then pelleted at 14,000 x g and resuspended in 300 to 500 µl of LB. 100 µl aliquots were plated onto selective media and incubated inverted overnight at 37°C.

3.6.6.3. Preparation of Electrocomponent *E. coli* Cells

Wash and Resuspension Buffer

10% glycerol
Sterilize by filtration through 0.4 µM syringe filter or autoclave for 15 minutes.

Typically, 20 ml of cells were grown in LB or LBK at 37°C until OD_{600}=0.4 to 0.5, pelleted at 17,400 x g in 50 ml centrifuge bottles in a JA-20 Beckman rotor and washed three times in 10% glycerol, then resuspended in the same buffer at a concentration of $1/100^{th}$ the original starting volume. 70 µl of the resulting suspension was aliquoted into pre-chilled Eppendorf tubes, flash-freezed in liquid nitrogen and stored at –80°C until further use.

3.6.6.4. Electroporation of *E. coli*

On ice, 1 to 2 µl of ethanol precipitated DNA was mixed with 30 µl of electrocompetent cells, transferred in a 0.1 cm gapped electroporation cuvette (BioRad), placed in a electroporator (BioRad GenePulser) and the cells electro-transformed at 1.8 kV for 5.0 milliseconds. It is very important that DNA be ethanol precipitated prior to

use to eliminate any salt prior to electroporation. The transformed cells were diluted with 1.0 ml of LB or LBK, the suspension placed into an Eppendorf tube and the cells allowed to recuperate in a 37°C shaker (250 rpm) for one hour. The cells were then pelleted at 14,000 x g and resuspended in 300 to 500 µl of LB or LBK. 100 µl aliquots were plated onto selective media and incubated inverted overnight at 37°C.

3.6.6.5. Preparation of Electrocompetent *V. cholerae*

Wash and Resuspension Buffer

137 mM Sucrose
10% (vol/vol) Glycerol
The solution was sterilized by autoclaving for 15 minutes and stored at –4°C.

Typically, *V. cholerae* was grown in 50 ml of LB at 37°C until OD_{600}=0.8. On ice, the cells were pelleted at 9,000 x g in 250 ml centrifuge bottles in a JA-14 Beckman rotor and washed three times in pre-chilled wash buffer. After the third wash, the cells were pelleted and resuspended in the same buffer at a concentration of $1/100^{th}$ the original starting volume. 100 µl of the resulting suspension was aliquoted into pre-chilled Eppendorf tubes, flash-freezed in liquid nitrogen and stored at –80°C until further use.

3.6.6.6. Electroporation of *V. cholerae*

Because *V. cholerae* produces a number of exonucleases, one has to work extremely fast. On ice, very quickly 100 µl of cells and 5 µl of plasmid DNA (approximately 200 ng) were mixed, transferred into a pre-chilled 0.2 cm electroporation cuvette (BioRad) and the cells were electro-transformed at 2.4 kV for 4.0 milliseconds. Immediately, the transformed cells were diluted with 1.0 ml of LB, the suspension transferred into a test tube and the cells allowed to grow on a 37°C shaker set at 250 rpm for one to two hours. The cells were then pelleted, resuspended in 100 µl of LB, plated

onto selective LB plates containing 100 μg/ml streptomycin and the selectable antibiotic. The plates were then incubated inverted at 37°C.

3.6.7. Selection of Recombinants

3.6.7.1. pBluescript-Based Recombinants

pBluescript-KS (+/-) (Stratagene) (see Fig. 2.1) is a 2961 bp phagemid, containing a multiple cloning site within the β-galactosidase (*lacZ*) gene that allows α-complementation for blue/white colour selection of transformants on LB plates containing IPTG and X-gal. Upstream of this gene, is an inducible *lac* promoter allowing for fusion protein expression. The KS description indicates that transcription of the *lacZ* gene progresses from KpnI to SacI. This vector also contains f1 (filamentous phage) origins of replication allowing for isolation of single-stranded sense (+) or antisense (-) DNA when the host is infected with helper phage. In the absence of helper phage, it has a ColE1 origin of replication. The presence of an ampicillin resistance gene (*bla*) allows for antibiotic selection of recombinants.

3.6.7.2. pMAKSAC-Based Recombinants

pMAKSAC (A/B) (see Fig. 2.2) is a suicide vector [Favre & Viret, 2000] containing a temperature sensitive origin of replication derived from pMAK700 as well as the *sacB* gene and multiple cloning site from pKNG01. It has an *oriT* for conjugational transfer and a chloramphenicol resistance gene (*cat*) as a selectable marker. The A and B designates the orientation of the fragment containing the *sacB* gene and polylinker, to the *cat* gene. In pMAKSACA this fragment is in opposite orientation to the chloramphenicol resistance gene whereas in pMAKSACB, it is in the same. The *B. subtilis sacB* gene,

Fig. 2.1. pBluescript KS+ cloning vector. From Stratagene.

Fig. 2.1

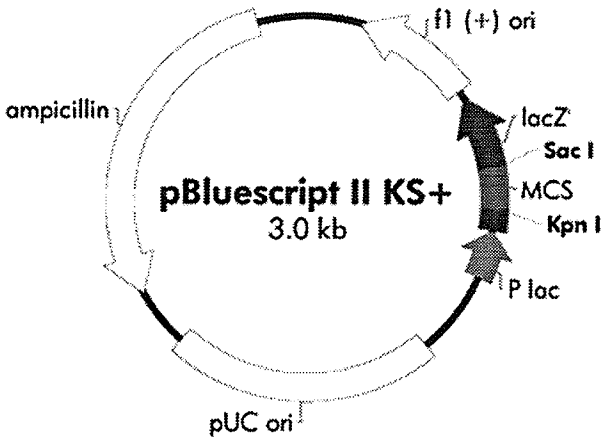
f1 (+) ori
ampicillin
lacZ'
Sac I
MCS
Kpn I
pBluescript II KS+
3.0 kb
P lac
pUC ori

Fig. 2.2. pMAKSACA and pMAKSACB vectors. See Favre & Viret, 2000, for further details.

Fig. 2.2

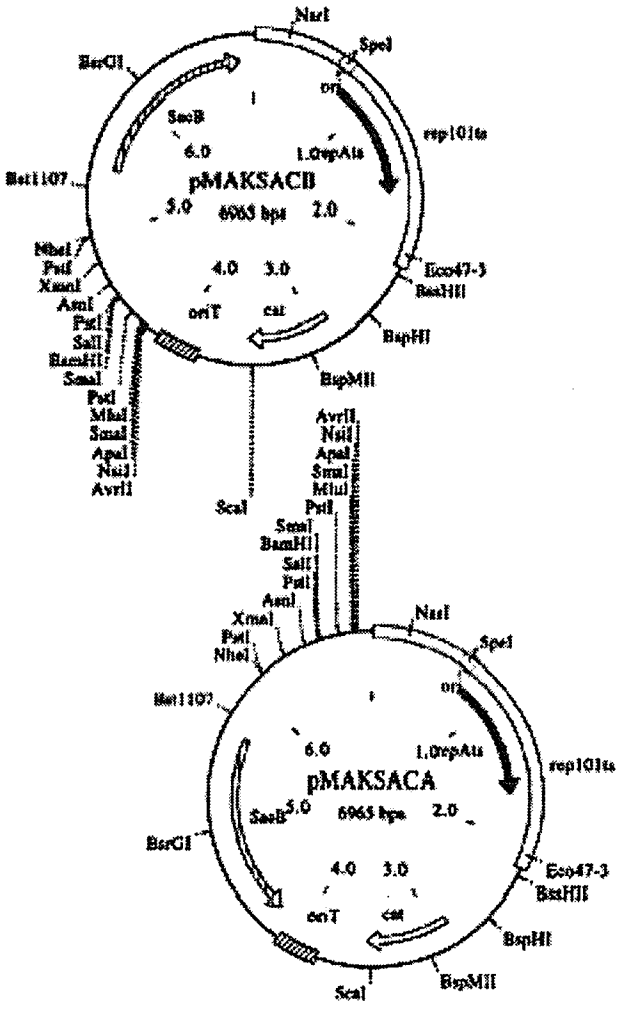
pMAKSACB
6965 bps
pMAKSACA
6965 bps
NaeI
SpeI
ori
rep101ts
SacB
BsrGI
Bst1107I
NheI
PstI
XmaI
AsnI
SalI
BamHI
SmaI
ApaI
NsiI
AvrII
MluI
Eco47-3
BstHII
BspHI
BspMII
ScaI
onT
cat

Fig. 2.3. Creating chromosomal deletions using pMAKSACA/B. The protocol is based on the procedure of Favre and Viret [Favre & Viret, 2000].

Fig. 2.3

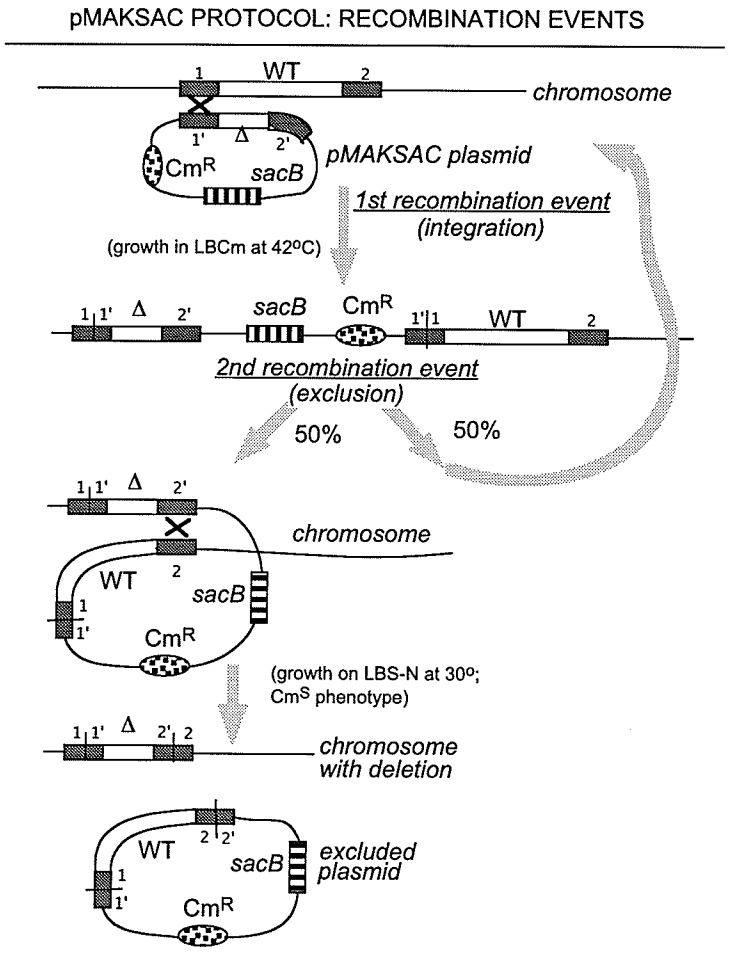
pMAKSAC PROTOCOL: RECOMBINATION EVENTS
WT
chromosome
pMAKSAC plasmid
CmR
sacB
1st recombination event
(integration)
(growth in LBCm at 42°C)
2nd recombination event
(exclusion)
50%
50%
chromosome
(growth on LBS-N at 30°;
CmS phenotype)
chromosome
with deletion
excluded
plasmid

which encodes levansucrase is one of the most popular counterselectable markers. In gram positive organisms, expression of this gene is harmless where as in gram negative bacteria, it is lethal. The mechanism of this toxicity is not well understood, but presumably it is because of the accumulation of levans (high molecular weight fructose polymers) in the periplasmic membrane, which may be toxic to the bacterium (http://www.protocol-online.org/biology-forums/posts/7391.html).

3.6.7.3. Cloning into pMAKSAC

In a typical case, the gene of interest which was flanked by approximately 1000 bp 5' and 3' ends was amplified by PCR and cloned into pBluescript using standard techniques as described above. A deletion was then created through restriction enzyme subcloned into pMAKSAC. Because this vector has a temperature sensitive origin of replication, all plates and cultures for plasmid DNA isolation were grown at 30°C.

3.6.7.4. Chromosomal Integration Procedure with pMAKSAC

The following protocol and all information regarding this procedure can be found in Favre and Viret [Favre & Viret, 2000] (see Fig. 2.3). The pMAKSAC-based construct carrying the desired gene harbouring the deletion with approximately 1000 bp 5' and 3' flanks was electroporated (or conjugated) into the relevant bacterial strain, in this case, *V. cholerae*. The electroporated cells were grown in LB or SOC medium at 30°C for at least two hours (conjugation mixtures should be left overnight at 30°C before plating onto chloramphenicol-containing medium). This is because cells containing the pMAKSAC vectors grow slowly. The electroporation or conjugation mixtures were plated onto LB containing 17 μg/ml chloramphenicol (LBCm) and the plates were incubated inverted at 30°C for greater than or equal to 24 hours. A number of transconjugant/transformant

colonies were pooled into 500 µl 1xPBS buffer, diluted in 10-fold steps up to 10,000-folds and 100 ml of each dilution plated out onto 42°C pre-warmed LBCm plates. All plates were incubated at 42°C. A pool (5 to 10) of well-isolated colonies was streaked onto a fresh 42°C pre-warmed LBCm plate. Plate(s) still showing colonies at the highest dilution of the cell suspension (often the plate with the 10^{-2} or 10^{-3} dilution) were used. The freshly streaked plates were incubated at 42°C. 10 to 20 DNA minipreps from isolated colonies were set-up in liquid LBCm and grown at 42°C. After plasmid DNA isolation was carried out, the remainder of each miniprep culture were kept at 4°C. 20 µl of the isolated DNA was run on an agarose gel and the colony(ies) of choice for further work corresponded to DNA minipreps which did not contain any visible plasmid (beware of the fact that certain amounts of chromosomal DNA are often still visible). 2 ml of LB containing 5% sucrose but without NaCl (LBS-N) was inoculated with 10 µl of the miniprep culture of choice that was kept at 4°C. The cultures were grown at 30°C for two to six hours after which, 100 µl of 10^{-3} to 10^{-7} diluted culture was plated out onto fresh LBS-N plates and grown at 30°C overnight. Colonies were then pick-plated onto LBCm and LB plates and grown at 30°C. Using the master LB plate, colonies were screened for chloramphenicol sensitivity. The colonies of choice (chloramphenicol sensitive) were then grown overnight in liquid LB at 30°C and chromosomal DNA isolation was carried out. PCR was performed on each isolated DNA to determine whether the chromosomal deletion event had occurred.

If the gene of interest is assayable, one may want to screen for its presence at each step of the procedure. This is because some genes may be unstable in this system. If this

were the case, one may try to plate out the electroporation/conjugation cultures directly at 42°C without the 30°C intermediary step.

3.7. Site-Directed Mutagenesis

PCR Reaction Components

100-300 ng	Template DNA
5 µl	10X Pfu or Pfx PCR Buffer
5 µl	50 mM $MgSO_4$
5 µl	10 mM dNTPs (Invitrogen)
5 µl	10 mM Mutagenic Primer
1 to 2 µl	Pfu (Stratagene or Fermantas) or Pfx DNA Polymerase

The volume was brought up to 50 µl with sterile double distilled water.

PCR Reaction Cycling Parametres

Segment 1	1X	94°C	5 minutes (Denaturation)
Segment 2	30X	94°C	30 seconds (Denaturation)
		60°C[a]	30 seconds (Annealing)
		68°C	1 minute per kb (Synthesis)
Segment 3	1X	68°C	7 minutes (Final Synthesis)
		4°C	∞

[a]This is the step at which primers anneal, therefore the temperature was adjusted accordingly (typically approximately 5°C below the T_m of the primer). It is best to have a T_m of greater than 60°C (Stratagene).

Site-directed mutagenesis was based on the QuikChange site-directed mutagenesis kit (Stratagene) as well as the method described by Makarova et al. [Makarova, et al, 2000]. Briefly, following PCR amplification in a reaction described above using the primers described in Table 3A, 10 to 20 µl of product was digested with DpnI to restrict any surplus parental DNA. *E. coli* XL1Blue (Stratagene) was then chemically transformed as described above and plated on selective media. The plates were grown inverted overnight at 37°C.

3.8. Isolation of Inside-Out Membrane Vesicles

3.8.1. Isolation of Inside-Out Membrane Vesicles from *E. coli*

Solution I

3.8 g KCl (100 mM)
3.0 g Tris-HCl (50 mM)
per 500 ml
The pH was adjusted to 8.0 with HCl.

Solution II

2.4 g Tris-HCl (200 mM)
per 100 ml
The pH was adjusted to 8.0 with HCl.

Solution III

34.0 g Sucrose (1.0 M)
2.4 g Tris-HCl (200 mM)
per 100ml
The pH was adjusted to 8.0 with HCl.

Solution IV

2.0 g KCl (100 mM)
17.0 g Sucrose (250 mM)
1.8 g HEPES (50 mM)
per 200 ml
The pH was adjusted to 7.5 with Tris base.

30 ml overnight cultures of *E. coli* EP432 transformants, in LBK plus 100 μg/ml ampicillin, 15 μg/ml kanamycin and 17.5 μg/ml chloramphenicol, were used to inoculate two 2000 ml Erlenmeyer flasks containing 750 ml of LBK plus the same antibiotics at a concentration of 1:100. Growth was carried out at 37°C until OD_{600} reached approximately 0.8 to 0.9 after which, the cells were collected by centrifugation in 250 ml centrifuge bottles in a JA-14 Beckman rotor at 12,400 x g for 10 minutes at 4°C. The cell pellets were then washed once in 125 ml of Solution I, centrifuged at 12,400 x g for 10 minutes, resuspended in 10 ml of pre-warmed Solution II and diluted with 10 ml of pre-

warmed Solution III. 100 µl of 0.1 M EDTA (pH 8.0) and 20 mg of lysozyme were added and incubation took place for 20 minutes with gentle shaking at 37°C. To stop the lysozyme, 200 µl of 1 M $MgSO_4$ was added and the sphaeroplasts were spun-down in 50 ml centrifuge bottles at 17,400 x g in a Beckman JA-20 rotor for 10 minutes at 4°C. The pellet was resuspended in a 20 ml isoosmotic buffer (10 ml Solution I, 10 ml Solution II, 10 mM $MgSO_4$) and again centrifuged for 10 minutes at 17,400 x g at 4°C. On ice the resulting pellet was resuspended in 20 ml ice-cold Solution IV after which 1 mM DTT, 20 µg/ml pepstatin A, 1 mM phenylmethylsulfonyl flouride (PMSF), which blocks the active serine in serine proteases, and approximately 5 mg/L DNase was added. The solution was passed twice through the French Press (American Instrument Company, Incorporated) set at "1000" on the scale, MED ratio (3000 psi) into clean 50 ml centrifuge bottles. The unbroken cells were pelleted by centrifugation at 17,400 x g for 20 minutes at 4°C. The supernatant was then ultracentrifuged in an Optima LE-80K ultracentrifuge (Beckman-Coulter) at 257,090 x g for 1.5 hours at 4°C using the 70Ti rotor (Beckman). The supernatant was carefully removed and the membrane pellet resuspended in 500 to 1000 µl of Solution IV containing all inhibitors, but no DNase, with a 1.0 cc syringe (Becton Dickinson & Company) using a 23G 1 needle (Becton Dickinson & Company), then a 25G 5/8 needle (Becton Dickinson & Company). 75 µl to 100 µl of inside-out of vesicles were aliquoted into Eppendorf tubes, flash frozen in liquid nitrogen and stored at –80°C until further use. The total protein concentration was determined as described below. One can determine if the vesicles are indeed inside-out by checking whether they are able to form a transmembrane pH gradient at the expense of ATP hydrolysis since the

membrane module i.e., the ion translocating part of the ATPase enzyme will be facing the vesicular exterior (see Fig. 2.4).

3.8.2. Isolation of Inside-Out Membrane Vesicles from *V. cholerae*

***Vibrio* Vesicle Buffer**

10 mM	MOPS
10% (w/v)	Glycerol
0.2 M	K_2SO_4
25 mM	$MgSO_4$

Cells were grown with vigorous aeration (250 rpm) in two 2000 ml flasks containing 500 ml of LB at 37°C to mid-log phase (OD_{600} approximately equal to 1.3 to 1.5). The cells were then cooled in on ice for 30 minutes, harvested by centrifugation in 250 ml centrifuge bottles, in a JA-14 rotor (Beckman-Coulter) at 12,400 x g, 4°C for 10 minutes. Cells were then washed twice in ice-cold *Vibrio* Vesicle Buffer, by resuspending and pelletting them at 12,400 x g, 4°C for 10 minutes. After the second wash, the pellet was resuspended in the same buffer and 1 mM DTT, 20 μg/ml Pepstatin-A, 1 mM phenylmethylsulfonyl flouride (PMSF) and 5 mg/L DNase added. The suspension was then passed twice through the French Press (American Instrument Company, Incorporated) set at "1000" on the scale, MED ratio into 50 ml centrifuge bottles. Unbroken cells were removed by centrifugation in JA-20 rotor (Beckman-Coulter) at 23,680 x g for 20 min. The membrane vesicles were then pelleted by ultracentrifugation in Ti70 rotor (Beckman-Coulter) at 257,090 x g at 4°C for 90 minutes. The supernatant was carefully decanted and the vesicles washed once by resuspending then in *Vibrio* Vesicle Buffer (without DNase) containing DTT, Pepstatin-A and PMSF as above and ultracentrifuging for 90 minutes at 257,090 x g at 4°C. The final membrane

pellet was then resuspended in the same buffer. The vesicles were aliquoted (50-75 μl) into pre-chilled Eppendorf tubes, flash frozen in liquid nitrogen and stored at -80°C.

3.9. Measuring Changes in ΔpH and Δψ in Inside-Out Membrane Vesicles

***E. coli* Experimental Buffer**

100 mM	KCl
250 mM	Sucrose
50 mM	HEPES
10 mM	$MgSO_4$

***V. cholerae* Experimental Buffer**

200 mM	K_2SO_4
10%	Glycerol
10 mM	Tris
25 mM	$MgSO_4$

ΔpH measurements (Acridine Orange)

Scan Mode	Time
Emission Wavelength	528.0 nm
Excitation Wavelength	492.0 nm

Δψ measurements (Oxonol V)

Scan Mode	Time
Emission Wavelength	630.0 nm
Excitation Wavelength	595.0 nm

For experiments with *E. coli* vesicles, a series of Experimental Buffers were prepared with varying pHs (6.0, 6.5, 7.0, 7.5, 8.0, 8.5, 9.0), using MES for pH 6.0 to 6.5, HEPES for pH 7.0 to 8.0 and Tris for pH 8.5 to 9.0. For experiments with *V. cholerae* vesicles, a series of Experimental Buffers were prepared from pH 6.0 to pH 9.0, using H_2SO_4. NaOH or KOH was never used for adjustment. The $Na^+(Li^+)/H^+$ antiport activity was registered using acridine orange/oxonol V fluorescence dequenching (Fig. 2.4). $MgSO_4$ was added to a final concentration of 10 mM to each experimental buffer prior to the assay. 2 ml of buffer was aliquoted into a four-sided quartz cuvette with a 10 mM

Fig. 2.4. Analysis of inside-out membrane vesicles (the acridine orange fluorescence dequenching assay). This approach is based on the fact that some weak amines emit light upon illumination (fluorescence). Acridine orange penetrates the membrane only in its uncharged form and does not when it is protonated. In Na^+-free medium, H^+ are pumped into the vesicle, resulting in the uptake of acridine orange (titrates internal acid) leading to a decrease in fluorescence - ***quenching***. After addition of Na^+, Na^+/H^+ exchange leads to efflux of acridine orange (titrates external acid) resulting in a rise in fluorescence - ***dequenching***. The ratio ***D/Q*** is used as a measure of the activity of the Na^+/H^+ antiporter.

Fig. 2.4

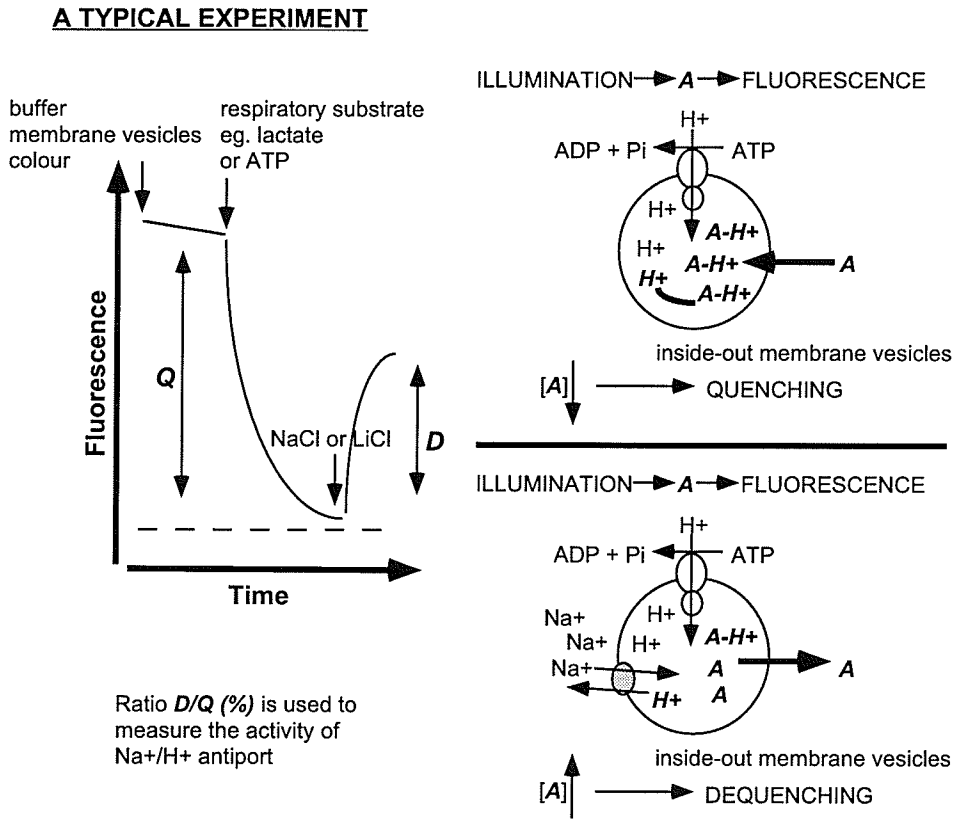
A TYPICAL EXPERIMENT
buffer
membrane vesicles
colour
respiratory substrate
eg. lactate
or ATP
Fluorescence
Q
NaCl or LiCl
D
Time
Ratio D/Q (%) is used to measure the activity of Na+/H+ antiport
ILLUMINATION → A → FLUORESCENCE
H+
ADP + Pi
ATP
H+
A-H+
H+
A-H+
A
H+
A-H+
inside-out membrane vesicles
[A]
QUENCHING
ILLUMINATION → A → FLUORESCENCE
H+
ADP + Pi
ATP
Na+
Na+
Na+
H+
H+
A-H+
A
A
H+
A
inside-out membrane vesicles
[A]
DEQUENCHING

light path (Hellma Canada Limited), then 1 to 2 μl of 10 mM acridine orange (Sigma) or 1 to 2 μl of 0.5 μM Oxonol V (Fluka Biochemika) prepared in water. The solution was mixed and the steady-state level of fluorescence recorded on a RF-1501 spectrofluorophotometre (Shimadzu Scientific Instruments Incorporated) equipped with a Multistirrer magnetic stirrer (Scinics Company, Limited), using the RF-1500 Series Communications Program Pack (Shimadzu Scientific Instruments Incorporated) and the above parameters. Then, approximately 200 μg of inside-out vesicles was added to the cuvette until a new steady-state level was achieved. After that, 20 μl of 1 M lactate (pH in the stock solution should be adjusted to 7.5 with Tris) to a final concentration of 10 mM was added until a new steady-state level of fluorescence was obtained. Then, 10 μl of 2 M LiCl or 2 M NaCl was added to final concentration of 10 mM (unless otherwise stated) until a new steady-state was observed.

In the case of experiments with *E. coli* vesicles in the presence of AP, the only modifications were as follows: 50 mM HEPES was replaced with 50 mM BTP-HCl (pH 7.5) and $MgSO_4$ was substituted for $MgCl_2$.

In the case of *V. cholerae* vesicles, the only modifications were as follows: Since the degree of respiration dependent ΔpH formation varied upon the addition of lactate to inside-out membrane vesicles, succinate-Tris (pH 7.5) to a final concentration of 10 mM was used as a respiratory substrate (the resulting degree of transmembrane pH gradient was always robust). With respect to studies with ATPase, 10 mM ATP replaced succinate. Because chloride precipitates out in the presence of Ag^+, as far as assays carried out with $AgNO_3$, the experimental buffer contained no Cl^- ions.

Some of the advantages of utilising inside-out membrane vesicles to study $Na^+(Li^+)/H^+$antiport in bacteria are as follows: (i) it is easy to study ion translocation across the membrane since the vesicles can be loaded with fluorescent probes allowing for the analysis of Na^+ and H^+ transport mechanisms across the vesicular membrane (see Fig. 3.4); (ii) the external and internal pH, ionic and chemical composition of the membrane vesicle can be easily manipulated. Some of the disadvantages of this system are as follows: (i) is not as pure as purified protein incorporated into proteoliposomes; (ii) one never knows whether the protein will survive the isolation. For example a loosely bound periplasmic component can be lost during the process.

3.10. Protein Determination

***DC* Protein Assay Reagent A**
Sodium Hydroxide

***DC* Protein Assay Reagent B**
Folin Reagent (mixture)

***DC* Protein Assay Reagent S**
Sodium dodecyl sulfate

***DC* Protein Assay Reagent A'**
Add 20 µl of Reagent S to every 1.0 ml of Reagent A
that will be required for the assay.

Relative protein concentrations were determined using the Standard Assay Protocol as described in the *DC* (Detergent Compatible) Protein Assay Kit manual (Bio-Rad). Protein standards were prepared containing a series of concentrations of bovine serum albumin (BSA) from 0.2 mg/ml to 5.0 mg/ml in the same buffer as the sample. The kit has been designed so that one can analyse membrane proteins with the use of Reagent A'. Next 100 µl of each standard was aliquoted into clean test tubes (blank, sample buffer)

and 500 µl of Reagent A' was added. The tubes were then mixed by shaking. Next, 4.0 ml of Reagent B was placed into each tube and the tubes mixed by vigorous shaking. After 15 to 20 minutes, the absorbance was read at 750 nm and a graph was prepared by plotting OD_{750} versus BSA in µg. Protein samples were typically analysed in 5 to 20 µl aliquots in a total volume of 100 µl. The assay was carried out as above.

3.11. SDS-Polyacrylamide Gel Electrophoresis

Standard SDS Loading Buffer

12.5 ml	Tris-HCl/SDS (pH 6.8)
30 ml	10% SDS
10 ml	Glycerol
5.0 ml	β-mercaptoethanol
5-10 mg	Bromphenol Blue (enough to give dark blue colour to the solution)

The volume was brought up to 100 ml with sterile double-distilled water, then divided into 1.0 aliquots and stored at –20°C.

Separating Gel (12%)

6.5 ml	Double-Distilled Water
7.5 ml	1 M Tris (pH 8.8)
0.2 ml	10% SDS
6.0 ml	40% Bis-AA (29:1, 3.3% C) (Bio-Rad)
300 µl+20 µl	APS + TMED (BioRad)

Stacking Gel

2.5 ml	1 M Tris (pH 6.8)
0.1 ml	10% SDS
1.25 ml	40% Bis-AA (29:1, 3.3% C) (Bio-Rad)
150 µl	APS (Bio-Rad)
10 µl	TEMED (BioRad)

Running Buffer (5X)

15 g/L	Tris (0.125 M)
72 g/L	Glycine (0.96 M)
5.0 g/L	SDS (0.5%)

The solution was filtered through 0.45 µM filter and store at 4°C. One volume of 5X stock was diluted with four volumes double-distilled water for electrophoretic run.

Staining Solution

50% (v/v)	Methanol
0.05% (v/v)	Coomassie Brillliant Blue R-250 (Bio-Rad)
10% (v/v)	Acetic Acid
40%	Distilled Water

The solution was prepared in distilled water.
Coomassie Brilliant Blue R was disolved in methanol before adding acetic acid and water.
The solution was stored for up to six months.
If precipitate appeared after prolonged storage, the solution was filtered.

Destaining Solution

7%	Acetic Acid
15%	Methanol

The Mini-PROTEAN II Electrophoresis Cell was assembled according to the manufacturer instructions (Bio-Rad). SDS-PAGE was performed according to the protocol provided by the Mini-PROTEAN II Electrophoresis Cell Manual (Bio-Rad). Briefly, a separating gel was prepared by combining all the reagents above accept the APS and TEMED. A comb was placed into the assembled gel sandwich consisting of two glass plates separated by a gel spacer and a mark was placed 1 cm below the teeth of the comb (level to which separating gel should be poured). After degassing, APS and TEMED were then added to the separating gel and it was pipetted within the gel sandwich using a pipet. The layer was immediately overlayed with isobutanol using a Pasteur pipet affixed with a bulb. The gel was allowed to polymerize for 45 minutes to one hour. After polymerization, the overlay was rinsed off copiously with water and the area above the separating gel dried with a filter paper. Next, a stacking gel was prepared by combining all ingredients except the APS and TMED. A comb was then placed within the gel sandwich. After degassing, the APS and TMED were added to the stacking gel and it was poured into the apparatus until the teeth of the comb were completely covered.

The gel was allowed to polymerize for 30 to 45 minutes. The comb was removed and the wells rinsed with distilled water before adding the running buffer. Protein samples were diluted into Standard SDS Loading Buffer and heated at 42°C for 20 to 30 minutes prior to loading. Samples were loaded into the wells under the running buffer using a Hamilton syringe along with prestained SDS PAGE Low Range Standards (BioRad) and electrophoresis was conducted at 100 V. The gel was then stained for 1 hour with Staining Solution. Destaining of gels was then carried out in Destaining Solution typically for 2-5 hours.

3.12. Western Immunoblotting

Because polyclonal antibodies are generally cheaper than monoclonal antibodies and a large quantity can be produced relatively quickly, anti-NhaD antibodies were produced by Genemed Synthesis, Incorporated using their standard rabbit polyclonal technique against the following peptide from a cytoplasmic IX-X loop of Vc-NhaD: ^{316}AKNDEAALKRIGSVVPFDVFRSISHA^{341}C (C-terminal cysteine added for coupling.) The antibodies were affinity purified using the above peptide coupled to SulfoLink Coupling Gel (Pierce). The procedure recommended by the manufacturer was followed, except that the antibodies were eluted from the column in 0.5 ml fractions into Eppendorf tubes containing 50 µl of glycerol and 50 µl of 1 M Tris-HCl (pH 7.5) to prevent antibody precipitation.

Membrane vesicles from different *V. cholerae* strains were isolated as described above. Aliquots containing 100 µg of total membrane protein were incubated on ice for 15 minutes in 200 µl of 0.1 M sodium carbonate. The samples were then pelleted by

ultracentrifugation at 540478 x g in a TLA 100.3 Beckman rotor for 30 minutes. The membrane pellet was re-suspended in 200 µl of a Standard SDS-PAGE Loading Buffer and incubated at 42°C for 30 minutes with shaking. For electrophoresis, 20 µl of sample was loaded per lane. Proteins were resolved in 12% polyacrylamide gels and transferred onto a PVDF Western Blotting membrane (Boehringer Mannheim GmbH) using semi-dry transfer. The membranes were blocked at room temperature with 10% skim milk powder dissolved in PBS with 1% TWEEN 20 (Sigma) (PBST) for 30 minutes. Then the membrane was incubated with the affinity purified anti-NhaD antibodies at a dilution of 1:3000 in 2% skim milk powder dissolved in PBST. The blot was rinsed 5 times for 5 minutes each with PBST, and incubated for 30 minutes with Goat Anti-Rabbit IgG Horseradish Peroxidase Conjugate (BioRad) at a dilution of 1:3000 in 2% skim milk powder dissolved in PBST. The blot was rinsed 5 times for 5 minutes each with PBST. Immunoreactive proteins were visualized using the Amersham Enhanced Chemiluminescence kit as recommended by the manufacturer. A Fluoro Chem™ 8900 was used to detect the resulting signal [Habibian et al., 2005].

3.13. Computer Analysis of DNA and Amino Acid Sequences

Genomic sequence analysis of *V. cholerae* was carried out using the Genome Database posted by The Institute for Genomic Research (TIGR). Derived amino acid sequences were aligned using BLASTP 2.0.9 and TopopredII [Claros and von Heijne, 1994] was used to predict amino acids located within transmembrane segments. Public databases maintained by the National Center for Biotechnology Information (http://www.ncbi.nlm.nih.gov), namely the NCBI Conserved Domain Database

(http://www.ncbi.nlm.nih.gov/Structure/cdd) and the NCBI Clusters of Orthologous Groups of Proteins (http://www.ncbi.nlm.nih.gov/COG) were searched and the sequences aligned using ClustalW [Higgins, et. al., 1994]. The obtained alignment was used by Dr. P. C. Loewen (Department Microbiology, U of M) to construct phylogenetic trees with the PROTDIST FITCH, RETREE and DRAWGRAM components of PHYLIP package (http://evolution.genetics.washington.edu/phylip). As well, sequences were analysed using The Membrane Transport Protein Classification database maintained by M. Saier and colleagues (http://www-biology.ucsd.edu/~msaier/transport).

4. RESULTS AND DISCUSSION

4. RESULTS AND DISCUSSION

4.1. Cloning and Functional Expression in *E. coli* of Vc-NhaD, Na^+/H^+ Antiporter of *V. cholerae*

4.1.1. Introduction

The mechanisms of Na^+/H^+ antiport and its role in *V. cholerae* physiology are still poorly investigated. As mentioned, in *Escherichia coli*, a pair of two electrogenic Na^+/H^+ antiporters, NhaA and NhaB, have been studied in great detail [Padan & Schuldiner, 1994; Padan & Schuldiner, 1996] and deletion of the *nhaA* gene in *E. coli* impairs cell growth at alkaline pH in the presence of NaCl or LiCl [Padan & Schuldiner, 1994]. Surprisingly, a *nhaA*-deficient mutant strain of *V. cholerae* was able to grow in the presence of up to 1.0 M NaCl over a pH range from 7.0 to 9.5 [Vimont & Berche, 2000] implying the existence of an additional system involved in pH-regulation and halotolerance. To further study the role of Na^+/H^+ antiport in *V. cholerae*, we have cloned and characterized a new Na^+/H^+ antiporter, Vc-NhaD. The *nhaD* gene from *V. cholerae* is very similar to the recently identified *nhaD* from *V. parahaemolyticus* (see below).

4.1.2. Cloning of the *nhaD* Gene

First, we screened the *V. cholerae* genome database posted by The Institute for Genomic Research (TIGR) with the BLAST program using the DNA sequence of NhaD from *V. parahaemolyticus* [Nakamura et al., 1994] as a query. The corresponding open reading frame (ORF) was indeed found. Both DNA and derived amino acid sequences obtained showed very high degrees of similarity to the *V. parahaemolyticus* counterpart, with 78% identities in the case of NhaD amino acid sequences. This putative Vc-NhaD

Fig. 4.1. Construction of pBLDL. The*V. cholerae nhaD* gene was generated by PCR using chromosomal DNA isolated from *V. cholerae* strain O395-N1 as a template and was directionally cloned into pBluescript-KS+ as an EcoR1/BamHI fragment, as described in "Materials and Methods". Figure made using DNA Strider Version 1.3.f14.

Fig. 4.1

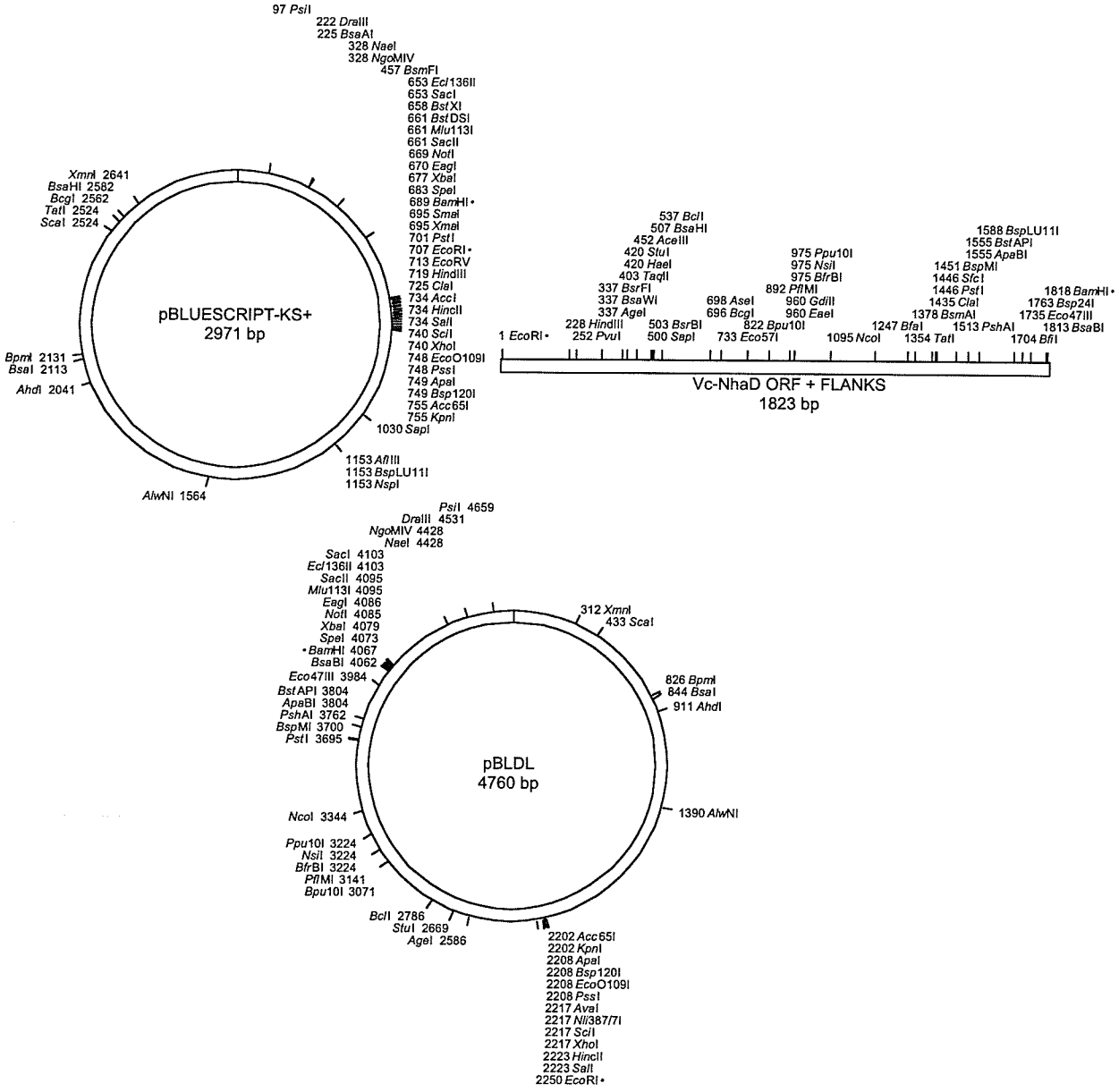
pBLUESCRIPT-KS+
2971 bp
97 PsiI
222 DraIII
225 BsaAI
328 NaeI
328 NgoMIV
457 BsmFI
653 Ecl136II
653 SacI
658 BstXI
661 BstDSI
661 Mlu113I
661 SacII
669 NotI
670 EagI
677 XbaI
683 SpeI
689 BamHI
695 SmaI
695 XmaI
701 PstI
707 EcoRI
713 EcoRV
719 HindIII
725 ClaI
734 AccI
734 HincII
734 SalI
740 SciI
740 XhoI
748 EcoO109I
748 PssI
749 ApaI
749 Bsp120I
755 Acc65I
755 KpnI
1030 SapI
1153 AflIII
1153 BspLU11I
1153 NspI
AlwNI 1564
XmnI 2641
BsaHI 2582
BcgI 2562
TatI 2524
ScaI 2524
BpmI 2131
BsaI 2113
AhdI 2041
537 BclI
507 BsaHI
452 AceIII
420 StuI
420 HaeI
403 TaqII
337 BsrFI
337 BsaWI
337 AgeI
228 HindIII
252 PvuI
503 BsrBI
500 SapI
698 AseI
696 BcgI
733 Eco57I
822 Bpu10I
892 PflMI
960 GdiII
960 EaeI
975 Ppu10I
975 NsiI
975 BfrBI
1095 NcoI
1247 BfaI
1378 BsmAI
1446 SfcI
1446 PstI
1435 ClaI
1354 TatI
1513 PshAI
1588 BspLU11I
1555 BstAPI
1555 ApaBI
1451 BspMI
1818 BamHI
1763 Bsp24I
1735 Eco47III
1704 BfiI
1813 BsaBI
1 EcoRI
Vc-NhaD ORF + FLANKS
1823 bp
pBLDL
4760 bp
PsiI 4659
DraIII 4531
NgoMIV 4428
NaeI 4428
SacI 4103
Ecl136II 4103
SacII 4095
Mlu113I 4095
EagI 4086
NotI 4085
XbaI 4079
SpeI 4073
BamHI 4067
BsaBI 4062
Eco47III 3984
BstAPI 3804
ApaBI 3804
PshAI 3762
BspMI 3700
PstI 3695
NcoI 3344
Ppu10I 3224
NsiI 3224
BfrBI 3224
PflMI 3141
Bpu10I 3071
BclI 2786
StuI 2669
AgeI 2586
312 XmnI
433 ScaI
826 BpmI
844 BsaI
911 AhdI
1390 AlwNI
2202 Acc65I
2202 KpnI
2208 ApaI
2208 Bsp120I
2208 EcoO109I
2208 PssI
2217 AvaI
2217 Nli3877I
2217 SciI
2217 XhoI
2223 HincII
2223 SalI
2250 EcoRI

ORF together with its flanking regions was directionally cloned into the pBluescript vector, as described below, yielding the pBLDL construct (Fig. 4.1).

The *V. cholerae nhaD* gene was cloned by PCR using chromosomal DNA isolated from *V. cholerae* strain O395-N1 as a template, as described in "Materials and Methods". Primers ECF (5'-TAG CAT GAA TTC TAA AAA ATG ATG AAT AAA CAA CCA TTT CTA AGC-3' [an introduced *EcoR*I site is underlined]) and BM (5'-CAT TAC GGA TCC AGA TCC GTA ATA ACT CC-3' [an introduced *BamH*I site is underlined]) were used. Following a "hot start" (94°C for 5 min), PCR was carried out with 30 cycles of amplification of 30 seconds at 94°C, 30 seconds at 60°C, and 110 seconds at 68°C. The resulting 1837 bp PCR product containing the putative *nhaD* ORF together with 154 bp-long 5' and 230 bp-long 3' flanking sequences, was directionally cloned into the pBluescript II KS+ (Stratagene) vector as an *Eco*RI-*Bam*HI fragment yielding the pBLDL construct (Fig. 4.1). The 1837 bp PCR insert was sequenced and found to be identical to the sequence reported by TIGR.

4.1.3. Effect of Vc-NhaD on the Growth of ΔNhaA,ΔNhaB *E. coli*

The pBLDL plasmid was transformed into *E. coli* strain EP432 bearing disruptions in the *nhaA* and *nhaB* genes for further characterization. Vc-NhaD restored the ability of EP432 to grow in the presence of high concentrations of LiCl or NaCl, verifying the functional expression of this antiporter in *E. coli* (Fig. 4.2). To assess the physiological effect of the Vc-NhaD expressed in EP432, the growth of EP432/pBLDL transformant cells was monitored in LBK medium supplemented with 100 mM LiCl at pH from 6.0 to 8.4 as described in "Materials and Methods". Because Li^+ is much more toxic to cells than Na^+, one can use relatively low LiCl concentrations to evaluate salt resistance.

Fig. 4.2. Vc-NhaD protects cells of the Δ*nhaA*Δ*nhaB* strain of *E. coli* EP432 from external LiCl. The pBLDL plasmid, which contains Vc-NhaD (●), was used to transform *E. coli* strain EP432 bearing disruptions of *nhaA* and *nhaB* genes. For control experiments, cells of EP432 were transformed with "empty" pBluescript vector (○). The growth experiment was carried out as described in "Materials and Methods." Briefly, overnight cultures of EP432 transformants were grown aerobically in LBK medium and the appropriate antibiotics. Test tubes containing 2.0 ml of LBK supplemented with 100 mM LiCl adjusted to the desirable pH with 60 mM HEPES-Tris were inoculated with the overnight cultures, to have a starting OD_{600} of 0.05. Ampicillin at a concentration of 100 μg/ml, kanamycin 30 μg/ml and chloramphenicol 17.5 μg/ml was added to all experimental media. After 16 hours at 37°C, growth of *E. coli* was measured as the absorbance of the bacterial suspension at 600 nm. Represents the average of five independent experiments. The standard deviation is shown.

Fig. 4.2

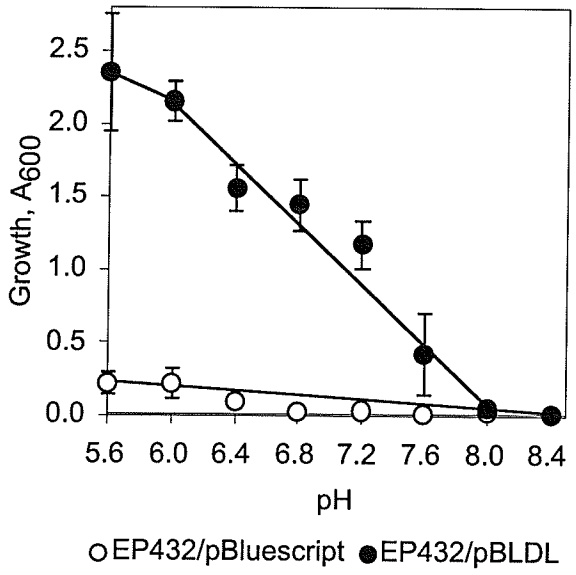
2.5
2.0
1.5
1.0
0.5
0.0
Growth, A_{600}
5.6 6.0 6.4 6.8 7.2 7.6 8.0 8.4
pH
EP432/pBluescript
EP432/pBLDL

eliminating unwanted osmotic effects. EP432/pBluescript-KS+ transformed cells were used as a control in the experiment. As one can see from Fig. 4.2, Vc-NhaD restored the ability of EP432 to grow in the presence of LiCl at pH 6.0 to 7.6, whereas the growth of EP432/pBluescript-KS+ was prevented at any pH tested. However, protection against LiCl offered by Vc-NhaD was considerably less pronounced in more alkaline media (Fig. 4.2).

4.1.4. Characterization of the Vc-NhaD in Inside-Out Membrane Vesicles

Direct measurement of the Vc-NhaD activity was performed in everted sub-bacterial membrane vesicles prepared from EP432/pBLDL and EP432/pBluescript-KS+ as described in "Materials and Methods". The antiport activities, expressed as percent restoration of the lactate-induced fluorescence quenching, revealed that introduction of the *nhaD* gene restored the Na^+-dependent H^+ translocation in membranes of EP432, confirming the functional expression of the *V. cholerae* antiporter in *E. coli* at the biochemical level (Fig. 4.3).

The most striking feature of Vc-NhaD turned out to be the pH-profile of its activity. Vc-NhaD was found to be active at pH 7.0, had a sharp maximum of activity close to pH ~8.0 and was totally inactive at pH 8.75 (Fig. 4.4).

The affinity of a Na^+/H^+ antiport system for translocated alkali cations is a feature important for the overall Na^+ homeostasis. In order to assess the affinity of Vc-NhaD for Na^+, we titrated the dequenching response in sub-bacterial vesicles isolated from EP432/pBLDL by the concentration of added NaCl at pH 8.0 (pH optimum of activity) (Fig. 4.5). These measurements yielded the concentration of Na^+ required for a half-maximal response ($[Na^+]_{1/2}$ = 1.1 mM). Although $[Na^+]_{1/2}$ is only indirectly related to the

Fig. 4.3. Na^+/H^+ antiport activity measured at pH 8.0 in inside-out membrane vesicles prepared from EP432/pBluescript (left trace) or EP432/pBLDL (right trace) cells. Inside-out membrane vesicles were isolated as described in "Materials and Methods." Protein content in membrane vesicles was determined by the Bio-Rad Detergent Compatible Protein Assay Kit as recommended by the manufacturer, using BSA as a standard. Briefly, aliquots of vesicles (~200 mg) were resuspended in buffer containing 100 mM KCl, 250 mM sucrose, 10 mM $MgSO_4$, 0.5 μM acridine orange and 50 mM HEPES-Tris adjusted to pH 8.0. The $Na^+(Li^+)/H^+$ antiporter activity was measured by the acridine orange fluorescence dequenching method [Harel-Bronstein et al., 1995]. At the indicated times, respiration-dependent formation of the transmembrane pH gradient was iniated by the addition of 10 mM Tris-D-lactate and the resulting quenching of acridine orange fluorescence was monitored in a Shimadzu RF-1501 spectrofluorometre with the excitation at 492 nm and emission at 528 nm. Na^+/H^+ antiporter activity was detected upon the addition of 10 mM NaCl, which resulted in collapse of the ΔpH. Fluorescence is shown as arbitrary units. Representative of a typical trace.

Fig. 4.3

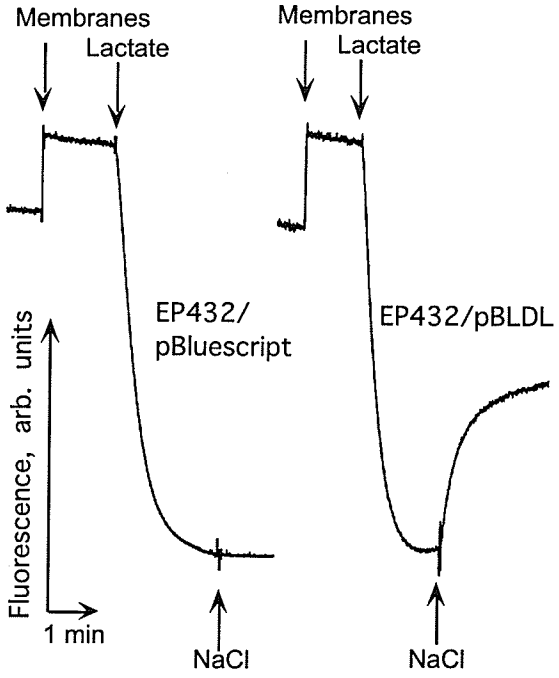
Membranes
Lactate
Membranes
Lactate
EP432/
pBluescript
EP432/pBLDL
Fluorescence, arb. units
1 min
NaCl
NaCl

Fig. 4.4. pH profile of Vc-NhaD activity measured in acridine orange fluorescence dequenching in EP432/pBLDL inside-out membrane vesicles. $Na^+(Li^+)/H^+$ antiport activity was measured in inside-out membrane vesicles resuspended in buffer adjusted to the indicated pH with 50 mM HEPES-Tris as described in Fig. 4.3. Activity is expressed as percent of the initial fluorescence quenching. 10 mM NaCl (○) or 10 mM LiCl (●) were used to initiate dequenching. Representative of a typical experiment.

Fig. 4.4

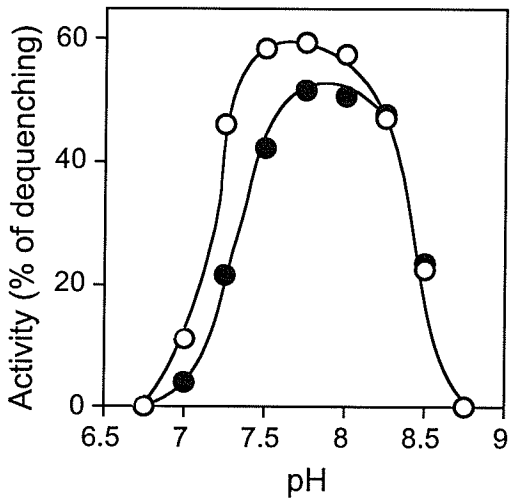

Fig. 4.5. Determination of the concentration of Na^+ required for half-maximal response of Vc-NhaD in inside-out membrane vesicles derived from EP432/pBLDL cells. Measurements were done at pH 8.0 with the final concentration of added NaCl varying from 0.5 to 20 mM. All the other conditions are as in Fig. 4.3. A $[Na^+]_{1/2}$ value of 1.1 mM was determined. The data points represent the average of two independent experiments.

Fig. 4.5

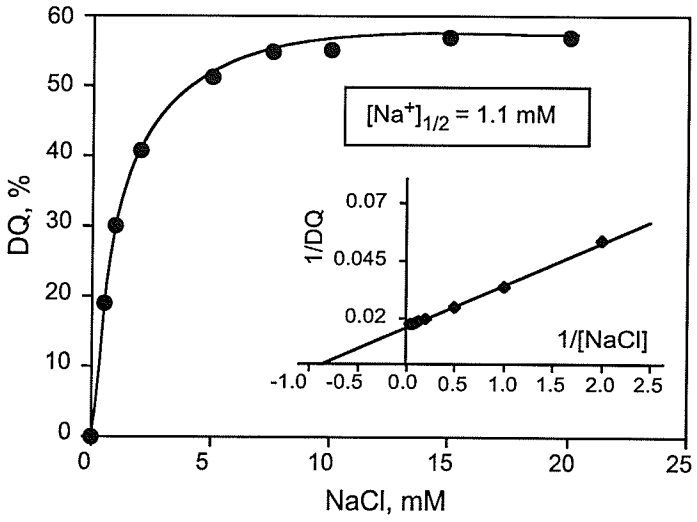
60
50
40
30
20
10
0
DQ, %
0
5
10
15
20
25
NaCl, mM
[Na+]1/2 = 1.1 mM
0.07
0.045
0.02
1/DQ
-1.0
-0.5
0.0
0.5
1.0
1.5
2.0
2.5
1/[NaCl]

actual K_m of the antiporter, this easily assessable parameter is a standard measure of the antiporter affinity [Nakamura et al., 1996]. The value of $[Na^+]_{1/2}$ for Vc-NhaD was comparable to that found previously for Ec-NhaA (0.2 mM at pH 8.0) [Nakamura et al., 1996], characterizing Vc-NhaD as an antiporter with a rather high affinity for transported alkali cation (Fig. 4.5).

4.1.5. Discussion

We found that the membrane of *V. cholerae* contains a Na^+/H^+ antiporter, Vc-NhaD, in addition to the "standard" pair of bacterial antiporters, NhaA and NhaB. Vc-NhaD was found to be a functional Na^+/H^+ antiporter, complementing an *E. coli* Δ*nhaA*Δ*nhaB* mutant phenotype. Most interestingly, Vc-NhaD demonstrated a unique pH-profile of activity different from that of any bacterial Na^+/H^+ antiporter described so far. In two different pH-dependent bacterial antiporters, Ec-NhaA and Vp-NhaD, the activity increases with the rise in pH [Gerchman et al., 1993; Nozaki et al., 1998]. It has been shown that Vp-NhaD is inactive at pH 7.5 and displays maximal activity in the pH range from 8.5 to 9.0 [Nozaki et al., 1998]. This, therefore, characterizes Vp-NhaD as a functional analog of Ec-NhaA antiporter, which has a very similar pH-profile [Gerchman et al., 1993; Olami et al., 1997]. Activity of another bacterial Na^+/H^+ antiporter, Ec-NhaB, does not depend on pH at all [Padan & Schuldiner, 1994; Padan & Schuldiner, 1996]. In contrast, Vc-NhaD displays a sharp pH optimum of activity at pH close to 8.0 (Fig. 4.4).

Noticeably, introduction of the *nhaD* gene into the double ΔNhaAΔNhaB *E. coli* mutant confers significant resistance against added LiCl over the pH range from 6.0 to

7.6 with decrease at more alkaline pHs (Fig. 4.2). One may ask why an antiporter, which is apparently inactive at pH below 7.0 (Fig. 4.4), provides the cell with the most efficient protection against external Li^+ (as well as Na^+) at pH 6.0 - 7.2 (Fig. 4.2)? It should be noted in this connection that in the experiments with sub-bacterial vesicles the experimental buffer is equivalent to the cell cytoplasm. Thus, pH-profiles of activity measured in such assays reflect the dependence of antiport on intracellular rather than extracellular pH. At acidic external pH, transmembrane circulation of K^+ rather than Na^+ is responsible for the maintenance of more alkaline pH in the bacterial cytoplasm [Booth, 1985]. Thus, in acidic media, K^+-related pH homeostatic mechanisms could maintain the cytoplasmic pH in EP432 cells at levels sufficient for operation of Vc-NhaD encoded in pBLDL. In addition, rates of $Na^+(Li^+)$ influx could be lower at acidic pH. Ikegami and co-authors reported similar results for *Enterococcus hirae* cells with both Na^+/H^+ antiporter and Na^+-ATPase deleted [Ikegami et al., 2000]. The double deletion did not prevent growth in high Na^+ medium at pH 5.5. The authors concluded that H^+ and Na^+ homeostasis in this bacterium at low pHs is maintained by a decreased Na^+ influx and normally functioning K^+ uptake rather than by active export of alkali cations [Ikegami et al., 2000].

4.2. Mutational Analysis and Biochemical Properties of Vc-NhaD

4.2.1. Introduction

As discussed in the "Literature Review," Na^+/H^+ antiporters are universal secondary ion transporters in bacteria. Typically, they expel toxic Na^+ and Li^+ ions from the cytoplasm at the expense of the pmf, thus playing an important role in cytoplasmic Na^+ and pH homeostasis and providing energy for Na^+ symports (see Padan &

Schuldiner, 1992; Padan and Schuldiner, 1994; Padan et al., 2001; Busch & Saier, 2002 for review). The Na^+/H^+ antiport in a bacterial cell is often mediated by antiporters of different types working in concert. Major enterobacterial antiporters, Ec-NhaA [Goldberg et al., 1987] and Ec-NhaB [Pinner et al., 1992], have been extensively characterized in *Escherichia coli* (see Padan et al., 1989; Taglict et al., 1991; Pinner et al., 1993; Taglicht et al., 1993; Dibrov & Taglicht, 1993; Dibrov, 1993; Gerchman et al., 1993; Pinner et al., 1994; Rimon et al., 1995; Inoue et al., 1995; Olami et al., 1997; Noumi et al., 1997; Gerchman et al., 2001, also Padan et al., 2001 for a review, and Galili et al., 2002; Rimon et al., 2002; Tzubery et al., 2004; Hunte et al., 2005 for recent progress). The genome of pathogenic *Vibrio cholerae* encodes as many as seven putative structural genes/operons of Na^+/H^+ antiporters [Heidelberg, 2000]. The physiological basis for such apparent redundancy could be in part explained by recent findings of additional, predominantly regulatory, functions of certain bacterial Na^+/H^+ antiporters, affecting processes such as antibiotic efflux [Krulwich et al., 2001b], transcription of the Pho operon [Pragai et al., 2001], the initiation of sporulation [Kosono et al., 2000] and endospore germination [Southworth et al., 2001].

Studying Na^+/H^+ antiport in *V. cholerae*, we have cloned a new Na^+/H^+ antiporter from *Vibrio cholerae*, Vc-NhaD, and expressed it in its functional form in the ΔNhaAΔNhaB strain of *E. coli* (see Section 4.1). As mentioned, a distinctive feature of Vc-NhaD is its pH dependence with a sharp maximum of activity at pH~8.0 (Fig. 4.4) [Ostroumov et al., 2002]. This distinguishes Vc-NhaD from other major enterobacterial antiporters. Indeed, Ec-NhaB from *E. coli* is pH-independent while the activity of Ec-NhaA gradually increases upon pH shift from 7.0 to 8.0, reaching a plateau [Taglicht et

al., 1991]. Curiously, homologous NhaD from *V. parahaemolyticus* exhibits a pH-dependence similar to Ec-NhaA rather than Vc-NhaD [Nozaki et al., 1998].

The Na^+/H^+ antiporters of NhaD-type are widely distributed in nature, being found in the genomes of pathogenic vibrios, nitrogen-fixing symbionts, magnetotactic cocci, photosynthetic bacteria, as well as in higher plants (Fig. 4.6A). In obligate intracellular parasites of the *Chlamydia* genus, NhaD serves as a sole Na^+/H^+ antiporter [Häse et al., 2001; Dibrov et al., 2004]. However, very little is known about the molecular mechanisms of cation exchange mediated by these proteins. In the absence of a detailed crystal structure, identification of functionally important residues in antiporters by site-directed mutagenesis remains one of the most informative approaches. Since Na^+/H^+ antiporters are exchanging cations, negatively charged residues are obvious primary targets for mutagenesis (see, for example Inoue et al., 1995; Tzubery et al., 2004). In our primary work, Dr. E. Ostroumov and I found that mutation of three polar residues, D344, T345 (TSM X and loop IX-X) and D393 (within TSM XI) severely affects the Na^+-dependent proton transfer mediated by Vc-NhaD (location of these mutations is given in Fig. 4.6B; results are presented in Ostroumov et al., 2002). In the next study we extended these observations by mutating Vc-NhaD residues that are conserved in NhaD homologues from different organisms (see Fig. 4.6A). In particular, the following questions were addressed: (i) Are other conserved polar residues besides D344, T345 and D393 functionally important, as well? (ii) Are any of the conserved His residues involved in the pH response of Vc-NhaD, such as His-225 in Ec-NhaA [Gerchman et al., 1993; Rimon et al., 1995]? (iii) Is R305 in Vc-NhaD (which is an analog of His-225 of Ec-NhaA, see Fig. 4.7) also involved in the pH response? I was solely responsible for

Fig. 4.6. *In silico* analysis of Vc-NhaD. Panel A. Partial alignments of representative NhaD proteins. Amino acid sequence of the protein from *Arabidopsis thaliana* (*Ath*, accession no. AAG51773) was used as a query for BLAST. The sequences used were found in *Microbulbifer degradans* (*Md*, ZP_00064921), *Rhodobacter sphaeroides* (*Rsp*, ZP_00007535), *Shewanella oneidensis* (*Son,* AAN54009), *Vibrio cholerae* (*Vc*, AAF96911), *Vibrio parahaemolyticus* (*Vp*, BAC61394), *Vibrio vulnificus* (*Vv*, AAO08110), *Magnetococcus* sp. (*Mg*, ZP_00288831), *Chlamyidophila pneumoniae* (*Cpn*, BAA99222), *Chlamydia trachomatis* (*Ctr*, AAC68454), and *Bradyrhizobium japonicum* (*Bja*, NP_770379). Conserved residues targeted for mutagenesis in Vc-NhaD are underlined; (*) indicates polar residues conserved in all aligned sequences. The sequences may be divided into three subgroups, with proteins within subgroups sharing higher degrees of identity/similarity. The largest one includes NhaD-like proteins from bacteria that are free-living or have a free-living stage in their life cycle (Subgroup 1, last 7 rows). Chlamydial proteins (from obligate intracellular parasites, rows 3-4) comprise the second subgroup (Subgroup 2). The third subgroup includes NhaD from nitrogen-fixing symbiont *Bradyrhizobium japonicum* and higher plant *A. thaliana*. See the text for more details. **Panel B.** Distribution of probed residues in putative transmembrane segments of the Vc-NhaD molecule. Conserved residues were mutated into alanines, except for D154 and N394, which were mutated into glycines. C163, C181 and C355 were substituted by serine residues. Strongly conserved residues (that is, conserved in all sequences are aligned in Fig. 4.6A) are given in bold-face. Shown also are functionally important residues D344, T345 and D393 characterized previously. See text for discussion.

Fig. 4.6A

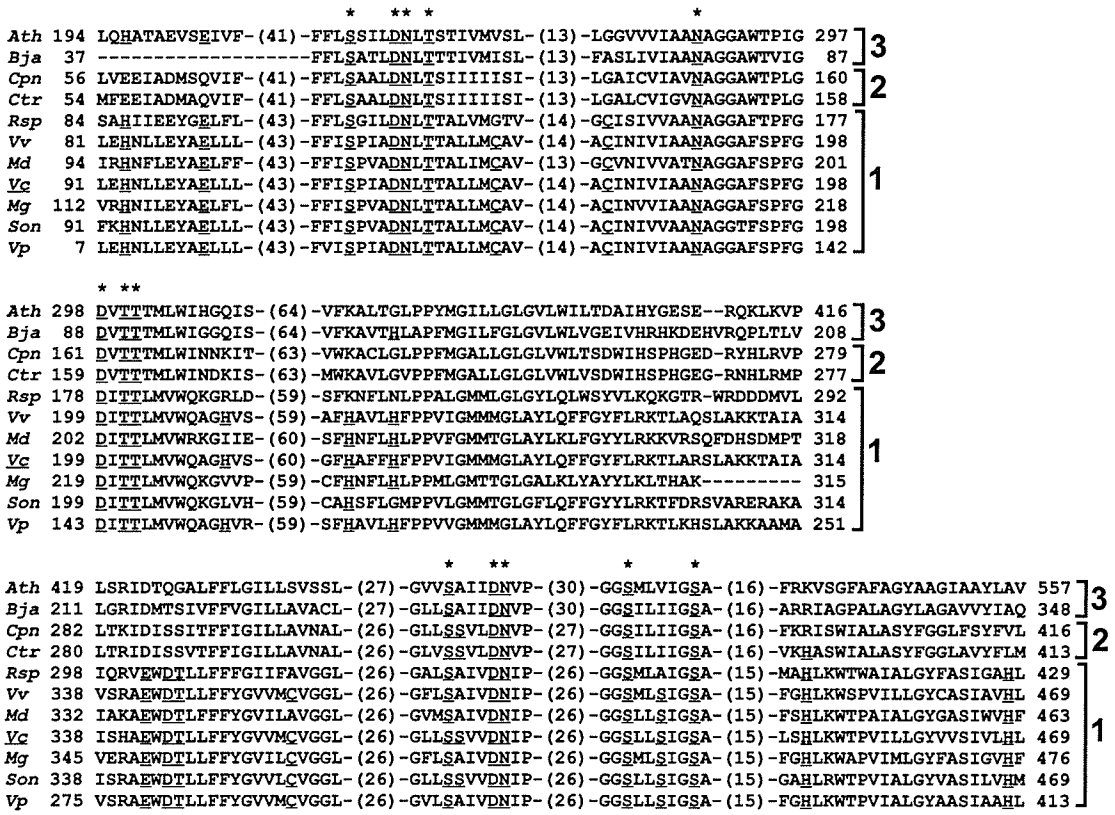
Ath 194 LQHATAEVSEIVF-(41)-FFLSSILDNLTSTIVMVSL-(13)-LGGVVVIAANAGGAWTPIG 297
Bja 37 ----------FFLSATLDNLTTTIVMISL-(13)-FASLIVIAANAGGAWTVIG 87
Cpn 56 LVEEIADMSQVIF-(41)-FFLSAALDNLTSIIIIISI-(13)-LGAICVIAVNAGGAWTPLG 160
Ctr 54 MFEEIADMAQVIF-(41)-FFLSAALDNLTSIIIIISI-(13)-LGALCVIGVNAGGAWTPLG 158
Rsp 84 SAHIIEEYGELFL-(43)-FFLSGILDNLTTALVMGTV-(14)-GCISIVVAANAGGAFTPFG 177
Vv 81 LEHNLLEYAELLL-(43)-FFISPIADNLTTALLMCAV-(14)-ACINIVIAANAGGAFSPFG 198
Md 94 IRHNFLEYAELFF-(43)-FFISPVADNLTTALIMCAV-(13)-GCVNIVVATNAGGAFSPFG 201
Vc 91 LEHNLLEYAELLL-(43)-FFISPIADNLTTALLMCAV-(14)-ACINIVIAANAGGAFSPFG 198
Mg 112 VRHNILEYAELFL-(43)-FFISPVADNLTTALLMCAV-(14)-ACINVVIAANAGGAFSPFG 218
Son 91 FKHNLLEYAELLL-(43)-FFISPVADNLTTALLMCAV-(14)-ACINIVVAANAGGTFSPFG 198
Vp 7 LEHNLLEYAELLL-(43)-FVISPIADNLTTALLMCAV-(14)-ACINIVIAANAGGAFSPFG 142
Ath 298 DVTTTMLWIHGQIS-(64)-VFKALTGLPPYMGILLGLGVLWILTDAIHYGESE--RQKLKVP 416
Bja 88 DVTTTMLWIGGQIS-(64)-VFKAVTHLAPFMGILFGLGVLWLVGEIVHRHKDEHVRQPLTLV 208
Cpn 161 DVTTTMLWINNKIT-(63)-VWKACLGLPPFMGALLGLGLVWLTSDWIHSPHGED-RYHLRVP 279
Ctr 159 DVTTTMLWINDKIS-(63)-MWKAVLGVPPFMGALLGLGLVWLVSDWIHSPHGEG-RNHLRMP 277
Rsp 178 DITTLMVWQKGRLD-(59)-SFKNFLNLPPALGMMLGLGYLQLWSYVLKQKGTR-WRDDDMVL 292
Vv 199 DITTLMVWQAGHVS-(59)-AFHAVLHFPPVIGMMMGLAYLQFFGYFLRKTLAQSLAKKTAIA 314
Md 202 DITTLMVWRKGIIE-(60)-SFHNFLHLPPVFGMMTGLAYLKLFGYYLRKKVRSQFDHSDMPT 318
Vc 199 DITTLMVWQAGHVS-(60)-GFHAFFHFPPVIGMMMGLAYLQFFGYFLRKTLARSLAKKTAIA 314
Mg 219 DITTLMVWQKGVVP-(59)-CFHNFLHLPPMLGMTTGLGALKLYAYYLKLTHAK--------- 315
Son 199 DITTLMVWQKGLVH-(59)-CAHSFLGMPPVLGMMTGLGFLQFFGYYLRKTFDRSVARERAKA 314
Vp 143 DITTLMVWQAGHVR-(59)-SFHAVLHFPPVVGMMMGLAYLQFFGYFLRKTLKHSLAKKAAMA 251
Ath 419 LSRIDTQGALFFLGILLSVSSL-(27)-GVVSAIIDNVP-(30)-GGSMLVIGSA-(16)-FRKVSGFAFAGYAAGIAAYLAV 557
Bja 211 LGRIDMTSIVFFVGILLAVACL-(27)-GLLSAIIDNVP-(30)-GGSILIIGSA-(16)-ARRIAGPALAGYLAGAVVYIAQ 348
Cpn 282 LTKIDISSITFFIGILLAVNAL-(26)-GLLSSVLDNVP-(27)-GGSILIIGSA-(16)-FKRISWIALASYFGGLFSYFVL 416
Ctr 280 LTRIDISSVTFFIGILLAVNAL-(26)-GLVSSVLDNVP-(27)-GGSILIIGSA-(16)-VKHASWIALASYFGGLAVYFLM 413
Rsp 298 IQRVEWDTLLFFFGIIFAVGGL-(26)-GALSAIVDNIP-(26)-GGSMLAIGSA-(15)-MAHLKWTWAIALGYFASIGAHL 429
Vv 338 VSRAEWDTLLFFYGVVMCVGGL-(26)-GFLSAIVDNIP-(26)-GGSMLSIGSA-(15)-FGHLKWSPVILLGYCASIAVHL 469
Md 332 IAKAEWDTLFFFYGVILAVGGL-(26)-GVMSAIVDNIP-(26)-GGSLLSIGSA-(15)-FSHLKWTPAIALGYGASIWVHF 463
Vc 338 ISHAEWDTLLFFYGVVMCVGGL-(26)-GLLSSVVDNIP-(26)-GGSLLSIGSA-(15)-LSHLKWTPVILLGYVVSIVLHL 469
Mg 345 VERAEWDTLLFFYGVILCVGGL-(26)-GFLSAIVDNIP-(26)-GGSMLSIGSA-(15)-FGHLKWAPVIMLGYFASIGVHF 476
Son 338 ISRAEWDTLLFFYGVVLCVGGL-(26)-GLLSSVVDNIP-(26)-GGSLLSIGSA-(15)-GAHLRWTPVIALGYVASILVHM 469
Vp 275 VSRAEWDTLLFFYGVVMCVGGL-(26)-GVLSAIVDNIP-(26)-GGSLLSIGSA-(15)-FGHLKWTPVIALGYAASIAAHL 413
3
2
1
3
2
1

Fig. 4.6B

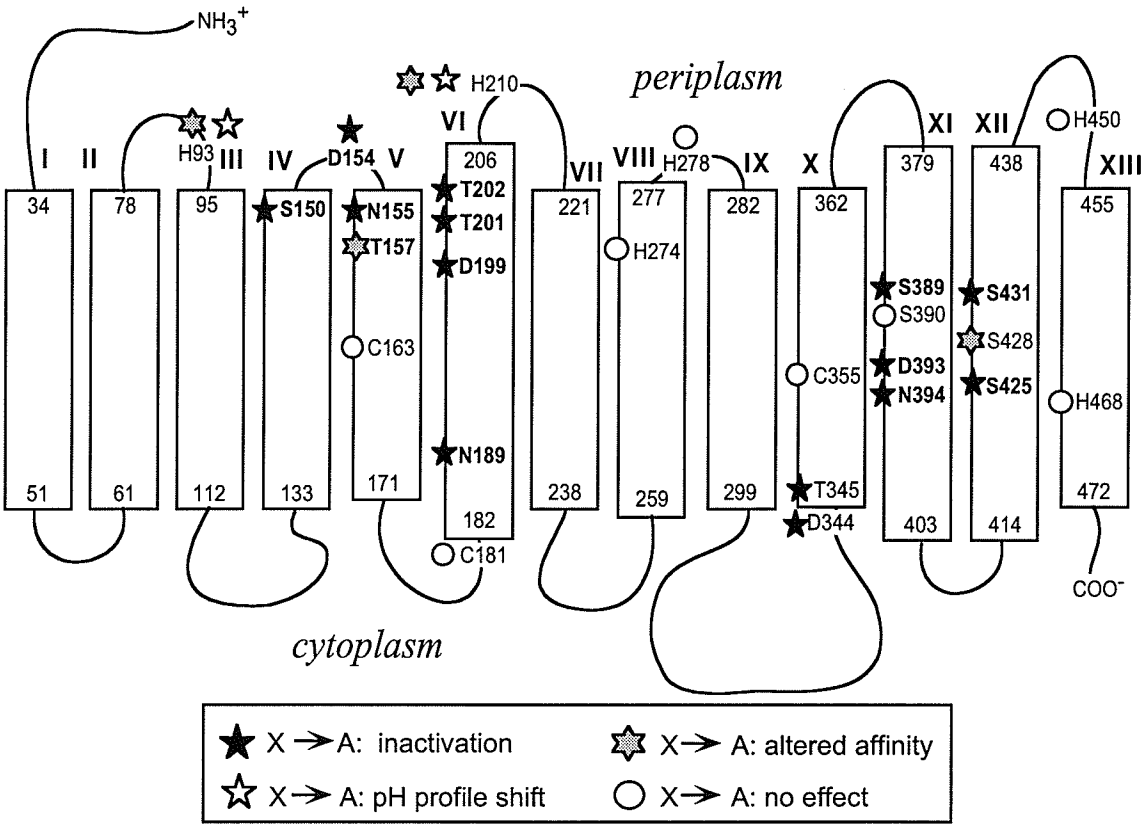
NH3+
periplasm
H210
VI
206
T202
T201
D199
N189
182
C181
I
II
H93
III
IV
D154
V
34
78
95
S150
N155
T157
C163
171
51
61
112
133
VII
221
238
VIII
H278
277
H274
259
IX
282
299
X
362
C355
T345
D344
XI
379
S389
S390
D393
N394
403
XII
438
S431
S428
S425
414
H450
XIII
455
H468
472
COO-
cytoplasm
X → A: inactivation
X → A: altered affinity
X → A: pH profile shift
X → A: no effect

all experiments dealing with (ii) and (iii), while Dr. R. Habibian in our lab contributed mostly to (i).

We identified three distinct clusters of functionally important polar residues dispersed through the protein. Cluster 1 is associated with TMS IV-VI at the periplasmic side of the protein (Fig. 4.6B), cluster 2 is at the opposite side facing cytoplasm (TMS X) (Fig. 4.6B) and cluster 3 in TMS XI-XII (Fig. 4.6B) is located in the middle of the transmembrane segments. Together with residues H93 and H210, which control the pH profile of the antiport and its affinity to alkali cations, these clusters may form a transmembrane relay of charged/polar residues involved in the attraction, coordination and translocation of transported ions, in a striking similarity to the recently reported structure of phylogenetically distant Ec-NhaA [Hunte et al., 2005].

In this work we also mutagenized the arginine residue, R305, of the conserved KTLX(R/H)SLA motif (Fig. 4.7). This motif was previously shown to be involved in pH control in Ec-NhaA. In the laboratory of Dr. E. Padan, they found that substitutions H225S and H225C did not affect the pH profile of activity, whereas H225R shifted it toward acid and H225D toward alkaline pH; the H225A variant showed very low activity over the pH range 7.5 to 9.0. The authors concluded that the capacity of a residue in position 225 to form hydrogen bonds may be important for the pH regulation [Gerchman et al., 1993; Rimon et al., 1995].

The motif containing H225 is conserved among NhaA antiporters from different species (Fig. 4.7). A similar sequence is also present in NhaD-type proteins from *V. vulnificus, V. parahaemolyticus* [Nozaki et al., 1998] and *V. cholerae* (see Section 4.1, Fig. 4.7). Based on the similarity in pH profiles of activity, it has been hypothesized that H249 of Vp-NhaD is a functional analog of H225 of Ec-NhaA [Nozaki

Fig. 4.7. Partial protein sequence alignment of the putative pH-sensing motif. The motif containing H225 is conserved among NhaA antiporters from different *Vibrio* species. A similar sequence is also present in NhaD-type proteins from *V. parahaemolyticus* and *V. cholerae*. See the text for further details.

Fig. 4.7

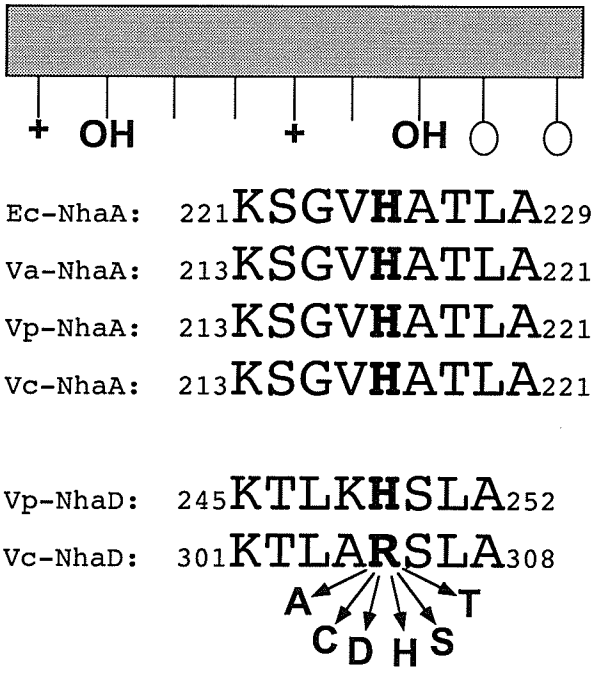
+ OH + OH
Ec-NhaA: 221KSGVHATLA229
Va-NhaA: 213KSGVHATLA221
Vp-NhaA: 213KSGVHATLA221
Vc-NhaA: 213KSGVHATLA221
Vp-NhaD: 245KTLKHSLA252
Vc-NhaD: 301KTLARSLA308
A
T
C D H S

et al., 1998]. In an apparent accord with such a hypothesis, Vc-NhaD, which has R305 in place of H in this conserved motif (Fig. 4.7), exhibits the pH dependence similar to that of the H225R variant of Ec-NhaA (shifted toward acid pH). It should be noted, however, that the location of the conserved motif in Ec-NhaA and Vc-NhaD is probably different. In Ec-NhaA, the H225-containing segment is located at the edge of a short transmembrane segment (TMS) facing the cell exterior [Olami et al., 1995], whereas the hydrophobicity profile of Vc-NhaD predicts the location of the corresponding motif in the cytoplasmic loop connecting TMS IX and X (Fig. 4.7). We therefore analyzed the possible role of the arginine residue in the ^{301}KTLARSLA^{308} motif in Vc-NhaD in pH regulation by site-directed mutagenesis.

4.2.2. Site-Directed Mutagenesis of *nhaD*

Primers used for mutagenesis are listed in Table 3A. Site-directed mutagenesis was performed using the QuikChange site-directed mutagenesis kit (Stratagene) as described in "Materials and Methods". The mutagenic oligonucleotide primers were designed to create or remove specific restriction enzyme sites (listed in Table 3A). As a template for mutagenesis, the plasmid pBLDL (pBluescript II KS+ [Stratagene] containing the *nhaD* gene together with the 154 bp-long 5' and 230 bp-long 3' flanking sequences as a 1837 bp *EcoR*I-*BamH*I insert) was used (see Section 4.1). Mutated plasmid DNA was isolated from selected transformant clones and digested by appropriate restriction enzymes to check for the presence of desired mutation. Finally, validity of all mutants was confirmed by DNA sequencing.

4.2.3. *In silico* Analysis of Vc-NhaD

NhaD homologues in various organisms were identified through a BLASTP [Altschul et al., 1997] search against the NCBI (Bethesda, MD) nonredundant protein database (Fig. 4.6A). A putative membrane topology model of NhaD from *V. cholerae* (Fig. 4.6B) was constructed using the Topopredict II [Claros & von Heijne, 1994] and HMMTOP [Tusnady & Simon, 1998] programs. The 3D-diagram showing the recently reported structure of Ec-NhaA [Hunte et al., 2005] in relation to the functionally important residues of Vc-NhaD was prepared by Dr. P. Loewen (Department of Microbiology, U of M) using VMD [Humphrey et al., 1996].

4.2.4. Strategy for Mutagenesis

Fig. 4.6A illustrates the strategy adopted for choosing the target amino acids for mutagenesis. It shows partial alignments of representative NhaD-like proteins from different organisms. Sequences presented in Fig. 4.6A may be divided into three subgroups, with proteins within subgroups sharing higher degrees of identity/similarity. The largest one includes NhaD-like proteins from bacteria that are free-living or have a free-living stage in their life cycle (Subgroup 1, last 7 rows in Fig. 4.6A). Chlamydial proteins (from obligate intracellular parasites, rows 3-4 in Fig. 4.6A) comprise the second subgroup (Subgroup 2). The third subgroup includes NhaD from nitrogen-fixing symbiont *Bradyrhizobium japonicum* and higher plant *A. thaliana*.

Thirteen polar/charged residues are conserved in all aligned sequences (highlighted and marked by asterisk in Fig. 4.6A). In Vc-NhaD these residues are S150, D154, N155, T157, N189, D199, T201, T202, S389, D393, N394, S425, and S431. From this list, D393 was previously mutagenized [Ostroumov et al., 2002], in a study that also included

E100, E342, D344, and T345 which are conserved in antiporters belonging to Subgroup 1, as well as the weakly conserved E251. The remaining residues were investigated in this study. Target residues were changed into Ala, except D154 and N394, which were changed into Gly. Our aim was to eliminate charged side chains in the chosen positions, so either substitution seemed appropriate. Although replacement with Gly could have caused confirmational flexibility, mutagenesis to this residue just simplified the screening of mutant clones by restriction analysis.

In addition to the fully conserved residues, six His residues, H93, H210, H274, H278, H450, and H468, are conserved at least partially in proteins belonging to Subgroup 1 (Fig. 4.6A). They could have a role in determining the pH response of the antiporter because of their physiologically relevant pK_a. Indeed, as mentioned above, mutation of conserved H225 in Ec-NhaA alters the pH response of the antiporter [Gerchman et al., 1993; Rimon et al., 1995]. All six conserved His residues were mutated. Finally, R305 and surrounding residues of the conserved ^{301}KTLARSLA^{308} motif were also targeted for analysis.

4.2.5. Characterization of Vc-NhaD Mutants in Membrane Vesicles

Isolation of membrane vesicles was carried out as described in "Materials and Methods."

4.2.5.1. Mutagenesis of Conserved Histidines in Vc-NhaD

Fig. 4.8 summarizes the results of substituting the conserved His residues in Vc-NhaD with Ala. In inside-out sub-bacterial vesicles, H274A, H278A, H450A, and H468A did not change the $Na^+(Li^+)/H^+$ antiport activity significantly, but H93A and

Fig. 4.8. Effect of His to Ala substitutions on the pH profile of activity of Vc-NhaD. Experimental conditions are as in Fig. 4.4. The activity of wild-type Vc-NhaD with 10 mM NaCl is shown for the reference (○). 10 mM LiCl (▲). 10 mM NaCl (■). Representative of a typical experiment.

Fig. 4.8

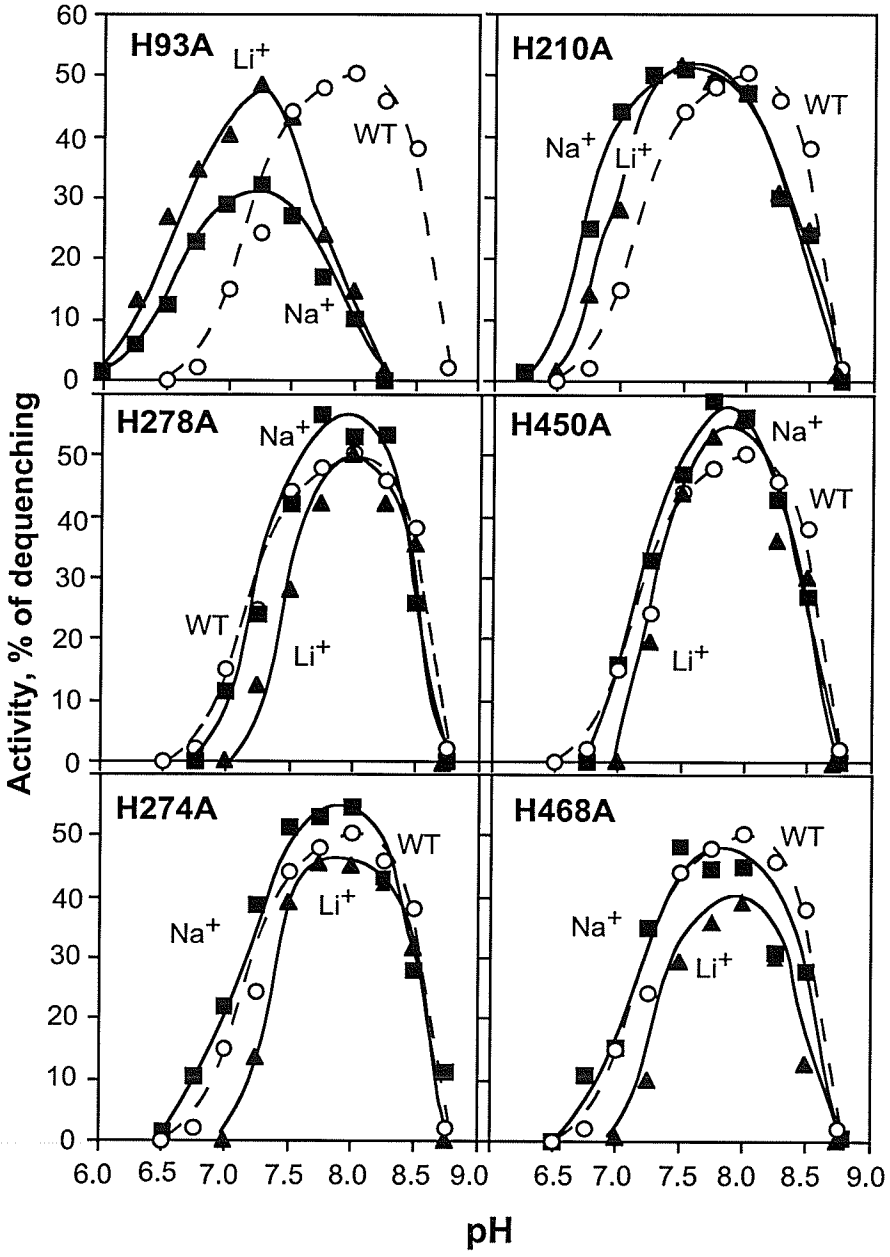
H93A
Li+
WT
Na+
H210A
WT
Na+
Li+
H278A
Na+
WT
Li+
H450A
Na+
WT
Li+
H274A
WT
Na+
Li+
H468A
WT
Na+
Li+
Activity, % of dequenching
pH
0
10
20
30
40
50
60
6.0
6.5
7.0
7.5
8.0
8.5
9.0

H210A variants displayed an acidic shift of the pH profile of the antiport for both alkali cations (Fig. 4.8). The shift was more pronounced in the H93A variant, which also responded differently to Na^+ and Li^+ ions, showing higher activity with Li^+ (Fig. 4.8). To assess further the affinity of H93A and H210A variants to alkali cations, the concentrations of Na^+ and Li^+ required for half-maximal response (apparent K_m values) at pH 7.75 were determined in sub-bacterial vesicles (Table 4). Despite the fact that the apparent K_m is only indirectly related to the actual K_m of the antiporter, this readily measurable parameter is commonly used to characterize antiporter affinity to substrate ions (for example, see [Gerchman et al., 2001]). The apparent K_m of H93A for Na^+ was found to be approximately 7-fold higher than in the wild type while its apparent K_m for Li^+ was unaffected (Table 4). By contrast there was only a slight increase in the apparent K_m of H210A for Li^+ (Table 4).

4.2.5.2. Mutagenesis of Conserved Polar/Charged Residues in Vc-NhaD

Computer modeling of the Vc-NhaD membrane topology suggests that the highly conserved residues S150A, D154G, N155A, T157A, D199A, T201A and T202A may form a compact "constellation" on the periplasmic side of the protein (see Fig. 4.6B).

Variants S150A, D154G, N155A, D199A, T201A, T202A and N189A failed to complement the Li^+-sensitive growth phenotype in EP432 and analysis of activity in sub-bacterial vesicles confirmed that they were unable to mediate the Na^+- and Li^+-dependent H^+ transport at pH 6.5 to 8.75 [Habibian et al., 2005]. Immunodetection confirmed that this was not due to the impaired expression and/or targeting of mutant variants [Habibian et al., 2005]. EP432 cells expressing the T157A variant showed slower growth in the presence of 100 mM LiCl; the T157A variant also exhibited lower activity in vesicle

Table. 4. Affinity of different Vc-NhaD variants for alkali cations

Mutation	Apparent K_m, mM (pH 7.75)	
	Na^+	Li^+
Wild Type	1.1	2.1
S390A	1.1	2.1
T157A	9.5	39.8
S428A	5.5	17.9
H93A	7.1	1.9
H210A	1.3	4.3

assays [Habibian et al., 2005] and a decreased affinity for alkali cations ([Habibian et al., 2005] and Table 4). Furthermore, the comparison of apparent K_m values revealed a difference in responses of the mutated antiporter to alkali cations with Na^+ becoming the preferred substrate ([Habibian et al., 2005] and Table 4).

It has been found that D393 in TMS XI, as well as D344 and T345 at the cytoplasmic end of TMS X, are functionally important (Fig. 4.6B; [Ostroumov et al., 2002]). Another four nearby polar/charged residues are conserved in NhaD antiporters (Fig. 4.6A), including S389 and N394 in TMS XI as well as S425 and S431 in TMS XII. In addition, S428 is conserved in proteins belonging to Subgroup 1, while S390 is replaced by alanine in many cases (Fig. 4.6A). These residues were mutagenized to Ala (except N394 which was replaced by Gly), and the antiport activities were assayed in sub-bacterial vesicles of transformed EP432 [Habibian et al., 2005]. The activity of the S390A variant was unaffected compared to native protein [Habibian et al., 2005], but mutation of conserved S389, N394, S431 and S425 prevented $Na^+(Li^+)$-dependent H^+ transfer in vesicles completely (Fig. 4.6B; [Habibian et al., 2005]). The S428A and T157A variants displayed similar slow growth of EP432 transformants in LiCl-containing medium, lowered activity in vesicles and different response to Na^+ and Li^+ [Habibian et al., 2005]. The K_m of S428A for Na^+ was 5.5 times higher than that of the wild type antiporter while its K_m for Li^+ was almost 9-fold elevated (Table 4).

Since a number of Vc-NhaD variants were unable to complement the EP432 phenotype and catalyze $Na^+(Li^+)$-dependent H^+ transfer in sub-bacterial vesicles, levels of their expression in the EP432 membranes were examined by Western blotting. It confirmed that the mutations did not interfere with either the expression or targeting to the membrane [Habibian et al., 2005]. Expression levels of all inactive variants in EP432

except S431A were comparable to that of the wild type protein and even for S431A the slightly reduced levels cannot account for the complete absence of activity.

4.2.5.3. Mutational Analysis of the KTLX(R/H)SLA Motif

As mentioned, Vc-NhaD has a distinct pH profile of activity peaking at pH ~8.0. This part of the study was designed to analyze the possible functional role of R305 of the ^{301}K-T-L-A-R-S-L-A^{308} motif in Vc-NhaD by site-directed mutagenesis. The data obtained suggest that R305 is involved not only in control of the pH response, but also in coupling of the H^+ and $Na^+(Li^+)$ fluxes in Vc-NhaD.

We found that R305H is a novel type of mutation that affects both the pH response and coupling of ion fluxes in a Na^+/H^+ antiporter. Membrane vesicles isolated from antiporter-less *Escherichia coli* cells expressing the R305H variant of Vc-NhaD formed severely reduced transmembrane proton gradient (ΔpH) upon addition of respiratory substrates (Fig. 4.9A, compare the upper and lower groups of tracks). In contrast to the wild type vesicles, ΔpH formed here was insensitive to Δψ-dissipating ionophore, valinomycin (Fig. 4.9A). These observations indicated that the membranes containing the R305H variant of Vc-NhaD are partially uncoupled, i.e. leaky for protons in the absence of added substrate alkali cation.

If membranes containing the R305H protein are more leaky for H^+ compared to the wild type, one could expect that enzymatic generation of the proton gradient in such membranes should be more sensitive to protonophoric uncouplers. We therefore measured formation of the respiration-driven ΔpH in wild type and R305H membranes in the presence of 100 nM CCCP (Fig. 4.9B). Wild type vesicles treated with this low

Fig. 4.9. Na^+/H^+ antiport activity measured at pH 7.5 in inside-out membrane vesicles prepared from EP432/pBLDL or EP432/pR305H. Inside-out membrane vesicles were isolated and analysed as described in "Materials and Methods" and as per Fig. 4.3. **Panel A.** R305H mutation results in membranes leaky for H^+. R305H formed severely reduced ΔpH upon addition of lactate, which was insensitive to the Δψ-dissipating ionophore, valinomycin. **Panel B.** 100 nM CCCP imitates the effect of the R305H mutation on ΔpH formation in wild type vesicles. Wild type vesicles treated with the protonophoric uncoupler, CCCP, were still able to form ΔpH upon the addition of lactate, but the magnitude and rate was similar to non-treated R305H vesicles. CCCP almost completely arrested ΔpH formation in the R305H vesicles.

Fig. 4.9

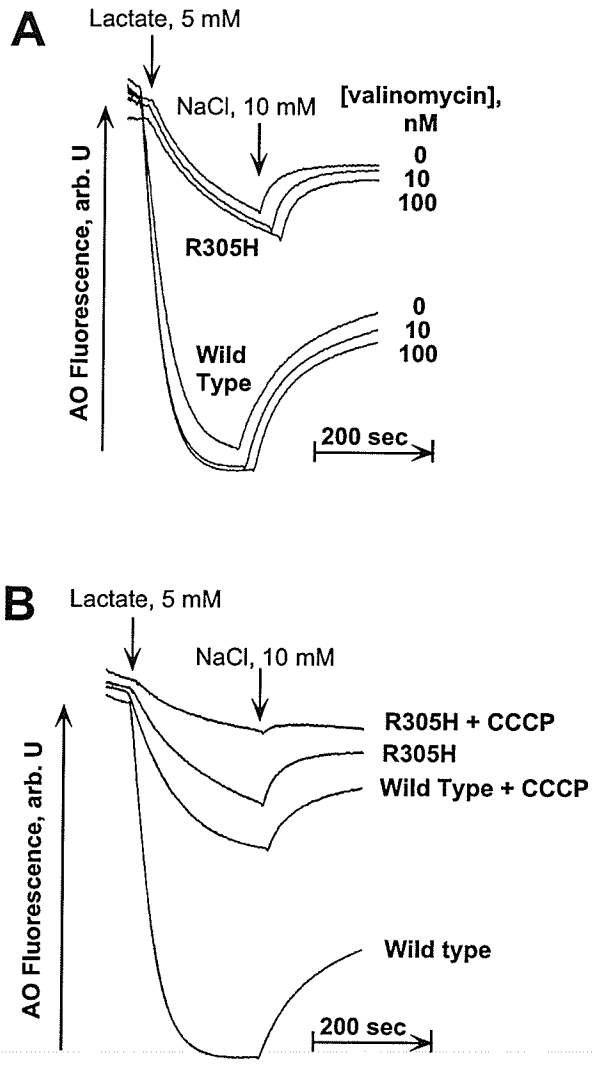
A
Lactate, 5 mM
NaCl, 10 mM
[valinomycin], nM
0
10
100
R305H
0
10
100
Wild Type
AO Fluorescence, arb. U
200 sec
B
Lactate, 5 mM
NaCl, 10 mM
R305H + CCCP
R305H
Wild Type + CCCP
Wild type
AO Fluorescence, arb. U
200 sec

concentration of uncoupler were still able to form sizable ΔpH upon addition of respiratory substrate. The magnitude and rate of this response were similar to those in non-treated R305H vesicles, in accord with the assumption that the R305H variant of Vc-NhaD acts as "endogenous" protonophore. Furthermore, treatment of the R305H vesicles with the same concentration of CCCP arrested the formation of the respiratory ΔpH almost completely (Fig. 4.9B, upper track).

At the same time, the pH profile of activity was practically unaffected by the R305H substitution (Fig. 4.10). Taken together, these observations strongly suggest that the R305H substitution results in H^+ uniport through Vc-NhaD in the absence of Na^+ or Li^+ ions. To the best of our knowledge, this is the first example of a single amino acid substitution affecting the coupling of ion fluxes via a Na^+/H^+ antiporter.

To assess the physiological effects of other R305 substitutions, pBLDL derivatives with the corresponding mutations in *nhaD* were introduced into the antiporter-deficient *E. coli* strain, EP432. Examination of the pH profiles of mutated Vc-NhaD in inside-out membrane vesicles revealed that at least in one variant its pH optimum is shifted toward acidic pH (Fig. 4.10). Indeed, elimination of the positive charge at the 305 position in the R305A variant resulted in pH optima for both Na^+ and Li^+ simultaneously shifted by a single pH unit. Two polar substitutions (R305T and R305S variants) displayed hardly any "acidic shift," while the R305H variant was moderately shifted. Both R305D and R305C variants showed somewhat lower overall activity compared to wild type antiporter, which, in principle, could be due to a slightly lowered expression of the respective variants. However, it does not explain why both of these variants, especially R305D, show different responses to Li^+ and Na^+ ions. Furthermore, in both cases the pH

Fig. 4.10. pH profiles of activity of R305 substitutions. Experimental conditions are as in Fig. 4.4. The activity of wild-type Vc-NhaD with 10 mM NaCl is shown for the reference (○). 10 mM LiCl (■). 10 mM NaCl (▲). Representative of a typical experiment.

Fig. 4.10

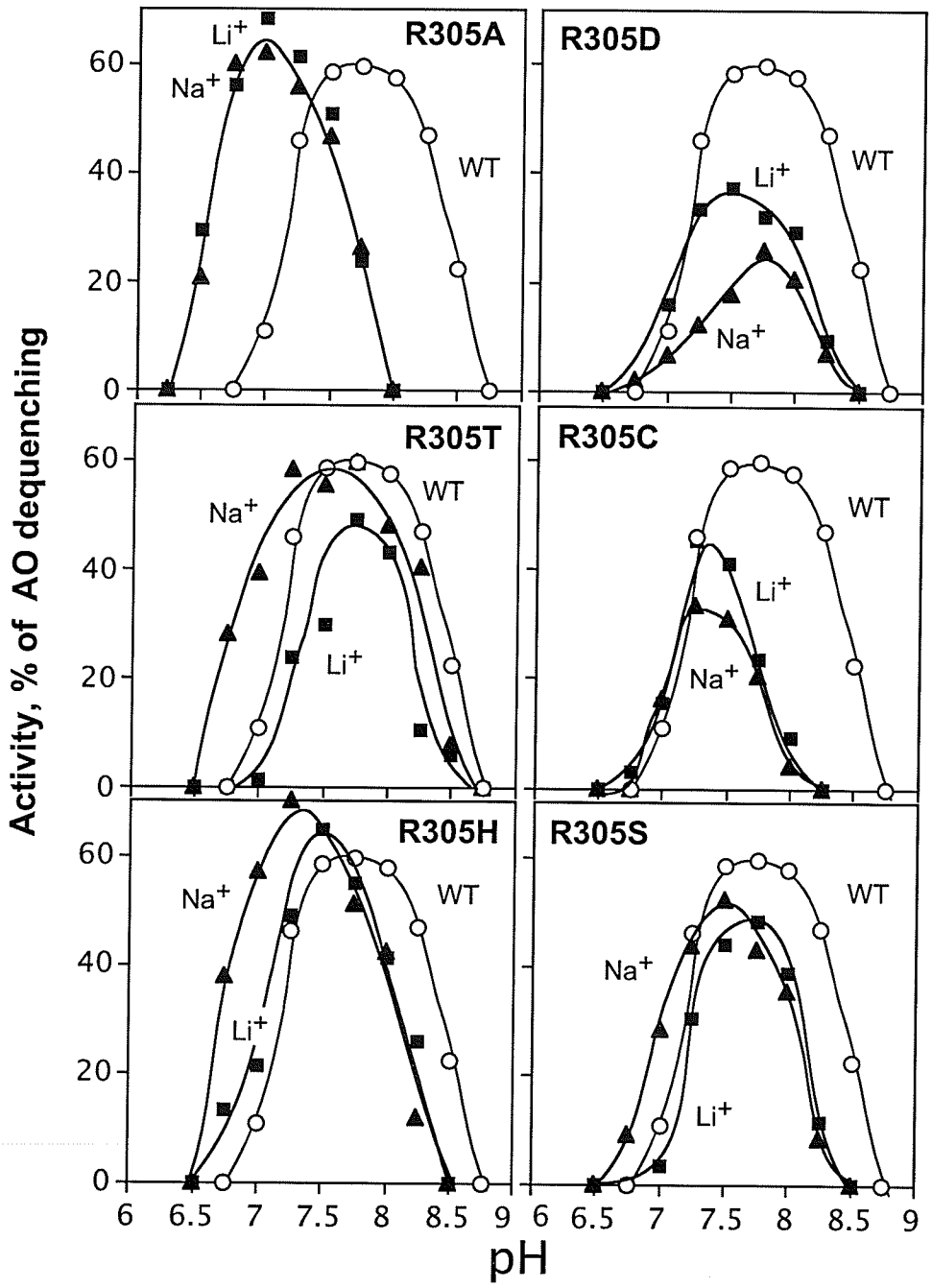
R305A
R305D
R305T
R305C
R305H
R305S
Li+
Na+
WT
Activity, % of AO dequenching
pH
0
20
40
60
6
6.5
7
7.5
8
8.5
9

profiles were narrower than in wild type, with the absence of activity at more alkaline pH (Fig. 4.10). These "deformations" of pH profiles of antiport should be due to the effect of the introduced mutations on activity rather than on expression levels.

4.2.6. Discussion

The present study is the first to provide an extensive molecular analysis of a Na^+/H^+ antiporter of the NhaD-type. The general methodology of the analysis of mutant variants of Na^+/H^+ antiporters has been developed over the past decade, primarily in works by Padan and co-workers (see, for example Galili et al., 2002; Padan et al., 2004). This methodology allows differentiation between residues that regulate the pH response of an antiporter and those involved in the translocation of cations. The first group of residues are expected to (i) have a pK in the physiological pH range, (ii) change the pH profile of antiport when mutated without an effect on the K_m of antiport and (iii) maintain the altered pH profile of the mutant variant assayed at saturating concentrations of substrate alkali cations. In terms of function, such residues could form an allosteric "built-in pH sensor" [Galili et al., 2002; Padan et al., 2004] or belong to the intramolecular H^+ translocation pathway.

The second group of residues, those involved in cation translocation, should (i) be associated with transmembrane segments, (ii) be able to interact with translocated cations, and (iii) affect the K_m of antiport when mutated without affecting the wild type pH profile, at least at saturating concentrations of alkali cations. Obviously, such residues could affect ion translocation either directly (i.e., by providing ligands for the coordination of transported cations) or indirectly (being important for the overall protein structure or conformational changes associated with ion translocation without direct

Fig. 4.11. Possible analogies between functionally important residues in Ec-NhaA and Vc-NhaD. The structure of Ec-NhaA is shown on the left along with a listing of conserved residues known to have a role in antiport. A listing of residues from Vc-NhaD in equivalent positions is included on the right. In both cases, a group of negatively charged/polar residues in the middle of the structure might form the putative cation-binding site with two other groups at opposite sides facilitating the access of ions to this active site.

Fig. 4.11

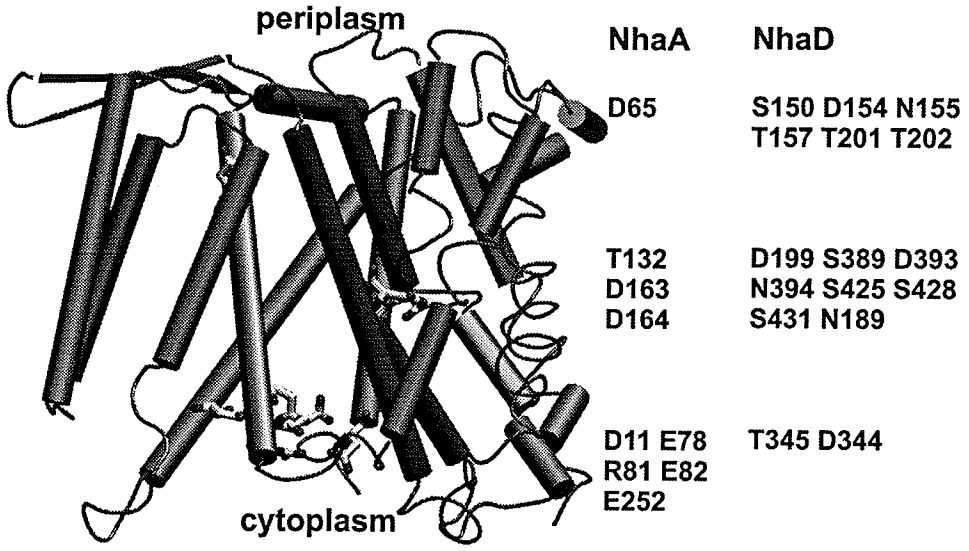
periplasm
cytoplasm
NhaA
NhaD
D65
S150 D154 N155
T157 T201 T202
T132
D163
D164
D199 S389 D393
N394 S425 S428
S431 N189
D11 E78
R81 E82
E252
T345 D344

interaction with substrate cations). Finally, some residues might be involved in both the pH response and ion translocation, for example if protons and alkali cations are sharing at least some segments of the same translocation pathway. Applying the above criteria to the functionally important residues identified in Vc-NhaD, one can classify S150, D154, N155, N189, D199, T201, T202, D344, T345, S389, D393, N394, S425 and S431 as ones involved, either directly or indirectly, in ion translocation. All these residues are either polar or charged and thus can coordinate or repel cations. They are located within hydrophobic segments of Vc-NhaD or at the membrane-water interface. Mutation of any of them arrests the overall reaction of cation-proton antiport over a pH range from 6.0 to 9.0. This is not due to the interference of mutations with expression/targeting [Habibian et al., 2005]. Although a somewhat lowered level of variant S431A in the membranes was detected [Habibian et al., 2005], it far exceeded the expression of Vc-NhaD from its chromosomal gene in *Vibrio cholerae* (Fig. 4.23B). A very low abundance is one of the characteristic features of bacterial Na^+/H^+ antiporters. For example, Ec-NhaA, the major antiporter of *E. coli*, remains immunochemically undetectable in the membrane unless it is overexpressed, *in trans* [Rimon et al., 1998]. Therefore, it seems highly unlikely that impaired expression or targeting is the reason for the lack of activity of S431A. Furthermore, it definitely cannot account for the difference in responses of T157A and S428 to Na^+ and Li^+ [Habibian et al., 2005]. Most likely, it is the altered affinity of these variants to alkali cations that causes their lowered activity (Table 4). It is significant that these residues are all evolutionarily conserved (Fig. 4.6A), whereas S390 is replaced by alanine in a number of NhaD proteins (Fig. 4.6A). Not surprisingly, S390 is not essential for the activity of Vc-NhaD. Its substitution by alanine does not affect either the pH profile of activity or apparent K_m for alkali cations ([Habibian et al., 2005] and Table 4).

Charged/polar residues associated with TMSs have been implicated in the ion translocation mediated by a variety of Na^+-dependent transporters. The Na^+-binding sites of the Na^+-motive ATPases from *Propionigenium modestum* and *Acetobacterium woodii* are thought to be formed by closely positioned conserved D, T and N residues [Kaim et al., 1997; Rahlfs & Müller, 1997]. Hydroxyl groups provided by S and T residues are critical for the activity of such diverse Na^+-motive proteins as the proline transporter in *E. coli* [Quick et al., 1996], the Na^+-dependent oxaloacetate decarboxylase [Jockel et al., 2000], the Na^+/iodide symporter [De La Vieja et al., 2000] and the glutamate transporter GLT-1 [Zhang & Kanner, 1999]. Most importantly, recent analysis of the structure of Ec-NhaA clearly shows that D163, D164 and T132 are parts of the catalytic site in this bacterial Na^+/H^+ antiporter (Fig. 4.11) [Hunte et al., 2005]. Two residues definitely involved in the alkali cation binding and/or translocation, T157 and S428, are located in the TMSs V and XII, respectively (Fig. 4.6B), and variants of both show markedly lower affinity to Li^+ compared to Na^+ (Table 4), supporting the idea of Li^+ having more stringent structural requirements for binding to the antiporter.

Functionally important amino acids identified in Vc-NhaD form three major clusters (Fig. 4.6B). Cluster 1 includes S150, D154, N155, T157, D199, T201 and T202 in neighboring TMS IV, V and VI. Cluster 2, presumably located at the opposite side of the transmembrane segments, includes D344 and T345 in TMS X [Ostroumov et al., 2002]. Finally, Cluster 3, located in the middle of TMSs XI-XII, includes S389, D393, N394, S425, S428 and S431. This distribution presents distinct parallels to the recently reported structure of Ec-NhaA resolved at 3.45Å [Hunte et al., 2005], which provides important insights into the function of bacterial Na^+/H^+ antiporters. In particular, a negatively charged funnel, with E78, E82, E252 and D11 at its entrance, leads from the

cytoplasm to a putative catalytic site in the middle of the membrane containing the charged/polar residues D163, D164, T132 and D133. On the opposite side of the protein, a shallow, negatively charged funnel with D65 at its tip connects the periplasm to the central cation-binding site [Hunte et al., 2005]. The arrangement allows for the access of substrate ions through the funnels to the catalytic site, which could operate in the alternating-access mode [Hunte et al., 2005]. It is tempting to speculate that Vc-NhaD, though phylogenitically unrelated, shares these structural elements. Cluster 1 in TMSs IV-VI together with H93 and H210 may represent an analogue of the shallow negatively charged funnel on the periplasmic side of Ec-NhaA, attracting cations towards the putative catalytic site in the middle of the protein made up of Cluster 2 in TMSs XI and XII. Of note, five or six oxygen ligands are required to coordinate an alkali cation [Glusker, 1991; Harding, 2004] and residues of Cluster 2, S389, D393, S425, S428 and S431 will suffice in this respect. Finally, the pair of D344 and T345 on TMS X and N189 of TMS VI may be part of the funnel that facilitates the ion access from the cytoplasmic side. Thus, despite their distant phylogenetic relationships, different groups of bacterial Na^+/H^+ antiporters may share common structural features and catalytic mode. Possible similarities between Ec-NhaA and Vc-NhaD outlined above are summarized (Fig. 4.11). It should be stressed here though that a crystal structure of Vc-NhaD is required to determine the location of each residue.

Of all conserved residues examined, only H93 and H210 contribute to the pH response of Vc-NhaD (Fig. 4.8). Interestingly, these histidines are located in short periplasmic loops flanking Cluster 1 of functionally important residues in TMS IV-VI (Fig. 4.6B). The acidic shift of the pH profile of activity in these variants can be explained by the protonatable side chains of these residues being involved in initial H^+

binding, such that their elimination results in a higher concentration of protons being required for maximal activity. On the other hand, the effect of H210A and H93A mutation on the apparent K_m for alkali cations suggests that these residues also contribute to the coordination of Na^+ (in the case of H93) or Li^+ (H210) instead of H^+ at some stage of the catalytic cycle. The effects of mutations in H93, H210 and in residues of Cluster 1 are in accord with the concept that periplasmic parts of TMSs IV-VI together with flanking loops form a funnel with low selectivity which channels substrate cations toward the putative catalytic site associated with TMSs XI-XII.

The distribution of functionally important residues in the Vc-NhaD molecule suggests that two groups of transmembrane segments, TMSs IV-VI and TMSs X-XII, may be located close to one another. Since the Cys-less variant of Vc-NhaD is fully active [Habibian et al., 2005], the helical packing of Vc-NhaD, as well as the precise membrane topology of the antiporter, may be probed by Cys-scanning mutagenesis. In particular, introducing pairs of Cys residues at appropriate locations and applying different cross-linking reagents, one may estimate the distances between TMSs of interest.

The major conclusion from the R305 mutational analysis is that a single amino acid substitution, R305H, creates proton conductance through the Vc-NhaD in the absence of added alkali cations. It is supported by the following observations: (i) In Na^+-free medium, the enzymatic generation of ΔpH in membranes containing the mutated antiporter (R305H vesicles) is of lower magnitude compared to the wild type Vc-NhaD-containing membranes (wild type vesicles) (Fig. 4.9A); (ii) The ΔpH generation rate in R305H vesicles but not in wild type vesicles is insensitive to valinomycin in the presence

Fig. 4.12. pR305H protects the cells of *E. coli* EP432 from external LiCl. The pR305H plasmid, which contains Vc-NhaD (closed squares) bearing a R305H mutation, was used to transform *E. coli* strain EP432 bearing disruptions of *nhaA* and *nhaB* genes. For control experiments, cells of EP432 were transformed with "empty" pBluescript vector. The growth experiment was carried out as described in "Materials and Methods" and as per Fig. 4.2 in LBK medium buffered to pH 7.2. Representative of five independent experiments. The standard deviation is shown.

Fig. 4.12

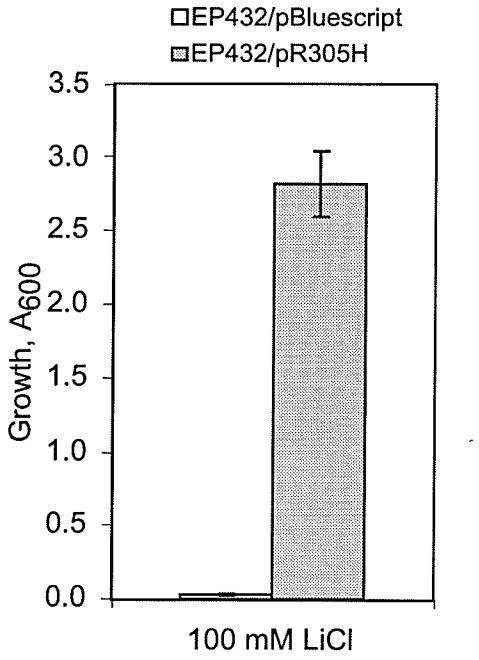
EP432/pBluescript
EP432/pR305H
3.5
3.0
2.5
2.0
1.5
1.0
0.5
0.0
Growth, A_{600}
100 mM LiCl

of K^+ ions (Fig. 4.9A); (iii) Addition of protonophorous uncoupler, CCCP, to wild type vesicles mimics the effect of R305H mutation on the generation of ΔpH (Fig. 4.9B).

These findings strongly suggest that the R305H mutation converts Vc-NhaD into a proton uniporter in the absence of Na^+ or Li^+. In the presence of alkali cations, however,the R305H variant of Vc-NhaD is still able to catalyze $Na^+(Li^+)/H^+$ exchange, as is illustrated in Fig. 4.9. This suggestion is supported experimentally by the cation-proton antiport activity measured in sub-bacterial vesicles containing R305H (Fig. 4.9 and 4.10) and by protection of the EP432 mutant provided by R305H variant of the antiporter against lethal concentrations of lithium (Fig. 4.12).

4.3. Toward Pharmacology of Na^+/H^+ Antiport in *V. cholerae*: Effects of 2-Aminoperimidine on Vc-NhaA and Vc-NhaD

4.3.1. Introduction

Specific inhibitors are valuable tools in biochemical studies of transport proteins. However, despite a long history of studies, no specific inhibitor has been so far reported for any member of the major enterobacterial antiporter family, NhaA. For NhaD antiporters, there is no known specific inhibitor, either. Because of their great physiological importance, Na^+/H^+ antiporters in bacterial pathogens such as *V. cholerae* are prospective targets for pharmacological agents.

The R-substituted guanidinium ions such as amiloride (Fig. 4.13, structure formula (3) and (4)) and its analogues [Lang, 2003] are competitive inhibitors of mammalian Na^+/H^+ antiporters belonging to the NHE family [Lang, 2003]. They have proven to be very valuable tools in the study of biochemistry, physiology and pharmacology of these membrane transporters. Amiloride also inhibits the Na^+/H^+ antiport in tonoplast and

plasmalemma of higher plants, algae and yeast [Blarka & Blumwald, 1991; Katz et al., 1994; Darley et al., 2000]. However, the only bacterial antiporter that is definitely sensitive to amiloride (with IC_{50} = 6 μM, as determined in purified protein reconstituted into proteoliposomes) is Ec-NhaB [Pinner et al., 1995]. An earlier report suggests that amiloride may be also effective against the Na^+/H^+ antiporter of methanogenic bacteria [Schonheit & Beimborn, 1985].

The ability of amiloride-type compounds to inhibit Na^+/H^+ antiporters is due to the presence of the small guanidine group, which mimics structurally the tri-hydrated Na^+ ion and thus can compete with Na^+ for the alkali cation-binding site of the antiporter [Lang, 2003; Natochin, 1982]. In spite of extensive screening of many of the common amiloride derivatives, none have been found to inhibit Ec-NhaA [Pinner et al., 1995]. Data obtained in our lab during the past few years showed that Vc-NhaD is also resistant to amiloride and its derivatives. These negative results could be interpreted in two ways: (i) The Na^+ binding sites of NhaA and NhaD are different from that of the amiloride sensitive antiporters; (ii) The Na^+ binding sites of NhaA,D types-antiporters are similar to that of the amiloride sensitive antiporters but are not accessible to the amilorides. By serendipity, we came across AP and noticed its similarity to amiloride, in that both compounds contain a guanidine group (Fig. 4.13).

The AP molecule, a known sulfate precipitant and potent inhibitor of cholinesterases [Shalitin et al., 2002], consists of a guanidine group fused to a naphthalene moiety (Fig. 4.13, structure formulas (1) and (2)). Crystallographic studies [Yokoyama et al., 1995] show that AP exists as a cation (2-perimidinylammonium ion) in two tautomeric forms, the $=NH_2^+$ tautomer (Fig. 4.13, structure formula (1)) and the

Fig. 4.13. 2-aminoperimidine structure formulae. AP cation (2-perimidinylamonium ion) exists in two tautomeric forms, the NH_2^+ tautomer (structure formula (1)) and the NH_3^+ one (structure formula (2)). The overall structure of AP resembles that of an R-substituted guanidinium ion (structure formula (3)), which includes amiloride (structure formula (4)) and its analogues.

Fig. 4.13

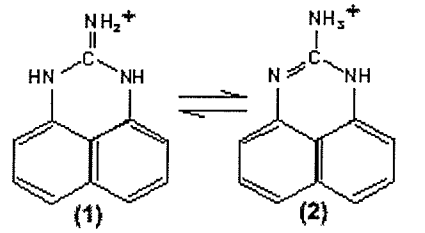

(1) (2)

2-aminoperimidine

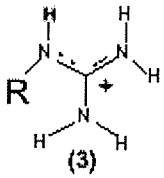

(3)

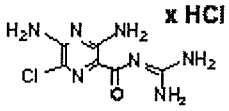

(4) *amiloride*

$-NH_3^+$ one (Fig. 4.13, structure formula (2)). Since AP has a pK_a of 9.5, it would be mostly cationic in the physiological pH range. The hydrophobic naphthalene moiety of AP (Fig. 4.13) suggests that the cationic form of AP is membrane permeable. Alternatively, the unprotonated form of AP may cross the membrane by passive diffusion and undergo reprotonation at the opposite side of the membrane.

We examined the effects of AP on Vc-NhaD and NhaA antiporters from *V. cholerae* and *E. coli*. For these studies, the *nhaA* gene from *V. cholerae* has been cloned and expressed in *E. coli* as described below.

4.3.2. Cloning of the *nhaA* Gene of *V. cholerae* and its Functional Expression in *E. coli*

We screened the *V. cholerae* genome database posted by The Institute for Genomic Research (TIGR) with the BLAST program using the DNA sequence of the NhaA from *V. parahaemolyticus* as a query and identified the corresponding open reading frame. As in the case of NhaD, both genes showed very high degrees of similarity, with 86% identities at the level of NhaA amino acid sequences. This putative Vc-NhaA ORF together with its flanking regions was cloned into the pBluescript vector, as described below, yielding the pBA construct.

pBA was constructed in partnership with Arthur Winogrodzki of our laboratory. Briefly, the *nhaA* gene was cloned by PCR using chromosomal DNA from *V. cholerae* strain O395-N1 as a template, which was isolated as described above. Primers NHAAF (5'-AAG CCG GAA TGG GCC CTC AGC CTT TTC GGA TGT GG-3') and NHAAR (5'-TTT GGT ATG GTC GAC CAG AGT CGA GTT GTG CTT TCA GTG C-3') were used. Following PCR, the resulting PCR product containing the putative Vc-NhaA ORF

Fig. 4.14. Construction of pBA. The*V. cholerae nhaA* gene was generated by PCR using chromosomal DNA isolated from *V. cholerae* strain O395-N1 as a template and was cloned into pBluescript-KS+ as an ApaI fragment, as described in "Materials and Methods". Figure made using DNA Strider Version 1.3.f14.

Fig. 4.14

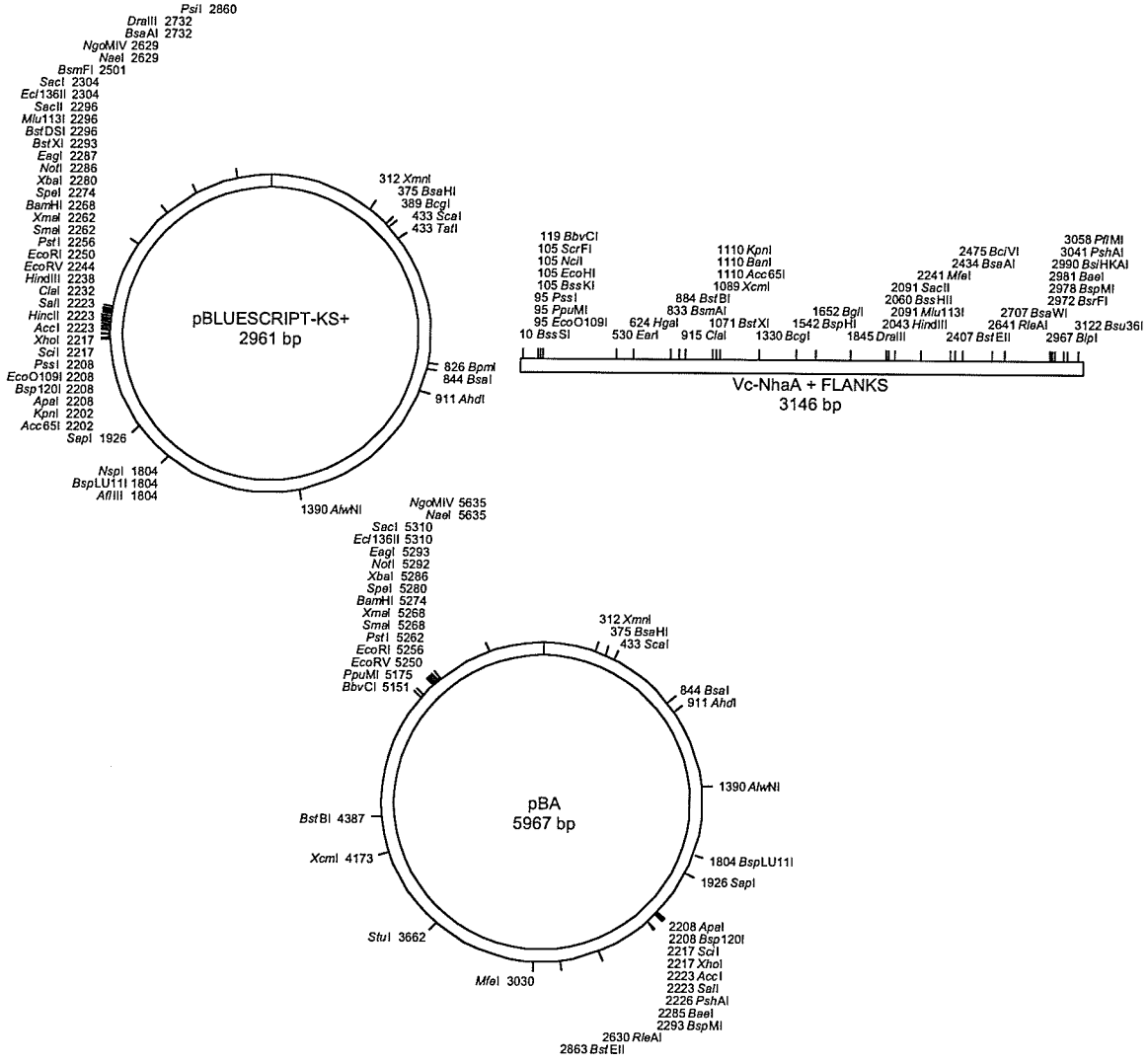
pBLUESCRIPT-KS+
2961 bp
Psi I 2860
DraIII 2732
BsaAI 2732
NgoMIV 2629
NaeI 2629
BsmFI 2501
SacI 2304
Ecl136II 2304
SacII 2296
Mlu113I 2296
BstDSI 2296
BstXI 2293
EagI 2287
NotI 2286
XbaI 2280
SpeI 2274
BamHI 2268
XmaI 2262
SmaI 2262
PstI 2256
EcoRI 2250
EcoRV 2244
HindIII 2238
ClaI 2232
SalI 2223
HincII 2223
AccI 2223
XhoI 2217
SciI 2217
PssI 2208
EcoO109I 2208
Bsp120I 2208
ApaI 2208
KpnI 2202
Acc65I 2202
SapI 1926
NspI 1804
BspLU11I 1804
AflIII 1804
1390 AlwNI
312 XmnI
375 BsaHI
389 BcgI
433 ScaI
433 TatI
826 BpmI
844 BsaI
911 AhdI
Vc-NhaA + FLANKS
3146 bp
119 BbvCI
105 ScrFI
105 NciI
105 EcoHI
105 BssKI
95 PssI
95 PpuMI
95 EcoO109I
10 BssSI
624 HgaI
530 EarI
884 BstBI
833 BsmAI
915 ClaI
1110 KpnI
1110 BanI
1110 Acc65I
1089 XcmI
1071 BstXI
1330 BcgI
1652 BglI
1542 BspHI
1845 DraIII
2475 BciVI
2434 BsaAI
2241 MfeI
2091 SacII
2060 BssHII
2091 Mlu113I
2043 HindIII
2707 BsaWI
2641 RleAI
2407 BstEII
3058 PflMI
3041 PshAI
2990 BsiHKAI
2981 BaeI
2978 BspMI
2972 BsrFI
3122 Bsu36I
2967 BlpI
pBA
5967 bp
NgoMIV 5635
NaeI 5635
SacI 5310
Ecl136II 5310
EagI 5293
NotI 5292
XbaI 5286
SpeI 5280
BamHI 5274
XmaI 5268
SmaI 5268
PstI 5262
EcoRI 5256
EcoRV 5250
PpuMI 5175
BbvCI 5151
312 XmnI
375 BsaHI
433 ScaI
844 BsaI
911 AhdI
1390 AlwNI
1804 BspLU11I
1926 SapI
2208 ApaI
2208 Bsp120I
2217 SciI
2217 XhoI
2223 AccI
2223 SalI
2226 PshAI
2285 BaeI
2293 BspMI
2630 RleAI
2863 BstEII
MfeI 3030
StuI 3662
XcmI 4173
BstBI 4387

Fig. 4.15. Vc-NhaA protects the cells of *E. coli* EP432 from external LiCl. The pBA plasmid, which contains Vc-NhaA (■) was used to transform *E. coli* strain EP432 bearing disruptions of *nhaA* and *nhaB* genes. For control experiments, cells of EP432 were transformed with "empty" pBluescript vector (❐). The growth experiment was carried out as described in "Materials and Methods" and as per Fig. 4.2. Representative of five independent experiments. The standard deviation is shown.

Fig. 4.15

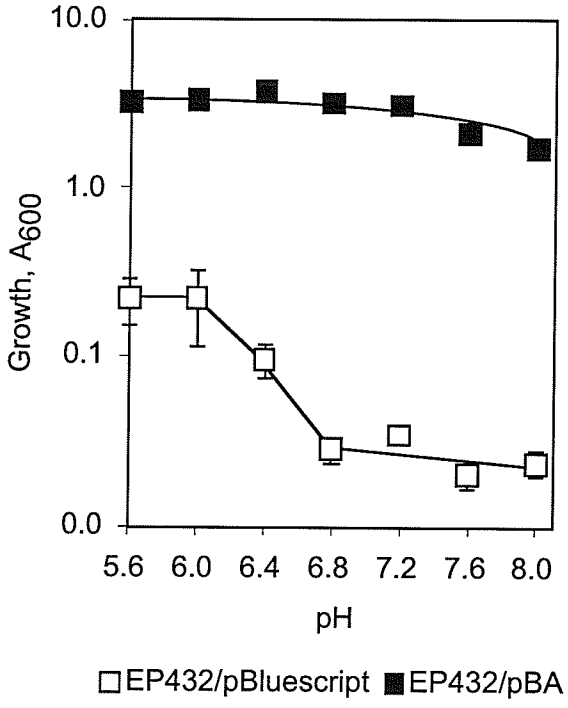
10.0
1.0
0.1
0.0
Growth, A_{600}
5.6 6.0 6.4 6.8 7.2 7.6 8.0
pH
EP432/pBluescript
EP432/pBA

together with 5' and 3' flanking sequences, was cloned into the pBluescript II KS+ (Stratagene) vector as an *Apa*I fragment yielding the pBA construct (Fig. 4.14). The clone used for further study, had the insert in opposite orientation to P_{lac}. This design allows for the expression of Vc-NhaA from its own promoter. The insert containing the *nhaA* gene was sequenced and found to be identical to the sequence reported by TIGR.

The pBA construct was introduced into EP432 host as described above, and functional expression of Vc-NhaA was confirmed by measuring the growth of transformants in the LBK medium supplemented with the concentration of LiCl lethal to the parental strain (Fig. 4.15).

4.3.3. The Specificity of 2-Aminoperimidine

Initial experiments regarding the inhibitory effect of AP on Ec-NhaA were performed in inside-out sub-bacterial vesicles derived from *E. coli* over-expressing Ec-NhaA and in proteoliposomes containing pure Ec-NhaA in collaboration with the laboratory of Dr. E. Padan. It was found that AP specifically inhibited the $Na^+(Li^+)/H^+$ antiport activity mediated by Ec-NhaA in both systems, but not Ec-NhaB [Dibrov et al., 2005].

To examine the specificity of AP towards *V. cholerae* antiporters, we repeated these experiments using inside-out sub-bacterial vesicles isolated from cells of *E. coli* EP432 expressing Vc-NhaA or Vc-NhaD. Similar to Ec-NhaA, Vc-NhaA was found to be sensitive to AP. Determination of IC_{50} gave 3.4 μM for 10 mM Na^+ and 3.7 μM for 1.0 mM Li^+ at pH 7.5 (Fig. 4.16A), indicating a very similar cation binding site of the two homologous NhaA antiporters. However, the cation-proton antiport was unaffected by

Fig. 4.16. AP specifically inhibits antiporters of NhaA type. Panel A: AP inhibits the Na^+/H^+ antiport (○) and Li^+/H^+ antiport (●) in inside-out membrane vesicles isolated from EP432 cells expressing Vc-NhaA. **Panel B:** Vc-NhaD is resistant to AP. Measurements were carried out under the same conditions of Vc-NhaA using inside-out membrane vesicles isolated from EP432 cells expressing Vc-NhaD. Open circles, Na^+/H^+ antiport activity; closed circles, Li^+/H^+ antiport activity. Representative of a typical experiment.

Fig. 4.16

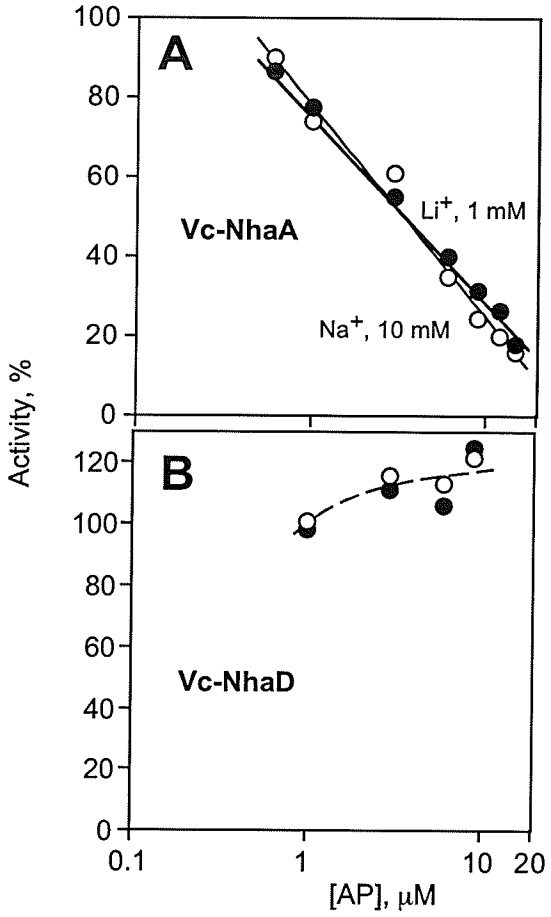
A
Vc-NhaA
Li+, 1 mM
Na+, 10 mM
B
Vc-NhaD
Activity, %
[AP], μM
100
80
60
40
20
0
120
0.1
1
10
20

the inhibitor in the case of Vc-NhaD (Fig. 4.16B). Thus, AP specifically inhibits bacterial Na^+/H^+ antiporters of the NhaA-type, while Vc-NhaD is resistant to AP.

4.3.4. Discussion

In this part of study, we found that AP inhibits the activity of Vc-NhaA with an IC_{50} close to 3.4 μM for Na^+/H^+ antiport (Fig. 4.16A). When assayed in sub-bacterial vesicles, AP also inhibits Ec-NhaA [Dibrov et al., 2005], but neither the heterologous Ec-NhaB [Dibrov et al., 2005] nor the Vc-NhaD (Fig. 4.16B) antiporters.

The identification of AP as a specific inhibitor of NhaA-type antiporters provides the first insight into the differences in pharmacological profiles of bacterial antiporters of NhaA and NhaD type. Also, AP is a new tool, which could be useful in future studies of ligand-protein interactions in NhaA-type antiporters. From the physiological point of view, AP could be used for selective inhibition of NhaA-type antiporters in growing bacterial cultures.

4.4. The Possible Physiological Role of NhaD in *V. cholerae*

4.4.1. Introduction

Na^+/H^+ antiporters are key elements in bacterial membrane energetics, maintaining pH homeostasis, $[Na^+]_{in}$ and osmoregulation. In addition, as discussed in the "Literature Review," a number of non-traditional, predominantly regulatory functions of these proteins have been uncovered during the past few years. The first attempt to reveal the role of Vc-NhaD in salt resistance of *V. cholerae* has been recently made by Herz *et al.* [Herz et al., 2003]. Using a *nhaD*-disrupted mutant of *V. cholerae*, the authors found that, in contrast to NhaA and NhaB, Vc-NhaD is not critical for export of toxic alkali cations.

This finding raised a question about the actual direction of the cation exchange mediated by Vc-NhaD in *V. cholerae*. It is conceivable that *in vivo* Vc-NhaD counteracts Vc-NhaA and Vc-NhaB, operating to import $Na^+(Li^+)$ in exchange for internal protons. If so, its primary role *in vivo* might be the regulation of cytoplasmic pH and internal $[Na^+]$ rather than contribution to halotolerance. We tried to address this question by comparing the phenotypes of Δ*nhaD* mutant of *V. cholerae* and cells overexpressing Vc-NhaD (see below sections).

As also discussed in the "Literature Review", some additional clues about the possible physiological role of NhaD come from the phylogenetic association of NhaD-type proteins with ArsB/NhaD superfamily of permeases and COG 1055, indicating possible relation of Vc-NhaD to arsenite/arsenate/phosphate metabolism in V. *cholerae*.

To probe the possible physiological role of Vc-NhaD, a chromosomal *nhaD* deletion mutant of *V. cholerae* was constructed as described below.

4.4.2. Construction of Chromosomal Deletion of *nhaD*.

In this part of the study we used *V. cholerae* strain O395-N1 *toxT::lacZ* (kindly provided by Dr. C. C. Häse, Oregon State University) and its isogenic Δ*nhaD* derivative, carrying an in-frame deletion in the Vc-NhaD ORF, DD1. DD1 was obtained by homologous recombination. The sequence containing Vc-NhaD ORF together with flanking sequences was amplified from genomic DNA by PCR using primers MADLF (5'-CAT CGA CAT CCA TGC ATC AAT CAA CAC CGC-3') and BM (5'-CAT TAC GGA TCC AGA TCC GTA ATA ACT CC-3' [a *BamH*I site is underlined]). The PCR product was cloned into HincII/BamHI digested pBluescript KS+ as a HincII/BamHI

fragment yielding the pBELD construct (*Vc-nhaD* with 919 bp 5'- and 230 bp 3'-flanks) (Fig. 4.17). pBELD was digested with *SnaB*I and self-ligated to generate an in-frame deletion of 241 residues (50.5% of the protein, S60-K301 residues removed) leaving 1078 bp 5'- and a 768 bp 3'-flanks. The resulting construct was named pΔSnaBL. The ΔNhaD insert was excised with *Hinc*II and *Ecl*136II, sub-cloned into the *Xmn*I site of suicidal vector pMAKSACB [Favre & Viret, 2000] (Fig. 4.18) and introduced into the *V. cholerae* O395-N1 chromosome following sucrose selection as described in [Favre & Viret, 2000]. Chromosomal deletion was verified by PCR using genomic DNA isolated from obtained sucrose-resistant, chloramphenicol-sensitive clones and oligonucleotide primers BM and ECF (5'-TAG CAT GAA TTC TAA AAA ATG ATG AAT AAA CAA CCA TTT CTA AGC-3'). One of the clones showing a shorter PCR product (1094 bp *vs.* 1817 in the parental strain) was selected, named DD1, and used in this study (Fig. 4.19).

4.4.3. Direction of Cation/Proton Exchange Mediated by Vc-NhaD

Comparing the salt resistance of EP432 transformants expressing electrogenic antiporter Vc-NhaA (stoichiometry of $2H^+/1Na^+$) or Vc-NhaD, we have found, that the latter protein failed to protect the growth against external Li^+ in alkaline media (Fig. 4.20). Indeed, already at pH 7.6, growth of EP432/pBLDL cells is considerably inhibited by 100 mM LiCl; at higher pH values, there was practically no growth, while EP432/pBA cells grew normally at pH 8.0 and even at pH 8.4 reached OD_{600} of app. 0.3 (Fig. 4.20). This could happen if Vc-NhaD, in contrast to Vc-NhaA, is an electroneutral antiporter, so that the direction of ion exchange is governed solely by the magnitudes of ΔpH and ΔpNa on the membrane.

Fig. 4.17. Construction of pBELD. The*V. cholerae nhaD* gene plus upstream and downstream shoulders was generated by PCR using chromosomal DNA isolated from *V. cholerae* strain O395-N1 as a template and was cloned into pBluescript-KS+ as an HincII/BamHI fragment, as described in "Materials and Methods". Figure made using DNA Strider Version 1.3.f14.

Fig. 4.17

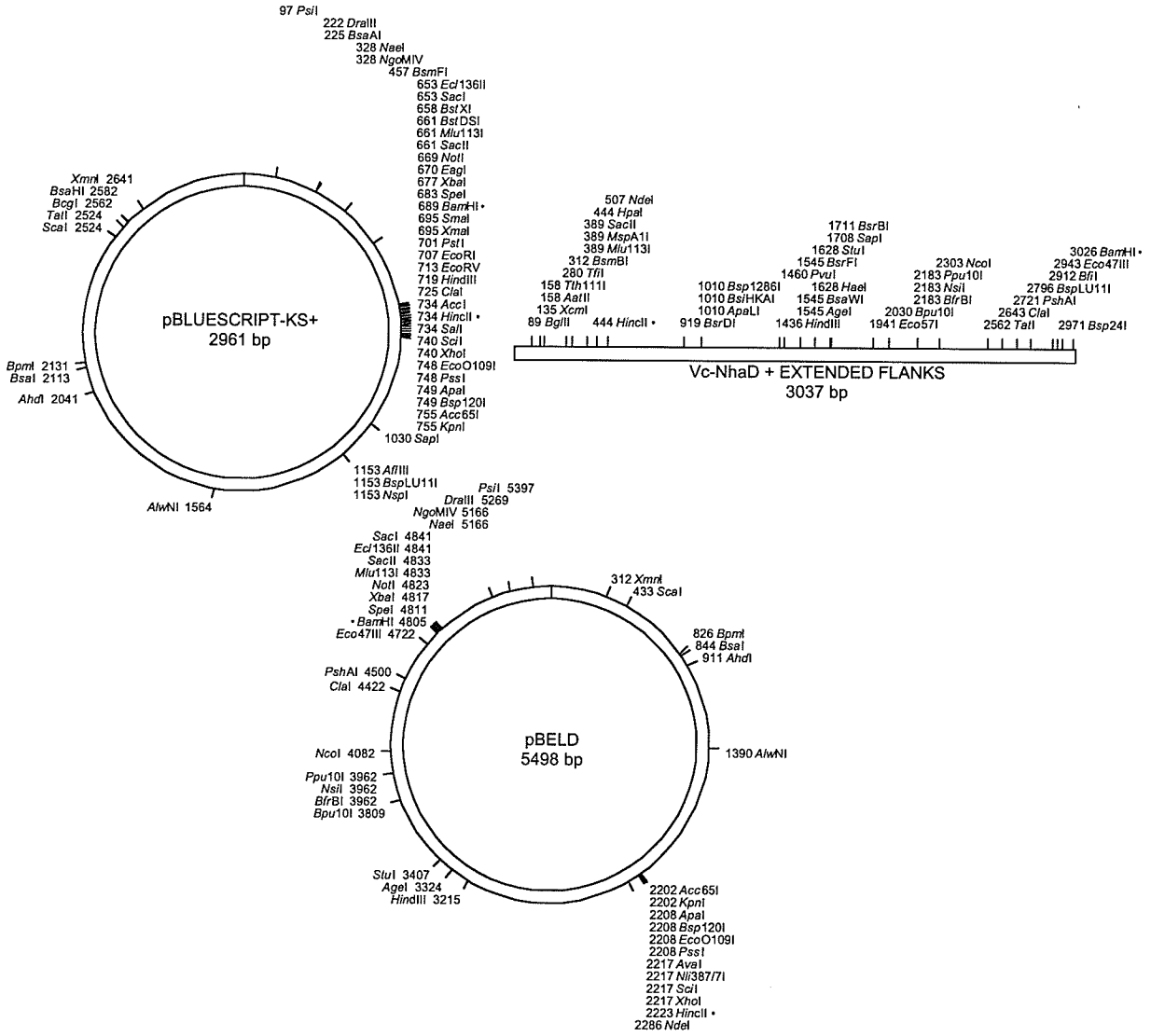
pBLUESCRIPT-KS+
2961 bp
97 PsiI
222 DraIII
225 BsaAI
328 NaeI
328 NgoMIV
457 BsmFI
653 Ecl136II
653 SacI
658 BstXI
661 BstDSI
661 MluI13I
661 SacII
669 NotI
670 EagI
677 XbaI
683 SpeI
689 BamHI •
695 SmaI
695 XmaI
701 PstI
707 EcoRI
713 EcoRV
719 HindIII
725 ClaI
734 AccI
734 HincII •
734 SalI
740 SciI
740 XhoI
748 EcoO109I
748 PssI
749 ApaI
749 Bsp120I
755 Acc65I
755 KpnI
1030 SapI
1153 AflIII
1153 BspLU11I
1153 NspI
PsiI 5397
DraIII 5269
NgoMIV 5166
NaeI 5166
SacI 4841
Ecl136II 4841
SacII 4833
MluI13I 4833
NotI 4823
XbaI 4817
SpeI 4811
• BamHI 4805
Eco47III 4722
PshAI 4500
ClaI 4422
NcoI 4082
Ppu10I 3962
NsiI 3962
BfrBI 3962
Bpu10I 3809
StuI 3407
AgeI 3324
HindIII 3215
2202 Acc65I
2202 KpnI
2208 ApaI
2208 Bsp120I
2208 EcoO109I
2208 PssI
2217 AvaI
2217 NlI387I
2217 SciI
2217 XhoI
2223 HincII •
2286 NdeI
312 XmnI
433 ScaI
826 BpmI
844 BsaI
911 AhdI
1390 AlwNI
XmnI 2641
BsaHI 2582
BcgI 2562
TatI 2524
ScaI 2524
BpmI 2131
BsaI 2113
AhdI 2041
AlwNI 1564
Vc-NhaD + EXTENDED FLANKS
3037 bp
507 NdeI
444 HpaI
389 SacII
389 MspA1I
389 MluI13I
312 BsmBI
280 TfiI
158 Tth111I
158 AatII
135 XcmI
89 BglII
444 HincII •
919 BsrDI
1010 Bsp1286I
1010 BslHKAI
1010 ApaLI
1436 HindIII
1545 BsaWI
1545 AgeI
1628 StuI
1628 HaeI
1711 BsrBI
1708 SapI
1545 BsrFI
1460 PvuI
1941 Eco57I
2030 Bpu10I
2303 NcoI
2183 Ppu10I
2183 NsiI
2183 BfrBI
2562 TatI
2643 ClaI
3026 BamHI •
2943 Eco47III
2912 BfiI
2796 BspLU11I
2721 PshAI
2971 Bsp24I

Fig. 4.18. Construction of pMADLS. First pBELD was digested with *SnaB*I and self-ligated to generate an in-frame deletion of 241 residues (S60-K301 residues removed) leaving 1078 bp 5'- and a 768 bp 3'-flanks. The resulting construct was named pΔSnaBL. The ΔNhaD insert was excised with *Hinc*II and *Ecl*136II, sub-cloned into the *Xmn*I site of suicidal vector pMAKSACB. Figure made using DNA Strider Version 1.3.f14.

Fig. 4.18

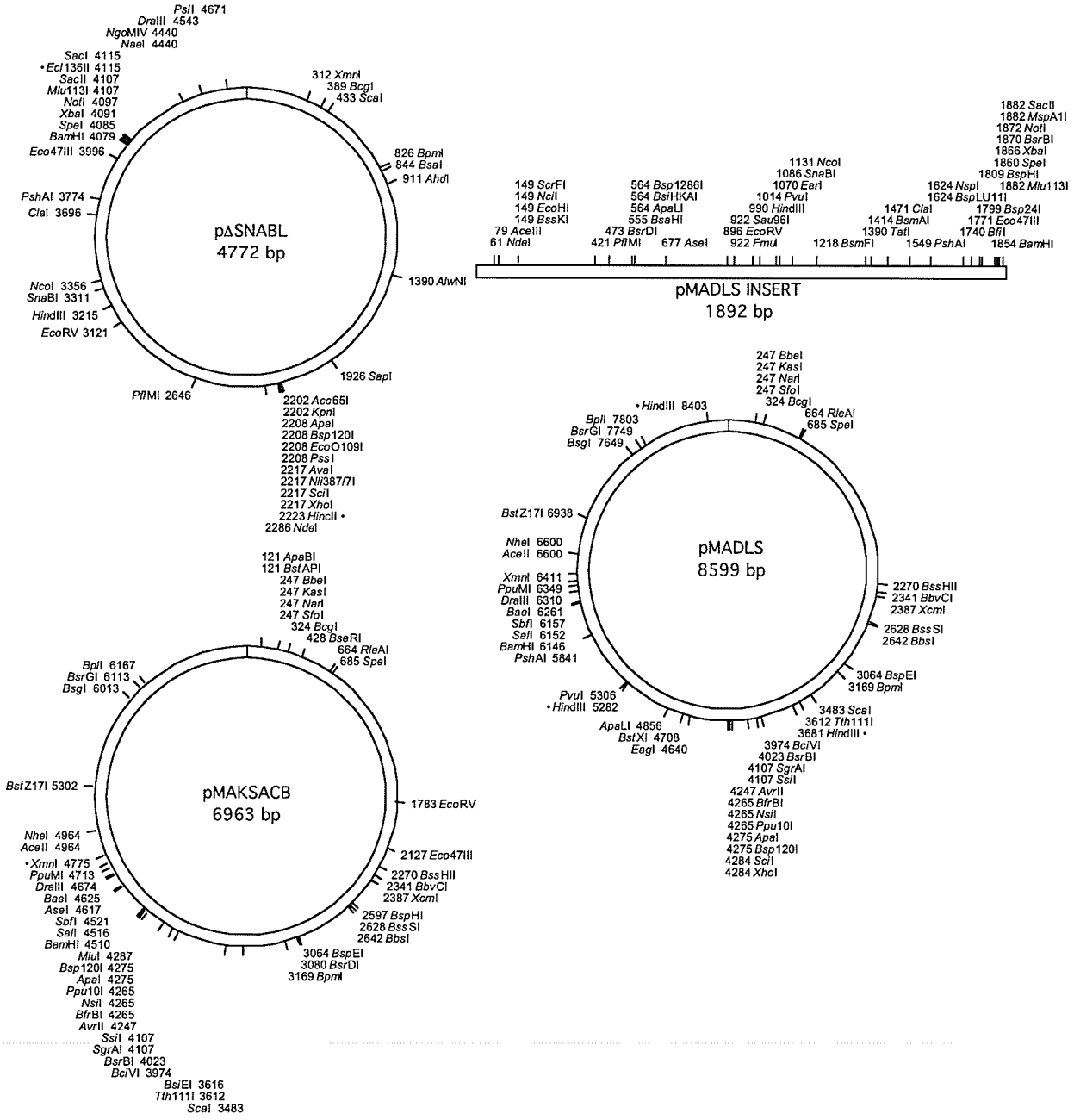
pΔSNABL
4772 bp
pMADLS INSERT
1892 bp
pMADLS
8599 bp
pMAKSACB
6963 bp

Fig. 4.19. PCR on chromosomal DNA isolation from five separate putative Δ*nhaD* clones. Clone #3 was used for further characterization.

Fig. 4.19

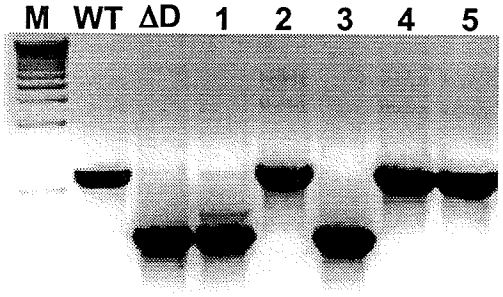

Fig. 4.20. Growth of *E. coli* EP432 in 100 mM LiCl expressing Vc-NhaD and Vc-NhaA at varying pHs. pBLDL plasmid contains Vc-NhaD (●) and pBA contains Vc-NhaA (■). For control experiments, cells of EP432 were transformed with "empty" pBluescript vector (○). All other conditions are as in Figs. 4.2 and 4.15. Representative of five independent experiments. The standard deviation is shown.

Fig. 4.20

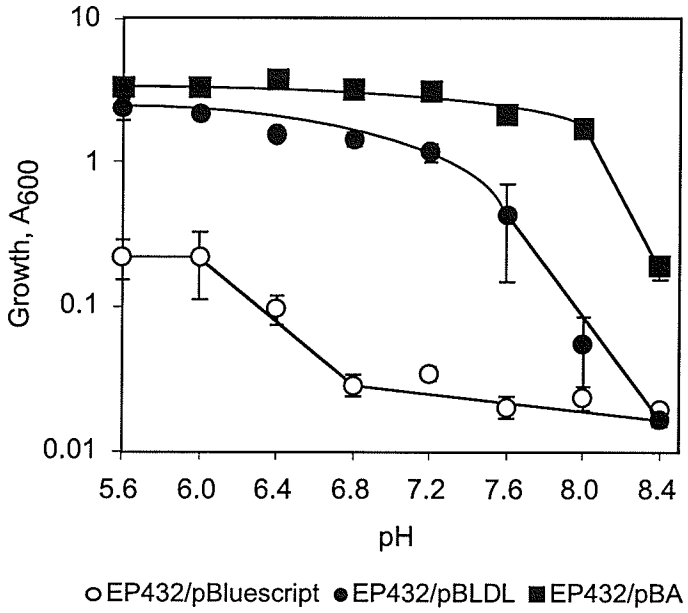
10
1
0.1
0.01
Growth, A_{600}
5.6
6.0
6.4
6.8
7.2
7.6
8.0
8.4
pH
EP432/pBluescript
EP432/pBLDL
EP432/pBA

The general thermodynamic equation describing the operation of antiporter exchanging ***n*** protons per each Na^+ (or Li^+) ion is:

$$\mathbf{\Delta pNa = n\Delta pH + (n\text{-}1)\Delta\psi}$$

Therefore, both ΔpH and Δψ can drive the sodium transport in this case. For the electroneutral antiporter (***n*** = 1), it will be:

$$\mathbf{\Delta pNa = \Delta pH}$$

Then, at low external pH, where ΔpH on the membrane (acidic outside) is sufficiently high, an electroneutral antiporter is expected to mediate the outwardly directed flux of Na^+ or Li^+. This also explains why, while the pH optimum for the Na^+/H^+ and Li^+/H^+ exchange mediated by Vc-NhaD is close to pH 8.0 [Dzioba et al., 2001; Ostroumov et al., 2002] when measured in inside-out vesicles (Fig. 4.21A, crosses), this antiporter is able to protect the growth of the antiport-deficient *E. coli* strain, EP432, against external LiCl (Fig. 4.21A, closed circles) at pH < 7.6.

Thus, in the simple model system of antiporterless EP432, the chemiosmotic behavior of introduced Vc-NhaD seems to be simple and could be explained by the above thermodynamic equations. But in its natural host, *V. cholerae*, Vc-NhaD operates in concert with primary Na^+ pumps and other antiporters, most importantly, electrogenic Vc-NhaA and Vc-NhaB. This makes the analysis of Vc-NhaD here more complicated.

Measuring the growth of *V. cholerae* cells bearing the chromosomal Vc-NhaD deletion vs. wild type and cells overexpressing Vc-NhaD, we found that even at lower external pH (pH 6.0), Vc-NhaD inhibits the growth in medium containing 180 mM LiCl (Fig. 4.21B). Indeed, in this case the deletion of *nhaD* results in more than two-fold increase in growth (Fig. 4.21B). This indicates that under these conditions the ΔpH

Fig. 4.21. Physiology of Vc-NhaD. Panel A: Vc-NhaD fails to protect antiporter-less EP432 cells against toxic LiCl at alkaline external pH. Growth of EP432/pBLDL transformants (●) or parental EP432 (○) was measured after 15 hours of aerobic growth in LBK supplemented with 0.1M LiCl at the indicated pH (left ordinate). Growth conditions are as in Fig. 4.2 except the starting pH was adjusted by the addition of 60 mM BTP-HCl. Crosses (✚), pH profile of Vc-NhaD activity measured in inside-out membrane vesicles derived from EP432/pBLDL (right ordinate). Conditions are as in Fig. 4.4. **Panel B:** Overexpression of Vc-NhaD hinders the growth of *V. cholerae* in LiCl-supplemented LBK media (starting pH adjusted with 60 mM HEPES-MES in the case of pH 6.0 and 60 mM HEPES-Tris in the case of pH 8.0). Growth conditions are as described in "Materials and Methods." Briefly, test tubes containing 2.0 ml of medium were inoculated with colonies taken from LB-grown plates. The cells were grown aerobically at 37°C. Open bars, parental O395-N1 strain; closed bars, DD1 mutant; hatched bars, DD1/pBLDL transformant. Representative of five independent experiments. The standard deviation is shown.

Fig. 4.21

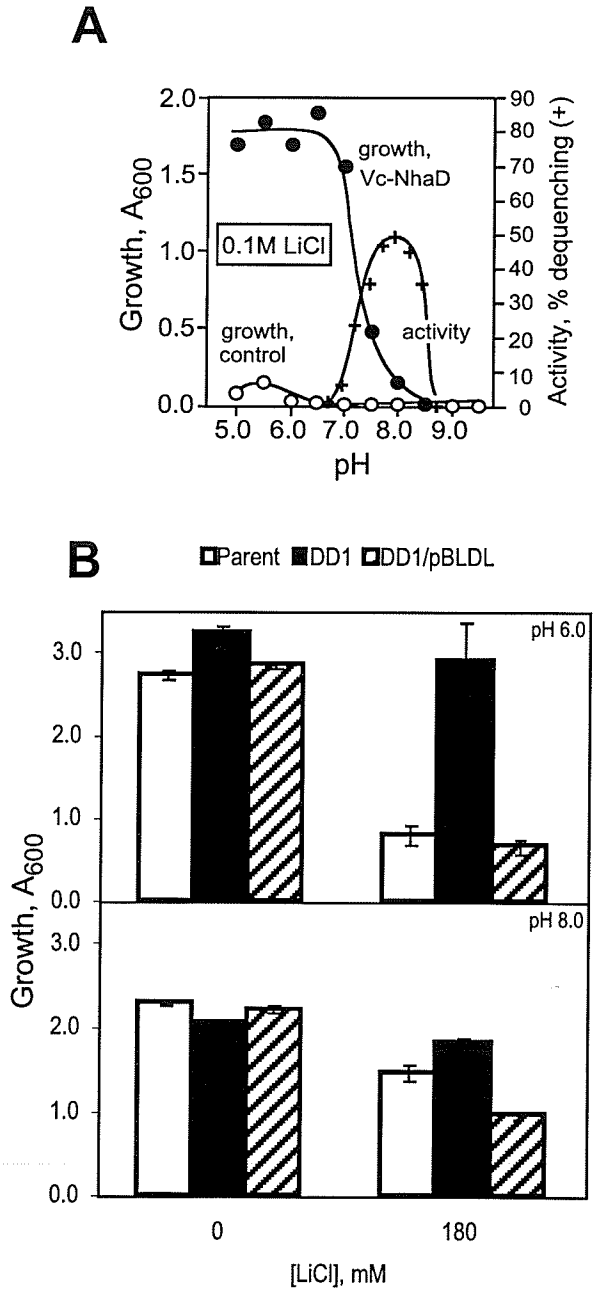
A
2.0
1.5
1.0
0.5
0.0
Growth, A_{600}
90
80
70
60
50
40
30
20
10
0
Activity, % dequenching (+)
growth, Vc-NhaD
0.1M LiCl
growth, control
activity
5.0 6.0 7.0 8.0 9.0
pH
B
Parent DD1 DD1/pBLDL
pH 6.0
pH 8.0
3.0
2.0
1.0
0.0
Growth, A_{600}
0
180
[LiCl], mM

existing on the *V. cholerae* membrane is such that at steady-state the intracellular concentration of Li^+ in cells expressing functional Vc-NhaD is still poisoning. Therefore, under conditions of heavy Li^+ load, Vc-NhaD is a major route for the alkali cation uptake at any pH.

The following questions are to be answered here: (i) Why in the absence of functional Vc-NhaD, do high concentrations of external Li^+ not poison the cells of *V. cholerae* at pH 6.0? (ii) Why at pH 6.0 is the difference in growth between wild type and Δ*nhaD* mutant even somewhat greater than at alkaline pH? (iii) Why being expressed in EP432 Vc-NhaD expels alkali cations at acidic pHs but apparently imports them in *V. cholerae*?

The most probable explanations are: (i) It is well known that at low external pHs Na^+ and Li^+ are not accumulated by bacterial cells as readily as at alkaline pHs [Ikegami et al., 2000]. The reason for that is not investigated, but most probably it is due to the pH dependence of $Na^+(Li^+)$-substrate symporters, which provide general routes of entry for alkali cations *in vivo*. (ii) In acidic growth media, relatively weak NhaB is the only Li^+ exporting mechanism available [Pinner et al., 1992; Pinner et al., 1993; Padan & Schuldiner, 1994; Padan & Schuldiner, 1996] while NhaA is virtually inactive due to its steep pH dependence [Gerchman et al., 1993; Olami et al., 1997]. In alkaline media, NhaA is fully active, extruding alkali cations very efficiently [Gerchman et al., 1993; Olami et al., 1997]. Thus the detrimental effect of NhaD on growth is naturally more pronounced at low pHs. (iii) Due to the presence of electrogenic Vc-NhaA and Vc-NhaB, acting to acidify the cytoplasm, at any given external pH the internal pH in *V.*

cholerae is apparently lower then in EP432. Therefore, the resulting ΔpH should be higher in EP432 and sufficient for export of $Li^+(Na^+)$ via Vc-NhaD at low external pH.

Summing up, our data suggest that *in vivo* Vc-NhaD counteracts electrogenic $Na^+(Li^+)$ extrusion through Vc-NhaA,B shortcircuiting transmembrane flux of alkali cations (at least, to some extent). It seems paradoxical to allow the operation of an electroneutral Na^+/H^+ antiporter in the membrane which contains a pair of electrogenic NhaA and NhaB exchangers, because it should result in a futile cycle for $Na^+(Li^+)$. However, the same membrane contains also a primary Na^+ pump, NQR, and secondary Na^+-extruding enzymes, Vc-NhaA and Vc-NhaB. This abundance of Na^+-extruding systems apparently require an additional element of the Na^+ cycle, which would mediate the uptake of Na^+ ions to keep intracellular $[Na^+]$ above K_m values for electrogenic Na^+ exporters. This would ensure the effectiveness of transmembrane Na^+ circulation in *V. cholerae*. On the other hand, operation of Vc-NhaD would undoubtedly prevent overacidification of the cytoplasm due to the functioning of Vc-NhaA,B. Importantly, the Vc-NhaD-mediated Na^+ entry route does not depend on either the motility status of the cell (as in the case of Na^+-driven flagellar motor) or the availability of a Na^+-symported substrate (another natural way of bringing Na^+ ions into the cytoplasm). All this defines Vc-NhaD as an important tool in the homeostasis of cytoplasmic pH and ionic composition.

Fig. 4.22. Panel A: Phylogenetic tree of representative members of the ArsB/NhaD superfamily of permeases. The sequences used were found in *Microbulbifer degradans* (accession no. ZP_00064921), *Rhodobacter sphaeroides* (ZP_00007535), *Desulfotalea psychrophila* (CAG35577), *Shewanella oneidensis* (AAN54009), *Photobacterium profundum* (CAG20988), *Vibrio cholerae* (AAF96911), *Vibrio parahaemolyticus* (BAC61394), *Vibrio vulnificus* (AAO08110), *Magnetococcus* sp. (ZP_00288831), *Chlamydia pneumoniae* (BAA99222), *Chlamydia trachomatis* (AAC68454), *Populus euphratica* (CAD91128), *Arabidopsis thaliana* (AAG51773), *Psychrobacter* sp. (ZP_00146388), *Exiguobacterium* sp. (ZP_00184376), *Lactobacillus plantarum* (CAD62747), *Pseudomonas aeruginosa* (AAG05666), *Pseudomonas putida* (AAN67546), *Pseudomonas fluorescens* (ZP_00265393), *Pseudomonas syringiae* (AAO57267), *Methylobacillus flagellatus* (ZP_00350170), *Escherichia coli* (AAG58634), *Yersinia pseudotuberculosis* (CAH20025), and *Symbiobacterium thermophilum* (BAD39878). Underlined proteins are functionally characterized transporters. **Panel B:** Putative Pho-box in the upstream region of *nhaD* from *V. cholerae*. Consensus sequence and its variations are taken from [Wanner B. L. 1996]. Solid vertical lines show strong conservation; dotted lines show a weaker conservation at a given position.

Fig. 4.22A

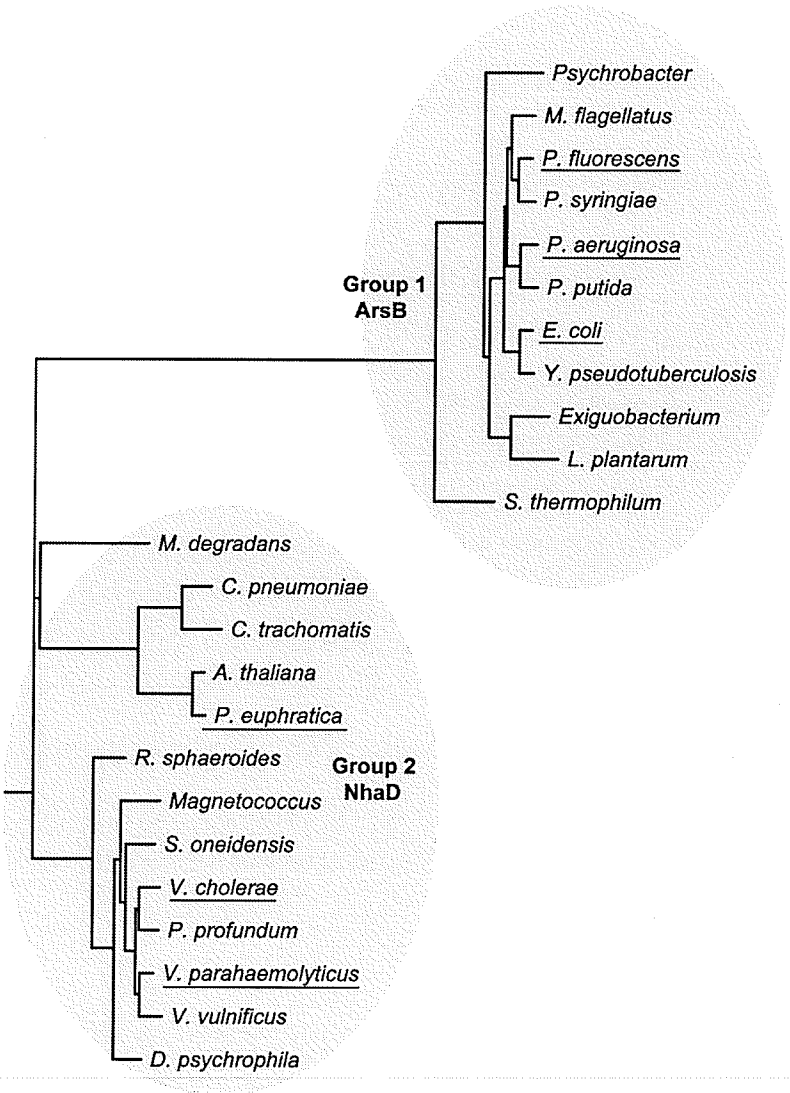
Psychrobacter
M. flagellatus
P. fluorescens
P. syringiae
P. aeruginosa
P. putida
E. coli
Y. pseudotuberculosis
Exiguobacterium
L. plantarum
S. thermophilum
Group 1
ArsB
M. degradans
C. pneumoniae
C. trachomatis
A. thaliana
P. euphratica
R. sphaeroides
Magnetococcus
S. oneidensis
V. cholerae
P. profundum
V. parahaemolyticus
V. vulnificus
D. psychrophila
Group 2
NhaD

Fig. 4.22B

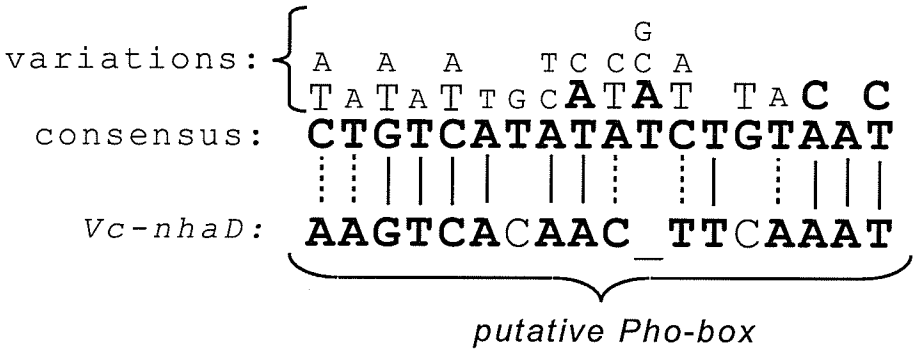
variations:
G
A A A TCCCA
TATATTGCATATTACC
consensus:
CTGTCATATATCTGTAAT
Vc-nhaD:
AAGTCACAAC_TTCAAAT
putative Pho-box

4.4.2. Vc-NhaD Modulates Arsenate Resistance and Net Inorganic Phosphate Transport in *V. cholerae*

Phylogeny of representative NhaD and ArsB amino acid sequences (Fig. 4.22) suggest that the two types of transporters evolved from a common ancestral protein. However, a significant evolutionary distance separates a branch containing functionally characterized Na^+/H^+ antiporters of NhaD-type from the group of proteins that mediate efflux of arsenite.

On the other hand, the upstream region of the *Vc-nhaD* gene contains a sequence AAGTCACAACTTCAAAT, which is similar to the *E. coli* Pho box consensus, a typical regulatory element of genes belonging to the phosphate regulon (see Fig. 4.22B). We therefore undertook investigation of a possible role of Vc-NhaD in the phosphate, arsenate, and arsenite transport of *V. cholerae*.

Growth of *V. cholerae* cells possessing an intact chromosomal copy of *Vc-nhaD* was found to be highly sensitive to As(III) in the form of arsenite. Already at 0.1 mM, the growth was almost completely inhibited (Fig. 4.23A, empty circles). Deletion of *Vc-nhaD* did not affect the sensitivity to arsenite (Fig. 4.23A, closed squares), thus demonstrating that Vc-NhaD does not act as an arsenite permease. This is in accord with the pylogenetic analysis predicting a divergent evolution of the ArsB and NhaD-type transporters (see Fig. 4.22A).

However, the resistance of *V. cholerae* to As(V) in the form of arsenate was clearly Vc-NhaD-dependent (Fig. 4.23B). 7.5 mM arsenate added to buffered LBK medium severely inhibited the growth in Vc-$NhaD^+$ cells over the pH range 6.4 to 7.6 (Fig. 4.23B, closed circles). In contrast, the ΔNhaD cells of DD1 showed progressively higher arsenate resistance when the pH was raised from 6.0 to 7.2 (closed triangles), so that at

Fig. 4.23. Role of Vc-NhaD in arsenic resistance of *Vibrio cholerae*. Panel A: Chromosomal deletion of *nhaD* gene does not affect the sensitivity of *V. cholerae* to As(III) in the form of arsenite. Wild type (○) and ΔVc-NhaD strain (■) were grown for 15 hours at 37°C in LBK medium (pH 7.2 adjusted with 60 mM HEPES-Tris) supplemented with varying concentrations of arsenite. Growth conditions are as described in Fig. 4.19. **Panel B:** Chromosomal copy of *nhaD* (○, ●) or *nhaD* expressed *in-trans* from pBLDL (□, ■) renders *V. cholerae* cells sensitive to As(V) in the form of arsenate at pH 6.5 to 7.8 (adjusted with 60 mM HEPES-Tris). Growth conditions are as in Fig. 4.19. Triangles, ΔVc-NhaD strain, DD1 (△, ▲). Open symbols, growth without added arsenate (control); closed symbols, growth in the presence of 7.5 mM Na^+-arsenate. Cells were grown aerobically in LBK medium buffered at indicated pH (adjusted with 60 mM HEPES-Mes in the case of pH 6.0-6.3 and HEPES-Tris in the case of pH 6.4-8.2) at 37°C for 15 hours. Average values of eight independent experiments are plotted. The standard deviation is shown.

Fig. 4.23

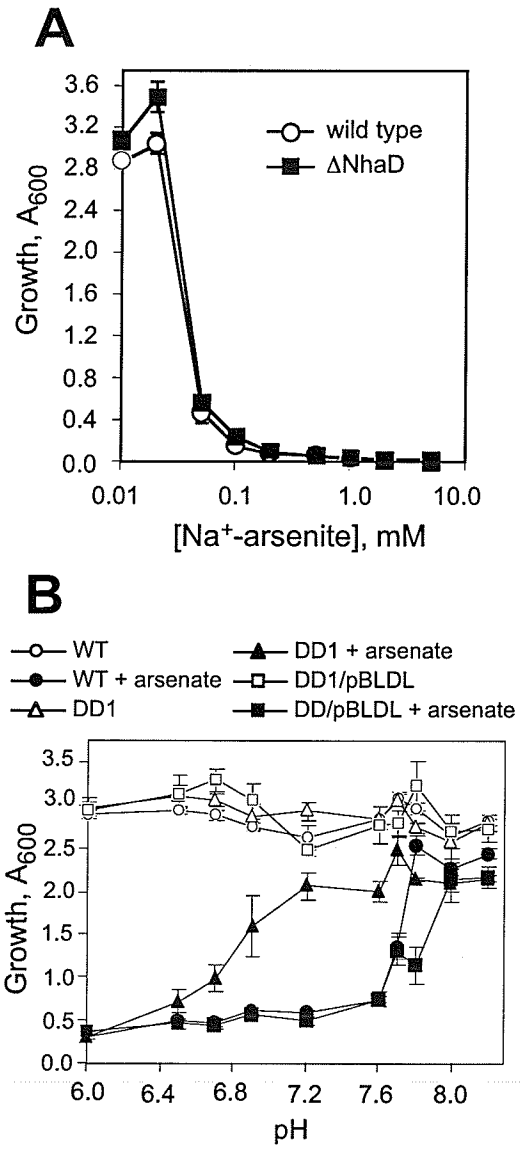
A
3.6
3.2
2.8
2.4
2.0
1.6
1.2
0.8
0.4
0.0
Growth, A_{600}
wild type
ΔNhaD
0.01
0.1
1.0
10.0
[Na^+-arsenite], mM
B
WT
WT + arsenate
DD1
DD1 + arsenate
DD1/pBLDL
DD/pBLDL + arsenate
3.5
3.0
2.5
2.0
1.5
1.0
0.5
0.0
Growth, A_{600}
6.0
6.4
6.8
7.2
7.6
8.0
pH

pH 7.2-7.6, added arsenate had no significant effect on the growth in this strain. At pH 7.8 and higher, cells were resistant to arsenate irrespectively of the presence of Vc-NhaD. Introduction of the *Vc-nhaD* gene on multicopy plasmid (pBluescript derivative, pBLDL [see Section 4.1]) restored the arsenate-sensitive phenotype in the DD1/pBLDL transformant (closed squares).

Elevated resistance to arsenate in the ΔNhaD mutant indicated possible alterations in P_i import. Arsenate is a competitive inhibitor of phosphate transport; mutations of the constitutive Pit system, importing P_i as a neutral metal-phosphate ($MeHPO_4$) complex in symport with H^+ [van Veen et al., 1994] conferred increased arsenate resistance in *E. coli* [Bennet & Malamy, 1970] and *B. subtilis* [Kay & Ghei, 1981]. If Vc-NhaD was related to the import of inorganic phosphate, one would expect that the addition of phosphate to the arsenate-containing growth medium should protect the Vc-NhaD$^+$ cells. Fig. 4.24A shows the growth of parental Vc-NhaD$^+$ strain (empty bars), DD1 strain (grey bars), and DD1/pBLDL (hatched bars) in buffered LBK medium (pH 7.2) supplemented with 7.5 mM arsenate in the presence of varying concentrations of P_i. As one can see, exogenous phosphate added on top of arsenate indeed protects, in a concentration-dependent manner, the growth of both parental strain and DD1 expressing the Vc-NhaD antiporter *in trans*. Furthermore, under the conditions of phosphate starvation, net P_i uptake by ΔNhaD cells was somewhat lower compared to the wild type (Fig. 4.24B, closed circles versus open circles). Being introduced *in trans*, *Vc-nhaD* complemented the P_i uptake deficiency, albeit partially (Fig. 4.24B, closed triangles).

In an attempt to analyze the possible mechanism by which Vc-NhaD is involved in phosphate transport, we examined the growth properties of DD1 cells expressing two

Fig. 4.24. Vc-NhaD modulates P_i uptake in *V. cholerae* cells. Panel A: K^+-phosphate added to the LBK medium supplemented with 7.5 mM Na^+-arsenate protects, in a concentration-dependent manner, growth of cells expressing Vc-NhaD from either a single chromosomal copy of *nhaD* (empty bars) or multicopy plasmid, pBLDL (hatched bars). For the control experiments, DD1 mutant cells were used (grey bars). Cells were grown aerobically in LBK medium (pH 7.2) at 37°C for 15 hours. Average values of eight independent experiments are plotted. Standard deviation is shown. **Panel B:** Deletion of Vc-NhaD results in lowered P_i uptake by whole cells of *V. cholerae* under the conditions of P_i starvation. These measurements were performed in collaboration with Dr. E. Padan (Hebrew University of Jerusalem). Empty circles, wild type cells (○); closed circles, DD1 cells (●); closed triangles, DD1/pBLDL transformant cells (▲). Results of a typical of three independent experiments are shown.

Fig. 4.24

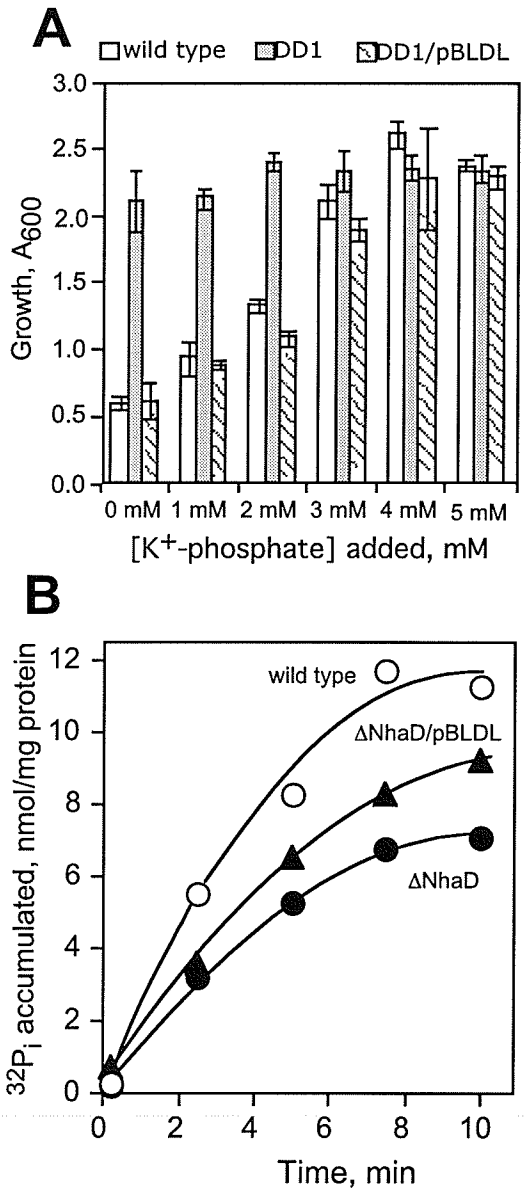
A
wild type
DD1
DD1/pBLDL
Growth, A_{600}
3.0
2.5
2.0
1.5
1.0
0.5
0.0
0 mM 1 mM 2 mM 3 mM 4 mM 5 mM
[K^+-phosphate] added, mM
B
$^{32}P_i$ accumulated, nmol/mg protein
12
10
8
6
4
2
0
wild type
ΔNhaD/pBLDL
ΔNhaD
0 2 4 6 8 10
Time, min

Fig. 4.25. The ability of Vc-NhaD to mediate Na^+/H^+ antiport is critical for its effect on arsenate sensitivity in *V. cholerae* cells. Panel A: pH profiles of antiport activity of different variants of Vc-NhaD were measured in the inside-out membrane vesicles isolated from EP432 transformants as described in Materials and Methods. Empty circles, wild type Vc-NhaD (○); open triangles, D199A variant (△); closed diamonds, T202A variant (♦). **Panel B:** Neither D199A nor T202A mutation prevents the expression and targeting of Vc-NhaD in *V. cholerae*. Immunodetection of different variants of Vc-NhaD in *V. cholerae* membranes was performed by Dr. J. Barrett with anti-Vc-NhaD antibodies as described in Materials and Methods. Chromosomal, Vc-NhaD expressed from a single chromosomal copy of *nhaD* gene; wild type, non-mutated antiporter expressed from pBLDL. **Panel C:** Only functional Vc-NhaD renders *V. cholerae* cells sensitive to external arsenate. Growth conditions as in Fig. 4.23. Representative of five independent experiments. The standard deviation is shown.

Fig. 4.25

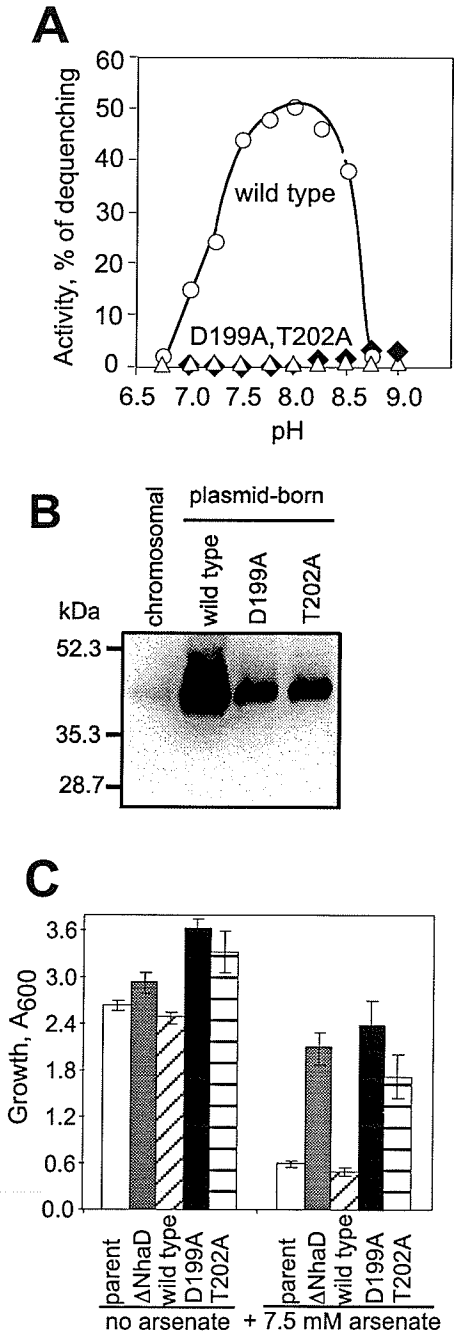
A
Activity, % of dequenching
60
50
40
30
20
10
0
wild type
D199A,T202A
6.5 7.0 7.5 8.0 8.5 9.0
pH
B
plasmid-born
chromosomal
wild type
D199A
T202A
kDa
52.3
35.3
28.7
C
Growth, A600
3.6
3.0
2.4
1.8
1.2
0.6
0.0
parent
ΔNhaD
wild type
D199A
T202A
parent
ΔNhaD
wild type
D199A
T202A
no arsenate
+ 7.5 mM arsenate

functionally impaired variants, D199A and T202A (Fig. 4.25). The pBLDL derivatives encoding these variants were first introduced into antiporter-deficient EP432 cells and the pH profiles of Na^+/H^+ antiport activity were determined in subbacterial vesicles (Fig. 4.25A). As one can see, both variants completely lost the ability to catalyze Na^+-dependent H^+ transfer over the pH range 6.75 to 9.0 (Fig. 4.25A).

As evidenced from the immunodetection data, neither mutation prevented the expression or targeting of Vc-NhaD. Indeed, being expressed from the plasmid in the DD1 strain of *V. cholerae*, both variants were present in the membrane preparations in amounts that were lower than that of the wild-type protein expressed from the same plasmid, but far exceeded the expression of Vc-NhaD from its chromosomal gene in the parental strain (Fig. 4.25B). A diffuse immunoreactive band of chromosomally encoded antiporter was barely detectable, indicating a very low abundance of Vc-NhaD in the wild-type *V. cholerae* membrane. This is apparently a common feature of bacterial Na^+/H^+ antiporters; Ec-NhaA, the major antiporter of *E. coli*, is also undetectable by Western blotting when expressed from a single chromosomal *nhaA* gene, yet it confers a wild-type phenotype [Rimon et al., 1998].

In contrast to the wild-type antiporters, both D199A and T202A variants failed to restore the arsenate sensitivity when expressed in DD1 cells (Fig. 4.25C). Thus, the influence of Vc-NhaD on phosphate (arsenate) transport is based on its ability to catalyse the Na^+/H^+ antiport.

When assayed in sub-bacterial vesicles, Vc-NhaD did not catalyse P_i/H^+ antiport; addition of phosphate or arsenate did not affect in any way the Na^+-dependent H^+ transport, as well (data not shown). Moreoever, when introduced *in trans*, Vc-NhaD did not complement a phosphate transport deficient strain of *E. coli* (Δ*pst*,Δ*pitA*,Δ*pitB*) (Fig.

Fig. 4.26. Vc-NhaD fails to complement *E. coli* strain AN3902. An *E. coli* strain (AN3902) bearing deletions of *pitA*, *pitB* and *pst* was transformed with pBLDL. The cells were grown aerobically in non-buffered LB medium supplemented with 5 mM glycerol-3-phospate or 5 mM Na_2HPO_4 at 37°C. Representative of five independent experiments. The standard deviation is shown.

Fig. 4.26

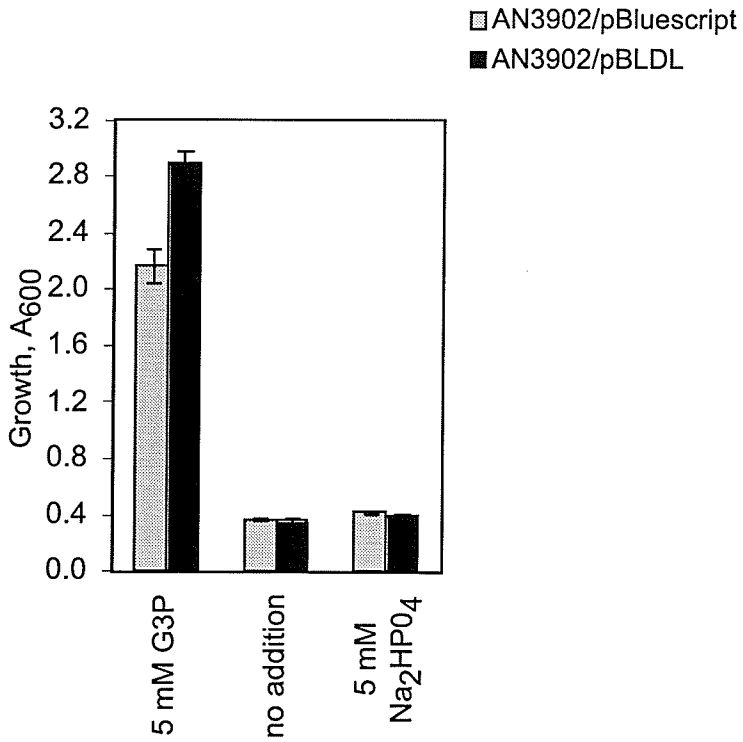
AN3902/pBluescript
AN3902/pBLDL
Growth, A_{600}
3.2
2.8
2.4
2.0
1.6
1.2
0.8
0.4
0.0
5 mM G3P
no addition
5 mM Na_2HPO_4

4.26). Therefore, it is unlikely that Vc-NhaD can use either phosphate or arsenate as a substrate ion. Instead, it could affect phosphate (arsenate) transport mediated by some other system(s) indirectly, for example, through changes in cytoplasmic [Na^+] and/or pH.

4.4.5. Discussion

In summary, the body of data accumulated so far, including growth data and the results obtained in sub-bacterial vesicles, show that *in vivo* Vc-NhaD mediates the influx rather than efflux of alkali cations in exchange for intracellular protons. Thus Vc-NhaD most probably operates as an electroneutral (or nearly electroneutral) $Na^+(Li^+)/H^+$ exchanger. This differentiates Vc-NhaD from electrogenic NhaA and NhaB-type antiporters. Direct measurement of the stoichiometry of Vc-NhaD is needed to check this possibility. Such measurements require functional reconstitution of purified antiporter into proteoliposomes, as it has been done with Ec-NhaA and Ec-NhaB [Taglict et al., 1993; Pinner et al., 1994]. Unfortunately, our attempts to isolate pure Vc-NhaD in amounts sufficient for the reconstitution were so far unsuccessful, but this goal will be pursued in the future studies.

Alkalinization of the cytoplasm by Vc-NhaD seems to play a central role in the regulation of phosphate transport and arsenate sensitivity in *V. cholerae.* As pointed out above, Vc-NhaD most probably regulates P_i transport by influencing some other P_i transport system of *V. cholerae.*

A number of phosphate transporters appear to exist in *V. cholerae*, which could be a possible target of regulation by Vc-NhaD. The genome of this organism contains two *pstSCAB*-like operons, VC0721-25 and VCA0070-73, encoding homologues of ABC-type ATPase with high affinity for P_i but low affinity for arsenate. It is induced only if

the external [P_i] falls below the millimolar range (see [van Veen, 1997] for an excellent review of microbial phosphate transporters). VCA0137 encodes a GlpT-type transporter, which in *E. coli* and other bacteria mediates the electroneutral antiport of phosphate (or arsenate) with glycerol-3-phosphate [van Veen, 1997]. GlpT has a much better selectivity for $H_2PO_4^-$ over HPO_4^{2-} [van Veen, 1997] suggesting that GlpT will contribute more to the overall uptake in acidic media, where phosphate and arsenate exist predominantly as monovalent anions. Thus GlpT-mediated uptake may account for the high arsenate sensitivity of *V. cholerae* cells at pH 6.0, which is however independent of the presence of functional Vc-NhaD (Fig. 4.23B).

VC2442 encodes the *V. cholerae* homologue of the Pit system, the major P_i uptake system in *E. coli*. It is constitutively expressed and mediates an electrogenic symport of $MeHPO_4$ or $MeHAsO_4$ complex with H^+ [Rosenberg et al., 1977; Rosenberg et al., 1979; van Veen et al., 1994; van Veen, 1997]. Importantly, since the overall transport reaction is limited by the dissociation of chemiosmotic H^+ from the protonated form of the transporter, Pit is most active at alkaline internal pH, and acidification of the cytoplasm strongly inhibits the transporter [van Veen, 1997]. Such behavior is consistent with the observed pH profile of Vc-NhaD-dependent arsenate sensitivity in *V. cholerae*, which is most pronounced at external pH > 7.2, where the bacterial cytoplasm is presumably more alkaline (Fig. 4.23B). Therefore, it is conceivable that Vc-NhaD may facilitate phosphate (arsenate) uptake via Pit by maintaining a sufficiently alkaline intracellular pH.

Another entry route for phosphate in *V. cholerae* is provided by the NptA-type transporter encoded by VC0676, which is homologous to the animal type II Na^+-dependent P_i cotransporters [Lebens et al., 2002]. Vc-NptA is the only *V. cholerae* phosphate transporter which has been cloned, expressed in *E. coli* and characterized

experimentally [Lebens et al., 2002]. Compared to other phosphate transporters, Vc-NptA has a rather low affinity for both P_i (300 μM) and Na^+ (75 mM) [Lebens et al., 2002]. Its contribution to the net P_i uptake in *V. cholerae* remains to be elucidated [Lebens et al., 2002], but the activity of Vc-NptA expressed in *E. coli* is dependent on external pH, doubling with the pH rise from 6.5 to 9.0 [Lebens et al., 2002]. Thus, like Pit, Vc-NptA could be influenced by the activity of Vc-NhaD through the modulation of cytoplasmic pH. At present, inorganic phosphate transport in *V. cholerae* remains underinvestigated, and a systematic analysis of mutants in P_i transport is needed to examine the mechanism of the Vc-NhaD effect on arsenate resistance and P_i uptake. In particular, it will be interesting to check whether ΔPit and ΔNptA chromosomal mutants of *V. cholerae* have phenotypes similar to the ΔVc-NhaD cells.

Though the exact molecular mechanism by which Vc-NhaD influences the phosphate (arsenate) transport in *V. cholerae* remains to be elucidated, it clearly depends on the ability of Vc-NhaD to catalyze Na^+/H^+ exchange (Fig. 4.25). Although it cannot be excluded at the moment that Vc-NhaD participates in P_i transport directly, for example, forming a complex with an as yet unidentified component of the *V. cholerae* membrane, the simplest explanation is that it just removes protons out of the cytoplasm thus permitting the Pit system (and, perhaps, Vc-NptA) to operate efficiently. This hypothesis also explains why at pH 8.0 and above *V. cholerae* cells are resistant to added arsenate irrespective of the presence of functional Vc-NhaD (Fig. 4.23B). Apparently, at higher external pH, the total level of the pmf on the membrane is not high enough to support Pit-mediated, pmf-driven import of phosphate (arsenate).

The simple experimental model presented in Fig. 4.23B, that is, monitoring the growth of *V. cholerae* in LB-based medium supplemented with 7.5 mM arsenate at different pH values, might be useful for the analysis of phosphate transport machinery in this bacterium. In particular, it could help to assess the relative contributions of Vc-Pit, Vc-NptA, and Vc-GlpT to the net inorganic phosphate uptake simply by comparing the pH profiles of arsenate sensitivity in corresponding mutants.

4.5. The Problem of Oxidative Phosphorylation in *V. cholerae*

4.5.1. Introduction

The membrane energetics of *V. cholerae* involves both H^+ and Na^+ as coupling ions. One of the general bioenergetic questions related to *V. cholerae,* is the one concerning the nature of the coupling ion (H^+ and/or Na^+) that energizes oxidative phosphorylation. The issue of energy requirements of oxidative phosphorylation in halotolerant *Vibrio* species is still somewhat controversial. Previous studies suggested that the free-living marine bacterium *V. alginolyticus* is able to use smf to energize ATP synthesis [Dibrov et al., 1986b]. Yet, following studies exploiting the reconstituted *V. alginolyticus* F_1F_0 enzyme, have demonstrated that it translocates H^+ ions rather than Na^+ [Dmitriev et al., 1991]. Na^+-coupled ATP synthesis driven by respiration or an artificial sodium ion gradient has also been reported in closely related *V. parahaemolyticus* [Sakai et al., 1989; Sakai-Tomita et al., 1991]. In organisms such as *Propionigenum modestum* and *Acetobacterium woodii*, F_1F_0-type ATPases were shown to transport Na^+ ions [Sakai et al., 1989; Sakai-Tomita et al., 1991; Krumholz et al., 1992], which led to the suggestion that the vibrional enzyme, too, might be Na^+-translocating [Dibrov et al., 1989].

However, the sequence of the *c* subunit of *V. cholerae* F_1F_0-ATPase suggested that this enzyme should translocate H^+ ions. More specifically, it lacks the characteristic Na^+-binding motif $Px_3Qx_{32}ET$, which is present in the *c* subunit of all sodium-motive ATPases of F_1F_0-type experimentally studied so far. Essentially the same motif ($Sx_3Qx_{28}ET$) could be identified in the K subunit of A/V-type Na^+ ATPases [Rahlfs & Müller, 1997].

It therefore seemed important to determine if the Vc-F_1F_0-ATPase, (i) was indeed crucial for oxidative phosphorylation in *V. cholerae*; and, (ii) used H^+ or Na^+ as a coupling ion as there was no experimental data obtained so far indicating the cationic specificity of the enzyme.

4.5.2. Construction of Chromosomal Deletion of *atpE*

The strain carrying a deletion of the *c* subunit of the F_1F_0-ATPase (DATPE1) was generated in the laboratory of Dr. C. Häse by homologous recombination in the course of the collaborative project. Briefly, sequences upstream and downstream of the F_0 *c* subunit were amplified from genomic DNA by PCR reactions using primer 1 (GGA CTA GTC TCC GGC TCG AAT AAT AA) and primer 2 (GGA ATT CCA CTT TAG GGG GTA G) for the region downstream of the *atpE* gene, and primer 3 (GGA ATT CTC CAA AGA TTC AAT GGG TAT TA) and primer 4 (AAT GGT CGA CAT CTC GTT TTA T) for the region upstream of *atpE*. Novel *Eco*RI sites were introduced at the 5' end of primers 2 and 3 to allow ligation of the two regions, which results in a complete deletion of the *atpE* gene. Novel *Spe*I and *Sal*I sites were introduced into primers 1 and 4, respectively, to allow direct cloning of the PCR product into the suicide vector

Fig. 4.27. Growth of the *V. cholerae* wild-type O395N1 and Δ*atpE* mutant derivative strains in liquid media. Cells were grown aerobically in M9 mineral medium (pH 7.5) supplemented with indicated substrates at 37°C overnight and resulting growth was measured as optical density at 600 nm. 5 mM CCCP was added at the time of inoculation where indicated. Results of a typical experiment from three independent experiments are shown. In other experiments, the results were nearly the same.

Fig. 4.27

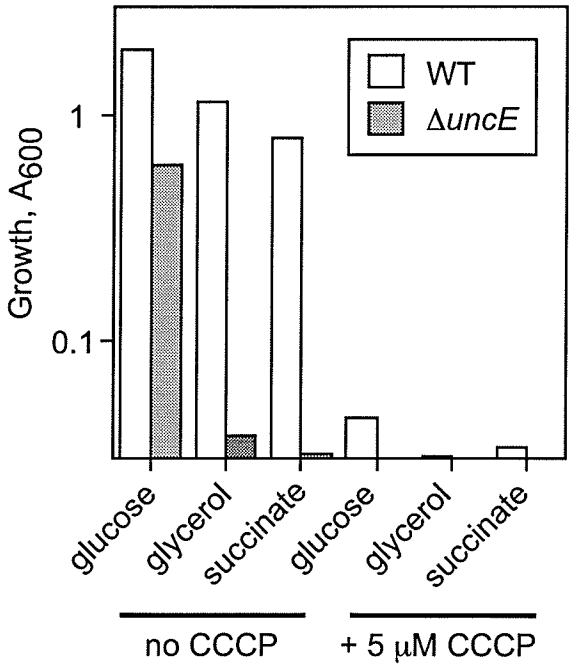
WT
ΔuncE
Growth, A600
1
0.1
glucose
glycerol
succinate
glucose
glycerol
succinate
no CCCP
+ 5 μM CCCP

pWM91 [Metcalf, et. al., 1996] and introduced into the *V. cholerae* O395-N1 *toxT::lacZ* chromosome following sucrose selection as described in [Donnenberg and Kaper, 1991].

4.5.3. Growth Properties of Δ*atpE* Mutant

To investigate the role of F_1F_0-ATPase in the physiology of *V. cholerae*, we used DATPE1, an *atp*⁻ mutant of the *V. cholerae* wild-type strain O395N1, carrying an in-frame deletion in *atpE*. Growth of the parent and mutant strains under various cultureconditions was analyzed. The DATPE1 mutant lacks subunit *c* of the membrane-embedded F_0 sector of F_1F_0-ATPase. Genetic elimination of the *c* subunit allows the inactivation of the enzyme without creating undesirable ion leakage through the mutant ATPase.

As shown in Fig. 4.27, the wild type cells were able to grow on either fermentable (glucose) or non-fermentable (succinate, glycerol) substrate. In contrast, the DATPE1 mutant grew only on fermentable substrate (glucose), therefore displaying a classical *unc*⁻ phenotype (Fig. 4.27). This finding clearly shows that the F_1F_0-ATPase in *V. cholerae* is indispensable for oxidative phosphorylation. Notably, very low (3 to 5 μM) concentrations of the protonophore uncoupler, CCCP, completely arrested the growth on non-fermentable substrates at pH 7.5 (Fig. 4.27) as well as at pH 8.5 (data not shown). The sensitivity of growth of the wild type cells to low concentrations of the protonophore suggested the involvement of proton rather than Na^+ as the coupling ion in this process.

Fig. 4.28. Formation of the ATP-dependent ΔpH measured in the inside-out sub-bacterial vesicles prepared from *V. cholerae*. Fluorometric assay with acridine orange was performed as described in "Materials and Methods". **Panel A:** wild-type (O395N1) *V. cholerae*. 1.0 mM Tris-ATP was added to the reaction mixture prior to the vesicles. **Panel B:** Δ*atpE* mutant. Formation of respiratory ΔpH was initiated by the addition of 5 mM succinate to the experimental mixture containing sub-bacterial vesicles. In the case of ATP-dependent ΔpH, 1.0 mM Tris-ATP was added to the reaction mixture prior to the vesicles.

Fig. 4.28

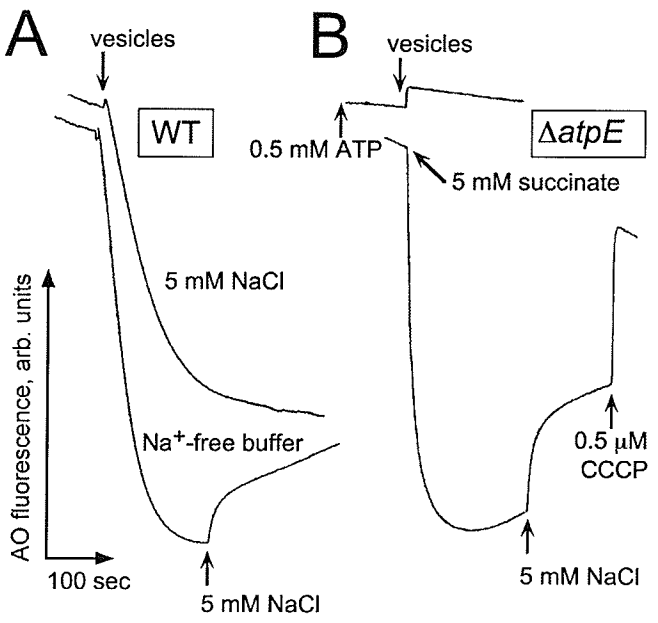
A
vesicles
WT
5 mM NaCl
Na+-free buffer
AO fluorescence, arb. units
100 sec
5 mM NaCl
B
vesicles
ΔatpE
0.5 mM ATP
5 mM succinate
0.5 μM
CCCP
5 mM NaCl

4.5.4. Characterization of the F_1F_0-ATPase in Membrane Vesicles

Next, we tested whether the hydrolysis of ATP results in proton transfer across the *V. cholerae* membrane. Addition of inside-out vesicles to an experimental buffer containing 0.5 mM Tris-ATP and 0.05 μM valinomycin resulted in an immediate proton uptake reflected by the rapid quenching of acridine orange fluorescence (Fig. 4.28A). No such effect was observed when ATP was not added. Valinomycin was added to the experimental mixture to maximize the magnitude of the formed ΔpH by dissipating the Δψ accompanying the transmembrane ion movement. Na^+ was not required for ATP-dependent ΔpH formation. Moreover, in the presence of 5 mM NaCl, the formation of ΔpH was slower and lower in magnitude (Fig. 4.28A, upper trace) compared to the Na^+-free buffer (Fig. 4.28A, lower trace), apparently because of the secondary Na^+/H^+ antiport. Indeed, the addition of 5 mM NaCl to the mixture after ΔpH had been established caused a partial dissipation of ΔpH (Fig. 4.28A, lower trace), a typical response of bacterial membranes capable of Na^+/H^+ antiport. Vesicles isolated from the Δ*atpE* mutant of *V. cholerae* lost the ability to generate ΔpH in response to the addition of ATP (Fig. 4.28B, upper trace) but not respiratory substrate, succinate (Fig. 4.28B, lower trace). Furthermore, secondary Na^+/H^+ exchange was not affected by the deletion (Fig. 4.28B). The addition of CCCP after the addition of NaCl collapsed the ΔpH completely (Fig. 4.28B, lower trace). Therefore, hydrolysis of ATP by the F_1F_0-ATPase of *V. cholerae* is directly coupled to the uphill proton movement across the membrane.

In the next series of experiments, we monitored the ATP-dependent formation of Δψ on the vesicular membrane (Fig. 4.29). As expected, the addition of ATP to the wild type vesicles resulted in a rapid generation of Δψ ("plus" in vesicular interior) at pH 7.5

Fig. 4.29. Measurements of ATP-dependent membrane electric potential ($\Delta\psi$) in sub-bacterial vesicles of *V. cholerae*. **Panel A, B:** wild-type (O395N1) *V. cholerae*. **Panel C:** Δ*atpE* mutant. Oxonol V was used instead of acridine orange. All other experimental conditions are described in "Materials and Methods".

Fig. 4.29

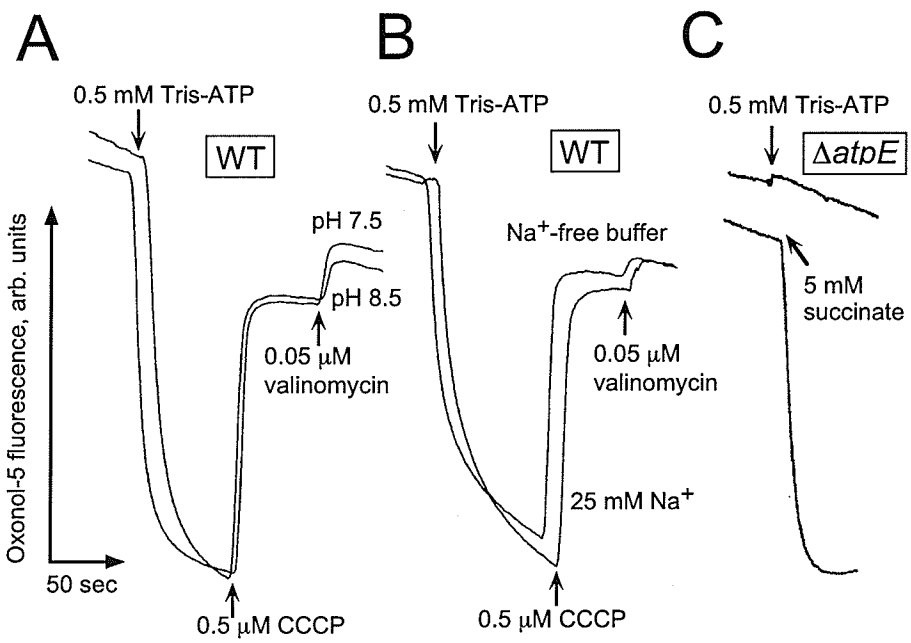
A
B
C
0.5 mM Tris-ATP
0.5 mM Tris-ATP
0.5 mM Tris-ATP
WT
WT
ΔatpE
pH 7.5
pH 8.5
0.05 μM valinomycin
Na+-free buffer
0.05 μM valinomycin
5 mM succinate
25 mM Na+
Oxonol-5 fluorescence, arb. units
50 sec
0.5 μM CCCP
0.5 μM CCCP

and 8.5 (Fig. 4.29A). Like the ATP-dependent formation of ΔpH, this process did not require Na^+ (Fig. 4.29B). The protonophore uncoupler, CCCP, collapsed the generated Δψ, so that the subsequent addition of valinomycin was practically without effect (Fig. 4.29A,B). These observations strongly suggest that the ion translocated by the ATPase is proton but not sodium. The magnitude of the ATP-dependent Δψ was the same at pH 7.5 and 8.5 (Fig. 4.29A). Vesicles of the DATPE1 mutant of *V. cholerae* were unable to generate Δψ in response to the addition of ATP, while a respiratory substrate provoked rapid formation of the electric potential on the membrane (Fig. 4.29C). Thus, the F_1F_0-ATPase of *V. cholerae* displays the behavior typical for proton-translocating ATPases of this type (see Schneider & Altendorf, 1987; Fillingame, 1990; Senior, 1990 for review). Hydrolysis of ATP by this enzyme is coupled to the formation of the pmf but not smf. Inability of the *V. cholerae* mutant lacking the functional F_1F_0-ATPase to grow on non-fermentable substrates (Fig. 4.27) clearly shows that this enzyme is critical for oxidative phosphorylation in this microorganism.

4.5.5. Discussion

At the beginning of this project, it was not clear whether the key element of membrane energetics, F_1F_0-ATPase of *V. cholerae,* is part of the H^+ or Na^+ cycle in this bacterium. The data reported above conclusively prove that in *V. cholerae*, despite the presence of a Na^+-translocating respiratory pump (NQR), a Na^+-dependent flagellar motor, a battery of Na^+/H^+ antiporters, a number of Na^+-symporters, and Na^+-dependent multidrug efflux pumps, the central membrane-related bioenergetic process, i.e.,

TABLE 5. Partial protein sequence alignment of the membrane fragments of *c* subunits (AtpE) of F_1F_0-type ATPases and K subunits (NtpK) of the archaeal/vacuolar ATPases[a]

F_1F_0-type H^+-ATPases		
E. coli	^{19}LAAI**G**AAI**G**IGILGG-19-FFIVMGLV**D**AIPMIAVGL^{70}	(79)
V. cholerae	^{18}LCAV**G**TAI**G**FAVLGG-19-MFIIAGLL**D**AVPMIGIVI^{69}	(85)
V. alginolyt.	^{18}LASL**G**TAI**G**FALLGG-19-MFIIAGLL**D**AVPMIGIVI^{69}	(84)
B. subtilis	^{12}LGAL**G**AGI**G**NGLIVS-19-MFMGIALV**E**ALPIIAVVI^{63}	(70)
E. hirae	^{12}GAAI**G**AGY**G**NGQVIS-19-MFIGVALV**E**AVPILGVVI^{63}	(71)
Yeast mito	^{17}IGLL**G**AGI**G**IAIVFA-19-AILGFALS**E**ATGLFCLMV^{68}	(74)
Human mito	^{82}VGVA**G**SGA**G**IGTVFG-19-AILGFALS**E**AMGLFCLMV^{143}	(151)
F_1F_0-type Na^+-ATPases		
A. woodii c3	^{20}IAGV**GP**GI**GQ**GFAAG-19-MLLGAAVA**ETT**GIYGLIV^{71}	(82)
A. woodii c1	^{44}VAGV**GP**GI**GQ**GFAAG-19-MLLGAAVA**ETS**GIFSLVI^{88}	(182)
A. woodii c1	^{120}IAGI**GP**GT**GQ**GYAAG-19-MLLGQAVA**QTT**GIYALIV^{171}	(182)
P. modestum	^{23}IAGI**GP**GV**GQ**GYAAG-19-MVLGQAIA**EST**GIYSLVI^{74}	(89)
T. maritima	^{26}IGAI**GP**GI**GE**GNIGA-19-MLLADAVA**ETT**GIYSLLI^{77}	(85)
F_1F_0-type ATPases, unknown cation		
M. genitalium	^{41}IAGSTVGIG**Q**GYIFG-19-IFIGSAVS**EST**AIYGLLI^{92}	(102)
M. pneumoniae	^{44}VGGATVGLG**Q**GYIFG-19-IFIGSAIS**ESS**SIYSLLI^{95}	(105)
U. urealyticum	^{50}LAAGAVGLM**Q**GFSTA-19-MIVGLALA**E**AVAIYALIV^{81}	(89)
S. pyogenes	^{9}LACFGVSLA**E**GFLMA-19-MILGVAFI**E**GTFFVTLVM^{60}	(65)
A/V-type H^+-ATPase		
Halobacterium	^{16}LAALAAGYAERGIGS-15-GLILTVLP**ET**LVILALVV^{63}	(71)
Sulfolobus	^{45}LAAIGAGVAVGMAAA-15-ILIFVAIGEGIAVYGILF^{92}	(101)
Yeast VMA11	^{30}LSCLGAAIGTAKSGI-15-SLIPVVMSGILAIYGLVV^{76}	(164)
	^{107}FACLSSGYAIGMVGD-15-IVLILIFS**E**VLGLYGMIV^{154}	(164)
A/V-type Na^+-ATPase		
E. hirae	^{24}FSGIGSAKGVGMTGE-15-ALILQLLPGTQGLYGFVI^{72}	(156)
	^{101}FTGLF**S**GIA**Q**GKVAA-15-GIIFAAMV**ET**YAILGFVI^{148}	(156)
C. trachomatis	^{14}LAMIGSAVGCGMAGV-15-IIGLSAMPSSQSIYGLIF^{62}	(141)
	^{89}SALLL**S**AFM**Q**GKCCV-15-SFASIGIV**ES**FALFAFVF^{136}	(141)
S. pyogenes	^{26}LSGMGSAYGVGKGGQ-15-ALILQLLPGSQGIYGFAI^{74}	(159)
	^{103}IVGYF**S**AKH**Q**GNVSV-15-GVILAAMV**ET**YAILAFVV^{150}	(159)
T. pallidum	^{14}ISAVGSALGLALAGQ-19-LLAFAGAPLTQTIYGFLL^{65}	(140)
	^{88}LGIAAS**ALS**Q**GRAAA-15-YLTIVGLC**ET**VALLVMVF^{135}**	(140)

Table 5 – Footnote

[a] Residues involved in cation binding are shown in inverted coloring. The Gly^{23} and Gly^{27} residues, creating the cavity for Asp^{61} in the *E. coli* enzyme [Girvin et al., 1998] are shown in boldface. The names of the organisms, sequence accession numbers in the NCBI protein database, and the references for experimentally studied proteins are as follows: *Escherichia coli* P00844 [Neilsen et al., 1981]; *Vibrio cholerae* AAF95908; *Vibrio alginolyticus* P12991, *Bacillus subtilis* P37815 [Santana et al., 1994]; *Enterococcus hirae* P26682 [Shibata et al., 1992] and BAA04271 [Kakinuma et al., 1993]; yeast mitochondria P00841 [Macino & Tazgoloff, 1979]; human mitochondria P05496 [Dyer & Walker, 1993]; *Acetobacter woodii* AAF01475 [Rahlfs & Müller, 1997] and AAF01474 [Rahlfs et al., 1999]; *Propionigenum modestum* CAA46895 [Kaim et al., 1997]; *Thermotoga maritima* AAD36682; *Mycoplasma genitalium* P47644; *Mycoplasma pneumoniae* AAC43654; *Ureaplasma urealyticum* AAF30542; *Streptococcus pyogenes* AAK33697 (AtpE) and AAK33254 (NtpK); *Halobacterium salinarum* BAA13179 [Ihara et al., 1997]; *Sulfolobus acidocaldarius* AAA72703 [Denda et al., 1989]; yeast vacuole P32842 [Umemoto et al., 1991]; *Chlamydia trachomatis* AAC67897; *Treponema pallidum* AAC65416. The total length of each protein is shown in parentheses on the right.

oxidative phosphorylation, is mediated by a H^+-dependent F_1F_0-ATPase. These experimental findings are further confirmed by the bioinformatics analysis.

The availability of the complete genome sequence of *Vibrio cholerae* [Heidelberg et al., 2000] allowed us to address the question of the nature of the coupling ion for its F_1F_0-ATPase also by comparing the sequence of its *c* subunit (AtpE) to the *c* subunits from ATPases with known cation specificities [Macino & Tzagoloff, 1979; Nielsen et al., 1981; Denda, et al., 1989; Umemoto, et al., 1991; Shibata et al., 1992; Kakinuma et al., 1993; Kaim et al., 1997; Rahlfs & Müller, 1997; Rahlfs et al., 1999]. An alignment of the membrane portions of this subunit (Table 5) showed that *V. cholerae* AtpE is very close to the H^+-conducting *c* subunits of the enzymes from *Escherichia coli*, *Bacillus subtilis*, *Enterococcus hirae*, and yeast and human mitochondria, but lacks the residues that are involved in Na^+-binding in the Na^+-dependent F_1F_0-ATPases from *Propionigenum modestum* and *Acetobacterium woodii* [Kaim et al., 1997; Rahlfs & Müller, 1997]. According to the model by Rahlfs and Müller [Rahlfs & Müller, 1997], the important determinant for Na^+-specificity of the F_1F_0-ATPase of *A. woodii* is the presence of the Na^+-binding motif that includes residues P^{25}, Q^{29}, E^{62}, and T^{63} (*A. woodii* c3 numbering, Table 5). The involvement of the latter three amino acid residues in Na^+-binding by the enzyme from *P. modestum* has been supported previously by site-specific mutagenesis data [Kaim et al., 1997]. The *c* subunit of the *V. cholerae* ATPase clearly lacked the predicted Na^+-binding motif (Table 5). Therefore, bioinformatics analysis is in full agreement with our experimental data, predicting that the *V. cholerae* ATPase should be specific for H^+ rather than Na^+ ions.

This motif was also missing in the *c* subunit from *V. alginolyticus*, which is 92% identical to the *V. cholerae* protein (Table 5). The reason(s) for the previously observed

Na^+-dependent ATP synthesis in *V. alginolyticus* [Dibrov et al., 1986b, Dibrov et al., 1989] and *V. parahaemolyticus* [Sakai et al., 1989; Sakai-Tomita, 1991] are not clear at this time. One possible explanation is that the addition of Na^+ ions to the whole cells could generate a temporary pmf that would not be immediately dissipated by the uncoupler. Such pmf generation could be due to the activity of any of the several Na^+/H^+ antiporters present in the cells of *Vibrio* sp. Another possible explanation is that the artificially imposed Na^+ gradient could drive reverse electron transport, leading to substrate-level phosphorylation in the cell cytoplasm, or stimulate some other biochemical process that would result in a temporary boost of ATP levels. It should be noted here that one cannot exclude the possible existence of an alternative Na^+-ATPase in *V. cholerae*, which could be repressed under the growth conditions used in this work. In addition to the *atp* operon encoding the F_1F_0-ATPase, the genome of *V. cholerae* contains three open reading frames (VC1033, VC1437, and VC2215) encoding P-type cation transport ATPases [E_1-E_2 ATPases [Silver, 1996; Rensing et al., 1999]. However, judging by the sequence similarity of VC1033 to the *E. coli* Zn^{2+} transporter ZntA [Sharma et al., 2000], and VC1437 and VC2215 to the *E. coli* Cu^+ transporter CopA [Rensing et al., 2000], they most probably transport divalent cations, which makes their involvement in oxidative phosphorylation highly unlikely. An inducible, two-gene ABC-type system extruding Na^+ ions, NatAB, has been reported in *Bacillus subtilis* [Cheng et al., 1997]. This transport system supposedly expels toxic Na^+ from the cytoplasm and stimulates K^+ uptake when the barrier function of cytoplasmic membrane is affected by uncouplers or alcohols [Cheng et al., 1997]. A number of genes encoding putative ABC-type transporters can be found in the *V. cholerae* genome, but neither of them shows

significant similarity to the bacillar *natAB* genes. These putative traffic ATPases of *V. cholerae* await their biochemical characterization.

The above analysis allows us to verify the existing predictions concerning the cation specificity of F_1F_0- and A/V-type ATPases. In *E. coli*, H^+ translocation through the F_0 portion of the F_1F_0-ATPase is mediated by Asp^{61} of the subunit *c* [Fillingame, 1990; Hoppe & Sebald, 1984; Rastogi & Girvin, 1999]. The acidic (Asp or Glu) residue in this position is conserved among *c* subunits of both H^+-dependent and Na^+-dependent F_1F_0 ATPases from various bacteria, as well as among the equivalent K subunits of the archaeal/vacuolar (A/V-type) ATPases (reviewed in [Blair et al., 1996], see Table 5). In Na^+-conducting *c* and K subunits, however, the Glu residue is followed by a hydroxyl-containing (Ser or Thr) residue, which apparently provides additional liganding groups, essential for binding alkali cations. A model of the membrane topology of the *c* subunit of *A. woodii*, consistent with the known structure of the *c* subunit from *E. coli* [Girvin et al., 1998; Rastogi & Girvin, 1999], showed that the conserved Pro and Gln residues located on the adjacent transmembrane segment could provide additional coordination axes for Na^+ binding [Rahlfs & Müller, 1997]. Indeed, when Kaim and Dimroth mutated those Gln and Ser/Thr residues, the Na^+-conductance by the *c* subunit from *P. modestum* was abolished but H^+-conductance was mostly unaffected [Kaim et al., 1997]. The membrane topology of the *c* subunit was identified as an additional factor affecting the cation selectivity of the ATPase. Thus, a double mutation Phe84→Leu, Leu87→Val in the *c* subunit was found to affect the Na^+-specificity of the *P. modestum* [Kaim & Dimroth, 1995] enzyme. Combining these data, Rahlfs and Müller proposed that there are two determinants for Na^+-specificity of the F_1F_0-ATPase of *A. woodii*: (i) an enlargement of the C-terminus of subunit *c* and (ii) the presence of the Na^+-binding motif

of P^{25}, Q^{29}, E^{62}, and T^{63} (see Table 5). However, analysis of multiple alignments of the sequences of the *c* subunits of F_1F_0-ATPases and K subunits of A/V ATPases (Table 5) shows that the length of the C-terminal extension is a poor predictor of the cation specificity of the enzyme. Indeed, the *c* subunit of the *V. cholerae* H^+-ATPase has a longer C-terminal fragment than both H^+-conducting proteins from *E. coli* and *B. subtilis*, and Na^+-conducting proteins from *A. woodii* and *P. modestum*. In contrast, the absence of the Na^+-binding motif $Px_3Qx_{28,32}ET$ correctly identified the *V. cholerae* enzyme as an H^+-ATPase. Likewise, the presence of a very similar sequence motif in the AtpE subunit from *Thermotoga maritima* suggests that its F_1F_0-ATPase is Na^+-dependent, which is consistent both with the preliminary transport data [Galperin et al., 1996; Galperin et al., 1997] and with the presence in its genome of two Na^+ pumps, NQR and a Na^+-translocating oxaloacetate decarboxylase [Häse et al., 2001; Dahinden et al., 2005].

4.6. The Role of NQR in the Sensitivity of *V. cholerae* to Ag^+

4.6.1. Introduction

The antibacterial effects of silver salts have been noticed since ancient times (for a review, see [Slawson et al., 1992; Silver & Phung 1996; Klasen, 2000]), and today, silver is used to control bacterial growth in a variety of applications, including dental work, catheters and burn wounds. Added at high (i.e., millimolar) concentrations, Ag^+ ions inhibit a number of enzymatic activities, reacting with electron donor groups, especially sulfhydryl groups [Slawson et al., 1992]. Although the antimicrobial effects of silver salts were noticed long ago, the molecular mechanism of the bactericidal action of Ag^+ in low concentrations i.e., micromolar, has not been elucidated.

In a study published almost 50 years ago, the uncoupler-like effects (stimulation of respiration and adenosinetriphosphatase activity) of micromolar concentrations of Ag^+ added to isolated mitochondria were documented by Chappell and Greville [Chappell & Greville, 1954]. This was done well before P. Mitchell formulated the chemiosmotic hypothesis revealing the role of the pmf in oxidative phosphorylation [Mitchell, 1991; Mitchell; 1996]. In the context of Mitchell's concept, the observation by Chappell and Greville suggests an ability of Ag^+ ions to collapse the pmf on the membrane. Paradoxically, to our knowledge no direct experimental evidence for the effect of Ag^+ on the pmf has been published since then. In 1982, Schreurs and Rosenberg mentioned (as an unpublished observation) that Ag^+ collapses the pmf on the membrane [Schreurs & Rosenberg, 1982]. However, neither the effective concentration of Ag^+, nor the experimental model used was specified in that communication.

On the other hand, NQR has been recognized to be one of the primary targets for low concentrations of Ag^+ ions in some bacteria [Semeykina & Skulachev, 1990; Hayashi et al., 1992]. In two independent studies, sub-micromolar concentrations of Ag^+ ions were shown to inhibit energy-dependent Na^+ transport in inside-out vesicles of alkalophilic *Bacillus* sp. FTU [Semeykina & Skulachev, 1990] and to inhibit purified NQR of *Vibrio alginolyticus* [Hayashi et al., 19920]. Later, in experiments with purified protein, Ag^+ was shown to irreversibly bind to the β-subunit of NQR (NqrF or Nqr6), causing enzyme denaturation and the loss of its FAD cofactor (see [Steubers et al., 1997]). These observations suggested that specific binding to NQR could be responsible for the bactericidal effect of low concentrations of Ag^+. However, no evidence that NQR indeed mediates the bactericidal action of Ag^+ *in vivo* had ever been presented. Moreover, like in *V. alginolyticus* [Tokuda et al., 1988], NQR is not critical for the

survival of *V. cholerae* [Häse & Mekalanos, 1998]. To investigate this long-standing issue, we decided to characterize the growth phenotype of a Δ*nqr* strain of *V. cholerae* and to measure directly the effect of Ag^+ ions on the proton-motive force on the membrane of the wild-type and ΔNQR strains.

4.6.2. Construction of Chromosomal Deletion of *nqr A-F*

The chromosomal DNQR1 strain of *V. cholerae* was a kind gift from Dr. C. Häse, Oregon State University and its construction is described in [Barquera et. al. 2000]. Briefly, deletion of the *nqr* operon was achieved by homologous recombination. The *nqr* operon and flanking sequences were amplified by PCR using the forward primer 5'-GCC GGC CTG CGT CCT GTC GCT CGT-3' and reverse primer 5'-GGA ACA CCA TCA CGG TTC AGT-3', which was cloned into pCR2.1 (Invitrogen). This construct was digested with NruI and self-ligated to produce an out-of-frame, internal deletion of the *nqr* operon (removes 114-447 nucleotides of *nqrA*, *nqrB-D* genes and 1-267 of *nqrF*). The Δ*nqr* insert was then subcloned into pWM91 suicide vector [Metcalf, W. et. al., 1996] and introduced into the *V. cholerae* O395-N1 *toxT::lacZ* chromosome following sucrose selection as described in [Donnenberg and Kaper, 1991]. This DNQR1 mutant has been used in [Barquera et al., 2000] as a host for the overexpression of NQR from a regulated P_{BAD} promoter, however its growth properties were not characterized.

4.6.3. Growth Properties of the Δ*nqr* Mutant

The DNQR1 mutant of the *V. cholerae*, carrying a deletion of the *nqr* operon, was able to grow normally in LB medium (Fig. 4.30) as well as in mineral media

supplemented with glucose at neutral pH at 37°C (data not shown). Studying the sensitivity of *V. cholerae* to Ag^+ ions, we found that growth in the wild type parent and DNQR1 mutant was equally sensitive to added Ag^+ ions (Table 6). In both strains, growth was completely arrested by 1.25 μM $AgNO_3$ added to the minimal growth medium. Therefore, the action of low concentrations of silver on the growth of *V. cholerae* could not be attributed to a specific binding to NQR.

4.6.4. Effect of Ag^+ Ions on ΔpH and Δψ in Membrane Vesicles

Next, we decided to measure directly the effect of Ag^+ ions on the membrane of the wild-type and DNQR1 strains of *V. cholerae.* The addition of sub-micromolar to low-micromolar concentrations of Ag^+ to inside-out membrane vesicles of *V. cholerae* induced a total collapse of the respiration-generated transmembrane pH gradient, ΔpH, irrespective of the presence of NQR in the membrane (Fig. 4.31A). Preincubation with Ag^+ completely prevented the formation of ΔpH in vesicles (Fig. 4.31A, upper trace). Noteworthy, in the presence of valinomycin, when Δψ does not limit the transmembrane ion flow, added Ag^+ provoked very fast dissipation of ΔpH, indicating that the resulting H^+ leakage is massive (Fig. 4.31C). In the next series of experiments, effect of Ag^+ ions on the membrane electric potential, Δψ, was measured with the Δψ-sensitive dye, Oxonol V. Fig. 4.32 shows that the addition of Ag^+ collapses also the respiration-generated membrane electric potential, Δψ, on the membrane of wild type *V. cholerae.* These measurements were performed in the absence of added Na^+ ions and using succinate (donating the electrons to the respiratory chain at the level of quinone, downstream of NQR) as a respiratory substrate (i.e., under the conditions when NQR is not active). In

Fig. 4.30. The deletion of *nqr* does not affect the growth of *V. cholerae* in LB medium at 37°C. Cells were grown aerobically as described in "Materials and Methods". Briefly overnight starters were prepared in LB medium and grown aerobically at 37°C. 250 ml flasks containing 20 ml of LB were inoculated with the overnight cultures to have a starting OD_{600} of 0.05. Growth was carried out at 37°C, 250 rpm. Parental, closed circles (●); DNQR1 (bearing deletion of *nqr*), closed triangles (▲). Representative of three independent experiments. The standard deviation is shown.

Fig. 4.30

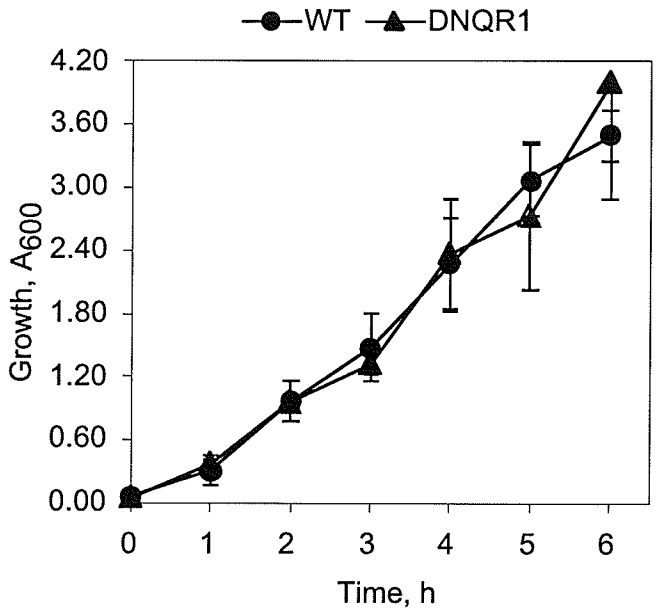
WT
DNQR1
4.20
3.60
3.00
2.40
1.80
1.20
0.60
0.00
Growth, A_{600}
0
1
2
3
4
5
6
Time, h

Table 6. Inhibition of *V. cholerae* growth by silver in M9 mineral medium

	optical density at 600 nm	
$AgNO_3$ (μM)	wild type	DNQR1
0	0.814	0.713
0.625	0.218	0.121
1.25	0.017	0.017
2.5	0.017	0.016
5	0.018	0.019
10	0.014	0.015

Fig. 4.31. Effects of Ag^+ on the H^+ permeability of the membrane measured in the inside-out membrane vesicles prepared from *V. cholerae*. Respiration-dependent formation of ΔpH was initiated by the addition of 10 mM Tris-succinate (downward arrows). Where indicated, 2.0 μM $AgNO_3$ was added to the vesicles (upward arrows). **Panel A**: Addition of Ag^+ after succinate collapses ΔpH generated in wild-type (upper trace) as well as ΔNQR membranes (lower trace). **Panel B**: Ag^+ prevents the formation of the respiration-dependent ΔpH. **Panel C**: Ag^+-induced ΔpH collapse is very fast in the presence of valinomycin.

Fig. 4.31

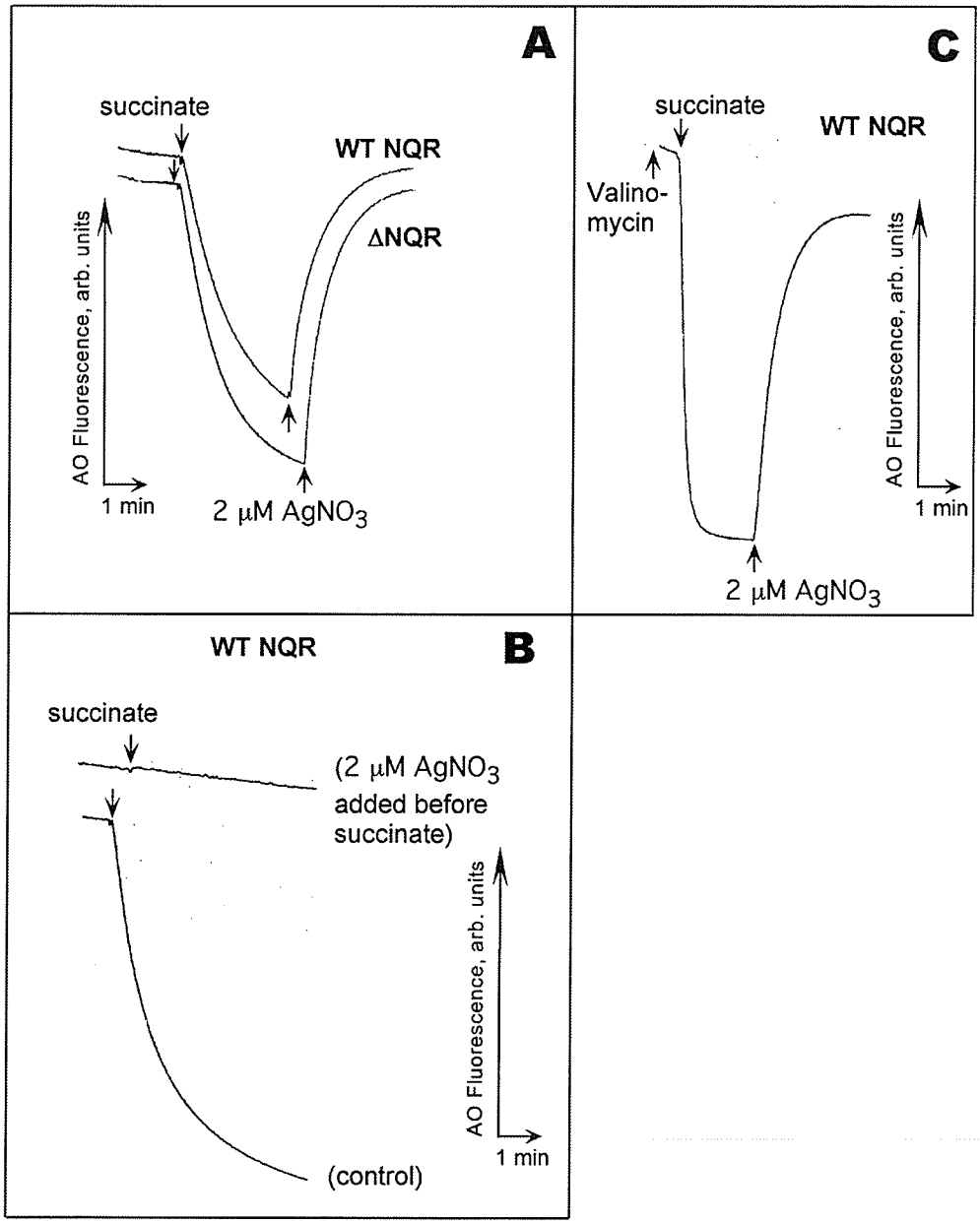
A
succinate
WT NQR
ΔNQR
AO Fluorescence, arb. units
1 min
2 μM AgNO3
C
succinate
WT NQR
Valino-
mycin
AO Fluorescence, arb. units
1 min
2 μM AgNO3
WT NQR
B
succinate
(2 μM AgNO3
added before
succinate)
AO Fluorescence, arb. units
1 min
(control)

Fig. 4.32. Effects of Ag^+ on $\Delta\psi$ in sub-bacterial vesicles of *V. cholerae*. The $\Delta\psi$-sensitive dye, Oxonol V was used instead of AO. 4.0 μM Ag^+ completely dissipates $\Delta\psi$ generated by respiration in vesicles derived from the strain possessing the wild-type NQR (upper trace). In the control experiment (lower trace), 0.2 μM valinomycin was added instead of $AgNO_3$.

Fig. 4.32

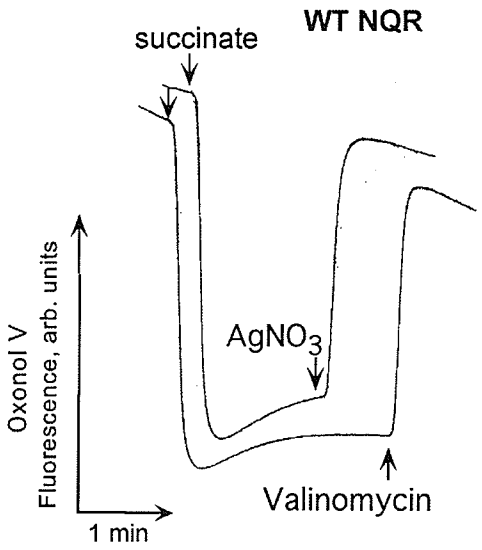
WT NQR
succinate
AgNO3
Valinomycin
Oxonol V
Fluorescence, arb. units
1 min

Fig. 4.33. The initial rate of ΔpH dissipation in the wild-type (○) and ΔNQR (▲) membrane vesicles as a function of [$AgNO_3$] added. A transmembrane pH gradient was generated by the addition of 10 mM Tris-succinate to the vesicles at pH 7.5 and varying concentrations of $AgNO_3$ were added after a steady-state ΔpH was reached. In each case, changes in AO fluorescence were monitored for 20 sec after Ag^+ addition. Initial dequenching rates are expressed in arbitrary fluorescence units per min.

Fig. 4.33

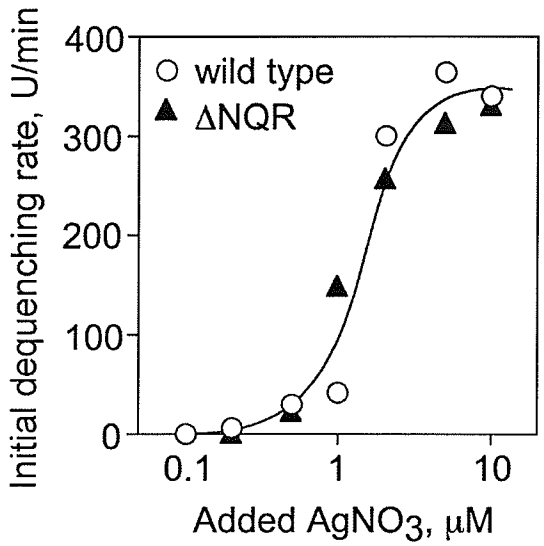
Initial dequenching rate, U/min
400
300
200
100
0
wild type
ΔNQR
0.1
1
10
Added AgNO3, μM

the control experiment, valinomycin was used instead of Ag^+ to collapse $\Delta\psi$ on the membrane (Fig. 4.32, lower trace). These data clearly demonstrate that the Ag^+-modified *V. cholerae* membrane is indeed leaky for protons.

To demonstrate that NQR does not contribute significantly into the overall H^+ leakage induced by Ag^+ ions, we measured the initial rate of ΔpH dissipation at different concentrations of added Ag^+ in vesicles isolated from either wild-type or ΔNQR cells (Fig. 4.33). We found that, in accordance with our growth experiments, the presence of NQR in the membrane is not required for the effect of Ag^+ ions (Fig. 4.33)

4.6.5. Discussion

The above data clearly demonstrate that the Ag^+-modified membrane is indeed leaky for protons and that loss of NQR does not alter the sensitivity of the mutant *V. cholerae* membrane to Ag^+ ions compared to the wild type. This suggests that another Ag^+-modified membrane protein(s) can cause the H^+ leakage, thus explaining the broad spectrum of the antimicrobial activity of Ag^+ ions.

The two most significant results of this project are: (i) the first (to our knowledge) direct experimental demonstration of the ability of Ag^+ ions to collapse the pmf; and, (ii) irrelevance of NQR as a specific target for such protonophore-like action of Ag^+. It is possible that the bactericidal action of low concentrations of Ag^+ in *V. cholerae* is not mediated by a specific target, but is due to proton leakage occurring through virtually any Ag^+-modified membrane protein, which results in complete de-energization of the membrane and inevitable cell death. Alternatively, some specific membrane protein could be a target for low concentrations of Ag^+ ions. Given the experimental data

obtained by Chappell and Greville with respect to the effect of Ag^+ on isolated mitochondria [Chappell & Greville, 1954], one could surmise that a target for low concentrations of Ag^+ ions would be common amongst bacterial and mitochondrial coupling membranes. In light of the results obtained in the present project (Fig 4.31B, upper trace) one such possibility may be succinate dehydrogenase (SDH), which is present in the mitochondrial inner membrane and in the cytoplasmic bacterial membranes. To attempt to identify a specific Ag^+ target, detailed analysis using a series of mutants, first of all, mutants lacking specific SDH subunits, is needed. Such experiments are planned for future studies.

In summary, both wild type and DNQR1 strains of *V. cholerae* were found to be equally sensitive to low-micromolar concentrations of Ag^+. Furthermore, the addition of low-micromolar Ag^+ to inside-out membrane vesicles of *V. cholerae* induced a total collapse of both the respiration-generated transmembrane pH gradient (ΔpH) and membrane electric potential ($\Delta\psi$) irrespective of the presence of Na^+ ions. This effect of Ag^+ was independent of the presence of the Na^+-translocating NADH:ubiquinone oxidoreductase (NQR), known as a specific target for sub-micromolar Ag^+, suggesting that the other Ag^+-modified membrane protein(s), possibly, one of SDH subunits, can cause the H^+ leakage, thus explaining the broad spectrum of the antimicrobial activity of Ag^+ ions.

4.7. The Role of the Na^+-Cycle in the Survival of *V. cholerae* at Elevated Temperature

4.7.1. Introduction

As a rule, membrane energetics in bacteria is based on the transmembrane circulation of H^+ (H^+ cycle). The pmf generated by primary H^+ pumps is used for osmotic, chemical and mechanical work (reviewed in [Harold & Maloney, 1996; Maloney & Wilson, 1996]). In many bacterial species, however, energetics employing Na^+ rather than H^+ as a primary coupling ion (Na^+ cycle) is an important adaptive mechanism enhancing the chances for survival under the conditions of dangerously lowered pmf. For example, in alkaline environments the pmf is lowered due to the opposite direction of its electric ($\Delta\psi$) and osmotic (ΔpH) constituents. The ability to use the Na^+ cycle under these circumstances may be crucial for survival [Skulachev, 1989; Skulachev, 1991].

As discussed in the Literature Review, growth of bacteria and archaea at high temperatures is limited by the increased permeability of the cytoplasmic membrane for ions resulting in low levels of the total pmf [Van de Vossenberg et al., 1995]. Remarkably, sodium ions are much less permeable compared to protons at any temperature [Van de Vossenberg et al., 1995]. Different microorganisms apparently use three distinct major strategies to cope with the arising proton leakage (see [Van de Vossenberg et al., 1998; Albers et al., 2001] and references therein): (i) psychrophilic and mesophilic bacteria, as well as archaea, are able to adjust the lipid composition of their membranes in order to limit the H^+ permeability at higher temperatures (so-called "homeo-proton permeability adaptation"); (ii) some thermophiles respond to the elevated

temperatures by a sharp increase in the H^+-extruding respiration [De Vrij et al., 1988]; (iii) anaerobic thermophiles use the Na^+ cycle instead of the H^+ cycle [Van de Vossenberg et al., 1998; Albers et al., 2001]. The use of a less permeable coupling cation in the latter case avoids the futile transmembrane circulation of H^+, thus enhancing the overall efficiency of energy transduction.

Since some mesophilic bacteria, including a number of important pathogens, possess both the primary Na^+ pumps and various smf consumers (see Häse et al., 2001), it seemed interesting to examine whether the Na^+ cycle may contribute to their survival at elevated temperatures. *Vibrio cholerae*, the aetiological agent of the severe human diarrheal disease cholera, is a typical mesophilic gram-negative bacterium with an optimal growth temperature of 37°C [Sahu et al., 1994; Kaper et al., 1995]. Its membrane contains, in the addition to the H^+-motive ATPase (see Section 4.5), essential elements of the Na^+ cycle, including the Na^+-translocating NADH:ubiquinone oxidoreductase (NQR) [Häse and Mekalanos, 1998], at least three functional Na^+/H^+ antiporters (Vc-NhaA, Vc-NhaB, Vc-NhaD) (see Sections 4.1, 4.2 & 4.3) [Herz et al., 2003], as well as Na^+ driven flagellar motor [Kojima et al., 1999]. The Na^+ cycle has been postulated [Bakeeva et al., 1986] and later experimentally proven [Häse and Mekalanos, 1999] to play a role in the virulence of *V. cholerae*. Data presented in this study strongly suggest that (i) in contrast to the primary Na^+ pump, NQR, and secondary Na^+ transporters such as NhaA, Vc-NhaD *in vivo* mediates import rather than export of alkali cations, and (ii) the transmembrane circulation of Na^+ is crucial for the survival of the mesophilic bacterium, *V. cholerae*, at 42°C.

4.7.2. Analysis of the Promoter Region of *nhaD* and *nqr*

As it is demonstrated in the above sections, Vc-NQR and Vc-NhaD represent two important and physiologically distinct sodium transporters of *V. cholerae*: Vc-NQR is a major primary system extruding Na^+ from the cytoplasm, while Vc-NhaD is a secondary ion exchanger which apparently translocates Na^+ in the opposite direction, thus presumably regulating intracellular pH and [Na^+] inside the cell. If the Na^+ cycle is important for the survival of bacteria under heat-shock conditions, it seemed natural to ascertain whether Vc-NQR (major exporter of Na^+) and Vc-NhaD (major importer of Na^+) contribute to the survivability of *V. cholerae* at elevated temperatures. Typically, the expression of proteins involved in heat shock response in bacteria is regulated by a specific sigma-factor, σ^{32} (for a review, see Yura & Nakahigashi, 1999; Arsene et al., 2000). The first indication that sodium circulation might be related to the heat response in *V. cholerae* came from promoter analysis. As Fig. 4.34 demonstrates, the putative promoters of both the *nqr* operon (encoding primary respiratory Na^+ pump, NQR) and the *nhaD* gene (encoding secondary Na^+/H^+ antiporter, Vc-NhaD) show clear similarity to the typical heat shock promoters controlled by σ^{32}. Of note, the degree of this similarity appears even higher if one ignores "mild" C→G substitutions, which occur not only in *nqrA* and *nhaD* promoters (underlined in Fig. 4.34), but also in such heat shock-inducible promoters as ones of *dnaK*, *grpE*, *groESl* or *dnaJ* (Fig. 4.34). We therefore examined the possible role of NQR and Vc-NhaD in survival of *V. cholerae* at elevated temperatures.

Fig. 4.34. Sequences of promoters of the *V. cholerae* genes annotated as heat shock ones, as well as of putative promoters of *nhaD* gene and *nqr* operon. The public database of TIGR (www.tigr.org) was used as a source of sequences. Positions of –35 and –10 regions were assigned by alignment with the consensus σ^{32} recognition sequence (*E. coli*).

Fig. 4.34

Heat shock promoters in *V. cholerae*

Gene/promoter		-35	Spacing	-10
dnaK	P1	**CCCTTGAAA**	TGGTTTTTGAAGA	**CCTTATTTA**
dnaK	P2	GGG**TTGAAA**	CCCGATTCTCCAT	**CCCCA**CATT
dnaJ	P1	AGT**TTGAA**G	AAGTTAACGACGATAAGA	AGTA**ATTGA**
dnaJ	P2	A**CAGATAAA**	GGCAACGGGATCCC	**CCTTATCTA**
ibpA	P1	AA**CTTGAAA**	TGGTTTTGAGTGA	**CCTTATATC**
groES1	P1	**CCCTTGA**TC	ACCAGCAGGATCGAAAG	**CGCCA**CCCT
groES1	P2	**CCCTTGGGA**	TATGGTGCAAGTTC	**CCCCACATA**
groES2	P1	**CCCTAGAAA**	AAATTTTTATTCC	**CCCTCTTGA**
groES2	P2	**CTCTTGAA**C	TTCGATTTTCTTA	**CCCTATTTA**
groES2	P3	**CGCGTGAAA**	CTGAGCTCATTTTGCA	AA**CAATCCT**
grpE	P1	A**CGTTGAA**C	GGCTTTTTCATAAGGTTTCCA	A**CCGATTTA**
grpE	P2	GG**CTTGAA**T	CAGAATTCATCGT	**CCCCATA**AT
hslJ	P1	ATA**TTGAAA**	AACTCCAATTG	**CTCCAT**AGG
hsp70	P1	**TTCTTGTAA**	GATTTGCTTTAAT	**CGCAATGCT**
htpX	P1	**CCCTTGT**GC	CTTCTAGGCTGCT	**CAGCATTTG**
htpX	P2	A**CCTTGT**TT	TTCAAATGGAAGA	A**CATATGTT**
htpG	P1	A**CCTTGAA**T	TTACATTTTTTGT	**CCATATCTC**
htpG	P2	**CACTTGCAC**	ATCAAGGTAA	TT**CCATTGA**
nqrA	P1	**C**G**TTTGAAA**	TTAAACAGTGATTCA	GGG**CATTGG**
nqrA	P2	T**GCTAGA**CT	ACAGCACCTGACAAATC	**CCCCACATG**
nhaD	P1	**CCTTTCTAA**	AAAATGATGAATAAAC	AA**CCATTTC**
nhaD	P2	AA**CTTGAA**G	CCGATCTTCAAGAGAA	GGGG**ATATC**
σ^{32} consensus		**CCCTTGAAA**	(13-17)	**CCCCAT-TA**

Fig. 4.35. Physiology of Vc-NhaD *vs.* Vc-NhaA expressed in antiporter-deficient *E. coli* EP432. Panel A: Being expressed in antiporter-less *E. coli*, Vc-NhaD protects growth against toxic LiCl at acid and neutral but not at alkaline pH of the medium (left ordinate, circles); in everted sub-bacterial vesicles isolated from EP432 expressing Vc-NhaD, it has the pH optimum of Li^+/H^+ antiport activity at ~8.0 (right ordinate, crosses). **Panel B:** Protection of EP432 growth against LiCl by expressed Vc-NhaA (left ordinate, black circles) and pH profile of the Vc-NhaA Li^+/H^+ antiport activity in everted vesicles (right ordinate, crosses). Cells of EP432 expressing either Vc-NhaD (**A**) or Vc-NhaA (**B**) were grown in LBK media buffered at indicated pH and supplemented with 0.1 M LiCl for 15 hours. Plotted are averages of five independent experiments. Bars show standard deviation. Antiport in vesicles was assayed with 10 mM LiCl at indicated pH as described in "Materials and Methods". Data shown are representatives of at least three independent experiments. The standard deviation is shown.

Fig. 4.35

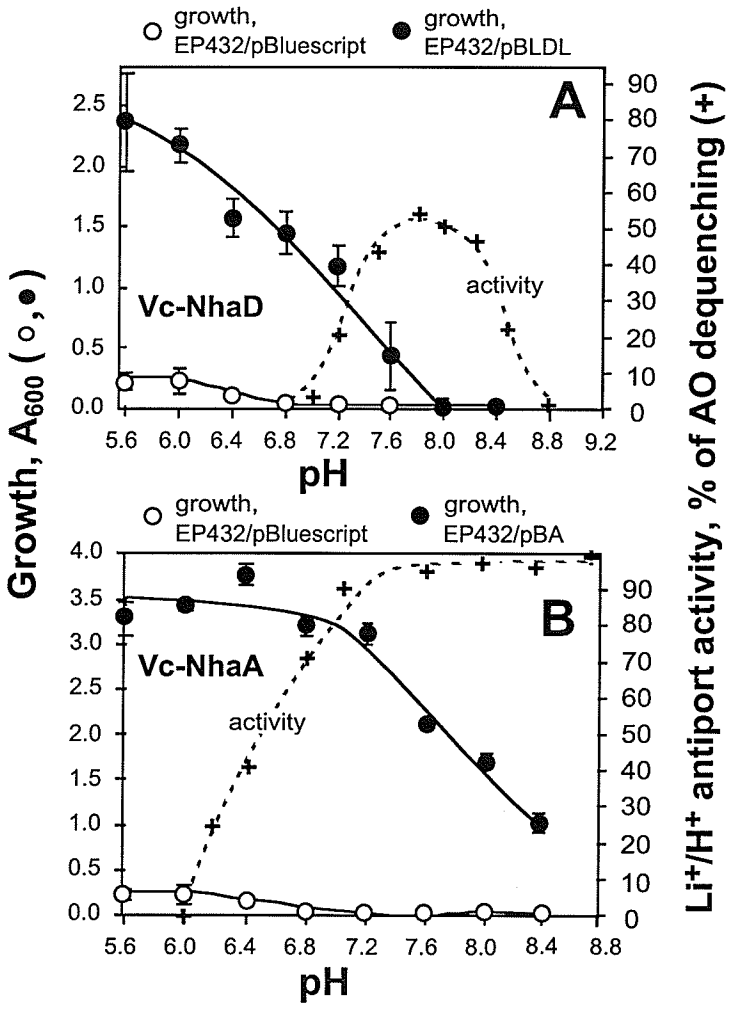
growth, EP432/pBluescript
growth, EP432/pBLDL
A
Vc-NhaD
activity
pH
growth, EP432/pBluescript
growth, EP432/pBA
B
Vc-NhaA
activity
pH
Growth, A600 (○,●)
Li+/H+ antiport activity, % of AO dequenching (+)

Fig. 4.36. In its native host, Vc-NhaD mediates import rather than export of alkali cations. Panel A: Deletion of *nhaD* does not affect overall Na^+ extrusion capacity of *V. cholerae* measured as Na^+/H^+ antiport in everted vesicles isolated from parental strain, O395N1 (empty symbols) and ΔNhaD strain, DD1 (closed symbols) grown in either LB medium (circles) or LB medium supplemented with 300 mM NaCl (triangles). **Panel B:** Growth of O395N1 (grey bars), DD1 (open bars), and DD1/pBLDL cells overexpressing Vc-NhaD (black bars) at pH 6.0 and 8.0. Bacteria were grown aerobically in LBK medium buffered at the desired pH and supplemented with indicated concentrations of LiCl. Shown are the averages from five independent experiments. The standard deviation is shown.

Fig. 4.36

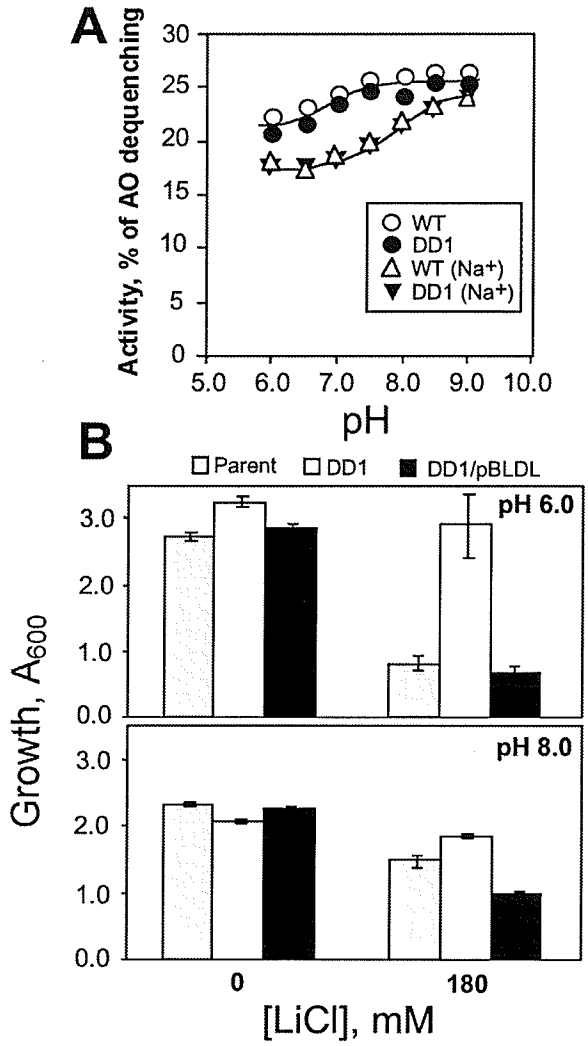
A
Activity, % of AO dequenching
30
25
20
15
10
5
0
5.0
6.0
7.0
8.0
9.0
10.0
pH
WT
DD1
WT (Na+)
DD1 (Na+)
B
Parent
DD1
DD1/pBLDL
pH 6.0
pH 8.0
Growth, A600
3.0
2.0
1.0
0.0
0
180
[LiCl], mM

4.7.3. The Place of Vc-NhaD in the Na^+ Cycle of *Vibrio cholerae*

It is well documented that NQR and Vc-NhaA play a major role in salt resistance of *V. cholerae*, extruding alkali cations from the cytoplasm [Barquera et al., 2002; Herz et al., 2003], while the inactivation of *nhaD* gene (encoding Vc-NhaD Na^+/H^+ antiporter) does not diminish the resistance to NaCl [Herz et al., 2003]. On the other hand, as shown here and in the above sections Vc-NhaD is chemiosmotically and physiologically active, when it is expressed in a model system of the antiporter-deficient *E. coli* strain, EP432 (see Sections 4.1 & 4.2 and Fig. 4.35A). To resolve an apparent contradiction concerning the role of Vc-NhaD, we compared its physiology in *E. coli* EP432 and *V. cholerae* (Fig. 4.35 and 4.36).

As already discussed, EP432 cells are devoid of two specific $Na^+(Li^+)/H^+$ antiporters, Ec-NhaA and Ec-NhaB, which renders them very sensitive to external alkali cations. As one can see from Fig. 4.31, 0.1M LiCl added to LBK medium abolished the growth of EP432 in the pH range 5.6-8.4 (left ordinate, empty circles). Introduction of Vc-NhaD expressed from multicopy plasmid, pBLDL, offers protection against lethal concentrations of Li^+, which is maximal at acidic external pH and progressively declines as the pH rises (Fig. 4.35A, left ordinate, closed circles). Already at pH 7.6 growth was severely inhibited (A_{600}<0.5) and no growth was detected beyond pH 8.0. This is not because of pH regulation of Vc-NhaD *per se*, as the pH profile of its activity peaks at ~8.0 (Fig. 4.35A, right ordinate, crosses). Again note that the activity of Vc-NhaD was determined in inside-out sub-bacterial vesicles, where the experimental pH imitates that of the cytoplasm. Thus, the effect of Vc-NhaD on the growth of EP432 transformants in the presence of Li^+ apparently reflects the thermodynamics of the Vc-NhaD-mediated antiport and suggests that ΔpH on the membrane (which progressively declines with the

rise of extracellular pH and turns into zero at pH_{out} ~8.0 [Padan et al., 1981]) but not $\Delta\psi$ (positive outside the cell) serves as a sole driving force for alkali cation export. In other words, it indicates that the antiport via Vc-NhaD is electroneutral.

Another antiporter from *V. cholerae*, Vc-NhaA, which belongs to the NhaA family of electrogenic Na^+/H^+ antiporters exchanging 2 H^+ per each Na^+ or Li^+ ion [Taglicht et al., 1993; Padan et al., 2001], behaves very differently when expressed in EP432 (Fig. 4.35B). Similarly to Vc-NhaD, this transporter reaches its maximal activity at alkaline pH but offers better protection against added Li^+ at acidic and neutral pH of the growth medium. However, in this case transformant cells were able to extrude toxic Li^+ ions and grow vigorously up to pH 8.4 (Fig. 4.35B, left ordinate, closed circles), when ΔpH on bacterial membrane is zero or even inverted (more acidic cytoplasm, see [Padan et al., 1981]). This is due to the ability of NhaA antiporters to use $\Delta\psi$ for the alkali cation extrusion.

If the antiport through Vc-NhaD is electroneutral, its direction in *V. cholerae* should be determined by magnitudes of ΔpH and $\Delta pNa^+(Li^+)$ on the membrane. In contrast to the simple case of EP432, both parameters in normal *V. cholerae* cells depend on the simultaneous operation of other ion-pumping systems, especially NhaA and NhaB antiporters which expel alkali cations and acidify the cytoplasm, thus maintaining palpable $\Delta pNa^+(Li^+)$ and minimizing ΔpH. Of note, both effects favour a backward direction of an electroneutral antiport presumably mediated by Vc-NhaD, i.e. import rather than export of alkali cations in salt-rich media. To probe the physiology of Vc-NhaD *in vivo*, the DD1 strain of *V. cholerae* bearing the Δ*nhaD* chromosomal deletion was used (Fig. 4.36). First, an overall Na^+ extrusion capacity was measured at different

pHs as Na^+/H^+ antiport in everted sub-bacterial vesicles (Fig. 4.36) isolated from O395N1 (open symbols) and DD1 (closed symbols) cells grown in regular LB medium (circles) or in LB supplemented with 0.3M NaCl (triangles). As one can see, elimination of functional Vc-NhaD did not affect the net Na^+ extrusion capacity, indicating that Vc-NhaD does not contribute into the export of Na^+ from *V. cholerae*. These data are in accord with the previously reported absence of effect of Vc-NhaD inactivation on NaCl resistance in *V. cholerae* [Herz et al., 2003]. Moreover, our growth experiments (Fig. 4.36B) showed that under high LiCl load, cells of the deletion mutant, DD1 (open bars) grew considerably better than both the parental O395N1 strain (grey bars) and DD1 overexpressing Vc-NhaD from multicopy plasmid (black bars). This clearly indicates that Vc-NhaD in *V. cholerae* acts to import rather than export alkali cations. Not surprisingly, the inhibitory effect of Vc-NhaD on growth in Li^+-rich medium was much less pronounced at alkaline pH (Fig. 4.36B, lower series of bars), where V_{max} of NhaA is many-fold higher (see [Padan et al., 2001] and references therein) thus allowing it to counterbalance the physiologically unfavourable activity of Vc-NhaD more efficiently. Taken together, the data presented in this thesis strongly suggest that, in contrast to NQR, Vc-NhaD mediates uptake of alkali cations in *V. cholerae*.

4.7.4. Growth Properties of Δ*nhaD* and Δ*nqr* Mutants at Elevated Temperatures

In a series of preliminary experiments, we analyzed the growth properties of the DNQR1 (DVc-NQR) and DD1 (DVc-NhaD) chromosomal mutants of *V. cholerae* at different temperatures. Cells were grown aerobically in standard LB medium (pH 7.0) at temperatures 37 to 42°C. At 37°C, there was no difference in the growth between wild

Fig. 4.37. Both NQR and Vc-NhaD enhance growth of *V. cholerae* at elevated temperatures. Cells of the parental strain, O395N1 (●), ΔNhaD strain, DD1 (■), and DNQR strain, DNQR1 (▲) were grown aerobically in LB medium at, **Panel A:** 37°C; **Panel B:** 40°C; or **Panel C:** 42°C. Data shown are representatives of three independent experiments. The standard deviation is shown.

Fig. 4.37

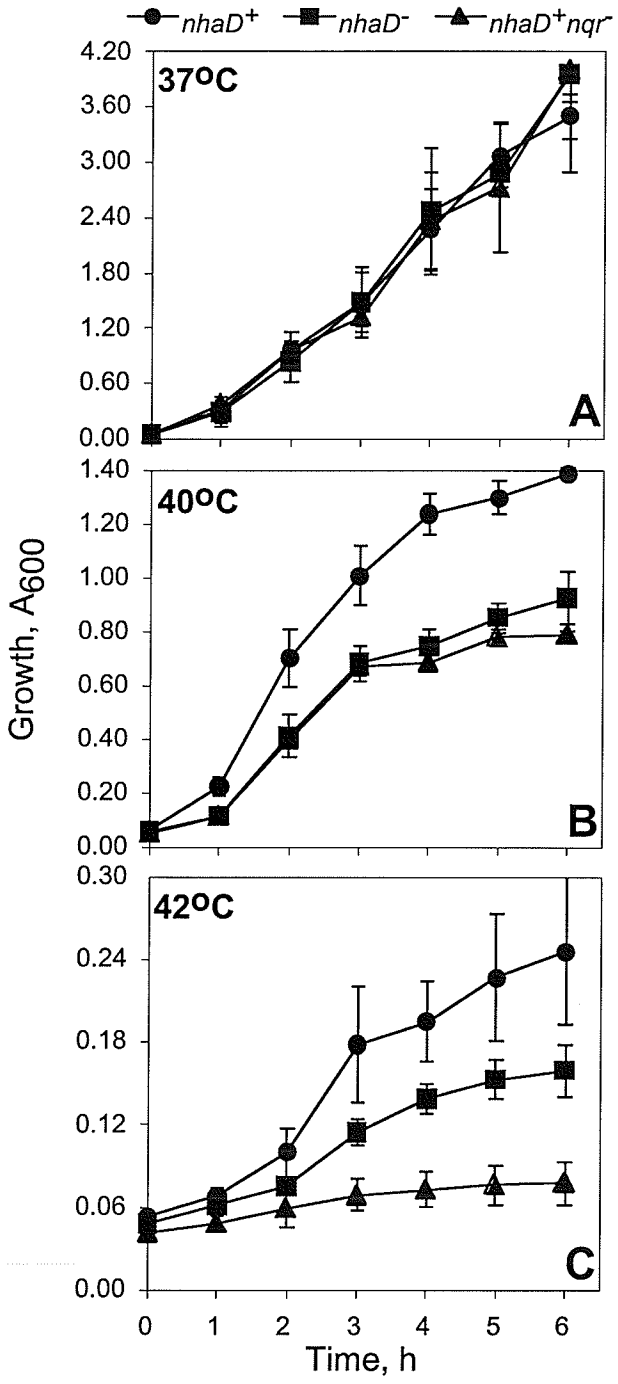
nhaD+
nhaD-
nhaD+nqr-
37°C
40°C
42°C
A
B
C
Growth, A600
Time, h
4.20
3.60
3.00
2.40
1.80
1.20
0.60
0.00
1.40
1.20
1.00
0.80
0.60
0.40
0.20
0.00
0.30
0.24
0.18
0.12
0.06
0.00
0
1
2
3
4
5
6

Fig. 4.38. Vc-NhaD expressed *in trans* in the ΔNhaD strain of *V. cholerae*, enhances the growth at high temperature during the first four hours. Shown is the average of two experiments. The standard deviation is shown.

Fig. 4.38

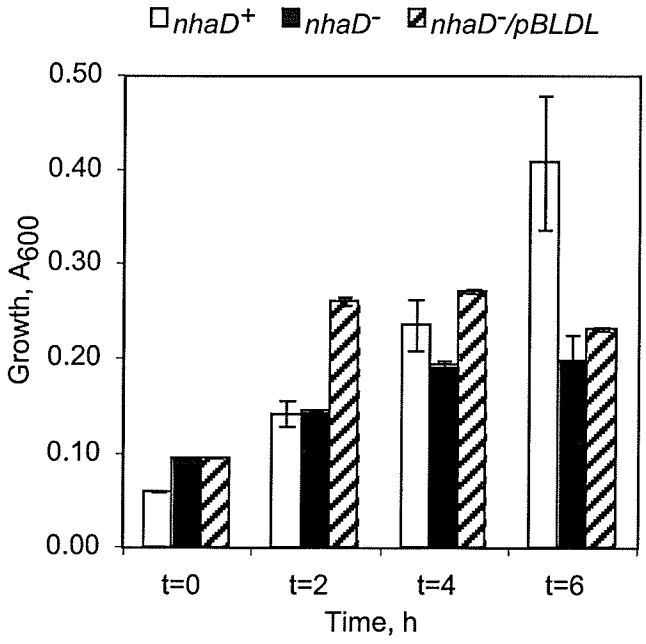
nhaD+
nhaD-
nhaD-/pBLDL
0.50
0.40
0.30
0.20
0.10
0.00
Growth, A600
t=0
t=2
t=4
t=6
Time, h

type cells and both mutants (Fig. 4.37A). However, as expected, the elimination of either NQR or Vc-NhaD resulted in the significant inhibition of growth at 40-42°C (Fig. 4.37B,C). Therefore, possessing the entire Na^+ cycle including its Na^+-exporting (NQR) as well as Na^+-importing (Vc-NhaD) elements, confers clear selective advantages to *V. cholerae* cells growing aerobically at elevated temperatures.

An attempt was made to demonstrate functional complementation of the DD1 growth phenotype by introduction of Vc-NhaD expressing plasmid, pBLDL into this strain (Fig. 4.38). As one can see, during the first 4 hours of growth, there was significantly better growth in the transformant culture as opposed to DD1 cells. However, this difference later disappeared. The reasons for that are not clear at the moment, but one could suggest that at high temperatures cells of *V. cholerae* have aproblem with maintanence of the plasmid. We also plan to check if Vc-NQR expressed *in trans* is able to complement the DNQR1 growth phenotype at high temperatures.

4.7.4. Discussion

The two major findings reported in the present study are: (i) that Vc-NhaD mediates influx rather than efflux of alkali cations in aerobically growing cells of *V. cholerae* and (ii) that transmembrane Na^+ circulation enhances growth of this mesophilic microorganism at elevated temperatures.

Despite the lack of stable functional complementation data (Fig. 4.38) at this moment, there is no doubt that the deletion of either Vc-NQR or Vc-NhaD renders cells of *V. cholerae* more sensitive to elevated temperatures. Therefore, the transmembrane circulation of Na^+ appears to be important for the survival of *V. cholerae* at elevated temperatures. As mentioned above, sodium ions are much less permeable compared to

protons at any temperature [Van de Vossenberg et al., 1995], and this is the reason why anaerobic thermophiles use the Na^+ cycle instead of the H^+ cycle. The use of a less permeable coupling cation in the latter case allows the avoidance of a futile transmembrane circulation of H^+, thus enhancing the overall efficiency of energy transduction. Therefore, the significance of transmembrane Na^+ circulation for survival at elevated temperatures is not constrained by the realm of anaerobic thermophiles as it was thought before [Van de Vossenberg *et al.*, 1998; Albers *et al.*, 2001]. Mesophilic microorganisms possessing a Na^+ cycle such as *V. cholerae*, in addition to the homeo-proton permeability adaptation, may exploit an alternative coupling ion in their membrane energetics thus enhancing their survival potential. Interestingly, both "Yin" (NQR, Na^+ exporter) and "Yang" (Vc-NhaD, Na^+ importer, see above sections) of *V.cholerae* Na^+ cycle seem to be important (Fig. 4.37B,C). Especially at critical temperature of 42°C (see Fig. 4.37C), contribution of NQR is more significant. This is not entirely surprising because NQR is a major primary Na^+ extruding mechanism, while re-entry of Na^+ during growth in rich LB-based medium could be efficiently mediated by Na^+-coupled symporters and the Na^+-motor (strain O395N1 is vigorously motile) as well as by non-specific Na^+ leakage through the membrane which is enhanced at high temperatures. Rather, the role of Vc-NhaD at high temperatures may be in the removal of excess of protons from the cytoplasm at the expense of smf generated by NQR. Whatever the interplay between NQR and Vc-NhaD really is, expression of both Na^+-motive enzymes appears to be under (at least partial) control of σ^{32} (Fig. 4.34). It will be interesting to monitor levels of expression of NQR and Vc-NhaD under conditions of temperature

stress. Our finding is the first report documenting the involvement of the Na^+ cycle in the heat-shock response of a mesophilic bacterium.

5. GENERAL CONCLUSIONS

5. GENERAL CONCLUSIONS

Vc-NhaD, Na^+/H^+ antiporter of *V. cholerae* representing a new class of bacterial Na^+/H^+ antiporters, has been cloned, functionally expressed in *E. coli* and extensively characterized for the first time.

Site-directed mutagenesis revealed a number of functionally important residues, whose intramolecular distribution intriguingly indicated similarity in the molecular organization of Vc-NhaD and the phylogenitically unrelated Ec-NhaA.

Equally interesting and most intriguing, was the finding that Vc-NhaD differs from any other characterized bacterial Na^+/H^+ antiporter, mediating *in vivo* the import rather than export of Na^+, thus presumably regulating both pH_{in} and Na^+_{in}. The importance of this is threefold: (i) it defines NhaD as an important part of the overall Na^+ cycle in *V. cholerae*, which is needed to complete the circulation of Na^+ ions irrespective of the motility status of the organism and the presence of Na^+-symported substrates; (ii) by removing H^+ from the cytoplasm, NhaD contributes to pH homeostasis in *V. cholerae*; (iii) the data obtained indicate that the peculiar mode of NhaD (functions backwards) is manifested in such different physiological traits as influencing phosphate uptake, arsenate sensitivity and survival at elevated temperature.

Also found is while Vc-NQR is not critical for either survival of *V. cholerae* at ambient temperature or sensitivity to Ag^+ ions, it is important (together with Vc-NhaD) for the survival of this mesophilic bacterium at elevated temperatures.

Another important contribution of this work is the confirmation that the central membrane-related bioenergetic process in *V. cholerae,* oxidative phosphorylation, is mediated by proton-motive, not sodium-motive F_1F_0-ATPase.

6. FUTURE PROSPECTS

6. FUTURE PROSPECTS

Future prospects would include:

(i) Cysteine scanning mutagenesis of Vc-NhaD to probe its topology. Dr. Habibian has constructed a cysteine-less Vc-NhaD mutant and has mutagenized several residues that are located within putative cytoplasmic and periplasmic loops, as well as within TMSs. He found that mutagenesis of all three cysteines into serine has no affect on the activity of the antiporter.

(ii) Purification and reconstitution Vc-NhaD for detailed studies. Several attempts thus far at placing Vc-NhaD under a controlled promoter have failed. Dr. Habibian has cloned Vc-NhaD into pET22b+, which places it under a T7 promoter. Unfortunately, we do not have a DE3 lysogenized EP432 strain to characterize it in an antiporterless background.

(iii) Detailed characterization of the "pH-sensing" motif ^{301}KTLARSLA^{308}, including characterization of K301A, T302A, S306A and R305,S306A mutants that have been constructed and complete characterizing the R305 residue.

(iv) Direct determination of internal pH in *nhaD*$^+$ and *nhaD*$^-$ *V. cholerae*. Does Vc-NhaD modulate phosphate (arsenate) transport in *V. cholerae* by alterations in cytoplasmic pH?

(v) Cloning and characterization of other Na^+/H^+ antiporters in *V. cholerae*. Vc-NhaA has been successfully cloned by Dr. Arthur Winogrodzki. Cloning of Vc-

NhaB is under way. Another interesting multisubunit Na^+/H^+ antiporter, Mrp, has been cloned and is currently being investigated in our laboratory. *V. cholerae* also has other putative Na^+/H^+ antiporters as discussed in the "Literature Review."

(vi) Production of Δ*nhaA*,Δ*nhaB*,Δ*nhaD* mutants and combinations thereof of *V. cholerae* to ascertain the effect on *V. cholerae* physiology.

(vii) Study phosphate transport in *V. cholerae*, which is currently under-studied.

7. REFERENCES

7. REFERENCES

Albers, S. V., van de Vossenberg, J. L. C. M., Diessen, A. J. M. and Konings, W. N. (2001) Bioenergetics and solute uptake under extreme conditions. *Extremophiles* **5**, 285-294.

Altschul, S. F., Madden, T. L., Schaffer, A. A., Zhang, J., Zhang, Z., Miller, W. and Lipman, D. J. (1997) Gapped BLAST and PSI-BLAST: a new generation of protein database search programs. *Nucleic Acids Res.* **25**, 3389-3402.

Arsene, F., Tomoyasu, T. and Bukau, B. (2000) The heat shock response of *Escherichia coli*. *Int J. Food Microbiol.* **10**, **55(1-3)**, 3-9.

Asai, I., Kojima, S., Kato, H., Nishioka, N., Kawagishi, I. and Homma, M. (1997) Putative channel components for the fast-rotating sodium-driven flagellar motor or a marine bacterium. *J. Bacteriol.* **179**, 5104-5110.

Avetisyan, A., Bogachev, A., Murtasina, R. and Skulachev, V. (1993) ATP-driven Na^+ transport and Na^+-dependent ATP synthesis in *Escherichia coli* grown at low delta-μH^+. *FEBS Lett.* **317**, 267-270.

Bakeeva, L. E., Chumakov, K. M., Drachev, A. L., Metlina, A. L., and Skulachev, V. P. (1986) The sodium cycle III. *Vibrio alginolyticus* resembles *Vibrio cholerae* and some other vibriones by flagellar motor and ribosomal 5S-RNA structures. *Biochim. Biophys. Acta.* **850**, 466-472.

Barkla, B. J. and Blumwald, E. (1991) Indentification of a 170-kDa protein associated with the vacuolar Na^+/H^+ antiport of *Beta vulgaris*. *Proc. Natl. Acad. Sci.* **88**, 11177-11181.

Barquera B., Häse C. C., Gennis R. B. (2001) Expression and mutagenesis of the NqrC subunit of the NQR respiratory Na^+ pump from *Vibrio cholerae* with covalently bound FMN. *FEBS Lett.* **492**, 45-49.

Barquera, B., Hellwig, P., Zhou, W., Morgan, J., Häse, C., Gosink, K. and Nilges, M. (2002a) Purification and characterization of the recombinant Na^+-translocating NADH:quinone oxidoreductase from *Vibrio cholerae*. *Biochemistry.* **41**, 3781-3789.

Barquera, B., Zhou, W., Morgan, J. E. and Gennis, R. B. (2002b) Riboflavin is a component of the Na^+-pumping NADH-quinone oxidoreductase from *Vibrio cholerae*. *Proc. Natl. Acad. Sci. USA.* **99**, 10322-10324.

Begum, A., Rahman, M. M., Ogawa, W., Mizushima, T., Kuroda, T. and Tsuchiya, T. (2005) Gene cloning and characterization of four MATE family multidrug efflux pumps from *Vibrio cholerae* non-O1. *Microbiol. Immunol.* **49**, 949-957.

Bennish, M. L. (1994) Cholera: pathophysiology, clinical features, and treatment. In *Vibrio cholerae and Cholera: Molecular and Global Perspectives*. Wachsmuth, I. K., Blake, P. A. and Olsvik, O. (eds). Washington, D. C., ASM Press, **pp.** 229-255.

Biber J., Custer M., Magagnin, S., Hayes, G., Werner, A., Lotscher, M., Kaissling, B. and Murer, H. (1996) Renal Na/P_i-cotransporters. *Kidney Int.* **49**, 981-985.

Birnboim, H. C. (1983) A rapid alkaline extraction method for the isolation of plasmid DNA. *Methods Enzymol.* **100**, 243-255.

Blair, D. F. and Berg, H. C. (1990) The MotA protein of *E. coli* is a proton-conducting component of the flagellar motor. *Cell* **60**, 439-449.

Blair, D. F. (1995) How bacteria sense and swim. *Annu. Rev. Microbiol.* **49**, 489-522.

Blair, A., Ngo, L., Park, J., Paulsen, I. T. and Saier Jr., M. H. (1996) Phylogenitic analyses of the homologous transmembrane channel-forming proteins of the F_1F_0-ATPases of bacterial, chloroplasts and mitochondria. *Microbiology* **142**, 17-32.

Blair, D. F. (2003) Flagellar movement driven by proton translocation. *FEBS Lett.* **545**, 86-95.

Blanco-Rivera, A., Leganes, F., Fernandez-Valiente, E., Calle, P. and Fernandez-Pinas, F. (2005) *mrpA*, a gene with roles in resistance to Na^+ and adaptation to alkaline pH in *Cyanobacterium anabaena* sp. PCC7120. *Microbiology*. **151**, 1671-1682.

Bogachev, A. V., Bertsova, Y. V., Barquera B. and Verkhovsky, M. I. (2001) Sodium-dependent steps in the redox reactions of the Na^+-motive NADH:quinone oxidoreductase from *Vibrio harveryi*. *Biochemistry*. **24**, 7318-7323.

Bolhuis, H., van Veen, H. W., Poolman, B., Driessen, A. J. and Konings, W. N. (1997) Mechanisms of multidrug transporters. *FEMS Microbiol. Rev.* **21**, 55-84.

Booth, I. R. (1985) Regulation of cytoplasmic pH in bacteria. *Microbiol. Rev.* **49**, 359-378.

Bott, M., Meyer, M. and Dimroth P. (1995) Regulation of anaerobic citrate metabolism in *Klebsiella pneumoniae*. *Mol. Microbiol.* **18**, 533-546.

Bott, M. (1997). Anaerobic citrate metabolism and its regulation in enterobacteria. *Arch. Microbiol.* **167**, 78-88.

Brown, M. H., Paulsen, I. T. and Skurray, R. A. (1999) The multidrug efflux protein NorM is a prototype of a new family of transporters. *Mol. Microbiol.* **31**, 394-395.

Buckles, E. L., Wang, X., Lockatell, C. V., Johnson, D. E. and Donnenberg, M. S. (2006) PhoU enhances the ability of extraintestinal pathogenic *Escherichia coli* strain CFT073 to colonize the murine urinary tract. *Microbiology* **152**, 153-160.

Busch W. and Saier, M. H. Jr. (2002) The transporter (TC) classification system. *Crit. Rev. Biochem. Mol. Biol.* **37**, 287-337.

Chapell, J. B. and Greville, G. D. (1954) Effect of silver ions on mitochondrial adenosine triphosphate. *Nature* **174**, 930-931.

Chen J., Morita, Y., Huda, M. N., Kuroda, T., Mizushima, T. and Tsuchiya, T. (2002) VmrA, a member of a novel class of Na^+-coupled multidrug efflux pumps from *Vibrio parahaemolyticus*. *J. Bacteriol.* **184**, 572-576.

Cheng, J., Guffanti, A. A., Krulwich, T. A. and Bechhofer, D. H. (1996) Chromosomal *tetA(L)* gene of *Bacillus subtilis*: regulation of expression and physiology of a *tetA(L)* deletion strain. *J. Bacteriol.* **178**, 2853-2860.

Cheng, J., Guffanti, A. and Krulwich, T. A. (1997) A two-gene ABC-type transport system that extrudes Na^+ in *Bacillus subtilis* is induced by ethanol or protonophore. *Mol. Microbiol.* **23**, 1107-1120.

Chiang, S. L., Taylor R. K., Koomey, M., and Mekalanos, J. J. (1995) Single amino acid substitutions in the N-terminus of *Vibrio cholerae* TcpA affect colonization, autoagglutination, and serum resistance. *Mol. Microbiol.* **17**, 1133-1142.

Claros, M. G. and von Heijne, G. (1994) TopPredII: an improved software for membrane protein structure predictions. *Comput. Appl. Biosci.* **10**, 685-686.

Colwell, R. R., and Huq, A. (1994) *Vibrios* in the environment: viable but nonculturable *Vibrio cholerae*. *In Vibrio cholerae and Cholera: Molecular and Global Perspectives*. Wachsmuth, I. K., Blake, P. A. and Olsvik, O. (eds). Washington D. C., ASM Press, **pp.** 117-113.

Colwell, R. (1996) Global climate and infectious disease: the cholera paradigm. *Science.* **274**, 2025-2031.

Dahinden, P., Auchli, Y., Granjon, T., Taralczak, M., Wild, M. and Dimroth, P. (2005) Oxaloacetate decarboxylase of *Vibrio cholerae*: purification, characterization, and expression of the genes in *Escherichia coli*. *Arch. Microbiol.* **183**, 121-129.

Daigle, F., Fairbrother, J. M. and Harel, J. (1995) Identification of a mutation in the *pst-phoU* operon that reduces pathogenicity of an *Escherichia coli* strain causing septicemia in pigs. *Infect. Immun.* **63**, 4924-4927.

Darley, C. P., van Wuytswinkel, O. C. M., van der Woude, K., Mager, W. H. and de Boer, A. H. (2000) *Arabidopsis thaliana* and *Saccharomyces cerevisiae* NHX1

genes encode amiloride sensitive electroneutral Na^+/H^+ exchangers. *Biochem. J.* **351**, 241-249.

de la Horra, C., Hernando, N., Lambert, G., Forster, I., Biber, J. and Murer, H. (2000) Molecular determinants of pH sensitivity of the type IIa Na/P_i cotransporter. *J. Biol. Chem.* **275**, 6284-6287.

De La Vieja, A., Dohan, O., Levy, O. and Carrasco, N. (2000) Molecular analysis of the sodium/iodide symporter: impact on thyroid and extrathyroid pathophysiology. *Physiol. Rev.* **80**, 1083-1105.

De Rosier, D. J. (1998) The turn of the screw: the bacterial flagellar motor. *Cell* **93**, 17-20.

De Vrij, W., Bulphuis, R. A. and Konings, W. N. (1988) Comparative study of energy-transducing properties of cytoplasmic membranes from mesophilic and thermophilic *Bacillus* species. *J. Bacteriol.* **170**, 2359-2366.

Dean, G. E., Macnab, R. M., Stader, J., Matsumura, P. and Burks, C. (1984) Gene sequence and predicted amino acid sequence of the MotA protein, a membrane-associated protein required for flagellar rotation in *Escherichia coli. J. Bacteriol.* **159**, 991-999.

Denda, K., Konishi, J., Oshima, T., Date, T. and Yoshida, M. (1989) A gene encoding the proteolipid subunit of *Sulfolobus acidocaldarius* ATPase complex. *J. Biol. Chem.* **264**, 7119-7121.

Di Berardino, M. and Dimroth, P. (1995) Synthesis of the oxaloacetate decarboxylase Na+ pump and its individual subunits in *Escherichia coli* and analysis of their function. *Eur. J. Biochem.* **231**, 790-801.

Di Berardino, M. and Dimroth, P. (1996) Aspartate 203 of the oxaloacetate decarboxylase *beta*-subunit catalyses both chemical and vectorial reaction of Na^+-pump. *EMBO J.* **15**, 1842-1849.

Dibrov, P., Lazarova, R., Skulachev, V. and Verkhovskaya, M. (1986a) The sodium cycle. I. Na^+-dependent motility and modes of membrane energization in the marine alkalotolerant *Vibrio alginolyticus. Biochim. Biophys. Acta.* **850**, 458-465.

Dibrov, P., Lazarova, R., Skulachev, V. and Verkhovskaya, M. (1986b) The sodium cycle. II. Na^+-coupled oxidative phosphorylation in *Vibrio alginolyticus* cells. *Biochim. Biophys. Acta.* **850**, 458-465.

Dibrov, P. A., Skulachev, V. P., Sokolov, M. V. and Verkhovskaya, M. L. (1988) The ATP-driven primary Na^+ pump in subcellular vesicles of *Vibrio alginolyticus. FEBS Lett.* **233**, 355-358.

Dibrov, P. A., Lazarova, R. L., Skulachev, V. P. and Verkhovskaya, M. L. (1989) A study on Na^+-coupled oxidative phosphorylation: ATP formation supported by artificially imposed ΔpNa and ΔpK in *Vibrio alginolyticus* cells. *J. Bioenerg. Biomembr.* **21**, 347-357.

Dibrov, P. A. (1993) Calcium transport mediated by NhaA Na^+/H^+ antiporter from *Escherichia coli*. *FEBS Lett.* **336**, 530-534.

Dibrov, P. A. and Taglicht, D. (1993) Mechanism of Na^+/H^+ exchange by *Escherichia coli* NhaA in reconstituted proteoliposomes. *FEBS Lett.* **336**, 525-529.

Dibrov, P. A., Rimon, A., **Dzioba, J.**, Winogrodzki, A., Shalitin, Y. and Padan, E. (2005) 2-Aminoperimidine, a specific inhibitor of bacterial NhaA Na^+/H^+ antiporters. *FEBS Letts.* **579**, 373-378.

Dibrov, P., Dibrov, E., Pierce, G. N. and Galperin, M. Y. (2005) Salt in the wound: a possible role of Na^+ gradient in Chlamydial infection. *J. Mol. Microbiol. Biotechnol.* **8**, 1-6.

Dimroth, P. (1980) A new sodium-transport system energized by the decarboxylation of oxaloacetate. *FEBS Lett.* **122**, 234-236.

Dimroth, P. and Thomer A. (1983) Subunit composition of oxaloacetate decarboxylase and characterization of the alpha chain carboxyltransferase. *Eur. J. Biochem.* **137**, 107-112.

Dimroth, P. (1987) Sodium ion transport decarboxylases and other aspects of sodium ion cycling in bacteria. *Microbiol. Rev.* **51**, 320-340.

Dimroth, P. (1994) Bacterial sodium ion-coupled energetics. *Antonie Van Leeuwenhoek.* **65**, 381-395.

Dimroth, P., Wang, H., Grabe, M. and Oster, G. (1999) *Proc. Natl. Acad. Sci. USA.* Energy transduction in the sodium F-ATPase of *Propionigenium modestum*. **96**, 4924-4929.

Dimroth P., Schink B. (1998) Energy conservation in the decarboxylation of dicarboxylic acids by fermenting bacteria. *Arch. Microbiol.* **170**, 69-77.

Dimroth, P. (2001) On the way towards the Na^+-binding site within the F_1F_0 ATPase of *Propionigenium modestum*. *Biochem. Soc. Trans.* **23**, 770-775.

Ding, Y., and Waldor, M. (2003) Deletion of a *Vibrio cholerae* ClC channel results in acid sensitivity and enhanced intestinal colonization. *Infect. Immun.* **71**, 4197-4200.

Dirita, V. J., Parsot, C., Jander, G., and Mekalanos, J. J. (1991) Regulatory cascade controls virulence in *Vibrio cholerae*. *Proc. Natl. Acad. Sci. USA.* **88**, 5403-5407.

Dmitriev, O. Yu, Krasnoselskaya, I. A., Papa, S. and Skulachev, V. P. (1991) F_1F_0-ATPase from *Vibrio alginolyticus*. Subunit composition and proton pumping activity. *FEBS Lett.* **284(2)**, 273-276.

Donnenberg, M. S. and Kaper, J. B. (1991) Construction of an *eae* deletion mutant of enteropathogenic *Escherichia coli* by using a positive-selectiion suicide vector. *Infect. Immun.* **59**, 4310-4317.

Dover, N. and Padan, E. (2001) Transcription of *nhaA*, the main Na^+/H^+ antiporter of *Escherichia coli*, is regulated by Na^+ and growth phase. *J. Bacteriol.* **183**, 644-653.

Dyer, M. R. and Walker, J. E. (1993) Sequences of members of the human gene family for the c subunit of mitochondrial ATP synthase. *Biochem. J.* **293**, 51-64.

Dzioba, J., Hase, C., Gosink, K., Galperin, M. and Dibrov, P. (2003) Experimental verification of a sequence-based prediction: F_1F_0-type ATPase of *Vibrio cholerae* transports protons, not Na^+ ions. *J. Bacteriol.* **185**, 674-678.

Dzioba, J., Ostroumov, E., Winogrodzki, A. and Dibrov, P. (2002) Cloning, functional expression in Escherichia coli and primary characterization of a new Na^+/H^+ antiporter, NhaD, of *Vibrio cholerae*. *Mol. Cell. Biochem.* **299**, 119-124.

Fan, B., Rosen, B. P. (2002) Biochemical characterization of CopA, the *Escherichia coli* Cu(I)-translocating P-type ATPase. *J. Biol. Chem.* **49**, 46987-46992.

Faruque S. M., Nair, G. B., and Mekalanos, J. J. (2004) Genetics of stress adaptation and virulence in toxigenic *Vibrio cholerae*. *DNA Cell Biol.* **23**, 723-741.

Favre, D. and Viret, J. F. (2000) Gene replacement in gram-negative bacteria: the pMAKSAC vectors. *Biotechniques* **28**, 198-200,202,204.

Felce, J. and Saier, M. H. Jr. (2004) Carbonic anhydrases fused to anion transporters of the SulP family: evidence of a novel type of bicarbonate transporter. *J. Mol. Microbiol. Biotechnol.* **8**, 169-176.

Fillingame, R. H. (1990) Molecular mechanism of ATP synthesis of the F_1F_0-type H^+-transporting ATP synthases. In *The Bacteria.* Krulwich, T. A. (ed). New York, Academic Press, vol. 12, **pp.** 345-391.

Finkelstein, R. A., Boesman-Finkelstein, M., Chang, Y. and Häse, C. C. (1992) *Vibrio cholerae* hemagglutinin/protease, colonial variation, virulence, and detachment. *Infect. Immun.* **60**, 472-478.

Finkelstein, R. A. (1996) Cholera, *Vibrio cholerae* O1 and O139, and other pathogenic *Vibrios.* In *Medical Microbiology 4th Edition.* Baron, S. (ed). The Medical Branch at Gavelston, The University of Texas, **ch.** 24.

Fletcher, M. (1996) Bacterial attachment in aquatic environments: a diversity of surfaces and adhesion strategies. In *Bacterial Adhesion: Molecular and Ecological Diversity*. Fletcher, M. (ed). New York, Wiley-Liss, **pp**. 1-24.

Francis, N. R., Sosinsky, G. E., Thomas, D. and DeRosier, D. J. (1994) Isolation, characterization and structure of bacterial flagellar motors containing the switch complex. *J. Mol. Biol.* **235**, 1261-1270.

Fujisawa, M., Kusomoto, A., Wada, Y., Tsuchiya, T. and Ito, M. (2005) NhaK, a novel monovalent cation/H^+ antiporter of *Bacillus subtilis*. *Arch. Microbiol.* **183**, 411-420.

Fukuoka, H., Yakushi, T., Kusumoto, A. and Homma, M. (2005) Assembly of the motor proteins, PomA and PomB, in the Na^+-driven stator of the flagellar motor. *J. Mol. Biol.* **351**, 707-717.

Galili, L., Rothman, A., Kozachkov, L., Rimon, A. and Padan E. (2002) Transmembrane domain IV is involved in ion transport activity and pH regulation of the NhaA Na^+/H^+ antiporter of *Escherichia coli*. *Biochemistry* **41**, 609-617.

Galperin, M. Y., Noll, K. M. and Romano, A. H. (1996) The glucose transport system of the hyperthermophilic anaerobic bacterium *Thermotoga neapolitana*. *Appl. Environ. Microbiol.* **62**, 2915-2918.

Galperin, M. Y., Noll, K. M. and Romano, A. H. (1997) Coregulation of β-galactoside uptake and hydrolysis by the hyperthermophilic bacterium *Thermotoga neapolitana*. *Appl. Environ. Microbiol.* **63**, 969-972.

Garcia, M. L., Guffanti, A. A. and Krulwich, T. A. (1983) Characterization of the Na^+/H^+ antiporter of akalophilic bacilli in vivo: $\Delta\psi$-dependent $^{22}Na^+$ efflux from whole cells. *J. Bacteriol.* **156**, 1151-1157.

Gardel, C. L. and Mekalanos, J. J. (1994) Regulation of cholera toxin by temperature, pH and osmolarity. *Methods Enzymol.* **235**, 517-526.

Gardel, C. L. and Mekalanos, J. J. (1996) Alterations in *Vibrio cholerae* motility phenotypes correlate with changes in virulence factor expression. *Infect. Immun.* **64**, 2246-2255.

Gerchman, Y., Olami, Y., Rimon, A., Taglict, D., Schuldiner, S. and Padan, E. (1993) Histidine-226 is part of the pH sensor of NhaA, a Na^+/H^+ antiporter in *Escherichia coli*. *Proc. Natl. Acad. Sci. USA.* **90**, 1212-1216.

Gerchman, Y., Rimon, A., Venturi, M. and Padan, E. (2001) Oligomerization of NhaA, the Na^+/H^+ antiporter of *Escherchia coli* in the membrane and its functional and structural consequences. *Biochemistry* **40**, 3403-3412.

Gill, D. M. (1976) The arrangement of subunits in cholera toxin. *Biochemistry* **15**, 335-348.

Girvin, M. E., Rastogi, V. K., Abildgaard, F., Markley, J. L. and Fillingame, R. H. (1998) Solution structure of the transmembrane H^+-transporting subunit c of the F_1F_0-ATP synthase. *Biochemistry* **37**, 8817-8824.

Glusker, J. P. (1991) Structural aspects of metal liganding to functional groups in proteins. *Adv. Protein Chem.* **42**, 1-76.

Goldberg, E. B., Arbel, T., Chen, J., Karpel, R., Mackie, G. A., Schuldiner, S. and Padan, E. (1987) Characterization of a Na^+/H^+ antiporter gene of *Escherichia coli*. *Proc. Natl. Acad. Sci. USA.* **84**, 2615-2619.

Gosink, K. and Häse, C. (2000) Requirements for conversion of the Na^+-driven flagellar motor of *Vibrio cholerae* to the H^+-driven motor of *Escherichia coli*. *J. Bacteriol.* **182**, 4234-4240.

Gupta, S. and Chowdhury, R. (1997) Bile affects production of virulence factors and motility in *Vibrio cholerae*. *Infect. Immun.* **65**, 1131-1134.

Habibian, R., **Dzioba, J.**, Barrett, J., Galperin, M. Y., Loewen, P. C. and Dibrov, P. (2005) Functional analysis of conserved polar residues in Vc-NhaD, Na+/H+ antiporter of *Vibrio cholerae*. *J. Biol. Chem.* **280**, 39637-39649.

Hamamoto, T., Hashimoto, M., Hino, M., Kitada, M., Seto, Y., Kudo, T. and Horikoshi, K. (1994) Characterization of a gene responsible for the Na+/H+ antiporter system of alkalophilic *Bacillus* species strain C-125. *Mol. Microbiol.* **14**, 939-946.

Harding M. M. (2004) The architecture of metal coordination groups in proteins. *Acta. Crystallogr. D. Biol. Crystallogr.* **60(Pt 5)**, 849-859.

Harel-Bronstein, M., Dibrov, P., Olami, Y., Pinner, E., Schuldiner, S. and Padan, E. (1995) MH1, a second-site revertant of an *Escherichia coli* mutant lacking Na^+/H^+ antiporters (*ΔnhaAΔnhaB*), regains Na^+ resistance and a capacity to excrete Na^+ in a $\Delta\mu H^+$-independent fashion. *J. Biol. Chem.* **270**, 3816-3822.

Harold F. M. and Maloney, P. C. (1996) Energy transduction by ion currents. In *Escherichia coli and Salmonella*. Neidhardt, F. C., Curtiss, R., Ingraham, J. L., Lin, E. C. C., Low, K. B., Magasanik, B., Reznikoff, W. S., Riley, M., Schaechter and M., Umbarger, H. E. (eds). Washington D. C.: ASM Press, **pp.** 283-306.

Häse, C. C., and Mekalanos, J. J. (1998) TcpP protein is a positive regulator of virulence gene expression in *Vibrio cholerae*. *Proc. Natl. Acad. Sci. USA.* **95**, 730-734.

Häse, C. C., and Mekalanos, J. J. (1999) Effects of changes in membrane sodium flux on virulence gene expression in *Vibrio cholerae*. *Proc. Natl. Acad. Sci. USA.* **96**, 3183-3187.

Häse, C. C. (2001) Analysis of the role of flagellar activity in virulence gene expression in *Vibrio cholerae*. *Microbiology* **147**, 831-837.

Häse, C. C., and Barquera, B. (2001) Role of sodium bioenergetics in *Vibrio cholerae*. *Biochim. Biophys. Acta.* **1505**, 169-178.

Häse, C. C., Fedorova, N. D., Galperin, M.Y. and Dibrov, P. (2001) Sodium ion cycle in bacterial pathogens: evidence from cross-genome comparisons. *Microbiol. Mol. Biol. Rev.* **65**, 353-370.

Hayashi, M., Miyoshi, T., Sato, M. and Unemoto, T. (1992) Properties of respiratory chain-linked Na^+-dependent NADH-quinone reductase in a marine *Vibrio alginolyticus*. *Biochim. Biophys. Acta.* **1099**, 145-151.

Hayashi M., Nakayama, Y., Yasui, M., Maeda, M., Furushi, K. and Unemoto, T. (2001) FMN is covalently attached to a threonine residue in the NqrB and NqrC subunits of Na^+-translocating NADH-quinone reductase from *Vibrio alginolyticus*. *FEBS Lett.* **488**, 5-8.

Hayashi, M., Nakayama, Y. and Unemoto, T. (2001) Recent progress in the Na^+-translocating NADH-quinone reductase from the marine *Vibrio alginolyticus*. *Biochim. Biophys. Acta.* **1505**, 37-44.

Heidelberg, J. F., Eisen, J. A., Nelson, W. C., Clayton, R. A., Gwinn, M. L., Dodson, R. J., Haft, D. H., Hickey, E. K., Peterson, J. D., Umayam, L., Gill, S. R., Nelson, K. E., Read, T. D., Tettelin, H., Richardson, D., Ermolaeva, M. D., Vamathevan, J., Bass, S., Qin, H., Dragoi, I., Sellers, P., McDonald, L., Utterback, T., Fleishmann, R. D., Nierman, W. C., White, O., Salzberg, S. L., Smith, H. O., Colwell, R. R., Mekalanos, J. J., Venter, J. C. and Fraser, C. M. (2000) DNA sequence of both chromosomes of the cholera pathogen *Vibrio cholerae*. *Nature* **406**, 477-483.

Heise, R., Müller, V. and Gottschalk, G. (1992) Presence of a sodium-translocating ATPase in membrane vesicles of the homoacetogenic bacterium *Acetobacterium woodi*. *Eur. J. Biochem.* **206**, 553-557.

Hellmer, J., Patzold, R. and Zeilinger, C. (2002) Identification of a pH regulated Na^+/H^+ antiporter of *Methanococcus jannaschii*. *FEBS Lett.* **527**, 245-249.

Herrington, D. A., Hall, R. H., Losonsky, G., Mekalanos, J. J., Taylor, R. K. and Levine, M. M. (1988) Toxin, toxin-coregulated pili, and the toxR regulon are essential for *Vibrio cholerae* pathogenesis in humans. *J. Exp. Med.* **168**, 1487-1492.

Herz, K., Vimont, S., Padan, E. and Berche, P. (2003) Roles of NhaA, NhaB, and NhaD Na^+/H^+ antiporters in survival of *Vibrio cholerae* in a saline environment. *J. Bacteriol.* **185**, 1236-1244.

Higgins, D., Thompson, J. and Gibson, T. G. (1994) ClustalW: improving the sensitivity of progressive sequence alignment through sequence weighting, position-specific gap penalities and weight matrix choice. *Nucleic Acid Res.* **22**, 4673-4680.

Hiramatsu, T., Kodama, K., Kuroda, T., Mizushima, T. and Tsuchiya, T. (1998) A putative multisubunit Na^+/H^+ antiporter from *Staphylococcus aureus*. *J. Bacteriol.* **180**, 6642-6648.

Hoppe, J. and Sebald, W. (1984) The proton conducting F_0 part of bacterial ATP synthases. *Biochim. Biophys. Acta.* **768**, 1-27.

Huda, M., Chen, J., Morita, Y., Kuroda, T., Mizushima, T. and Tsuchiya T. (2003) Gene cloning and characterization of VcrM, a Na^+-coupled multidrug efflux pump, from *Vibrio cholerae* non-O1. *Microbiol. Immunol.* **47**, 419-427.

Huda, M., Morita, Y., Kuroda, T., Mizushima, T. and Tsuchiya, T. (2001) Na+-driven multidrug efflux pump VcmA from *Vibrio cholerae* non-O1, a non-halophilic bacterium. *FEMS Microbiol. Lett.* **203**, 235-239.

Humphrey, W., Dalke, A. and Schulten, K. (1996) VMD: visual molecular dynamics. *J. Mol. Graph.* **14**, 33-38, 27-28.

Hung D. T., and Mekalanos, J. J. (2005) Bile acids induce cholera toxin expression in *Vibrio cholerae* in a ToxT-independent manner. *Proc. Natl. Acad. Sci. USA.* **102**, 3028-3033.

Hunte, C., Screpanti, E., Venturi, M., Rimon, A., Padan, E. and Michel, H. (2005) Structure of a Na^+/H^+ antiporter and insights into mechanism of action and regulation by pH. *Nature.* **435**, 1197-1202.

Huq, A., West, P. A., Small, E. B., Hug, M. I., and Colwell, R. R. (1984) Influence of water temperature, salinity, and pH on survival and growth of toxigenic *Vibrio cholerae* serovar 01 associated with live copepods in laboratory microcosms. *Appl. Environ. Microbiol.* **48**, 420-424.

Huq A., Huq, S., Grimes, D., O'Brien, M., Chu, K., Capuzzo, J., and Colwell, R. (1986) Colonization of the gut of the blue crab (*Callinectes sapidus*) by *Vibrio cholerae*. *Appl. Environ. Microbiol.* **52**, 586-588.

Ihara, K., Watanabe, S., Sugimara, K., Katagiri, I. and Mukohata, Y. (1997) Identification of a proteolipid from an extremely halophilic archaeon *Halobacterium salinarum* as an N,N'-dicyclohexyl-carbodiimide binding subunit of ATP synthase. *Arch. Biochem. Biophys.* **341**, 267-272.

Ikegami, M., Takahashi, H., Igarashi, K. and Kakinuma, Y. (2000) Sodium ATPase and sodium/proton antiporter are not obligatory for sodium homeostasis of *Enterococcus hirae* at acid pH. *Biosci. Biotechnol. Biochem.* **64**, 1088-1092.

Inoue, H., Noumi, T., Tsuchiya, T. and Kanazawa, H. (1995) Essential asparatic residues, Asp-133, Asp-163 and Asp-164, in the transmembrane helices of a Na^+/H^+ antiporter (NhaA) from *Escherichia coli*. *FEBS Lett.* **363**, 264-268.

Inoue, H., Sakurai, T., Ujike, S., Tsuchiya, T., Murakami, H. and Kanazawa, H. (1999) Expression of functional Na^+/H^+ antiporters from *Helicobacter pylori* in antiporter-deficient *Escherichia coli* mutants. *FEBS Lett.* **443**, 11-16.

Ito, M., Guffanti, A., Oudega, B. and Krulwich, T. A. (1999) *mrp*, a multigene, multifunctional locus in *Bacillus subtilus* with roles in resistance to cholate and Na^+ and in pH homeostasis. *J. Bacteriol.* **181**, 2394-2402.

Ito, M., Guffanti, A. A., Wang, W. and Krulwich, T. A. (2000) Effects of nonpolar mutations in each of the seven *Bacillus subtilis mrp* genes suggest complex interactions among the gene products in support of Na^+ and alkali but not cholate resistance. *J. Bacteriol.* **20**, 5663-5670.

Ivey, D. M., Guffanti, A. A., Zemsky, J., Pinner, E., Karpel, R., Padan, E., Schuldiner, S. (1993) Cloning and characterization of a putative Ca^{2+}/H^+ antiporter gene from *Escherichia coli* upon functional complementation of Na^+/H^+ antiporter-deficient strains by the overexpressed gene. *J. Biol. Chem.* **268**, 11296-11303.

Jockel, P., Di Berardino, M. and Dimroth, P. (1999) Membrane topology of the beta-subunit of the oxaloacetate decarboxylase Na^+ pump from *Klebsiella pneumoniae*. *Biochemistry* **38**, 13461-13472.

Jockel, P., Schmid, M., Steuber, J. and Dimroth, P. (2000) A molecular coupling mechanism for oxaloacetate decarboxylase Na^+ pump as inferred from mutational analysis. *Biochemistry* **39**, 131-143.

Jung H. (2001) Towards the molecular mechanism of Na^+/solute symport in prokaryotes. *Biochim. Biophys. Acta.* **1505**, 131-143.

Kaim, G. and Dimroth, P. (1995) A double mutation in subunit c of the Na^+-specific F_1F_0-ATPase of *Propionigenium modestum* results in a switch from Na^+ to H^+-coupled ATP synthesis in the *Escherichia coli* host cells. *J. Mol. Biol.* **253**, 726-738.

Kaim, G., Wehrle, F., Gerike, U. and Dimroth, P. (1997) Molecular basis for the coupling ion selectivity of F_1F_0 ATP synthases: probing the liganding groups for Na^+ and Li^+ in the c subunit of the ATP synthease from *Propionigenium modestum*. *Biochemistry* **36**, 9185-9194.

Kakinuma, Y., Kakinuma, S., Takase, K., Konishi, K., Igarashi, K. and Yamato, I. (1993) A gene encoding the 16-kDa proteolipid subunit of *Enterococcus hirae* Na^+-ATPase complex. *Biochem. Biophys. Res. Commun.* **195**, 1063-1069.

Kaper, J. B., Morris, J. O. Jr. and Levine, M. M. (1995) Cholera. *Clin. Microbiol. Rev.* **8**, 48-86.

Kato, S. and Yumoto, I. (2000) Detection of the Na^+-translocating NADH-quinone reductase in marine bacteria using a PCR technique. *Can. J. Microbiol.* **46**, 325-332.

Katz, A., Kleyman, T. R. and Pick, U. (1994) Utilization of amiloride analogs for characterization and labelling of the plasma membrane Na^+/H^+ antiporter from *Dunaliella salina*. *Biochemistry* **33**, 2389-2393.

Kitada, M., Kosono, S. and Kudo, T. (2000) The Na^+/H^+ antiporter of alkaliphilic *Bacillus* sp. *Extremophiles*. **4**, 253-258.

Klasen, H. J. (2000) A historical review of the use of silver in the treatment of burns. *Burns* **26**, 131-138.

Klose, K. E. (2001) Regulation of virulence in *Vibrio cholerae*. *Int. J. Med. Microbiol.* **291**, 81-88.

Kojima, S., Yamamoto, K., Kawagishi, I. and Homma M. (1999) The polar flagellar motor of *Vibrio cholerae* is driven by an Na^+ motive force. *J. Bacteriol.* **181**, 1927-1930.

Kosono, S., Haga K., Tomizawa, R., Kajiyama, Y., Hatano, K., Takeda, S., Wakai, Y., Hino, M. and Kudo, T. (2005) Characterization of a multigene-encoded sodium/hydrogen antiporter (sha) from *Pseudomonas aeruginosa*: its involvement in pathogenesis. *J. Bacteriol.* **187**, 5242-5248.

Kosono, S., Morotomi, S., Kitada, M. and Kudo, T. (1999) Analyses of a *Bacillus subtilis* homologue of the Na^+/H^+ antiporter gene which is important for pH homeostasis of alkaliphilic *Bacillus sp.* C-125. *Biochim. Biophys. Acta.* **1409**, 171-175.

Kosono, S., Ohashi, Y., Kawamura, F., Kitada, M. and Kudo, T. (2000) Function of a principal Na^+/H^+ antiporter, ShaA, is required for initiation of sporulation in *Bacillus subtilis*. *J. Bacteriol.* **182**, 898-904.

Kovach, M. E., Shaffer, M. D. and Peterson, K. M. (1996) A putative integrase gene defines the distal end of a large cluster of ToxR-regulated colonization genes in *Vibrio cholerae*. *Microbiology* **142**, 2165-2174.

Kovacikova, G. and Skorupski, K. (2001) Overlapping binding sites for the virulence gene regulators AphA, AphB and cAMP-CRP at the *Vibrio cholerae tcpPH* promoter. *Mol. Microbiol.* **41**, 393-407.

Kovacikova, G. and Skorupski, K. (2002) Regulation of virulence gene expression in *Vibrio cholerae* by quorum sensing: HapR functions at the *aphA* promoter. *Mol. Microbiol.* **46**, 1135-1147.

Krebs, W., Steuber, J., Gemperli, A. C. and Dimroth, P. (1999) Na^+ translocation by the NADH:ubiquinone oxidoreductase (complex I) from *Klebsiella pneumoniae*. *Mol. Microbiol.* **33**, 590-598.

Krishnan, H. H., Ghosh, A., Paul, K. and Chowdhury, R. (2004) Effect of anaerobiosis on expression of virulence factors in *Vibrio cholerae*. *Infect. Immun.* **72**, 3961-3967.

Krukonis, E. S., DiRita, V. J. (2003) From motility to virulence: Sensing and responding to environmental signals in *Vibrio cholerae*. *Curr. Opin. Microbiol.* **6**, 186-190.
Krulwich, T. A. (1983) Na^+/H^+ antiporters. *Biochim. Biophys. Acta.* **726**, 245-264.

Krulwich, T. A., Ito, M. and Guffanti, A. (2001a) The Na^+-dependence of alkaliphily in *Bacillus*. *Biochim. Biophys. Acta.* **1505**, 158-168.

Krulwich, T. A., Jin, J., Guffanti, A. and Bechhofer, D. (2001b) Functions of tetracycline efflux proteins that do not involve tetracycline. *J. Mol. Microbiol. Biotechnol.* **3**, 236-246.

Krulwich, T. A., Lewinson, O., Padan, E. and Bibi, E. (2005) Do physiological roles foster persistence of drug/multidrug-efflux transporters? A case study. *Nat. Rev. Microbiol.* **3**, 566-572.

Kudo, S., Magariyama, Y. and Aizawa, S. (1990) Abrupt changes in flagellar rotation observed by laser dark-field microscopy. *Nature* **346**, 677-680.

Kuroda, T., Shimamoto, T., Inaba, K., Tsuda, M. and Tsuchiya, T. (1994) Properties and sequence of the NhaA Na^+/H^+ antiporter of *Vibrio parahaemolyticus*. *J. Biochem, (Tokyo)*. **116**, 1030-1038.

Kuroda, T., Shimamoto, T., Mizushima, T. and Tsuchiya, T. (1997) Mutational analysis of amiloride sensitivity of the NhaA Na^+/H^+ antiporter from *Vibrio parahaemolyticus*. *J. Bacteriol.* **179**, 7600-7602.

Kuroda, T., Fujita, N., Utsugi, J., Kuroda, M., Mizushima, T. and Tsuchiya T. (2004) A major Li^+ extrusion system NhaB of *Pseudomonas aeruginosa*: comparison with the major Na^+ extrusion system NhaP. *Microbiol. Immunol.* **48**, 243-250.

Kuroda, T., Mizushima, T. and Tsuchiya, T. (2005) Physiological roles of three Na^+/H^+ antiporters in the halophilic bacterium *Vibrio parahaemolyticus*. *Microbiol. Immunol.* **49**, 711-719.

Lang, H. J. (2003) Chemistry of NHE inhibitors. In *The sodium-hydrogen exchange, from molecule to its role in disease.* Karmazin, M., Avkiran, N. and Fliegel, L. (eds). Boston: Kluwer Academic Publishers, **pp.** 239-253.

Laubinger, W. and Dimroth, P. (1987) Characterization of the Na^+-translocating stimulated ATPase of *Propionigenium modestum* as an enzyme of the F_1F_0 type. *Eur. J. Biochem.* **168**, 475-480.

Laussermair, E., Schwartz, E., Oesterhelt D., Reinke, H., Beyreuther, K., and Dimroth, P. (1989) The sodium-translocating oxaloacetate decarboxylase of *Klebsiella pneumoniae*. Sequence of the integral membrane-bound subunits beta and gamma. *J. Biol. Chem.* **264**, 14710-14715.

Lebens, M., Lindquist, P., Soderlund, L., Todorovic, M. and Carlin, N. (2002) The *nptA* gene of *Vibrio cholerae* encodes a functional sodium-dependent phosphate cotransporter homologous to the type II cotransporters of eukaryotes. *J. Bacteriol.* **184**, 4466-4474.

Lewinson, O., Padan, E. and Bibi, E. (2004) Alkalitolerance: a biological function for a multidrug transporter in pH homeostasis. *Proc. Natl. Acad. Sci. USA.* **101**, 14073-14078.

Libby, S. J., Goebel, W., Muir, S., Songer, G. and Heffron, F. (1990) Cloning and characterization of a cytotoxin gene from *Salmonella typhimurium*. *Res. Microbiol.* **141**, 775-783.

Liu, J., Xue, Y., Wang, O., Wei, Y., Swartz, T. H., Hicks, D. B., Ito, M., Ma, Y. and Krulwich, T. A. (2005) The activity profile of the NhaD-type $Na^+(Li^+)/H^+$ antiporter from the soda lake haloalkaliphile *Alkalimonas amylolytica* is adaptive for the extreme environment. *J. Bacteriol.* **187**, 7589-7595.

Lloyd, S. A., Tang, H., Wang, X., Billings, S. and Blair, D. F. (1996) Torque generation in the flagellar motor of *Escherichia coli*: evidence of a direct role for FliG but not for FliM or FliN. *J. Bacteriol.* **178**, 223-231.

Lowe, G., Meister, M. and Berg, H. C. (1987) Rapid rotation of flagellar bundles in swimming bacteria. *Nature* **325**, 637-640.

Macino, G. and Tzagoloff, A. (1979) Assembly of the mitochondrial membrane system. The DNA sequence of a mitochondrial ATPase gene in *Saccharomyces cerevisiae*. *J. Biol. Chem.* **254**, 4617-4623.

Macnab, R. M. (1996) Flagella and motility. In *Escherichia coli and Salmonella: cellular and molecular biology, 2nd edition.* Neidhart, F.C. Curtiss III, R., Ingraham, J. L., Lin, E. C. C., Low, K. B., Magasanik. B., Reznikoff, W. S., Riley, M., Schaechter, M. and Umbargar, H. E. (eds). Washington D. C.: ASM Press, **pp**. 123-146.

Magariyama, Y., Sugiyama, S., Muramoto, K., Maekawa, Y., Kawagishi, I., Imae, Y. and Kudo S. (1994) Very fast flagellar rotation. *Nature* **371**, 752.

Makarova, O., Kamberov, E. and Margolis, B. (2000) Generation of deletion and point mutations with one primer in a single cloning step. *Biotechniques* **29**, 970-972.

Maloney, P. C. and Wilson, T. H. (1996) Ion-coupled transport and transporters. In *Escherichia coli and Salmonella*. Neidhardt, F. C., Curtiss, R., Ingraham, J. L., Lin, E. C. C., Low, K. B., Magasanik, B., Reznikoff, W. S., Riley, M., Schaechter and M., Umbarger, H. E. (eds). Washington D. C.: ASM Press, **pp.** 283-306.

Manning, P. A. (1997) The *tcp* gene cluster of *Vibrio cholerae. Gene* **192**, 63-70.

McCarter, L. (1994a) MotX, the channel component of the sodium-type flagellar motor. *J. Bacteriol.* **176**, 5988-5998.

McCarter, L. (1994b) MotY, a component of the sodium-type flagellar motor. *J. Bacteriol.* **176**, 4219-4225.

Meister, M., Lowe, G. and Berg H. C. (1987) The proton flux through the bacterial flagellar motor. *Cell* **49**, 643-650.

Mekalanos, J. J., Swartz, D. J., Pearson, G. D., Harford, N., Groyne, F. and de Wilde, M. (1983) Cholera toxin genes: nucleotide sequence, deletion analysis and vaccine development. *Nature* **306**, 551-557.

Melo, A. M., Lobo, S. A., Sousa, F. L., Fernandes, A. S., Pereira, M. M., Hreggtvidsson, G. O., Kristjansson, J. K., Saraiva, L. M. and Teixeira, M. (2005) A *nhaD* Na^+/H^+ antiporter and *pcd* homologues are among the *Rhodotermus marinus* complex I genes. *Biochim. Biophys. Acta.* **1709**, 95-103.

Meng, Y. L., Liu, Z. and Rosen, B. P. (2004) As(III) and Sb(III) uptake by GlpF and efflux by ArsB in *Escherichia coli. J. Biol. Chem.* **279**, 18334-18341.

Merrell, D. S. and Camilli, A. (1999) The *cadA* gene of *Vibrio cholerae* is induced during infection and plays a role in acid tolerance. *Mol. Microbiol.* **34**, 836-849.

Merrell, D. S. and Camilli, A. (2000) Regulation of *Vibrio cholerae* genes required for acid tolerance by a member of the "ToxR-like" family of transcriptional regulators. *J. Bacteriol.* **182**, 5342-5350.

Metcalf, W. W., Jiang, W., Daniels, L. L., Kim, S. K., Haldimann, A. and Wanner, B. L. (1996) Conditionally replicative and conjugative plasmids carrying *lacZ* alpha for cloning, mutagenesis and allele replacement in bacteria. *Plasmid* **35**, 1-13.

Miller, C., Draser, B. and Feachem, R. (1984) Response of toxigenic *Vibrio cholerae* 01 to physico-chemical stresses in aquatic environments. *J. Hyg. (Lond).* **93**, 475-495.

Miller, V. L., Taylor R. K. and Mekalanos, J. J. (1987) Cholera toxin transcriptional activator *toxR* is a transmembrane DNA binding protein. *Cell* **48**, 271-279.

Miller, V. L. and Mekalanos, J. J. (1988) A novel suicide vector and its use in construction of insertion mutations: osmoregulation of outer membrane proteins and virulence determinants in *Vibrio cholerae* requires *toxR*. *J. Bacteriol.* **170**, 2575-2583.

Mitchell, P. (1961) Coupling of phosphorylation to electron and hydrogen transfer by a chemi-osmotic type of mechanism. *Nature* **191**, 144-148.

Mitchell, P. (1966) Chemiosmotic coupling in oxidative and photosynthetic phosphorylation. *Biol. Rev. Camb. Philos. Soc.* **41**, 445-502.

Morita, Y., Kodama, K., Shiota, S., Mine, T., Kataoka, A., Mizushima, T. and Tsuchiya, T. (1998) NorM, a putative multidrug efflux protein, of *Vibrio parahaemolyticus* and its homolog in *Escherichia coli*. *Antimicrob. Agents Chemother.* **42**, 1778-1782.

Morita Y., Kataoka, A., Shiota, S., Mizushima, T. and Tsuchiya, T. (2000) NorM of *Vibrio parahaemolyticus* is a Na^+-driven multidrug efflux pump. *J. Bacteriol.* **182**, 6694-6697.

Muramoto, K. and Macnab, R. M. (1998) Deletion analysis of MotA and MotB, components of the force-generating unit in the flagellar motor of *Salmonella*. *Mol. Microbiol.* **29**, 1191-1202.

Nakamura, T., Komano, Y., Itaya, E., Tsukamoto, K., Tsuchiya, T. and Unemoto, T. (1994) Cloning and sequencing of a Na^+/H^+ antiporter gene from the marine bacterium *Vibrio alginolyticus*. *Biochim. Biophys. Acta.* **1190**, 465-468.

Nakamura, T., Komano, Y. and Unemoto, T. (1995) Three aspartate residues in membrane-spanning regions of the Na^+/H^+ antiporter play a role in the activity of the carrier. *Biochim. Biophys. Acta.* **1230**, 170-176.

Nakamura, T., Enomoto, H. and Unemoto, T. (1996) Cloning and sequencing of *nhaB* gene encoding an Na^+/H^+ antiporter from *Vibrio alginolyticus*. *Biochim. Biophys. Acta.* **1275**, 157-160.

Nakamura, T., Fujisaki, Y., Enomoto, H., Nakayma, T., Takabe, T., Yamaguchi, N. and Uozumi, N. (2001) Residue aspartate-147 from the third transmembrane region of

Na^+/H^+ antiporter NhaB of *Vibrio alginolyticus* plays a role in its activity. *J. Bacteriol.* **183**, 5762-5767.

Nakayama, Y., Hayashi, M. and Unemoto, U. (1998) Identification of six subunits constituting Na^+-translocating NADH-quinone reductase from the marine *Vibrio alginolyticus*. *FEBS Lett.* **422**, 240-242.

Nakayama, Y., Hayashi, M., Yoshikawa, K., Mochida, K. and Unemoto, T. (1999) Inhibitor studies of a new antibiotic, korormicin, 2-n-heptyl-4-hydroxyquinolone-N-oxide and Ag^+ toward the Na^+-translocating NADH-quinone reductase from the marine *Vibrio alginolyticus*. *Biol. Pharm. Bull.* **22**, 1064-1067.

Natochin, Y. V. (1982) Mechanisms of drugs action on ion and water transport in renal tubular cells. *Progr. Drug Res.* **26**, 87-142.

Nielsen, J., Hansen F. G., Hoppe, J., Friedl, P., and von Meyenburg, K. (1981) The nucleotide sequence of the *atp* genes coding for the F_0 subunits a, b, c and the F_1 subunit delta of the membrane bound ATP synthase of *Escherichia coli*. *Mol. Gen. Genet.* **184**, 33-39.

Nishino, K. and Yamaguchi, A. (2001) Analysis of a complete library of putative drug transporter genes in *Escherichia coli*. *J. Bacteriol.* **183**, 5803-5812.

Noumi, T., Inoue, H., Sakurai, T., Tsuchiya, T. and Kanazawa, H. (1997) Identification and characterization of functional residues in a Na^+/H^+ antiporter (NhaA) from *Escherichia coli* by random mutagenesis. *J. Biochem.* **121**, 661-670.

Nozaki, K., Inaba, K., Tsuda, M., Tsuchiya, T. (1996) Cloning and sequencing of the gene for Na^+/H^+ antiporter of *Vibrio parahaemolyticus*. *Biochem. Biophy. Res. Commun.* **222**, 774-779.

Nozaki, K., Kuroda, T., Mizushima, T. and Tsuchiya, T. (1998). A new Na^+/H^+ antiporter, NhaD, from *Vibrio parahaemolyticus*. *Biochim. Biophys. Acta.* **1369**, 213-220.

Nye, M. B., Pfau, J. D., Skorupski, K. and Taylor R. K. (2000) *Vibrio cholerae* H-NS silences virulence gene expression at multiple steps in the ToxR regulatory cascade. *J. Bacteriol.* **182**, 4295-4303.

Ohyama, T., Igarashi, K. and Kobayashi, H. (1994) Physiological role of *chaA* gene in sodium and calcium circulations at high pH in *Escherichia coli*. *J. Bacteriol.* **176**, 4311-4315.

Okabe, M., Yakushi, T., Kojima, M. and Homma, M. (2002) MotX and MotY, specific components of the sodium-driven flagellar motor, colocalize to the outer membrane in *Vibrio alginolyticus*. *Mol. Microbiol.* **46**, 125-134.

Okabe, M., Yakushi, T. and Homma, M. (2005) Interactions of MotX with MotY and with the PomA/PomB sodium ion channel complex of the *Vibrio alginolyticus* polar flagellum. *J. Biol. Chem.* **280**, 25659-25664.

Olami, Y., Rimon, A., Gerchman, Y. and Padan, E. (1997) Histidine 225, a residue of the NhaA-Na^+/H^+ antiporter of *Escherichia coli* is exposed and faces the cell exterior. *J. Biol. Chem.* **272**, 1761-1768.

Ostroff, R. M., Wretlind, B. and Vasil, M. L. (1989) Mutations in the hemolytic-phospholipase-C operon result in decreased virulence of *Pseudomonos aeruginosa* PAO1 grown under phosphate-limiting conditions. *Infect. Immun.* **57**, 1369-1373.

Ostroumov, E., **Dzioba, J.**, Loewen, P. and Dibrov, P. (2002) Asp(344) and Thr(345) are critical for cation exchange mediated by NhaD, Na^+/H^+ antiporter of *Vibrio cholerae*. *Biochim. Biophys. Acta.* **1564**, 99-106.

Ottermann, K. M. and Miller J. F. (1997) Roles of motility in bacterial-host interactions. *Mol. Microbiol.* **24**, 1109-1117.

Ottow, E. A., Polle, A., Broché, M., Kangasjärvi, J., Dibrov, P., Zörb, C. and Teichmann, T. (2005) Molecular characterization of *PeNhaD1*: the first member of the NhaD Na^+/H^+ antiporter family from plant origin. *Plant Mol. Biol.* **58**, 75-88.

Padan, E., Zilberstein, D. and Schuldiner, S. (1981) pH homeostasis in bacteria. *Biochim. Biophys. Acta.* **650**, 151-166.

Padan, E., Maisler, N., Taglicht, D., Karpel, R. and Schuldiner, S. (1989) Deletion of *ant* in *Escherichia coli* reveals its function in adaptation to high salinity and an alternative Na^+/H^+ antiporter system(s). *J. Biol. Chem.* **264**, 20297-202302.

Padan E. and Schuldiner, S. (1992) In *Alkali Cation Transport Systems in Prokaryotes*. Bakker, E. (ed). Boca Raton, Florida.: CRC Press, **pp.** 3-24.

Padan, E. and Schuldiner, S. (1994) Molecular physiology of Na^+/H^+ antiporters, key transporters in circulation of Na^+ and H^+ in cells. *Biochim. Biophys. Acta.* **1185**, 129-151.

Padan, E. and Schuldiner, S. (1996) Bacterial Na^+/H^+ antiporters - molecular biology, biochemistry and physiology. In *The Handbook of Biological Physics, Vol. II, Transport Processes in Membranes.* Konings, W., Kaback, R. and Lolkema, J. (eds). Amsterdam, The Netherlands: Elsevier Science, **pp**. 501-531.

Padan, E. and Krulwich, T. A. (2000) Sodium Stress. In *Bacterial Stress Responses*. Storz, G. and Hengge-Aronis, R. (eds). Washington, D. C., ASM Press, **pp**.117-130.

Padan, E., Venturi, M., Gerchman, Y. and Dover, N. (2001). Na^+/H^+ antiporters. *Biochim. Biophys. Acta.* **1505**, 144-57.

Padan, E., Tzubery, T., Herz, K., Kozachkov, L., Rimon, A. and Galili, L. (2004) NhaA of *Escherichia coli*, as a model of a pH-regulated Na^+/H^+ antiporter. *Biochim. Biophys. Acta.* **1658**, 2-13.

Padan, E., Bibi, E., Ito, M. and Krulwich, T. A. (2005) Alkaline pH homeostasis: new insights. *Biochim. Biophys. Acta.* Epub ahead of print.

Parsot, C. and Mekalanos, J. J. (1990) Expression of ToxR, the transcriptional activator of the virulence factors in *Vibrio cholerae*, is modulated by the heat shock response. *Proc. Natl. Acad. Sci. USA*, **87**, 9898-9902.

Peterson, K. M. (2002) Expression of *Vibrio cholerae* virulence genes in response to environmental signals. *Curr. Issues Intest Microbiol.* **3**, 29-38.

Pfenninger-Li, X. D., Albracht, S. P., van Belzen, R. and Dimroth, P. (1996) NADH:ubiquinone oxidoreductase of *Vibrio alginolyticus*: purification, properties, and reconstitution of the Na^+ pump. *Biochemistry* **35**, 6233-6242.

Pinner, E., Padan, E. and Schuldiner, S. (1992) Cloning, sequencing, and expression of the *nhaB* gene, encoding a Na^+/H^+ antiporter in *Escherichia coli*. *J. Biol. Chem.* **267**, 11064-11068.

Pinner, E., Kotler, Y., Padan, E. and Schuldiner, S. (1993) Physiological role of nhaB, a specific Na+/H+ antiporter in Escherichia coli. *J. Biol. Chem.* **268**, 1729-1734.

Pinner, E., Padan, E. and Schuldiner, S. (1994) Kinetic properties of NhaB, a Na^+/H^+ antiporter from *Escherichia coli*. *J. Biol. Chem.* **269**, 26274-26279.

Pinner, E., Padan, E. and Schuldiner, S. (1995) Amiloride and harmaline are potent inhibitors of NhaB, a Na^+/H^+ antiporter from *Escherichia coli*. *FEBS Lett.* **365**, 18-22.

Pragai, Z., Eschevens, C., Bron, S. and Harwood, C. (2001) Bacillus subtilis NhaC, an Na^+/H^+ antiporter, influences expression of the *phoPR* operon and production of alkaline phosphatases. *J. Bacteriol.* **183**, 2505-2515.

Prakash, S., Cooper, G, Singhi, S. and Saier, M. H. (2003) The ion transporter superfamily. *Biochim. Biophys. Acta.* **1618**, 79-92

Putnoky, P., Kereszt, A., Nakamura, T., Endre, G., Grosskopf, E., Kiss, P. and Kondorosi, A. (1998) The *pha* gene cluster in *Rhizobium meliloti* involved in pH adaptation and symbiosis encodes a novel type of K^+ efflux system. *Mol. Microbiol.* **28**, 1091-1101.

Quick, M., Tebbe, S. and Jung, H. (1996) Ser57 in the Na^+/proline permease of *Escherichia coli* is critical for high-affinity proline uptake. *Eur. J. Biochem.* **239**, 732-736.

Rahav-Manor, O., Carmel, O., Karpel, R., Taglicht, D., Glaser, G., Schuldiner, S. and Padan, E. (1992) NhaR, a protein homologous to a family of bacterial regulatory proteins (LysR), regulates *nhaA*, the sodium proton antiporter gene in *Escherichia coli*. *J. Biol. Chem.* **267**, 10433-10438.

Rahlfs, S. and Müller, V. (1997) Sequence of subunit c of the Na^+-translocating F_1F_0-ATPase of *Acetobacterium woodii*: proposal for determinants of Na^+ specificity as revealed by sequence comparisons. *FEBS Lett.* **404**, 269-271.

Rahlfs, S., Aufurth, S. and Müller, V. (1999) The Na^+-F_1F_0-ATPase operon from *Acetobacterium woodii*. Operon structure and presence of multiple copies of *atpE* which encode proteolipids of 8- and 18kDa. *J. Biol. Chem.* **274**, 33999-34004.

Raskin, D., Bina, J. and Mekalanos, J. J. (2004) Genomic and Genetic Analysis of *Vibrio cholerae*. *ASM News* **70**, 57-62.

Rastogi, V. K. and Girvin, M. E. (1999) Structural changes linked to proton translocation by subunit c of the ATP synthase. *Nature* **402**, 263-268.

Reidl, J., and Klose, K. (2002) *Vibrio cholerae* and cholera: out of the water and into the host. *FEMS Microbiol. Rev.* **26**, 125-139.

Rensing C., Mitra, B. and Rosen B. P. (1997) The *zntA* gene of *Escherichia coli* encodes a Zn(II)-translocating P-type ATPase. *Proc. Natl. Acad. Sci, USA.* **94**, 14326-14331.

Rensing, C., Ghosh, M. and Rosen, B. P. (1999) Families of soft-metal-ion-transporting ATPases. *J. Bacteriol.* **181**, 5891-5897.

Rensing, C., Fan, B., Sharma, R., Mitra, B. and Rosen B. P. (2000) CopA: An *Escherichia coli* Cu(I)-translocating P-type ATPase. *Proc. Natl. Acad. Sci. USA.* **97**, 652-656.

Rich, P. R., Meunier, B. and Ward, F. B. (1995) Predicted structure and possible ionmotive mechanism of the sodium-linked NADH-ubiquinone oxidoreductase of *Vibrio alginolyticus*. *FEBS Lett.* **375**, 5-10.

Rimon, A., Gerchman, Y., Olami, Y., Schuldiner, S. and Padan, E. (1995) Replacements of histidine 226 of NhaA-Na^+/H^+ antiporter of *Escherichia coli*. Cysteine (H226C) or serine (H226S) retain both normal activity and pH sensitivity, aspartate (H226D) shifts the pH profile toward basic pH, and alanine (H226A) inactivates the carrier at all pH values. *J. Biol. Chem.* **270**, 26813-26817.

Rimon, A., Gerchman, Y., Kariv, Z. and Padan, E. (1998) A point mutation (G338S) and its suppressor mutations affect both the pH response o fthe NhaA Na^+/H^+ antiporter as well as growth phenotype of *Escherichia coli*. *J. Biol. Chem.* **273**, 26470-26476.

Rimon, A, Tzubery, T., Galili, L. and Padan, E. (2002) Proximity of cytoplasmic and periplasmic loops in NhaA Na^+/H^+ antiporter of *Escherichia coli* as determined by site-directed thiol cross-linking. *Biochemistry* **41**, 14897-14905.

Rosen, B. P. (1999) Families of arsenic transporters. *Trends Microbiol.* **7,** 201-212.

Rosen, B. P. (2002) Biochemsitry of arsenic detoxification. *FEBS Lett.* **529**, 86-92.

Rosenberg, H., Gerdes, R. G. and Chegwidden, K. (1977) Two systems for the uptake of phosphate in *Escherchia coli*. *J. Bacteriol.* **131**, 505-511.

Rosenberg, H., Gerdes, R. G. and Harold, F. M. (1979) Energy coupling to the transport of inorganic phosphate in *Escherichia coli* K-12. *Biochem. J.* **178**, 133-137.

Sagar , I. K., Nagesha, C. N. and Bhat, J. V. (1981) The role of trace elements and phosphate in the synthesis of vascular-permeability factor by *Vibrio cholerae*. *J. Med. Microbiol.* **14**, 243-250.

Sahu, G. K., Chowdhury, R. and Das, J. (1994) Heat shock response and heat shock protein antigens of *Vibrio cholerae*. *Infect. and Immun.* **62**, 5624-5631.

Saier, M. H. Jr. (1998) Molecular phylogeny as a basis for the classification of transport proteins from bacteria, archaea and eukarya. *Adv. Microb. Physiol.* **40**, 81-136.

Saier, M. H. Jr. (2000) A functional-phylogenetic classification system for transmembrane solute transporters. *Microbiol. Mol. Biol. Rev.* **64**, 354-411.

Sakai, Y. C., Moritani, M., Tsuda, M. and Tsuchiya, T. (1989) A respiratory-driven and artificially driven ATP synthesis in mutants of *Vibrio parahaemolyticus* lacking H^+-translocating ATPase. *Biochim. Biophys. Acta.* **973**, 450-456.

Sakai-Tomita, Y., Tsuda M. and Tsuchiya, T. (1991) Na^+-coupled ATP synthesis in a mutant of *Vibrio parahaemolyticus* lacking H^+-translocating ATPase activity. *Biochem. Biophys. Res. Commun.* **179**, 224-228.

Sambrook, J., Fritsch, E. F. and Maniatis, T. (1989) In *Molecular Cloning: A Laboratory Manaual.* Ford, N., Nolan, C., Ferguson, M., Ockler, M. (eds.) Cold Spring Harbour, New York, Cold Spring Harbour Laboratory.

Santana, M., Ionescu, M. S., Vertes, A., Longin, R., Kunst, F., Danchin, A. and Glaser, P. (1994) *Bacillus subtilis* F_1F_0-ATPase: DNA sequence of the *atp* operon and characterization of *atp* mutants. *J. Bacteriol.* **176**, 6802-6811.

Sarker, R. I., Ogawa, W., Tsuda, M., Tanaka, S., Tsuchiya, T. (1996) Properties of a Na^+/galactose (glucose) symport system in *Vibrio parahaemolyticus. Biochim. Biophys. Acta.* **1279**, 149-156.

Sato, T. and Kobayashi, Y. (1998) The *ars* operon in the *skin* element of *Bacillus subtilis* confers resistance to arsenate and arsenite. *J. Bacteriol.* **180**, 1655-1661.

Schmid, M., Wild, M. R., Dahinden, P. and Dimroth, P. (2002) Subunit gamma of the oxaloacetate decarboxylase Na^+ pump: interaction with other subunits/domains of the complex and binding site for the Zn^{2+} metal ion. *Biochemistry* **41**, 1285-1292.

Schneider, E. and Altendorf, K. (1987). Bacterial adenosine 5'triphosphate synthase (F_1F_0): purification and reconstitution of F_0 complexes and biochemical and functional characterization of *atp* mutants. *Microbiol. Rev.* **51**, 477-497.

Schonheit, P. and Beimborn, D. B. (1985) Presence of a Na^+/H^+ antiporter in *Methanobacterium thermoautotrophicum* and its role in Na^+ dependent methanogenesis. *Arch. Microbiol.* **142**, 354-360.

Schreurs, W. J. and Rosenberg, H. (1982) The effect of silver ions on transport and retention of phosphae in *Escherichia coli. J. Bacteriol.* **152**, 7-13.

Schuldiner, S. and Padan, E. (1994) Na^+/H^+ antiporters in *Escherichia coli* . In *Alkali Cation Transport Systems in Prokaryotes*. Bakker, E. (ed). Boca Raton, CRC Press, **pp**.26-46.

Schwarz, E., Oesterhelt, D., Reinke, H., Beyreuther, K. and Dimroth, P. (1988) The sodium ion translocating oxalacetate decarboxylase of *Klebsiella pneumoniae*. Sequence of the biotin-containing alpha-subunit and relationship to other biotin-containing enzymes. *J. Biol. Chem.* **263**, 9640-9645.

Semeykina, A. L. and Skulachev, V. P. (1990) Submicromolar Ag^+ increases passive Na^+ permeability and i

Senior, A. E. (1990) The proton-translocating ATPase of *Escherichia coli. Annu. Rev. Biophys. Chem.* **19**, 7-41.

Shalitin, Y., Segal, D and Gur, D. (2002) 2-aminoperimidine is an effector of cholinestrases. In *Proceedings of the XIth International Symposium on Cholinergic Mechanisms – function and dysfunction.* St. Moritz, Switzerland, **p.** 32.

Sharma, R., Rensing, C., Rosen, B. P. and Mitra, B. (2000) The ATP hydrolytic activity of purified ZntA, a Pb(II)/Cd(II)/Zn(II)-translocating ATPase from *Escherichia coli. J. Biol. Chem.* **275**, 3873-3878.

Shibata, C., Ehara, T., Tomura, K., Igarashi, K. and Kobayashi, H. (1992) Gene structure of *Enterococcus hirae* (*Streptococcus faecalis*) F_1F_0-ATPase, which functions as a regulator of cytoplasmic pH. *J. Bacteriol.* **174**, 6117-6124.

Shijuku, T., Yamashino, T., Ohashi, H., Saito, H., Kakegawa, T., Ohta, M. and Kobayashi, H. (2002) Expression of *chaA*, a sodium ion extrusion system of *Escherichia coli*, is regulated by osmolarity and pH. *Biochim. Biophys. Acta.* **1556**, 142-148.

Silver S. and Phung, L. T. (1996) Bacterial heavy metal resistance: new surprises. *Annu. Rev. Microbiol.* **50**, 753-789.

Silver, S. (1996) Transport of inorganic cations. In *Escherichia coli and Salmonella*, 2nd ed. Neidhardt, F. C., Curtiss III, R., Ingraham, J. L., Linn, E. C. C., Low, K. B., Magasanik, B., Reznikoff, W. S., Riley, M., Schaechter, M. and Umbarger, H. E. (eds). Washington, D. C.: ASM Press, **pp.** 1091-1102.

Sinai, A. P. and Bavoil, P. M. (1993) Hyper-invasive mutants define a Pho-regulated invasion pathway in *Escherichia coli*. *Mol. Microbiol.* **10**, 1125-1137.

Singleton, F. L., Attwell, R., Jangi, S., and Colwell, R. R. (1982) Effects of temperature and salinity on *Vibrio cholerae* growth. *Appl. Environ. Microbiol.* **44**, 1047-1058.

Skorupski, K. and Taylor, R. K. (1999) A new level in the *Vibrio cholerae* ToxR virulence cascade: AphA is required for transcriptional activation of the *tcpPH* operon. *Mol. Microbiol.* **31**, 763-771.

Skulachev, V. P. (1989) The sodium cycle: a novel type of bacterial energetics. *J. Bioenerg. Biomembr.* **21**, 635-647.

Skulachev, V. P. (1991) Chemiosmotic systems in bioenergetics: H^+-cycles and Na^+-cycles. *Biosci. Rep.* **11**, 387-441.

Slawson, R. M., Van Dyke, M. I., Lee, H. and Trevors, J. T. (1992) Germanium and silver resistance, accumulation and toxicity in microorganism. *Plasmid* **27**, 72-79.

Southworth, T. W., Guffanti, A. A., Moir, A. and Krulwich, T. A. (2001) GerN, an endospore germination protein of Bacillus cereus, is an Na^+/H^+-K^+ antiporter. *J. Bacteriol.* **183**, 5896-5903.

Speelmans, G., Poolman, B., Abee, T. and Konings, W. N. (1993) Energy transduction in the thermophilic anaerobic bacterium *Clostridium fervidus* is exclusively coupled to sodium ions. *Proc. Natl. Acad. Sci. USA.* **90**, 7975-7979.

Stader, J., Matsumura, P., Vacante, D., Dean, G. E. and Macnab, R. M. (1986) Nucleotide sequence of the *Escherichia coli motB* gene and site-limited incorporation of its product into the cytoplasmic membrane. *J. Bacteriol.* **166**, 244-252.

Steuber J. (2001) Na^+ translocation by bacterial NADH:quinone oxidoreductase: an extension to the complex-I family of redox pumps. *Biochim. Biophys. Acta.* **1505**, 45-56.

Steuber, J., Krebs, W. and Dimroth, P. (1997) The Na^+-translocating NADH:ubiquinone oxidoreductase from *Vibrio alginolyticus*-redox states of the FAD prosthetic group and mechanism of Ag^+ inhibition. *Eur. J. Biochem.* **249**, 770-776.

Stolz, B. and Berg, H. C. (1991) Evidence for interactions between MotA and MotB, torque-generating elements of the flagellar motor of *Escherichia coli. J. Bacteriol.* **173**, 7033-7037.

Sugiyama, S. (1994) Na^+-driven flagellar motors as a likely Na^+ re-entry pathway in alkaliphilic bacteria. *Mol. Microbiol.* **15**, 592.

Swartz , T. H., Ikewada, S., Ishikawa, O., Ito, M. and Krulwich, T. A. (2005) The Mrp system: a giant among monovalent cation/proton antiporters? *Extremophiles.* **9**, 345-354.

Taglicht, D., Padan, E. and Schuldiner, S. (1991) Overproduction and purification of a functional Na^+/H^+ antiporter coded by *nhaA* (*ant*) from *Escherichia coli. J. Biol. Chem.* **266**, 11289-11294.

Taglicht, D., Padan, E. and Schuldiner, S. (1993) Proton-sodium stoichiometry of NhaA, an electrogenic antiporter from *Escherichia coli. J. Biol. Chem.* **268**, 5382-5387.

Takeda E., Taketani, Y., Morita, K. and Miyamoto, K. (1999) Sodium-dependent phosphate co-transporters. *Int J. Biochem. Cell Biol.* **31**, 377-381.

Tamplin, M. L., Gauzens, A. L., Huq, A., Sack, D. A., and Colwell, R. R. (1990) Attachment of *Vibrio cholerae* serogroup O1 to zooplankton and phytoplankton of Bangladesh waters. *Appl. Environ. Microbiol.* **56**, 1997-1980.

Tang, H., Braun, T. F. and Blair D. F. (1996) Motility protein complexes in the bacterial flagellar motor. *J. Mol. Biol.* **261**, 209-221.

Taylor, R. K., Miller, V. L., Furlong, D. B. and Mekalanos, J. J. (1987) Use of *phoA* gene fusions to identify a pilus colonization factor coordinately regulated with cholera toxin. *Proc. Natl. Acad. Sci. USA.* **84**, 2833-2837.

Todar, K. (2005) *Vibrio cholerae* and asiatic cholera. In *Todar's Online Textbook of Bacteriology*. Todar, K. (ed). University of Wisconsin-Madison, Department of Bacteriology, http://textbookofbacteriology.net/cholera.html.

Tokuda, H., Asano, M., Shimamura, Y., Unemoto, T., Sugiyama, S. and Imae, Y. (1988) Roles of the respiratory Na^+ pump in bioenergetics of *Vibrio alginolyticus*. *J. Biochem.* **103**, 650-655.

Tusnady, G. E. and Simon, I. (1998) Principles governing amino acid composition of integral membrane proteins: application to topology prediction. *J. Mol. Biol.* **283**, 489-506.

Tzubery, T., Rimon A. and Padan, E. (2004) Mutation E252C increases drastically the K_m value for Na^+ and causes an alkaline shift of the pH dependence of NhaA Na^+/H^+ antiporter of *Escherichia coli*. *J. Biol. Chem.* **279**, 3265-3272.

Ueno, T., Oosawa, K. and Aizawa, S. (1992) M ring, S ring and proximal rod of the flagella basal body of *Salmonella typhimurium* are composed of subunits of a single protein FliF. *J. Mol. Biol.* **227**, 672-677.

Ueno, S., Kaieda, N and Koyama N. (2000) Characterization of a P-type Na^+-ATPase of a facultatively anaerobic alkaliphile, *Exiguobacterium aurantiacum*. *J. Biol. Chem.* **275**, 14537-14540.

Unemoto, N., Ohya, Y. and Anraku, Y. (1991) VMA11, a novel gene that encodes a putative proteolipid, is indispensable for expression of yeast vacuolar membrane H^+-ATPase activity. *J. Biol. Chem.* **266**, 24526-24532.

Unemoto, T. and Hayashi, M. (1993) Na^+-translocating NADH-quinone reductase of marine and halophilic bacteria. *J. Bioenerg. Biomembr.* **25**, 385-391.

Utsugi, J., Inaba, K., Kuroda, T., Tsuda, M. and Tsuchiya, T. (1998) Cloning and sequencing of a novel Na^+/H^+ antiporter gene from *Pseudomonas aeruginosa*. *Biochim. Biophys. Acta.* **1398**, 330-334.

van de Vossenberg, J. L. C. M., Ubbink-Kok, T, Elferink, M. G. L., Driessen, A. J. M. and Konings, W. N. (1995) Ion permeability of the cytoplasmic membrane limits the maximum growth temperature of bacteria and archaea. *Mol. Microbiol.* **18**, 925-932.

van de Vossenberg, J. L. C. M., Diessen, A. J. M. and Konings, W. N. (1998) The essence of being an extremophile: the role of the unique archael membrane lipids. *Extremophiles* **2**, 163-170.

van der Rest, M. E., Molenaar, D. and Konings, W. N. (1992a) Mechanism of Na^+-dependent citrate transport in *Klebsiella pneumoniae*. *J. Bacteriol.* **174**, 4893-4898.

van der Rest, M. E., Siewe, R. M., Abee, T., Schwarz, E., Oesterhelt, D. and Konings W. N. (1992b) Nucleotide sequence and functional properties of a sodium-dependent citrate transport system from *Klebsiella pneumoniae*. *J. Biol. Chem.* **267**, 8971-8976.

van Geest, M. and Lolkema J. S. (1996) Membrane topology of the sodium ion-dependent citrate carrier of *Klebsiella pneumoniae*. Evidence for a new structural class of secondary transporters. *J. Biol. Chem.* **271**, 25582-25589.

van Veen, H. W., Abee, T., Kortstee, G. J., Konings, W. N. and Zehnder, A. J. (1994) Translocation of metal phosphate via the phosphate inorganic transport system of *Escherchia coli*. *Biochemistry* **33**, 1766-1770.

van Veen, H. W. (1997) Phosphate transport in prokaryotes: molecules, mediators and mechanisms. *Antonie Van Leeuwenhoek.* **72**, 299-315.

Vimont, S. and Berche, P. (2000) NhaA, a Na^+/H^+ antiporter involved in environmental survival of *Vibrio cholerae*. *J. Bacteriol.* **182**, 2937-2944.

von Kruger, W. M., Humphreys, S. and Ketley, J. M. (1999) A role for the PhoBR regulatory system homologue in the *Vibrio cholerae* phosphate-limitation response and intestinal colonization. *Microbiology* **145**, 2463-2475.

Waditee, R., Hibino, T., Tanaka, Y., Nakamura, T., Incharoensakdi, A. and Takabe, T. (2001) Halotolerant cyanobacterium *Aphanothece halophytica* contains an Na^+/H^+ antiporter, homologous to eukaryotic ones, with novel ion specificity affected by C-terminal tail. *J. Biol. Chem.* **276**, 36931-36938.

Waldor, M. K. and Mekalanos, J. J. (1996) Lysogenic conversion by a filamentous phage encoding cholera toxin. *Science* **272**, 1910-1914.

Wanner, B. L. and Chang, B. D. (1987) The *phoBR* operon in *Escherichia coli* K-12. *J. Bacteriol.* **169**, 5569-5574.

Watnick, P., and Kolter, R. (1999) Steps in the development of a *Vibrio cholerae* El Tor biofilm. *Mol. Microbiol.* **34**, 586-595.

Wei, Y., Guffanti, A. A., Ito, M. and Krulwich, T. A. (2000) *Bacillus subtilis* YqkI is a novel malic/Na^+-lactate antiporter that enhances growth on malate at low protonmotive force. *J. Biol. Chem.* **275**, 30287-30292.

Werner, A. and Kinne, R. K. (2001) Evolution of Na-P_i cotransport systems. *Am. J. Physiol. Regul. Integr. Comp. Physiol.* **280**, R301-R312.

Wifling K. and Dimroth P. (1989) Isolation and characterization of oxaloacetate decarboxylase of *Salmonella typhimurium*, a sodium pump. *Arch. Microbiol.* **152**, 584-588.

Williams, S. G., Carmel-Harel, O. and Manning P. A. (1998) A functional homolog of *Escherichia coli* NhaR in *Vibrio cholerae*. *J. Bacteriol.* **180**, 762-765.

Willsky, G. R., Bennett, R. L., and Malamy, M. H. (1973) Inorganic phosphate transport in *Escherichia coli*: involvement of two genes which play a role in alkaline phosphatase regulation. *J. Bacteriol.* **113**, 529-539.

Wu, J. and Rosen, B. P. (1991) The ArsR protein is a trans-acting regulatory protein. *Mol. Microbiol.* **5**, 1331-1336.

Xu, C., Shi, W. and Rosen, B. P. (1996) The chromosomal *arsR* gene of *Escherichia coli* encodes a trans-acting metalloregulatory protein. *J. Biol. Chem.* **271**, 2427-2432.

Yakushi, T., Maki, S. and Homma, M. (2004) Interaction of PomB with the third transmembrane segment of PomA in the Na^+-driven polar flagellum of *Vibrio alginolyticus*. *J. Bacteriol.* **186**, 5281-5291.

Yamaguchi , S., Aizawa, S., Kihara, M., Isomura, M., Jones, C. J. and Macnab, R. M. (1986) Genetic evidence of a switching and energy-transducing complex in the flagellar motor of *Salmonella typhimurium*. *J. Bacteriol.* **168**, 1172-1179.

Yokoyama, T., Masuo, T., Akashi, H. and Zenki, M. (1995) The crystal structures of 2-aminoperimidine. *Bull. Chem. Soc. Jpn.* **68**, 1331-1336.

Yorimitsu, T. and Homma, M. (2001) Na^+-driven flagellar motor of *Vibrio*. *Biochim. Biophys. Acta.* **1505**, 82-93.

Yu, R. R. and DiRita, V. J. (2002) Regulation of gene expression in *Vibrio cholerae* by ToxT involves both antirepression and RNA polymerase stimulation. *Mol. Microbiol.* **43**, 119-134.

Yura, T. and Nakahigashi, K. (1999) Regulation of the heat-shock response. *Curr. Opin. Microbiol.* **2(2)**, 153-158.

Zhang, Y. and Kanner, B. I. (1999) Two serine residues of the glutamate transporter GLT-1 are crucial for coupling the fluxes of sodium and the neurotransmitter. *Proc. Natl. Acad. Sci. U.S.A.* **96**, 1710-1715.

Zhou, J., Sharp, L. L., Tang H. L., Lloyd S. A., Billings, S., Braun, T. F. and Blair D. F. (1998) Function of the protonatable site in the flagellar motor of *Escherichia coli*: a critical role for Asp32 of MotB. *J. Bacteriol.* **180**, 2729-2735.

Zhou, W., Bertsova, Y. V., Feng, B., Tsatsos, P., Verkhovskaya, M., Gennis, R. B., Bogachev, A. V. and Barquera, B. (1999) Sequencing and preliminary characterization of the Na^+-translocating NADH:ubiquinone oxidoreductase from *Vibrio harveyi*. *Biochemistry* **38**, 16246-16252.

Zhu, J., Miller, M. B., Vance, R. E., Dziejman, M., Bassler, B. L., and Mekalanos, J. J. (2002) Quorum-sensing regulators control virulence gene expression in *Vibrio cholerae*. *Proc. Natl. Acad. Sci. USA.* **99**, 3129-3134.

Zubkov, M. V., Fuchs, B. M., Eilers, H. Burkill, P. H. and Amann, R. (1999) Determination of total protein content of bacterial cells by SYPRO staining and flow cytometry. *Appl. Environ. Microbiol.* **65**, 3251-3257.